UNIVERSITÀ DEGLI STUDI FIRENZE

DOCTORAL PROGRAMME IN INDUSTRIAL ENGINEERING

Cycle XXXV

COORDINATOR Prof. Giovanni Ferrara

DeSA: Holistic Eco-Design Framework for Design and Sustainability Analysis in the Automotive Context

ING/IND-14

Doctoral Candidate
Dr. Antonacci Andrea

(signature)

Supervisor
Prof. Delogu Massimo

(signature)

Coordinator
Prof. (*Ferrara Giovanni*)

(signature)

Years 2019/2022

ISBN XXX–XX–XXXX–XXX–X
D/XXXX/XXXX/XX

Ai miei genitori Rosa e Vincenzo,

alla mia compagna Sara,

ai miei amici

Summary

The work is developed in the context of the automotive Life Cycle Sustainability Assessment (LCSA), and it is aimed to represent a valid support for assisting automotive designers in the early product development phase of single mono-material components. The final target of this research is to conceive a methodology/tool that takes into account at the same time and on the same level of importance both design and sustainability pillars (i.e., environment and economy). Starting from the following requirements:

- physical features and load case of the specific automotive case study
- functional and structural requirements
- available life cycle (LC) inventory data in terms of materials and manufacturing processes to be investigated
- vehicle features of the specific automotive case study (internal combustion engine vehicles (ICEV), battery electric vehicles (BEV))

The framework automatically generates different design alternatives evaluated through design and sustainability indicators developed in the methodology. These indicators are aggregated through MCDA methods in a single score index, based on which a ranking and the final choice of the most promising design option(s) are carried out.

The work defines a tool for analyzing and evaluating overall LC component installed to generic vehicles (gasoline, diesel, and electric). From a practical point of view, the tool is constituted by a series of models that:

- are flexible and tailorable for any generic case study
- adoptable by designers (or practitioners) for application to real case studies
- overcome the limitations and criticisms of current LCSA practices.

The conceived eco-design framework is developed and implemented within a computer-modeling tool developed in an integrated HyperWorks/MATLAB simulation environment. The utility of the research is highlighted through the application to several case studies, starting from physical/technical features and available inventory data provided by the designer as input/setting parameters.

The first part of the work defines the topic of the research, aiming to explain the relevance of the design for sustainability within the automotive LCSA context. An introduction to the LCA, LCC and S-LCA methodologies are provided and the importance of the eco-design tools in the determination of the overall LC impact is highlighted.

Chapter 1 is constituted by a State Of the Art (SOA) analysis regarding the considered topic: "Ecodesign methods/tools (EDM/T) in the automotive sector". The review includes both findings from research and practices usually adopted in current LCSA analyses. Literature data are collected and presented to support this section, from existing automotive LCSAs to studies that deal with the possible combination of sustainability pillars together to MCDA methods. Current approaches are described in detail, analyzed, and critically commented, evidencing the main points of criticism they are subject to. In the light of critical analysis, the enhancements with respect to existing literature are identified and translated into specific requirements the holistic eco-design tool has to fulfil.

Chapter 2 describes the eco-design framework, that is composed by the following four main phases:

- Screening: the generation of all the alternative design solutions that satisfy design requirements and are feasible from a technological point of view is performed;
- Design and Sustainability analysis: the description of the design, environmental and economic pillars, as well as the definition of related mid-point indicators are made;
- Optimization: the optimization of all the acceptable alternative design solutions that still satisfy design requirements and are feasible from a technological point of view is conducted - with the purpose to improve the sustainability, without compromising the mechanical performance;
- Classification: the calculation of product sustainability index and final ranking of optimized competing design alternatives are made.

Chapter 3 illustrates the application of the methodology to four case studies. The setting of parameters is explained in detail with the support of figures and tables in Appendices; in this phase it also included data collection, analysis and treatment performed by the Candidate. The results of the research are subdivided between two main sections: design and sustainability indexes calculated during the first phase of methodology (before optimization) and design and sustainability indexes calculated during the final phase of methodology (after optimization).

The results are critically discussed always in chapter 3. Finally the eco-design methodology is commented in chapter 4, placing particular emphasis on the enhancements of the research with respect to existing literature.

Table of Contents

List of Figures

List of Tables

Acronyms List

1D	Prismatic Shape
2D	Sheet Shape
3D	Three-dimensional Shape
AHP	Analytic Hierarchy Process
ARB	Arbitrary Scenario
AT	Acceptability threshold
B	Batch Size
BCs	Boundary Conditions
BEVs	Battery Electric Vehicles
BiW	Body-in-White
CBA-LCC	Cost Benefit Analysis LCC
CC	Climate Change
CFRPs	Carbon Fiber Reinforced Plastics
CI	Cost Index
cLCC	Conventional LCC
DeSA	Design and Sustainability Analysis
DfA	Design for Assembly
DfD	design for disassembly
DfDu	Design for durability
DfEE	Design for energy efficiency
DfM	Design for manufacturing
DfR	Design for recyclability
DfRem	Design for remanufacturing
DS	Design space
EDM/T	Ecodesign methods/tools
EI	Environmental Index
EL	Elasticity
eLCC	Environmental LCC
ELV	Elasticity Value
ELV^{ref}	Reference Elasticity Value
EMB	Engine Mounting Bracket
EoL	End-of-Life
ERV	Energy Reduction Value
EU-28	European Grid Mix
EXA	Exploratory approach
FEM	Finite Element Method
FL	Filtering level
FLCA	Front Lower Control Arm
FRV	Fuel Reduction Value
FU	The Functional Unit
G	Geometry
G&S	Goal and Scope definition
GFRP	Glass Fiber Reinforced Polymer
GHG	Green-House-Gas
G_t	Modified geometry
GUI	Graphic User Interface

ICEVs	Internal Combustion Vehicles
IGES	Initial Graphics Exchange Specification
ILCD	International Reference Life Cycle Data system
LC	Life Cycle
LCA	Life Cycle Assessment
LCC	Life Cycle Costing
LCI	Life Cycle Inventory
LCIA	Life Cycle Impact Assessment
LCIn	Life Cycle Interpretation
LCSA	Life Cycle Sustainability Assessment
LHS	Latin Hypercube Sampling
m	Component Mass
MAT	Material
MCDA	Multi-Criteria Decision Analysis
NDS	Non-design space
NPV	Net Present Value
OEMs	Original Equipment Manufacturers
par	Geometric parameter
PI	Performance Index
PR	Manufacturing process
PS	primary shape
PSL	Product Sustainability Level
$PSLV^{ref}$	Reference Product Sustainability Level Value
PUs	Process Units
RBE2	1D rigid element
RBE3	1D deformable element
REF	Reference Scenario
SB	System boundaries
SF	Substitution factor
SIMP	Simplified Isotropic Material with Penalization
S-LCA	Social-Life Cycle Assessment
sLCC	Societal LCC
SR	Surface Roughness
ST	Section Thickness
STEP	Standard for the Exchange of Product Data
TB	Torsion Bar
THR	threshold value
TO	Topology Optimization
To	Tolerance
TRA	Traditional approach
TRF	Top Roof
TTW	Tank-To-Wheel
WLTP	Worldwide Harmonized Light Vehicles Test Procedure
WTT	Well-To-Tank

Preface

Transportation plays a leading role within our global society and the development trends indicate a substantial growth in this sector over the coming decades. Considering the European Union, the transportation industry is currently the second largest contributor to anthropogenic Green-House-Gas (GHG) emissions; around 20% of these emissions are generated by road transport. Therefore, light-duty vehicles account for approximately 10% of total energy use and GHG emissions. According to the World Business Council for Sustainable Development, they could increase from roughly 700 million to 2 billion over the period 2000-2050. These concerns forecast a dramatic increase in air emissions, global fuel/electricity demand, and material requirements, with implications on energy security, climate change, and urban air quality.

In this context, sustainability is a crucial topic for automotive companies, and carmakers are subject to a strong regulatory pressure intended to make light-duty vehicles more environmentally sustainable. Such a scenario imposes that designers and product developers bind design performances with greater environmental commitment.

Therefore, this work proposes an innovative eco-design methodology to provide the automotive designer with the concept development phase of single mono-material components. Starting from the geometry and load case of the specific application, the method generates different design alternatives (both in terms of materials and manufacturing processes applied), which are evaluated under both performance and sustainability point of view. In particular, the assessment and selection steps are carried out through a single-score indicator based on a multi-objective approach.

Four automotive components are presented as automotive case studies which envisage the examination of a range of materials and manufacturing processes directly provided by the designer as an extension of the investigation field. The case studies results reveal the potentiality and utility of this approach: the developed framework generates, analyzes, and critically compares several design solutions obtained by combining different materials and manufacturing processes.

The choice of the most promising design options is performed based on the single-score indicator (as well as performance and sustainability pillars).

The work is developed in the context of the automotive Life Cycle Sustainability Assessment (LCSA), and it is aimed to represent a valid support for assisting automotive designers in the early product development phase of single mono-material components.

Therefore, it can be stated that the design and sustainability approach in the concept development stage of the product supports designers in their research to achieve the eco-design with less effort.

1. Introduction

The actual society is strongly dependent on transportation, and the development trends indicate substantial growth in this sector over the coming decades (Hawkins et al., 2012). The transportation industry (including all transport modes, from air to surface traffic) is currently the second largest contributor to anthropogenic Green-House-Gas (GHG) emissions within the European Union; around 20% of these emissions are generated by road transport, including both private/public and passenger/freight vehicles (Witik et al., 2011; Mayyas et al., 2012; Graedel and Allenby, 1998).

In detail, light-duty vehicles account for approximately 10% of total energy use and GHG emissions (Solomon et al., 2007a,b). In 2016 global vehicle registrations were estimated at around 1.32 billion units (Ward's auto, 2017) - nearly double the volume 20 years prior when vehicles-in-operation totaled 670 million in 1996 - and this number is expected to grow to 2.5 billion by 2050 (ITF, 2015). Light-duty vehicles are responsible for large-scale environmental and economic impacts at every life cycle stage (according to Jasinski et al., 2015):

- raw material and production stages, characterized by intensive resources and energy consumption;
- use stage, affecting global fuel demand (as well as global electricity demand for electric vehicles), air pollutants emissions, noise, and road accidents;
- End-of-Life (EoL) stage, causing the definition of complex waste management systems.

These concerns forecast a dramatic increase in air emissions, global fuel/electricity demand, and material requirements, with implications on energy security, climate change, and urban air quality (Ford et al., 2011; Hawkins et al., 2012; IPCC, 2013; Moawad et al., 2013; U.S. National Highway Traffic Safety Administration, 2012; U.S. EPA, 2013, 2014) as well as a corresponding increase of waste produced during the EoL (Berzi et al., 2013).

Against this background, many countries have put regulations to reduce fuel consumption and air emissions, including decisive actions and initiatives necessary to foster an industrial renaissance rooted in sustainability (such as high fuel taxes to promote energy conservation). Considering the European context, the environmental regulation (e.g., 2009/125/EC - Energy related products- ERP, 2009/443/EC - CO_2 emissions from light-duty vehicles, 2000/53/EC – End-of-Life vehicle – ELV) is a crucial driver for promoting the eco-innovation in the automotive sector. Thus, it leads to the developing of new materials and related technologies, reducing the environmental impact of vehicles and their components. However, pressure from stakeholders and Corporate strategies toward sustainability are the main drivers for the performance improvements of products into broader sustainability (Andriankaja et al., 2015; Pallaro et al., 2015). In order to produce vehicles with a lower environmental impact, the automotive Original Equipment Manufacturers (OEMs) are currently requested to target several technological challenges (Schmidt et al., 2004; Subic & Koopmans, 2010; Kelly et al., 2015). The main objectives include:

- Reduction of tailpipe emissions, hence reducing Greenhouse Gasses effect and improving air quality;
- Increase efficiency and hence reduce consumption of energy and natural resources;
- Increase recyclability and recoverability of vehicle parts. Thus, reducing landfilled waste and improving the circularity of materials (Subic & Koopmans, 2010).

1.1 Design for Sustainability in automotive industry

Sustainable development (Ness et al., 2007; Fauzi et al., 2019) has become crucial in recent years. Environmental and cost sustainability represented the main pillars for business and societal decision-making. As regards the industrial context, a key element to help policymakers, stakeholders, and customers to make decisions in the perspective of making society more sustainable is represented by the eco-design of new products (Sala et al., 2015; McArthur & Rasmussen, 2018; Leal Filho et al., 2018). Therefore, assessing Life Cycle (LC) sustainability has become crucial for decision support. Sustainable development indicators are widely used to evaluate technical performances and the sustainability profile of new products.

Such a trend adds more pressure on OEMs, as nowadays, vehicles also have to meet environmental targets besides the traditional ones (safety, performance, and functionality).

Sustainability provides that the needs of both the business customer and society are met while preserving the ecosystem (Ness et al., 2007). From this definition, the intrinsic complexity of the term "sustainability" derives from treating different issues within the product development process (such as social, ethical, environmental, and economic). In order to guarantee the car is an environmentally sustainable asset, design for sustainability follows the design-for-X principles (as shown in **Figure 1**).

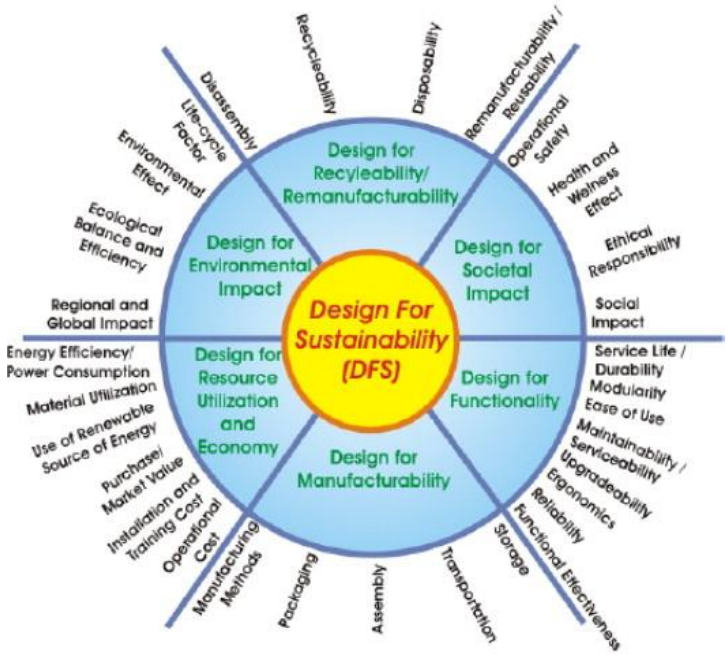

Figure 1. Major application fields of Design for Sustainability.

The design-for-X covers several areas of interest: manufacturing, durability, energy efficiency, and recyclability.

- Design for manufacturing (DfM): it is targeted to reduce both time and cost of production. The guidelines of DfM include product adoption at the company level, the product family, the product structure, and components. A derivative of DfM is the "Design for Assembly" (DfA), which focuses on assembly and fastening strategies (such as reducing the number of parts and part variations).

- Design for durability (DfDu): it has the scope to increase the time or amount of usage during which the product operates without failure; thus, designing the product to last longer leads to advantages in both resource consumption and waste generation.
- Design for energy efficiency (DfEE): It aims to reduce the energy consumed by vehicles during the use stage. In addition to improving the thermal efficiency of the engine, the use of lightweight materials represents an optimal solution: since rolling resistance and acceleration forces are directly proportional to vehicle weight (Cheah & Heywood, 2011; Ungureanu et al., 2007), mass is the critical factor in order to achieve significant reductions in energy consumption and air emissions. For instance, using plastics in lightweight vehicles saves 30 times more energy over the lifecycle than the energy required for fabrication (Mcauley, 2003).
- Design for recyclability (DfR): it envisages that EoL materials are processed out of one form and remade into a new product. Using recycled materials minimizes the consumption of virgin raw materials, energy, and water, thus leading to reduce waste, air/water pollution, and energy consumption. Another notable advantage of lowering the need for virgin materials is saving money by avoiding additional materials extraction. DfR includes design for disassembly (DfD) and design for remanufacturing (DfRem), which are strictly connected. On the one hand, DfD makes that a product is disassembled at minimum cost and effort, ensuring a fast disassembly process, and recovering a more significant proportion of system components. On the other hand, DfRem is targeted to return the vehicle assemblies and components to an "acceptable performance level" for reuse. A standard design guideline for recyclability is avoiding mixing materials in assemblies and minimizing the number of parts made of different materials. Such expedients facilitate the process of disassembling, sorting, and collecting materials, enhancing vehicle recyclability.

Therefore, considering design-for-X principles, the new trend in vehicle design aims not only to improve fuel efficiency but also to enhance driving performance while simultaneously lowering air emissions. In this regard, several materials and manufacturing selection methodologies have been developed to incorporate environmental concerns. Such methodologies can be classified based on multiple criteria:

- Design approach. The methodologies can emphasize the ease of manufacturability rather than environmental or economic sustainability aspects;
- A portion of vehicle LC. Some methods set up the design phase taking into account only a single LC stage, while others attempt to consider the entire lifetime;
- Quantitative/qualitative approaches. Some approaches provide guidelines based on qualitative selection methodologies, while others rate the materials and processes using quantitative indicators.

In conclusion, it directly derives that materials and manufacturing process selection is not led by a unique factor but is instead made up of a mixing of technical, economic, and environmental issues. It can be stated that significant challenges still lie ahead for the automotive industry to reach sustainability goals.

1.2 Challenges and methodologies for the automotive sector sustainability

To meet the challenging targets described above, automotive organizations struggle to mitigate the environmental effects in different ways, such as design for sustainability, cleaner technologies investment, and creation of value for the community (Maclean & Lave, 2003; Delogu et al., 2016). Concerning the design aspect, some of the most common approaches utilized by OEMs are as follow:

- Lightweighting (Hakamada et al., 2007; La Rosa et al., 2014; Mayyas et al., 2013; Raugei et al., 2015; Tharumarajah & Koltun, 2007);
- Optimization of manufacturing processes/technologies (Rödger et al., 2018; Simoes et al., 2016; Vinodh & Jayakrishna, 2011; Ferreira et al., 2020);
- Redesign vehicle assemblies/components and adopt more efficient materials to replace traditional ones (Inti et al., 2016; Koffler & Zahller, 2012; Poulikidou et al., 2016; Santos et al., 2017; Lopes et al., 2019; Spreafico, 2022).

Lightweight design is one of the main concerns for OEMs since it is proven to produce effective fuel demand reduction and tailpipe emission abatement. It can be achieved by reducing weight through material substitution and vehicle component redesign while maintaining vehicle size and satisfying consumer demand. It is strongly related to material selection, materials research advancements, and manufacturing technologies. Lightweighting concentrates on three main areas: the use of lightweight materials, the use of more robust materials, and design optimization. The first area envisages reducing vehicle weight and improving fuel economy by adopting low-density materials. On the other hand, the cost of these materials (such as aluminium, magnesium, carbon fiber reinforced polymers, and sandwich materials) and the difficulty involved in their manufacturability represent the significant obstacles to this solution. The second approach to lightweighting is based on using more robust materials (such as modified steel alloys and grades). This solution allows car designers to reduce vehicle weight through thinner gauges. The last area is design optimization, based on optimized cross-sectional shapes of structures; this solution enables better loading performance without increasing weight.

This innovative approach undoubtedly ensures several improvements, such as technical and driving features (e.g., performance, drive-ability, and road safety) and energy consumption (Kelly et al., 2015; Javadi et al., 2021). Compared to conventional design solutions, new materials and advanced components typically involve higher GHG emissions during the production and manufacturing stages. A clear example of this is represented by the adoption of Carbon Fiber Reinforced Plastics (CFRPs): With respect to conventional steels, CFRPs cause a more significant impact, both in raw materials acquisition (increased depletion of primary resources) and processing of semi-finished products (higher energy consumption and emissions) (Ciacci et al., 2010). At the same time, using new generation materials often involves more significant issues in EoL management (Dhingra & Das, 2014). The non-availability of separation processes and recycling technologies cause lower recoverability rates and a more considerable amount of waste in landfill (Diener & Tillman, 2016; Berzi et al., 2016); consider, for instance, the impossibility of separating different material fractions used in composites or sandwich materials. As a result, even if notable technical improvements are achieved, innovative design can lead to adverse effects on the overall product LC, mainly due to increased environmental burdens in production and EoL

stages (Kim & Wallington, 2013; Rousseaux et al., 2017; Das, 2000; Funazaki et al., 2003). Therefore, the material selection process needs to balance many aspects - technical performance and feasibility, materials recyclability, and the environmental impact of material production – and this leads to necessarily facing controversial issues and trade-offs (De Medina, 2006; Raugei et al., 2015; Andriankaja et al., 2015; Kelly et al., 2015).

The awareness and need for a more comprehensive sustainability approach where environmental evaluations are combined with economic ones to give a deeper insight for selecting the best trade-off among the dimensions of sustainability are arising among the scientific community and the industrial sector. This, in turn, brings to consider many conflicting environmental and economic factors (Schmidt & Taylor, 2008; Pallaro et al., 2015; Jasinski et al., 2015).

From the above discussion, it follows that novel design solutions within the automotive field need to be developed through dedicated eco-design methodologies, which consider mechanical performance, environmental and economic sustainability pillars at the same level of importance, both evaluated under the entire LC perspective. To meet this challenging issue Life Cycle Sustainability Assessment (LCSA) has been developed as a suitable approach for assessing the product sustainability in the early design phase (UNEP/SETAC, 2011; Zamagni et al., 2013), based on considerations related to the entire LC (Visentin et al., 2020; Costa et al, 2019). Such a methodology compares quantitatively different product concepts, provides insights about rooms for improvement (e.g., alternative materials or processes) and transparently describes the potential trade-off. The implementation of LCSA often brings to the adoption of Multi-Criteria Decision Analysis (MCDA) methods that support both product developers and designers to solve decision-making problems when a series of alternatives are evaluated based on multiple criteria (Aruldoss et al., 2013; Wang et al., 2009, Onat et al., 2020). It is clearly a LC-based methodology which integrates the three techniques LCA, LCC and S-LCA to represent the environmental, economic, and social dimension respectively (Finkbeiner et al. 2010). According to (Guinée, 2016), two basic approaches exist. The first, proposed by (Kloepffer, 2008; Finkbeiner et al. 2010), promotes LCSA (assessment) as a broadening of ISO-LCA to also include economic and social aspects; it is based on the "triple bottom line" model, also called "three-pillar", and relies on the scheme:

$$LCSA = LCA + LCC + SLCA$$

where:

LCA = the environmental Life Cycle Assessment, defined and standardized by the ISO 14040–44 (ISO14040 2006; ISO14044 2006);
LCC = the environmental Life Cycle Costing or the assessment of economic factors along the product LC (Hunkeler et al. 2008; Swarr et al. 2011);
SLCA = the evaluation of the social aspects (UNEP/SETAC 2009).

The second approach, proposed by (Guinée et al., 2011), promotes LCSA (analysis) as a transdisciplinary integrated frameworks of models to broaden the scope of current LCA from environmental impacts only to all three dimensions of sustainability, and to deepen the analysis at different level (products, sector, and economy), taking into account technological, economic, and behavioural relations, just to mention some (Guinée, 2016). Both approaches

have the common intent of broadening the impacts analysis from the environmental impacts to the economic and social ones; however they differ in terms of conceptual structure and modelling principles (Sala et al., 2013).

The majority of LCSA case studies published so far have focused on the scheme proposed by (Kloepffer, 2008) and addressed its applicability and practicability along with evaluating what kind of information can be obtained and how they can support the decision making process (Zamagni et al., 2013; Guinée, 2016). Therefore, the first approach will be followed and discussed in the present research. Therefore, in order to describe the LCSA methodology, it is also necessary to review and discuss the methodological aspects that constitute it: LCA, LCC, S-LCA, and MCDA.

1.2.1 Life Cycle Assessment (LCA) in automotive industry

Life Cycle Assessment (LCA) (Finnveden et al., 2009; ILCD, 2011; Mayyas et al., 2012a; WorldAutoSteel, 2012) is an environmental accounting methodology that allows the quantification and evaluation of environmental effects associated with a product, manufacturing process or specific service. It has established itself as the prevailing tool for:

- assessing the environmental effects of products, processes, or services;
- assisting with the optimization of the environmental performance of a product;
- comparing products to determine the most environmentally favourable ones.

The environmental effects quantified by LCA are expressed as potential impacts; the impact categories most frequently adopted are climate change, ozone depletion, tropospheric ozone creation, eutrophication, acidification, toxicological stress on human health and ecosystems, depletion of resources, and land use (Rebitzer et al., 2004). The methodology follows a "from cradle-to-grave" approach, beginning with raw materials gathered from the earth and ending at the point when all materials are returned to the earth. In this context, all stages of the product LC are evaluated from the interdependent perspective, implying that one operation leads to the next. Such an approach allows estimating the cumulative environmental impacts from the entire LC, including impacts not considered in more traditional analyses. For this reason, a more accurate picture of the actual environmental trade-offs in product and process selection is achievable. The LCA becomes an essential tool for decision-makers to identify the product, process, or service with the minimum environmental impact.

1.2.1.1 LCA methodology. A typical product LC is deemed to be made up of four main stages: raw materials acquisition, production, use, and EoL. **Figure 2** illustrates the typical LC stages and input/output measured, with their description reported below.

- Raw materials acquisition. The LC of a product begins with the removal of raw materials and energy sources from the earth; materials transportation from the point of acquisition to the point of processing is also comprised;
- Production. The production stage consists of three steps: materials manufacture (activities that convert raw materials into a semi-finished product, i.e., a form that

can be used to fabricate a finished product), product fabrication (activities that take the manufactured material and process it into a product that is ready to be filled or packaged), and filling/packaging/distribution of the manufactured product;

- Use/Reuse/Maintenance. All the activities associated with useful life-time are included in this stage. Actual use, reuse, and maintenance are considered; all energy demands and environmental wastes from both product storage and consumption are also taken into account in this phase;
- End-of-Life (EoL). The stage includes the energy requirements and environmental wastes associated with recovery, recycling, and disposal of the product.

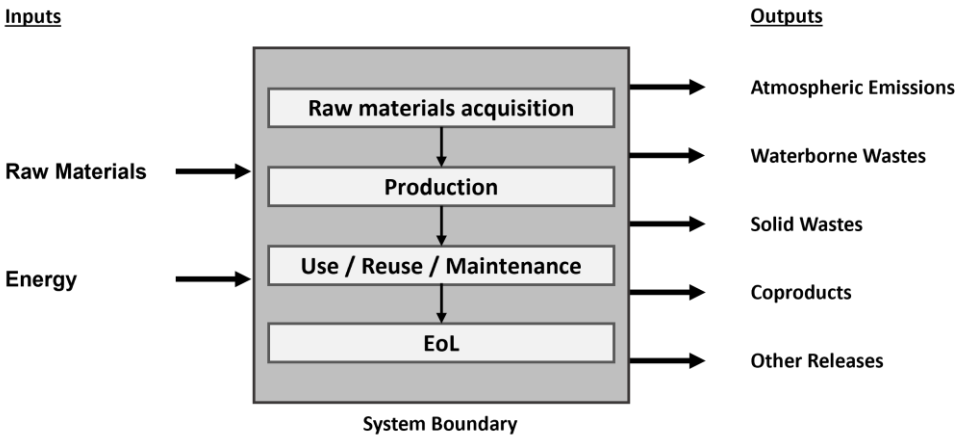

Figure 2. Main stages of product LC

The LCA methodology is supported by a set of standards from the ISO (Finkbeiner, 2006; ISO 14040, 2006; ISO 14044, 2006) and according to them it follows four phases: Goal and Scope definition (G&S), Life Cycle Inventory (LCI), Life Cycle Impact Assessment (LCIA) and Life Cycle Interpretation (LCIn). A brief description of the phases of a LCA study is reported below; in **Figure 3** the LCA framework with the interaction between phases is shown, according to UNI EN ISO 14040:2006 and UNI EN ISO 14044: 2006 (ISO 14040, 2006; ISO 14044, 2006).

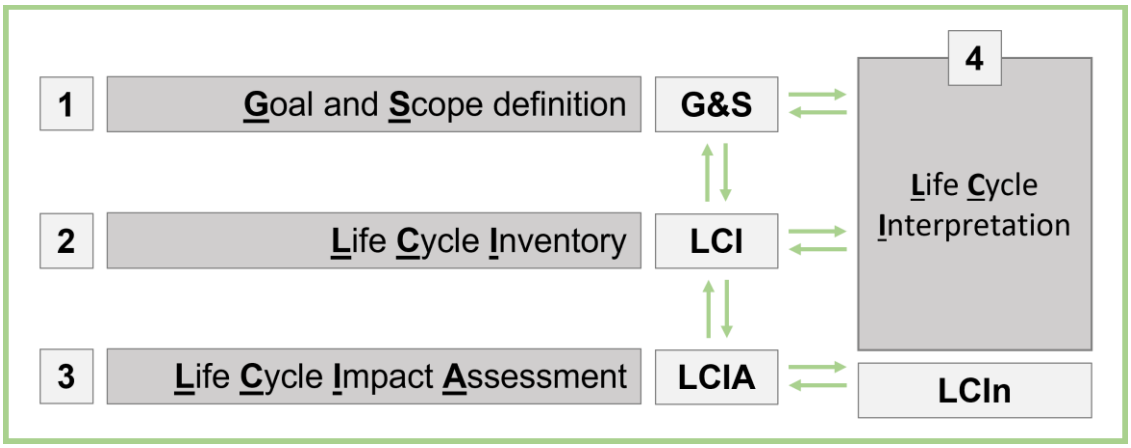

Figure 3. LCA framework and interaction between phases of the study.

1. Goal and Scope definition (G&S). G&S is the first phase of an LCA; it influences the entire study's progress and impacts the relevance of final results. G&S defines the purpose and method of including LC environmental impacts in the decision-making process, how accurate the results must be, and how the results should be interpreted and displayed to be meaningful and usable. Two essential elements for the development of the entire study are defined in the G&S: system boundaries and functional unit. The System boundaries (SB) define the product system; they comprehend all process units that describe the key elements of physical systems and define across which boundaries the exchange of elementary flows with nature takes place (Hiederer, 2011). Within the system, a distinction between "Foreground system" and "Background system" must be made: "Foreground" indicates the main object of the analysis. In contrast, "Background" represents all the activities required to realize the Foreground processes. Ideally, the product system should be modelled so that inputs and outputs at its boundaries are elementary flows. The Functional Unit (FU) describes the product system's primary function(s), indicating how much of this function is to be considered in the intended LCA study. FU enables different systems to be treated functionally equivalent, and reference flows are determined for each. FU is used to select one or more alternative (product) systems that might provide the same function(s).
2. Life Cycle Inventory (LCI). This inventory gathers and processes all data required in order to analyze the system described in the G&S. These are the exchanges with the ecosphere that are triggered during product LC: quantities of energy and raw materials, atmospheric emissions, waterborne emissions, solid wastes, and other releases attributed to product LC are quantified and allocated to the defined FU. LCI is composed of two main steps: data collection and Modelling. The Data collection collects and organizes all relevant data regarding product LC to depict the system's average behavior, including regular and nominal functioning and possible abnormal operation. The level of detail and accuracy by which data collection is performed influences the significance and truthfulness of the entire study. The final output of an LCI is a list of the amounts of consumed energy and materials and pollutants released to the environment; the results can be segregated by LC stage, media (air, water, and land), specific process, or any combination thereof. The Modelling determines and quantifies all elementary flows that characterize the product's environmental profile. G&S. strongly influences both data collection and Modelling. The outcomes of LCI become the input for the subsequent LCIA phase and provide feedback to G&S as initial scope settings often need adjustments.
3. Life Cycle Impact Assessment (LCIA). The LCIA phase evaluates potential human health and environmental impacts starting from the contributions of emissions, waste, and resources determined in the inventory analysis. An LCIA attempts to connect the product or process and its potential environmental impacts; all the elementary flows collected in the LCI are translated into an ensemble of environmental impact indicators. The results of LCIA should be seen as environmentally relevant impact potential indicators rather than predictions of actual environmental effects and represent the basis for the last phase of the LCA study, the interpretation. LCIA is composed of mandatory and optional steps. According to ISO 14040, Classification and Characterization are obligatory elements.
   The Classification assigns the elements of the LCI data to relevant impact categories such as climate change and toxicological stress land use. Whereas the Characterization determines the contribution of each classified elementary flow to the proper impact categories by multiplying it with the relative characterization

factors. For instance, within the global warming category, results are given in kg of CO_2 equivalents (eqv), and therefore, 1 kg of CO_2 quantified in the LCI would be indicated by 1 kg of CO_{2eqv} in the climate change impact category. CH_4, on the other hand, contributes 25 times more to climate change than CO_2; therefore, the characterization factor would be 25, and 1 kg of CH_4 from the LCI would be communicated as 25 kg of CO_2 equivalents in this category. Usually, Classification and Characterization are performed based on complete sets of LCIA methods developed by LCA experts; the appropriate method is chosen concerning the outputs defined in the G&S. Depending on association with specific environmental aspects, LCIA results are shared in various indicators which refer to different impact categories: Climate change, (Stratospheric) Ozone depletion, Human toxicity, Respiratory inorganics, Ionizing radiation, (Ground-level) Photochemical ozone formation, Acidification (land and water), Eutrophication (land and water), Eco-toxicity, Land use, Resource depletion (metals, minerals, fossil, nuclear and renewable energy sources, water). The impact categories can then be further processed into three areas of protection: Human health, Natural environment, Natural resources. Impact categories are typically called "midpoints," while the three protection areas are referred to as "endpoints". The type and number of impact categories taken into account in a study vary depending on the G&S. **Figure 4** shows a summary of the LCIA framework within the International Reference Life Cycle Data system (ILCD) (Hiederer, 2011).

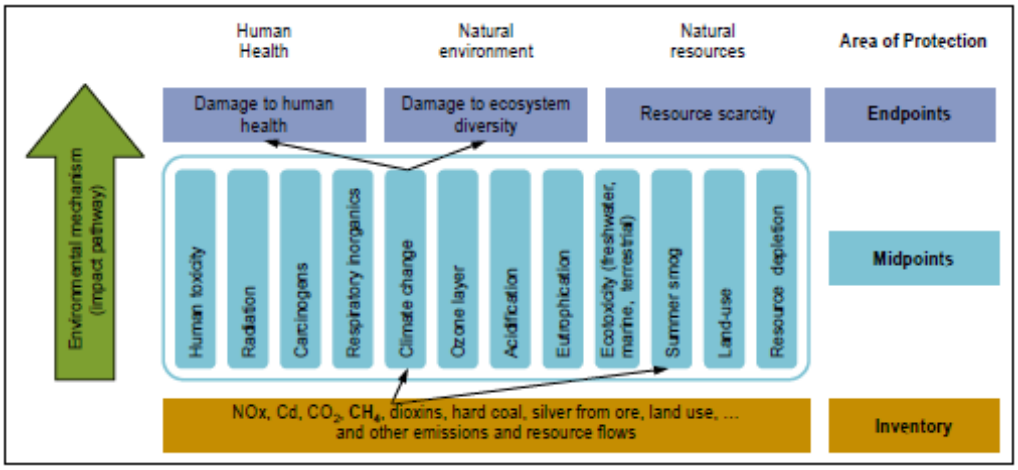

Figure 4. Summary of the LCIA framework within the ILCD (source: Hiederer, 2011).

The LCIA optional steps are Normalization and Weighting. Normalization normalizes the LCIA results through multiplication by factors representing the overall inventory of a reference (e.g., a whole country or an average citizen); normalized dimensionless LCIA results are obtained. Finally, Weighting evaluates the significance of the normalized LCIA results through multiplication by a set of weighting factors. The weighting factors reflect the different relevance that different impact categories (midpoint level related weighting) or areas of protection (endpoint level related weighting) have. The final output is represented by normalized and weighted LCIA results that can be summed up to a single-value impact indicator.

4. Life Cycle Interpretation (LCIn). In this phase, the study outcomes are evaluated to respond to the questions defined in the G&S. Results are collectively considered and analyzed in light of the accuracy, completeness, and precision of the LCI data collection. Additionally, the sensitivity of significant issues concerning their

influence on the overall results is evaluated. The final target of LCIn is double: on the one hand, improving the LCI model to meet the needs derived from the G&S. On the other hand, deriving robust conclusions and recommendations once the final results are available. Since the LCA must be constantly measured against its initial G&S and refined during its duration, the LCIn has continuous interactions with the other phases of the study (as shown in **Figure 3**).

1.2.1.2 LCA of vehicles. The LCA methodology has mainly been employed in the transportation sector and particularly in the automotive field for the following purposes:

- Estimating environmental profile of current vehicles and automotive components;
- Evaluating environmental progress from one product generation to the next.

As said in paragraph 1.2.1.1, the LCA analysis evaluates the environmental impacts involved by all stages that compose LC of the investigated system. Similarly to other products, the main LC stages of a car are production, use, and EoL (see **Figure 5**).

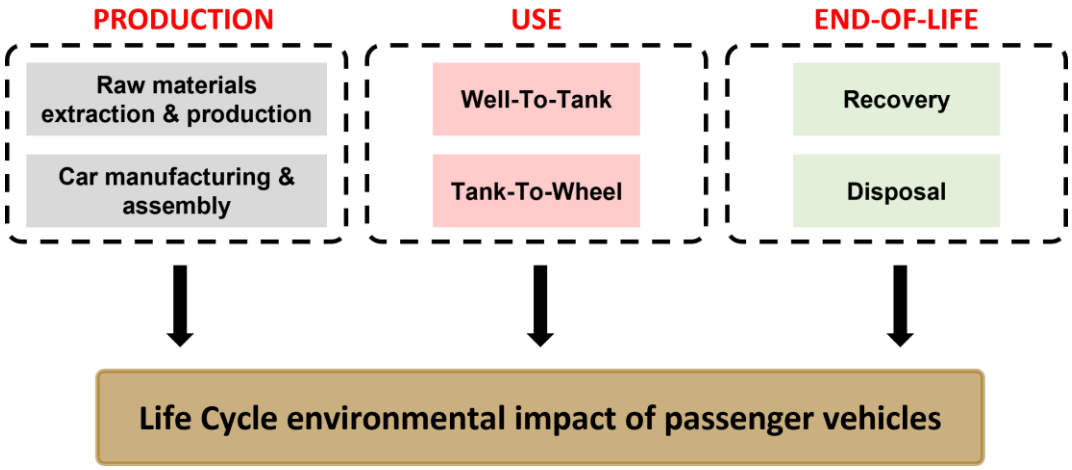

Figure 5. LC stages that determine the overall Life Cycle environmental impact of a vehicle.

The main LC stages of a car can be divided into Process Units (PUs) which in turn include the single processes. Below a brief description of PUs and processes is reported for each one of car LC stages:

1. Production. Production is the first stage of car LC, and it includes all manufacturing and assembly processes of vehicle components. It involves the following PUs and processes:
    - PU Raw materials extraction and production. Production of electricity, heat, steam and fuel for raw materials extraction and production of car components and spare parts;
    - PU Car manufacturing and assembling. Production of electricity, heat, steam and fuel for manufacturing and assembly activities.
2. Use. Use is the most complicated stage of car LC as it comprises both energy cycle and vehicle operation. It includes the following PUs and processes (defined according to different propulsion technology):

- PU Well-To-Tank (WTT). Considering Internal Combustion Vehicles (ICEV): Fuel transformation processes upstream to fuel consumption: fuel production from recovery or production of the feedstock, its transportation, conversion of the feedstock to the final fuel and subsequent storage, distribution, and delivery to the vehicle fuel tank. Considering Battery Electric Vehicles (BEV): Electricity transformation processes upstream to energy consumption: electricity production from specific grid-mix, distribution, and delivery to the vehicle battery.
- PU Tank-To-Wheel (TTW). Fuel/Energy consumption for car driving: energy required to drive the vehicle, exhaust, and evaporative emissions from the vehicle over its life-time.

3. End-of-Life. EoL is the final stage of car LC, and it includes all activities of recovery and disposal at the end of vehicle lifetime. It involves the following PUs and processes:
   - PU Recovery. Transportation of the vehicle to dismantling facilities, disassembly, shredding, materials recovery, energy recovery;
   - PU Disposal. Landfilling of waste materials and shredder residue.

Figure 6 illustrates the subdivision of the main LC stages of a car into PUs and single processes (considering both propulsion technologies – ICEVs and BEVs).

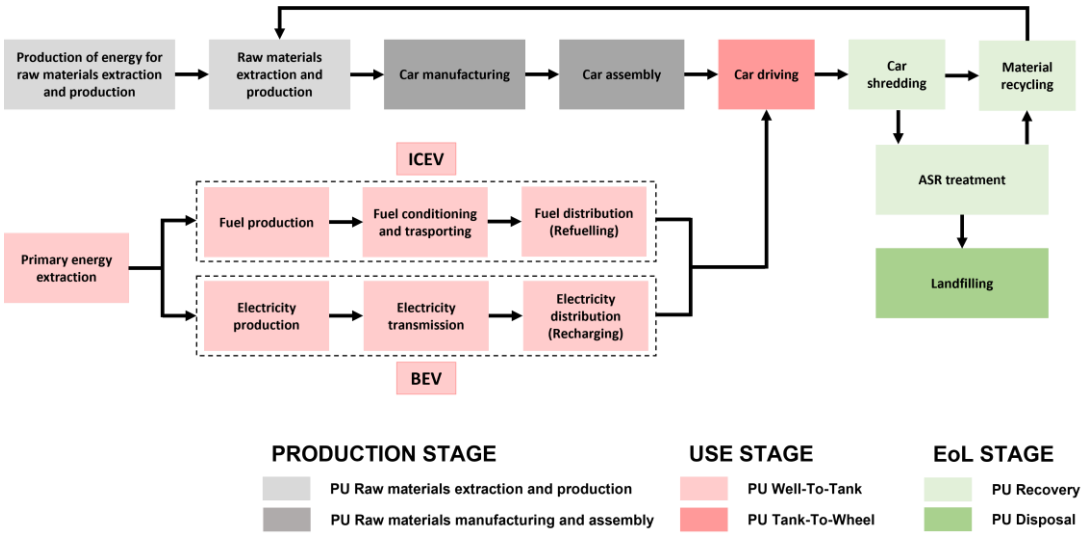

Figure 6. PUs and processes composing the main LC stages for a vehicle.

In literature three main typologies of automotive LCA study exist: LCA of an entire vehicle, LCA of a specific vehicle component and comparative LCA between two or more vehicle/component alternatives.

1.2.2 Life Cycle Costing (LCC) in automotive industry

Life Cycle Costing (LCC) can be defined as an economic accounting methodology that allows the quantification and evaluation of economic effects associated with a product, manufacturing process, or specific service. Unlike the LCA, there are currently no standards available for the LCC of products, processes, or services in a sustainability context (except

for the building sector, for which the ISO 15686-5:2008 Buildings and constructed assets -- Service-life planning -- Part 5: Lifecycle costing has been developed). In this context, the Code of Practice represents the primary reference for applying the methodology on Environmental Life Cycle Costing (Swarr et al., 2011), together with the publication of Hunkeler and colleagues (2008) (the starting point for the Code of Practice).

1.2.2.1 LCC methodology. This methodology calculates the total cost of a product (which can be goods, services, or technologies) induced throughout its life cycle. It is often used for supporting the decision process about the design, development, and purchase of products, processes, or activities. As already described in LCA, five primary life cycle stages significant for the LCC can be identified, including "Research, development, and design" as the starting point (Huppes et al., 2004):

- Research, development, and design.
- Primary production, beginning with the removal of raw materials and energy sources from the earth. Then, materials transportation from the point of acquisition to the point of manufacturing processing;
- Manufacturing, defined from three steps: materials manufacture (that converts raw materials into a semi-finished product), product fabrication (that takes the manufactured material and processes it into a product ready to be filled or packaged), and filling/packaging/distribution of the manufactured product;
- Use and maintenance, defined as all the activities associated with the product's useful lifetime. Actual use, reuse, and maintenance are considered, as well as all energy demands and economic wastes from both product storage and consumption;
- End-of-Life (EoL), that it includes the energy requirements and economic costs associated with recovery, recycling, and disposal of the product.

Many LCC approaches and variants exist; according to (Huppes et al., 2004) three main types of LCC can be distinguished based on their historical background:

- Cost Benefit Analysis LCC (CBA-LCC);
- Budget LCC and LCC as a Managerial Cost Accounting;
- LCC in a LCA context (LCA-LCC).

The LCA-type LCC originates from LCA context and attempts to include economic analysis to the environmental one. Common features are the use of functional unit (FU), the product system description, based on units/processes and flows (i.e., energy, materials, and waste). However, some open issues exist to make LCC a fully applicable methodology. The modelling cost and the analysis perspective are some examples. Indeed, since the LCA approach is based on a steady-state model, some authors claimed that even the LCC approach would be based on steady-state costs. Moreover, since the costs met along the product LC are generally sustained by different actors (such as materials suppliers and components producers), the difference between purchases and sales, the value added, is a tricky aspect to be considered. The perspective definition of the analysis seems to be a particular aspect of the LCC; its definition in the goal and scope phase could guide the following analysis assumptions and a coherent result interpretation. In the SETAC Code of practice, three different types of LCA-type LCC are proposed: Conventional LCC (cLCC), Environmental LCC (eLCC), and Societal LCC (sLCC). The differences are provided in **Figure 7**. The

differences between the several LCC typologies depend on four basic dimensions (according to Hunkeler et al., 2008):

1. Cost categories (budget cost, personnel cost, etc.);
2. Cost bearers (producer, user, society, etc.);
3. Cost models (steady-state, quasi-dynamic, etc.);
4. Cost aggregation (average yearly cost, Net Present Value (NPV), etc.).

The first dimension of LCC is self-explanatory: it defines the cost subdivided into several categories (like budget, personnel, supplies, etc.).

Whereas in the second dimension, LCC has to look at the cost bearer who determines the costs to be included in the economic analysis. According to Huppes et al., 2004, eight types of bearers are identified: producer, supply chain, owner, user, group, life cycle, country's society, and global society.

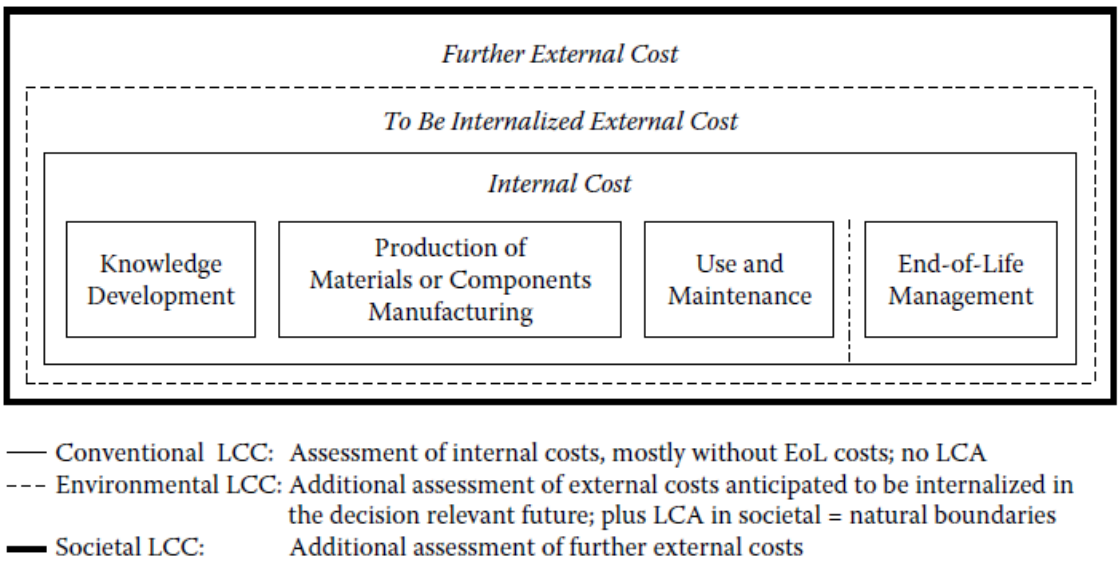

Figure 7. The three types of LCC: conventional LCC, environmental LCC and societal LCC.

Instead, the Code of practice proposes only three main perspectives: producer, consumer, and society – according the three LCC types defined above - conventional, environmental, and societal. It is generally considered that in the conventional LCC the perspective of one actor is assumed, either the manufacturer or the user; whereas one or more actors connected to the product LC can be included in the environmental LCC (mainly manufacturers and user).

Finally, In the societal LCC the perspective of the whole society is adopted and considered (Hunkeler et al., 2008).

The third dimension of LCC is the cost-model, i.e., how the time value of money is considered. Several types of models can be found (steady-state, quasi-dynamic, dynamic, etc.) (Huppes et al., 2004). The steady state model is the simplest one, assuming all processes to be constant in time. A dynamic model considers the development of all variables over time; instead, a quasi-dynamic model assumes that most of the variables remain constant in time, though they allow one or more of them to vary. Conventional and societal LCC generally apply quasi-dynamic models, while environmental LCC is generally

recommended to be set up as a steady-state method in order to allow a combined use of LCC and LCA results, stemmed from steady-state environmental methods (Hunkeler et al., 2008).

The last dimension of LCC is aggregation of costs/revenues. A total value, like Net Present Value (NPV), or a yearly flow, like an average cost per year are some examples (Hunkeler et al., 2008). The aggregation of LCC results is generally not handy but it can be recommended or not depending on the intended final use (Martinez-Sanchez, 2015).

Among the three proposed approaches – conventional LCC, environmental LCC and societal LCC - the most appropriate one was identified as the environmental LCC when the cost assessment is developed and integrated to the environmental LCA or even within a sustainability assessment (Schau et al., 2011). The environmental LCC is defined as *"An assessment of all costs associated with the life cycle of a product that are directly covered by any one or more of the actors in the product life cycle (e.g., supplier, manufacturer, user or consumer, or EOL actor) with complementary inclusion of externalities that are anticipated to be internalized in the decision-relevant future (…). Environmental LCC (eLCC) has to be accompanied by a life cycle assessment and is a consistent pillar of sustainability."* (see Hunkeler et al., 2008).

As an LCA-type LCC, the main phases of the eLCC study are the ones proposed the Code of Practice:

1. Goal and Scope Definition (G&S);
2. Economic Life Cycle Inventory (Economic LCI);
3. Economic Life Cycle Interpretation (LCIn).
4. Reporting and Critical Review.

1.2.2.2 <u>LCC of vehicles</u>. The LCC methodology has mainly been employed in the transportation sector and particularly in the automotive field for the following purposes:

- Estimating the cost profile of overall vehicles (Hunkeler et al., 2008; Wong et al., 2010; Kim et al., 2011; Cicconi et al., 2014), where LCC is applied to compare and identify the economic benefit expected from different power train systems or a different material;
- Evaluating the cost profile of automotive components (Roes et al., 2007; Khoonsari, 2009; Witik et al., 2011; Schau et al., 2011), where LCC is used on a single module to compare different design solutions in terms of economic expenditures during the production stage (as well as in terms of benefit during the use stage).

Then, in the automotive context, many actors are involved in product LC (i.e. materials suppliers, components producer, vehicle producer, user) and the decision of implementing a lightweight solution or not does make sense only if the production cost is compared with the benefits that this solution will produce in the use stage (in favour of the consumer).

As said in paragraph 1.2.2.1, the LCC analysis evaluates the costs involved by all stages that compose LC of the investigated system. Similarly to other products, the main LC stages of a car are production, use, and EoL. The main LC stages of a car can be divided into Process Units (PUs) which in turn include the single processes (as already described in the sub-paragraph *1.2.1.2 – LCA of vehicles* and shown in **Figure 6**).

1. Production, first stage of car LC, and it includes all manufacturing and assembly processes costs. It involves the following PUs and processes:
    - PU Raw materials extraction and production, with production of electricity, heat, steam and fuel for raw materials extraction and production of car components and spare parts;
    - PU Car manufacturing and assembling, with production of electricity, heat, steam and fuel for manufacturing and assembly activities.
2. Use, it comprises both energy cycle and vehicle operation costs. It includes the following PUs and processes (defined according to different propulsion technology):
    - PU Well-To-Tank (WTT). Considering Internal Combustion Vehicles (ICEV): Fuel transformation processes upstream to fuel consumption: fuel production from recovery or production of the feedstock, its transportation, conversion of the feedstock to the final fuel and subsequent storage, distribution, and delivery to the vehicle fuel tank. Considering Battery Electric Vehicles (BEV): Electricity transformation processes upstream to energy consumption: electricity production from specific grid-mix, distribution, and delivery to the vehicle battery.
    - PU Tank-To-Wheel (TTW). Fuel/Energy consumption for car driving: energy required to drive the vehicle, exhaust, and evaporative emissions from the vehicle over its life-time.
3. End-of-Life, the final stage of car LC, and it includes all costs related to recovery and disposal at the end of vehicle lifetime. It involves the following PUs and processes:
    - PU Recovery, with transportation of the vehicle to dismantling facilities, disassembly, shredding, materials recovery, energy recovery;
    - PU Disposal, where landfilling of waste materials and shredder residue are taken and occurred.

In the automotive sector LCC applications present a great variety in terms of level of development, types, dimensions and objective. Overall, LCC is considered a decision-making tool; indeed some authors carried out LCC studies to support consumers investment decisions (Cicconi et al., 2014) or to evaluate the life cycle cost to reduce Green House Gasses emissions relative to lightweight solutions (Kim et al., 2011). In other cases it is used to assess the economic part of a wider sustainability assessment of product (according to Schau et al., 2011).

1.2.3 Social Life Cycle Assessment (S-LCA) in automotive industry

Social Life Cycle Assessment (S-LCA) is the youngest analysis technique compared with other life cycle-based methodologies. It is a methodology aimed at assessing the potential social and socio-economic impacts of products/services throughout their life cycle (UNEP/SETAC 2009). Due to its recent launch, there is much room for progress in the theoretical foundations of social impact assessment, functional unit, system boundaries convergence, and indicators selection, among others (Mathe, 2014). Despite an increasing number of scientific articles dealing with S-LCA applications during the last few years, S-

LCA still presents many open issues (far from being resolved) that need further progress to operationalize the methodology fully.

1.2.3.1 *S-LCA methodology*. S-LCA developments and applications have been growing during last years, both as a stand-alone methodology and within a more comprehensive life cycle-based sustainability assessment (i.e., Life Cycle Sustainability Assessment – LCSA).

From the methodology point of view, despite the initiatives at the international and national levels, S-LCA still presents many open issues that need further progress for fully utilizing the methodology. Most of the scientific articles published so far have addressed the applicability of S-LCA by focusing on selecting suitable and relevant indicators and data collection, relying upon the existing guidelines (Feschet et al., 2012; Macombe, 2014; Neugebauer et al., 2014; Bocoum et al., 2015). However, the key aspects that make the analysis challenging (such as functional unit, system boundary definition, and the scope of the assessment (company vs. product)) are not questioned. Moreover, the lack of comprehensive and robust databases and the different social indicators (i.e., quantitative and qualitative) make the inventory phase a critical step. **Table 1** sums up the elements significantly affecting G&S, and inventory phases of the S-LCA, described as follows:

Table 1. Elements affecting the goal and scope and inventory phases of S-LCA applications.

Elements affecting S-LCA applications
Perspective
S-LCA as stand-alone methodology or within LCSA
Selection and prioritization of indicators
Functional unit
System boundaries
Background, foreground unit processes

- Perspective. It is the angle from which the analysis is carried out; it also includes the concept of "level of concern", i.e. who should care about the consequences of a decision/action (Macombe et al., 2013). Three levels of concern are identified – company, regional, state – and they represent three different levels of decision-making whose different and potentially competing concerns may be regarded as aspects of assessing the sustainable development of a project (Elghali et al., 2007). Then, the UNEP/SETAC guidelines provide, as guidance, a list of questions that need to be answered in the G&S phase of the study: Why is an S-LCA being conducted? What is the intended use? Who will use the results? What do we want to assess?
- S-LCA as stand-alone methodology or within LCSA. The S-LCA can be conducted as a stand-alone methodology (according to the UNEP/SETAC guidelines (UNEP/SETAC 2009)) or within LCSA. The two possibilities differ in the following three main aspects: definition of functional unit and system boundaries, due to the need of ensuring consistency among the life cycle-based methodologies applied in the framework, and number of indicators (Schau et al., 2012; Traverso et al., 2012; Martínez-Blanco et al., 2014).
- Selection and prioritization of indicators. As far as indicators are concerned, this is a challenging issue for two reasons: 1) there is not a clear distinction between impact

indicators and inventory indicators (Neugebauer et al., 2014); 2) a robust approach for indicators selection is seldom discussed and reported in a transparent way.

- Functional unit. One of the most discussed aspect in the papers is the use of functional unit (i.e., the product system's primary function(s), indicating how much of this function is to be considered in the intended S-LCA study). In particular, two main challenges are claimed: the first is how to link social indicators to the functional unit (Zamagni et al., 2011; Norris, 2013; Wu et al., 2014; Martínez-Blanco et al., 2015); whereas the second concerns the transferability of social inventory information at organisational level (company behaviour information) to the product system (Zamagni et al., 2011).
- System boundaries. According to the UNEP/SETAC guidelines, system boundaries should not be crossed by 'product flows' (economic flow) but only by elementary flows, similarly to LCA. However, two different approaches to system boundaries definition can be defined (Foolmaun & Ramjeeawon, 2012): on the one hand, the inclusion of only those parts of the LC which are directly influenced by the company performing the social assessment; and on the other hand, the inclusion of the entire LC, excluding the processes which can be considered non influential for the study.
- Background, foreground unit processes. In the S-LCA context, the discerning factors between foreground and background processes, and related data requirements, are the relevance of the process(es) and the level of interest and influence (according to Martínez-Blanco et al., 2014).
- Data sources, quality and geographic level. Data source and quality is an important theme in S-LCA since a great number of information (both quantitative and qualitative) is needed, and their availability and robustness is critical to the study results. The UNEP/SETAC propose examples of sources (i.e. report of international agencies, NGOs, web sites) where some information can be collected, nevertheless they do not expect to be exhaustive and often direct data collection is needed to get more representative and suitable data. Moreover, the use of generic data seems to be a trickier aspect in S-LCA than in LCA, because performances are more locally variable and dependent on companies' behaviours instead than on the technology system itself.

The main elements affecting the goal and scope and inventory phases of S-LCA applications, listed in **Table 1** and described previously, have been organized into a conceptual map (see **Figure 8**) for guiding practitioners in setting goal and scope and inventory phase of S-LCA studies (according to Zanchi, 2016).

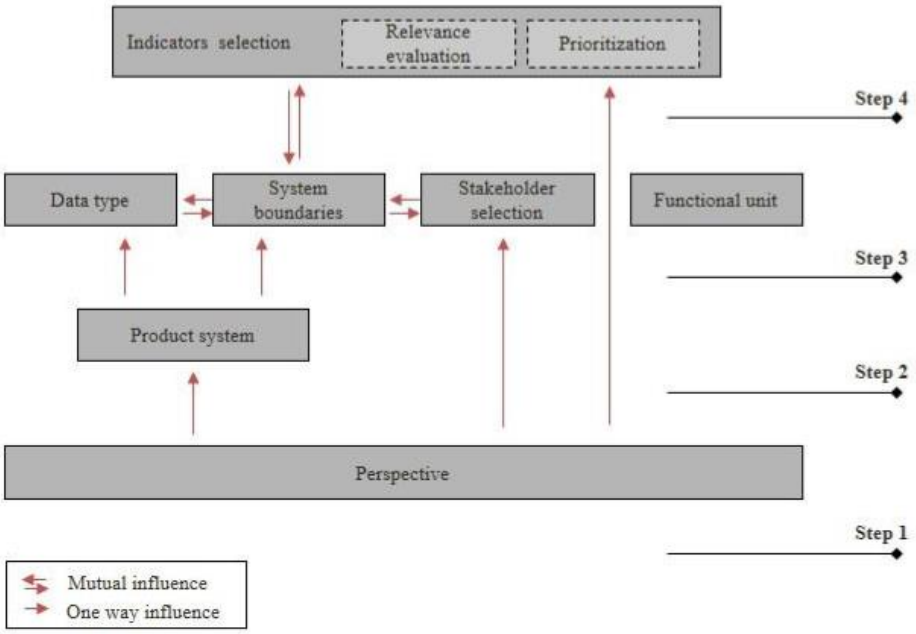

Figure 8. S-LCA Conceptual map (source: Zanchi, 2016).

This conceptual map was elaborated in which all the elements pointed out by the review were grouped into seven nodes. Each node represents a crucial point where a decision needs to be taken in order to carry out the analysis. The nodes are then placed into four steps representing a suggestion for an orderly procedure of analysis (but they can be faced also simultaneously); the single and double rows represent the influence among the nodes (one way, or mutual). The aim of the conceptual map is not to solve open methodological issues but to push practitioners in critically facing all of them and therefore contribute to the enhancement of the research in the S-LCA field (Zanchi, 2016).

1.2.3.2 *S-LCA of vehicles*. The conceptual map described before is then analysed with respect to the automotive sector, with the ultimate goal of contributing to the development of the S-LCA methodology tailored to the peculiarities and needs of the sector itself. For the novelty of this methodology applied to automotive context, it can be stated that (according to Zanchi, 2016):

- The analysis of the sector and its contribution to further tailoring the conceptual map to it highlighted that, when both complex products and value chains are involved (such as in the automotive sector or in the electronic and electrical equipment), both the information on social performances at product and company level are relevant.
- The company level provides a measure of the degree to which a company is able to manage the social aspects of concern along the value chain, independently from the product/service delivered, and according to its level of influence.
- Regarding the social information at product level, this is considered relevant too for two purposes: to build the profile of products also in relation to the social aspects, besides the technical, quality-related and environmental ones; to be able to better conceive and design products and services taking into account the social variable.

1.3 Eco-design methodology in automotive industry

From the above description of all the elements that characterize the LCSA, it follows that novel design solutions within the automotive field need to be developed through dedicated eco-design methodologies, which consider mechanical performance and sustainability pillars at the same level of importance, both evaluated under the entire LC perspective.

To meet this challenging issue, Life Cycle Sustainability Assessment (LCSA) has been developed as a suitable approach for assessing the product sustainability in the early design phase (UNEP/SETAC, 2011; Zamagni et al., 2013) based on considerations related to the entire LC (Costa et al., 2019; Visentin et al., 2020). Such a methodology compares quantitatively different product concepts, provides insights about rooms for improvement (e.g., alternative materials or processes), and transparently describes the potential trade-off.

The implementation of LCSA often brings the adoption of Multi-Criteria Decision Analysis (MCDA) methods which support both product developers and designers to solve decision- making problems when a series of alternatives are evaluated based on multiple criteria and alternatives (Aruldoss et al., 2013; Onat et al., 2020; Wang et al., 2009). Different types of MCDA methods exist, including Weighted Sum Method, Analytical Hierarchy Process, TOPSIS, VIKOR, ELECTRE, PROMETHEE, among others (Wang et al., 2009). A clear overview of them, in terms of advantages/disadvantages and sector, can be found in literature (Wang et al., 2009; Aruldoss et al., 2013).

In the automotive sector, MCDA methods have been applied in many domains, particularly in the material selection process (Jeya Girubha & Vinodh, 2012), impact of reverse logistics practices (Haji Vahabzadeh et al., 2015), technologies for fuel cells as the power systems for vehicles (Sadeghzadeh & Salehi, 2011), as well as to select the best fuel-based vehicles (Safaei Mohamadabadi et al., 2009).

MCDA methods have been extensively combined with the LCA, and recently they have become popular in the decision-making regarding sustainability of processes/products due to the multi-dimensionality of sustainability problems (Wang et al., 2009; Bachmann, 2012; Atilgan & Azapagic, 2016). Yet, the use of MCDA to integrate the three aspects of sustainability – environment, economy and society – within the LCSA framework is analysed by some authors in different sectors (Halog & Manik, 2011; Bachmann, 2012; Onat et al., 2016b; Onat et al. 2016a; Atilgan & Azapagic, 2016).

Besides the capability of combining different sustainability criteria and ranking alternatives, the integration of life cycle thinking methodologies (LCA, LCC, and S-LCA) and MCDA is thought a promising research area since could also enhance stakeholder involvement in LCSAs, as encouraged in the UNEP/SETAC guidelines. Therefore further work and practice would be needed in this sense.

A general State of Art (SoA) review is conducted considering the following topic: “Ecodesign methods/tools (EDM/T) in the automotive sector”. Literature offers a large series of papers dealing with eco-design within the automotive field, which vary significantly in terms of objective, type, complexity, and availability of inventory data (Rousseaux et al., 2017; Rossi et al., 2016). The majority of these researches apply analysis of sustainability as a supporting tool functional to validate lightweight design. Both the aspects of sustainability (economic (EC), environmental (EN), and social (SO)) and the design dimension (D) are considered in SoA review. The MCDA methods that can link together all of these dimensions

are considered (as well as the lightweight context (LW)). Therefore, a dataset of 120 papers is considered for the SoA review (reported in the following **Table 2**).

Starting from the design dimension (D) applied to lightweight context (LW), several studies (approximately 13%) present a framework for the design of automotive components from a weight reduction perspective. The problem of automotive component design is tackled through several optimization techniques. However, the most widely used is Topology optimization (TO), which is carried out to reduce the structure's weight without compromising the intended performance. For this reason, TO has its application in the automotive sector for lightweight components and fuel efficiency.

In this context, the reviewed papers perform topological optimization of various lightweight solutions: redesign and optimization of vehicle transmission (small formula racecar wheel upright (Chiandussi et al., 2004), rear suspension subframe (Jankovics and Barari, 2019 front lower control arm (Rahman et al., 2018; Yoo et al., 2017), steering knuckle (Srivastava et al., 2019)), redesign and optimization of engine parts (engine piston (Barbieri et al., 2017)), optimization of vehicle Body-in-White (automotive chassis (Cavazzuti et al., 2011), automotive dashboard (Mantovani et al., 2017), Tailor-Welded Blank Door (Li et al., 2015)). Instead, Lee and Kang, 2007, and Kamalakkannan et al., 2021 stand out for relevance, as they use different optimization techniques to innovative and light-weighted automotive components respect to a baseline design. However, no relevant reference is made to sustainability aspects of the considered studies, and the concept alternatives are obtained according to the classical design approach.

Table 2. SoA Review in the automotive sector (D = Design, EN = Environment, EC = Economy, SO = Society, LCSA = Life Cycle Sustainability Assessment, MCDA = Multi-Criteria Decision Analysis, LW = Lightweight).

Automotive SoA Review								
ID	**Reference**	**D**	**EN**	**EC**	**SO**	**LCSA**	**MCDA**	**LW**
1	Wang et al., 2009						X	
2	Rossi et al., 2016	X	X					
3	Delogu et al., 2015		X					X
4	Cecchel et al., 2018		X					X
5	Sun et al., 2017		X					X
6	Sun et al., 2019		X					X
7	Deng et al., 2019	X	X					
8	Fassi et al., 2021	X	X					X
9	Ghadimi et al., 2012		X	X	X	X	X	
10	Delogu et al., 2018		X					X
11	Russo & Matina, 2012	X	X					X
12	Russo & Rizzi, 2014	X	X					X
13	Reimer et al., 2020	X	X					

Automotive SoA Review [CONTINUE]								
ID	**Reference**	**D**	**EN**	**EC**	**SO**	**LCSA**	**MCDA**	**LW**
14	Salvado et al., 2015		X	X	X	X	X	
15	Saad et al., 2019		X	X	X	X	X	
16	Hapuwatte et al., 2016		X	X	X	X	X	
17	Zanchi, 2016		X	X	X	X	X	X
18	Atilgan & Azapagic, 2016		X	X	X	X	X	
19	Onat et al., 2016a		X	X	X	X	X	
20	Onat et al., 2016b		X	X	X	X	X	
21	Alves et al., 2010		X		X			
22	Andriankaja et al., 2009		X					X
23	Andriankaja et al., 2015		X					X
24	Das, 2011		X					X
25	Dhingra & Das, 2014		X					X
26	Duflou et al.,2009		X					X
27	Kelly et al., 2015		X					X
28	Koffler, 2013		X					X
29	Luz et al., 2010		X					X
30	Mayyas et al., 2012b		X					X
31	Park et al., 2013		X					X
32	Rajendran et al., 2012		X					X
33	Raugei et al., 2015		X					X
34	Schuh et al., 2013		X					X
35	Subic et al., 2010		X					X
36	Tharumarajah & Koltun, 2007		X					X
37	Tharumarajah & Koltun, 2010		X					X
38	Vinodh & Jayakrishna, 2011		X					X
39	Witik et al., 2011		X	X				X
40	De Medina, 2006		X					X
41	Geyer, 2007		X					X
42	Geyer, 2008		X					X
43	Joshi et al., 2004		X					X
44	Zah et al., 2006		X		X			X
45	Ribeiro et al., 2007		X					

Automotive SoA Review [CONTINUE I]								
ID	**Reference**	**D**	**EN**	**EC**	**SO**	**LCSA**	**MCDA**	**LW**
46	Weiss et al., 2000		X					
47	Baroth et al., 2012		X					X
48	Dubreuil et al., 2012		X					X
49	Edwards et al., 2014		X					X
50	Hamakada et al., 2007		X					X
51	Koffler & Zahller 2012		X					X
52	Li, 2004		X					X
53	Reppe et al., 1998		X					X
54	Saur et al., 1995		X					X
55	Schmidt et al., 2004		X					X
56	Cicconi et al., 2014			X				
57	Hunkeler et al., 2008			X				
58	Khoonsari, 2009			X				X
59	Kim et al., 2011		X	X				X
60	Ogden et al., 2004		X	X	X			
61	Roes et al., 2007		X	X				X
62	Schau et al., 2011		X	X				X
63	Ungureanu et al., 2007		X	X				X
64	Wong et al., 2010			X				
65	Mayyas et al., 2016	X	X	X	X			
66	Jasinski et al., 2015		X	X	X			
67	Schöggl et al., 2016		X	X	X			
68	Stoycheva et al., 2018		X	X	X	X	X	
69	Kaspar et al., 2018	X	X	X			X	
70	Choudry et al., 2018	X	X	X				
71	Choudry, Kaspar et al., 2018	X	X	X				
72	Choudry, Muller et al., 2018	X	X	X			X	
73	Choudry, Sandmann and Landgrebe, 2018	X	X	X				
74	Del Duce et al., 2013		X					X
75	Der et al.,2019	X	X					X
76	Kaluza et al., 2017	X	X					X
77	Lewis & Kelly, 2012		X					X

Automotive SoA Review [CONTINUE II]								
ID	**Reference**	**D**	**EN**	**EC**	**SO**	**LCSA**	**MCDA**	**LW**
78	Del Pero et al., 2017		X					X
79	Chien et al., 2012		X	X			X	
80	Danilecki et al., 2016		X					
81	Delogu et al., 2016		X					X
82	Delogu et al., 2017		X					X
83	Egede, 2017		X					
84	Hawkins et al., 2012		X					
85	Hawkins et al., 2013		X					
86	Soo & Subic, 2014		X					X
87	Castro & Parreiras, 2018						X	
88	Kaspar and Vielhaber, 2016	X						X
89	Kaspar et al., 2019		X	X				X
90	Sakundarini et al., 2013	X	X				X	X
91	Choudry, Kaspar and Greinacher, 2019		X	X				
92	Cui et al., 2008	X						X
93	Cui et al., 2011	X						X
94	Chu et al., 2019	X	X	X			X	X
95	Baumann et al., 2013				X			
96	Blom & Solmar, 2009				X			
97	Braithwaite, 2001		X	X	X			
98	Chang et al., 2015		X		X			
99	Ekener-Petersen et al., 2014				X			
100	Karlewski, 2016				X			
101	Macombe et al., 2013				X			
102	Manik et al., 2013				X		X	
103	Reuter et al., 2014				X			
104	Schau et al., 2012		X	X	X			X
105	Singh, 2014				X			
106	Vermeulen et al., 2012		X	X	X			
107	Gemechu et al., 2017		X			X		
108	Merulla et al., 2019	X						X
109	Jankovics & Barari, 2019	X						X

Automotive SoA Review [CONTINUE III]								
ID	**Reference**	**D**	**EN**	**EC**	**SO**	**LCSA**	**MCDA**	**LW**
110	Chiandussi et al., 2004	X						X
111	Cavazzuti et al., 2011	X						X
112	Rahman et al., 2018	X						X
113	Mantovani et al., 2017	X						X
114	Srivastava et al., 2019	X						X
115	Yoo et al., 2017	X						X
116	Barbieri et al., 2017	X						X
117	Li et al., 2015	X						X
118	Lee et al., 2019	X						X
119	Lee & Kang, 2007	X						X
120	Kamalakkannan et al., 2021	X						X

If we consider the environmental pillar, from the SoA review it is evident that most papers deal with LCA analysis in lightweighting perspective (i.e., EN and LW in **Table 2**) (approximately 35%), highlighting that environmental sustainability (related to CO_2 reduction through mass savings of vehicles) is a topic discussed in the scientific community and by companies in the automotive industry in the last decades. In this context, Delogu et al., 2015, Cecchel et al., 2018 and Sun et al., 2017, 2019 stand out for relevance, as they compare innovative and light-weighted automotive alternatives with a baseline design performing LCA of solutions. These studies perform very detailed assessments of the considered car assets, assuming different impact categories to express the final results and including all LC stages (mainly production, use and EoL). That said, no reference is made to performance/design requirements of the considered components and the concept alternatives are assessed on the assumption they are rigorously equivalent from a functional perspective. From this perspective, Deng et al., 2019 and Fassi et al., 2021 exceed the researches above, as they carry out sustainability assessment on a design equivalence basis. Deng et al., 2019 performs the LCA of flax fiber reinforced polymers (FRPs) and glass FRPs (GFRPs) in automotive structural applications. The generalized Rule-Of-Mixture (ROM) model and the Ashby material selection method are combined to define a criterion for equivalent design. Fassi et al., 2021 presents an interesting example of a design process driven by sustainability targets. The work assesses the design of plastic automotive parts by considering a series of alternative materials and manufacturing technologies: the minimization of environmental impacts is achieved through the application of optimization methods, both at design and manufacturing level.

Regarding the economic perspective (i.e., EC in **Table 2**), five papers uniquely discuss the economic aspect (only 4% of the total). Among them, Khoonsari, 2009 and Schau et al., 2011 deal with components generally using the LC cost model focused on manufacturing and develop their studies according to two different perspectives: manufacturer and user. In some cases, when the user perspective is assumed the component acquisition cost is used as representative for the whole production stage, while in other studies the direct production

expenditure is summed up to the use stage and EoL (Witik et al., 2011). Also considering the lightweight perspective, LCC is used to compare traditional materials for a given component (i.e. steel) with innovative and lightweight ones (i.e. Aluminium, composites) with the aim of evaluating the component manufacturing costs and the expected use stage cost reduction due to mass saving (Ungureanu et al., 2007; Khoonsari, 2009, Witik et al., 2011). However, no reference is made to the performance/design requirements in the considered papers. The concept alternatives analyzed are economically assessed on the assumption that they are rigorously equivalent from a functional perspective.

Several product-oriented S-LCA studies targeted to the automotive sector was found and reviewed (i.e., SO in **Table 2**). Approximately 23% of the analyzed papers study the social aspect: they cover applications related to vehicle components/parts (Braithwaite, 2001; Schau et al., 2012; Baumann et al., 2013; Karlewski, 2016), alternative fuels (Blom & Solmar, 2009; Manik et al., 2013; Macombe et al., 2013; Ekener-Petersen et al., 2014), materials for automotive parts (Zah et al., 2006; Alves et al., 2010; Reuter et al., 2014; Singh, 2014), automotive shredder residue treatment (Vermeulen et al., 2012), and manufacturing technology (Chang et al., 2015). However, the analysis of the sector-specific publications in the field of social sustainability currently do not allow to fully tailor the conceptual map to the automotive sector (as discussed in the previous paragraphs), due to the limited sample, but it provides directions about some of the nodes of the conceptual map, in particular regarding system boundaries, indicators and stakeholders.

The integration of environmental and economic pillars with the traditional requirements in product design is gaining vital importance for many companies; for this reason, several authors attempt to provide a clear and transparent structure to calculate the LCA and LCC of a given product/system. Although several articles deal with LCA and LCC (approximately 12% of the total - i.e., EN and EC in Table 2), very few examples of combined LCC and LCA exist in the literature for the automotive sector. Typically, economic assessments are carried out separately from LCA; thus, equivalence in the system boundaries definition, functional unit, and other assumptions are not discussed. The integration of economic and environmental aspects encountered along the life cycle of an automotive product is discussed only in a few cases (Roes et al., 2007; Witik et al., 2011; Schau et al., 2011; Choudry, Kaspar, et al., 2018; Choudry, Muller, et al., 2018; Choudry, Sandmann and Landgrebe, 2018). LCA and LCC are based on the same goal and scope settings in these cases, but the final results are presented separately (without an integration of the results using MCDA methods). Among these automotive case studies, an attempt to connect LCA and LCC findings is offered by Witik et al., 2011, which calculates the breakeven point values corresponding to CO_2 and total life cycle cost. This analysis enables us to compare alternative solutions and select the best option regarding cost and environment trade-offs. In the same way, Schau et al., 2011 investigate the application of LCC as part of a broader sustainability assessment where SLCA and LCA are combined. LCA-type LCC is applied to a case study of remanufactured alternators, showing that the remanufacturing of vehicle parts is an important, fast-growing business with a large potential for cost and resource savings. Finally, (Jasinski et al., 2015) analysis is based on a different approach where economic, environmental, and social aspects are combined using the unique metric of monetary value.

Many papers presented in SoA refer to applicative eco-design case studies, where the assessment is guided and performed according to principles of LCSA methodology. Another substantial strand in literature on eco-design is represented by the development of dedicated

methods and tools that are ready for application to real case studies, considering all sustainability pillars integrated through MCDA methods. In this context, several articles concerns the above aspects (approximately 8% of SoA in **Table 2**, considering EN, EC, SO and MCDA labels). Ghadimi et al., 2012 and Delogu et al., 2018 are two interesting examples for this: both studies refine holistic assessment methods which integrate sustainability aspects (i.e., environmental, economic, and social pillars). The different sustainability issues are combined on the basis of a single-score indicator through the application of MCDA methods, the main setting parameters being the influencing factors for the product, the weight criteria, and the analytical hierarchy process. The authors validate the effectiveness of the conceived assessment methods through the application to specific case studies, which are proven to offer beneficial effects when considering the overall sustainability profile. Both researches are valid attempts to include sustainability within the concept development phase since they provide valuable support to designers and decision makers by measuring sustainable information and making it more transparent. Salvado et al., 2015, Saad et al., 2019, and Hapuwatte et al., 2016 refine holistic assessment methods by defining a single score index (representative of all sustainability pillars) in different industrial contexts within the automotive sector. The first study proposes a sustainability index to allow individual companies and their respective supply chains to gain information on their level of economic, social, and environmental sustainability; the authors use the Analytic Hierarchy Process (AHP) methodology to obtain the weights of the indicators. A supply chain case study in the automotive group was performed to illustrate the application of the suggested sustainability index. Saad et al., 2019 define a framework for sustainability assessment of manufacturing processes that covers the three sustainability dimensions; the proposed methodology combines objective and subjective weighting methods to reduce the uncertainty associated with subjective weighting. It also captures the interaction among different indicators using MCDA methods instead of traditional statistical methods. In order to make the model more robust, the authors also included a sensitivity analysis. Lastly, Hapuwatte et al., 2016 present a total life sustainability assessment of additively manufactured products through a single score called Product Sustainability Index (ProdSI). The authors validate the ProdSI matrices by conducting a case study with two iterations of additively manufactured products. Atilgan and Azapagic (2016) applied the Weighted Sum Method to integrate twenty life cycle sustainability indicators to evaluate alternative electricity supply options in Turkey. A mixture of environmental LCA indicators (i.e. abiotic resource depletion, global warming potential, and acidification potential), economic indicators (i.e. levelized cost, capital cost) and social indicators concerning employees and workers safety are employed. First equal importance is assumed, followed by additional evaluations concerning results sensitivity to weights variations. On the other hand, Onat et al. (2016a) developed a combined MCDA method to rank alternative vehicle technologies (i.e. internal combustion electric vehicle, hybrid electric vehicle, battery electric vehicle) utilizing TOPSIS and fuzzy set approaches. In this case macro-level indicators are used (e.g. GDP, total GHG emissions, water withdrawal), as representative for the economic, environmental, and social area, and they are evaluated according to decision-makers' judgments. Finally, Zanchi, 2016 presents a methodology where the integration of LCA, LCC, and S-LCA results is done with Multi-Criteria Decision Analysis (MCDA), identified as a suitable approach. In this way, MCDA helps decision-makers to choose the best option when a wide range of criteria has to be considered, and compensation needs to be avoided. After a review of the most used and suited MCDA methods, the author selected TOPSIS. This method develops a ranking of alternatives, assuming that the most preferred alternative should have the shortest distance from the positive ideal solution and the farthest distance from the negative ideal solution. A set of quantified social, economic, and environmental

sustainability indicators have been identified for the S-LCA, LCC, and LCA. An online survey was proposed to prioritize them according to experts from different sectors' judgment. The survey was mainly addressed to people in the automotive sector, both as industry members and as researchers in the sustainable transportation field and people working in the sustainability and Life Cycle Assessment area. Next, results from the survey were analyzed and treated by the intuitionistic fuzzy set method to avoid ambiguity and determine the weights of indicators needed for the TOPSIS method. The author verified the presented methodology on lightweight design for specific car components.

From the analysis of these papers, it is clear that the overall sustainability analysis is carried out downstream of the design process or it is performed only to validate alternative solutions whose conception/development have already been finalized (i.e., they are rigorously equivalent from a functional perspective). For these reasons, Russo & Matina, 2012, Russo & Rizzi, 2014 and Reimer et al., 2020, Kamalakkannan and Kulatunga, 2021 are the only studies that integrate the sustainability aspect within the design process by means of a systematic computer aided design procedure (considering D, and EN labels in **Table 2**). Russo & Rizzi, 2014 and Russo & Matina, 2012 present an approach implemented in a software framework which supports the designers to optimize component-based automotive solutions in a lightweight eco-design perspective. The refined method is based on the integration of Computer-Aided Engineering (CAE), Life Cycle Modeling (LCM) and LCA tools, which operate in direct connection with the Computer-Aided Design (CAD) environment. The framework assists product developers in the conception of different design alternatives obtained as a combination of material, shape, and manufacturing process through the use of structural optimization tools. Reimer et al., 2020 proposes a methodology targeted at supporting the conceptual design of lightweight body parts for Electric Vehicles (EVs), with a combined perspective on structural integrity and GHG emissions. The tool is based on an analytical method which integrates numerical design of different competing solutions and estimation of LC GHG impact, through an in-depth modelling of both part and vehicle-specific influencing factors. The results are combined in engineering diagrams that allow to systematically assess the implications of design choices on mechanical performances, lightweight potential and GHG emissions. The methodology is applied to a case study including a series of combinations of load cases, geometries, materials and use stage scenarios.

The studies above considered represent very interesting attempts to orientate design towards sustainability targets in a systematic way. That said, such methods are functional only to assist the designer in the generation of optimized solutions, but the conception phase and the data processing do not take place automatically, since the refined tools are not able to generate alternative design options on their own.

Finally, Kamalakkannan & Kulatunga, 2021 propose a Parametric Life Cycle Assessment (PLCA) approach to eco-design optimization at the early design stage. This model reflects the characteristics of the environmental and design performance of the entire product LC as an objective function, allowing designers to optimize the design and mitigate environmental impacts without performing scenario analysis. The methodology is applied to two case studies, including combinations of parameters and multiple scenarios, demonstrating the approach's effectiveness for eco-design optimization and decision making. However, this approach is challenging to develop parametric models that show entire LC characteristics in a single function because of the complexity and uncertainty of product design.

1.4 Critical analysis of current eco-design methodologies

The outcomes of the SoA review on automotive eco-design can be summarized in the following key points, emphasizing the limits and weaknesses of existing literature:

- Several papers define methodologies (applied to different automotive case studies) that deal with the sole design perspective, which is used to optimize solutions that are not analyzed from a sustainability point of view;
- the vast majority of papers is represented by applicative case studies that deal with the sole sustainability issue (i.e., environment, economy, society), which is used to validate solutions that have been already finalized from a design point of view;
- a limited number of applicative LCSA case studies takes into account at the same time both design and sustainability pillars, but results are provided separately for the different aspects (such as structural integrity, functionality, and environmental impact), thus not enabling a proper evaluation of the effects that innovative solutions involve on the integrated design/sustainability profile;
- only a few papers deal with the development of eco-design methods targeted at investigating different design options, but both concept generation and modelling process are not carried out through an automated procedure.

1.5 Objective of the work

In light of critical analysis, the present research proposes an innovative eco-design framework (Design and Sustainability Analysis - DeSA) for assisting automotive designers in the early product development phase of single mono-material components. The methodology takes into account at the same time and on the same level of importance both design and sustainability pillars (i.e., environment and economy) starting from:

- physical features and load case of the specific automotive case study
- functional and structural requirements
- available LC inventory data in terms of materials and manufacturing processes to be investigated and analyzed
- vehicle features of the specific automotive case study (internal combustion engine vehicles (ICEV), Battery electric vehicles (BEV))

The framework automatically generates different concept solutions evaluated through design and sustainability indicators. Such indicators are aggregated within a single score index developed through MCDA methods, based on which the final ranking and the choice of the most promising design option(s) are carried out. The conceived eco-design framework is developed and implemented within a computer-modeling tool developed in an integrated HyperWorks/MATLAB simulation environment.

Potentiality and utility of the research are highlighted through the application to four case studies, starting from physical/technical features of the generic component and available inventory data directly provided by the designer as input/setting parameters. Finally, critical discussion and concluding remarks are presented based on several case studies outcomes.

The work aims to create a tool for analyzing and evaluating overall LC components mounted to generic vehicles (gasoline, diesel, and electric). From a practical point of view, the tool is constituted by a series of models that:

- can be adopted by practitioners for application to real case studies
- are flexible and tailorable for any generic case study
- overcome, or at least reduce the limitations and criticisms of current LCSA practices presented in the previous paragraph.

Below, the enhancements for existing literature that the eco-design framework intends to fulfill are reported.

- The methodology automatically generates a series of design options starting from physical features, load cases, and functional/structural requirements, directly provided by the designer.
- The alternatives are subject to a simultaneous and integrated design/sustainability assessment by means of specific indexes. The ranking and the choice of the most promising design option(s) are carried out based on an overall single score obtained through MCDA methods.
- The framework is implemented within an automated simulation tool, specifically developed to be easily adaptable to objectives and constraints of whichever case study, as well as easily usable by professionals in the automotive industry. The added value of the conceived tool is enabling designers to clearly identify potentialities and criticalities of the considered alternatives, thus representing valuable support for decision-making in the eco-design field.

2. Materials & Method

The proposed eco-design approach defines an innovative framework that compare competing design solutions for mono-material components within the automotive field, considering design and sustainability aspects since the concept development stage. With regard to the environmental and economic assessment, the method evaluates the entire LC of the design alternatives, including all stages, from raw materials extraction up to the final disposal of EoL materials, passing through manufacturing, use and recovery/recycling processes. The multi-criteria assessment is based on an integrated single score index (i.e., Product Sustainability Level, PSL), based on a series of input data belonging to four areas:

- design data: main physical and technological features of the automotive component;
- environmental sustainability data: LCI data used to environmentally assess the overall component LC;
- economic sustainability data: LCI data used to economically assess the overall component LC;
- vehicle features: parameters and operating conditions that define the component operational stage.

The overall methodology is implemented within an automated simulation tool developed in MATLAB/Hypermesh environment and it is composed by the following four main sections:

1. Screening: generation of all the alternative design solutions that satisfy design requirements and are feasible from a technological point of view (feasible solutions);
2. Design and Sustainability analysis: description of design, environmental and economic pillars, and definition of related mid-point indicators (obtaining the acceptable solutions);
3. Optimization: optimization of all the acceptable alternative design solutions that still satisfy design requirements and are feasible from a technological point of view (acceptable and optimized solutions);
4. Classification: calculation of PSL index and final ranking of optimized competing design alternatives.

Figure 9 provides a scheme of the overall approach; whereas **Figure 10** describes the four DeSA main phases, that are explained in detail in the following paragraphs.

2.1 Screening

The main objective of the screening phase is identifying all feasible design solutions, defined as all solutions that at the same time satisfy design requirements and are feasible from a technological point of view. The starting point of the screening is the creation and development of the production database, which provides the entirety of possible design solutions, obtained as a combination of material and manufacturing technology. The database includes all materials and processes that are available to the designer, and it is structured in two major sections (**Table 3**):

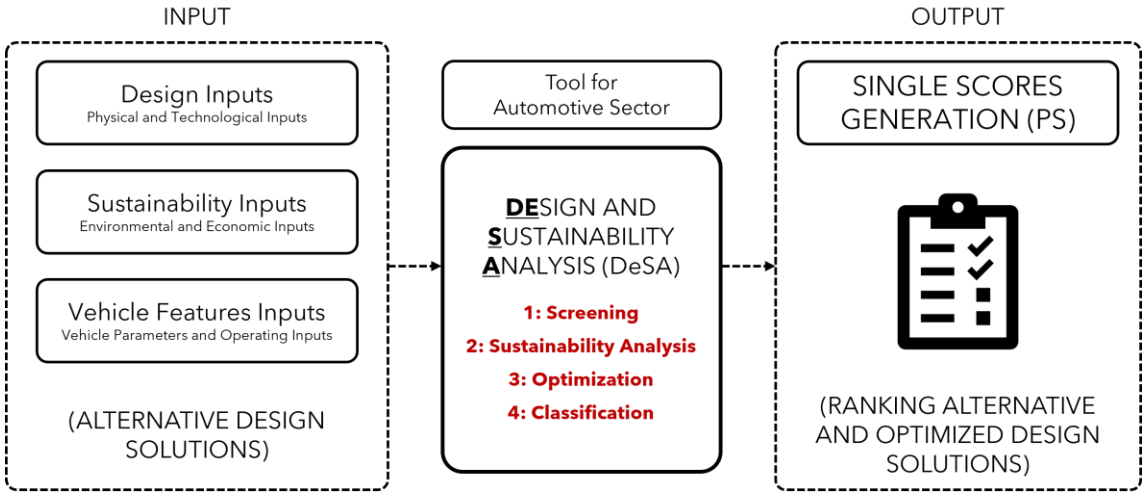

Figure 9. DeSA framework.

- Materials. Materials are organized into classes belonging to macro-families: metals (ferrous and non-ferrous materials), polymers (elastomers, thermoplastics, and thermosets), glasses/ceramics, and hybrids materials (composites, foams, and natural materials);
- Manufacturing technologies. Processes are classified into a hierarchical order and characterized in terms of the following features according to the Ashby theory (Ashby, 2011): applicable materials (subset of materials to which the manufacturing process can be applied), applicable primary shapes (shapes that can be made through the process), and process properties related to the component to be designed.

Table 3. Production database overview.

Production database		
Materials	**Manufacturing technologies**	
Macro-families: 1. Metals (ferrous, non-ferrous materials); 2. Polymers (elastomers, thermoplastics, and thermosets); 3. Glasses/Ceramic; 4. Hybrids (composites, foams, and natural materials).	Applicable materials	Applicable shapes: Prismatic (1D) Sheet (2D) Three-dimensional (3D)
		Process properties: Component mass (m) Section thickness (ST) Batch size (B) Tolerance (To) Surface roughness (SR)

As said, each manufacturing technology is characterized by a set of attributes (applicable materials and shapes, process properties). These information can be conveniently displayed as simple binary matrices. They provide the selection tools we need for the screening phase. In the production database two types of matrices are present:

- Shape-process compatibility matrix (see **Table 4**);

- Material-process compatibility matrix (see **Table 5**).

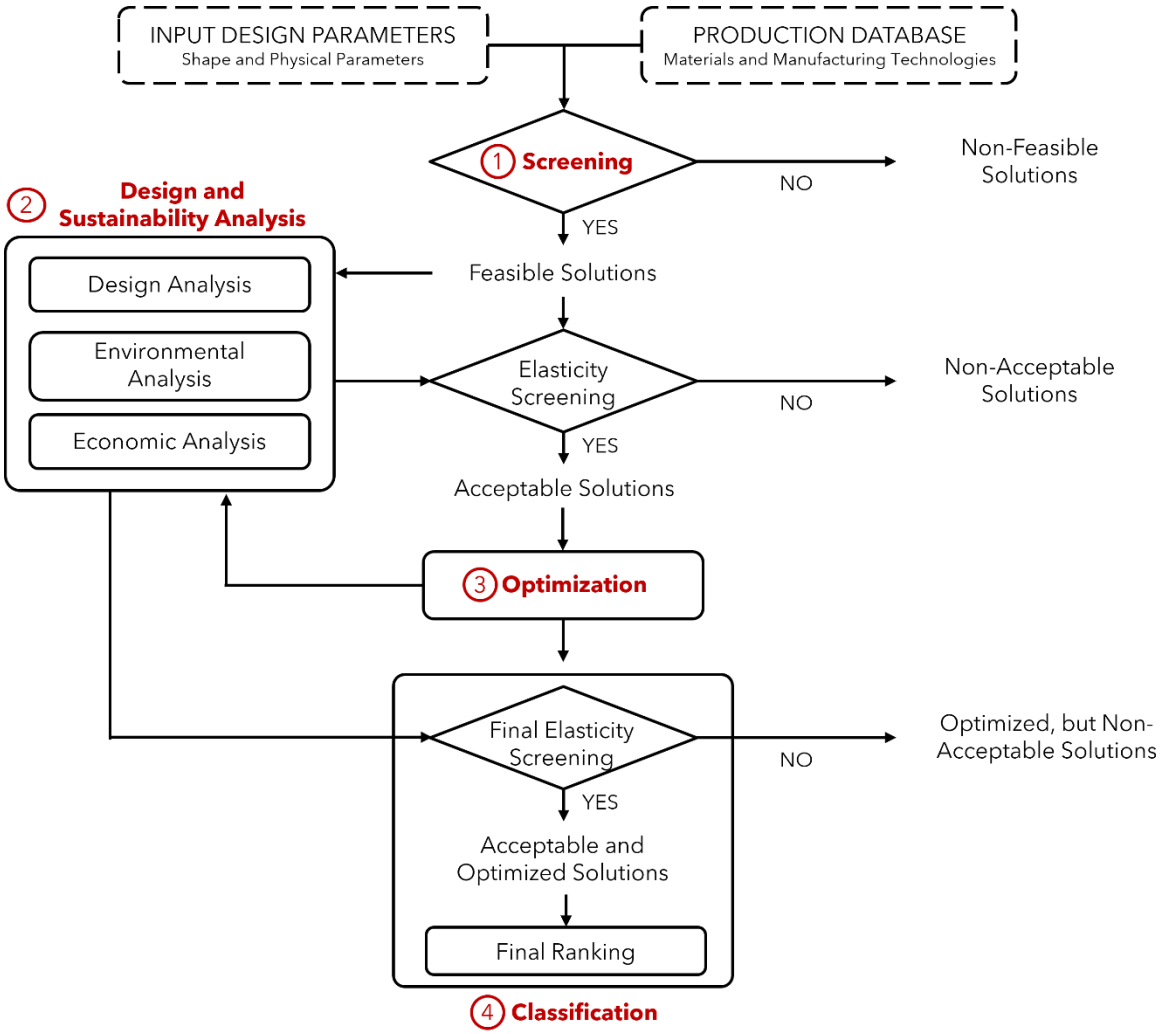

Figure 10. DeSA framework main phases.

Table 4 and **Table 5** show a simplified representation of binary matrices defined in the production database. The shape-process matrix (as well as the material-process matrix) displays the links between primary shapes (or materials) and manufacturing processes, with compatible combinations marked by value "1" that identify the linkage; the value "0" indicates non-compatibility between the process and the primary shape (or material) selected. Its use for screening is straightforward: specify the shape (or material) and read off the processes or the reverse: specify the process and read off the shapes (or material).

The next step of the screening stage is the definition by the designer of the following types of design constraints (**Table 6**):

- primary shape constraint. The designer selects the primary shape of the component based on the specific case study, choosing between the options provided by the production database (Prismatic-1D, Sheet-2D, Three-dimensional-3D);
- process constraints. The designer defines acceptability ranges for process properties (i.e., the requirements on physical and technological features which characterize the specific case study).

Table 4. Shape-process compatibility matrix simplified representation.

Shape-process compatibility matrix			
Process	**Shape**		
	Prismatic (1D)	Sheet (2D)	Three-dimensional (3D)
Process 1	1	0	1
Process 2	0	1	0
…	…	…	…
Process K	1	1	0

Table 5. Material-process compatibility matrix simplified representation.

Material-process compatibility matrix				
Process	**Material**			
	Material 1	Material 2	…	Material M
Process 1	1	0	…	0
Process 2	1	1	…	0
…	…	…	…	…
Process K	0	1	…	1

Table 6. Input data: design constraints.

Design Constraints	
Primary shape	**Process constraints**
Prismatic-1D Sheet-2D Three-dimensional-3D	Component mass (m) - $[m_{min}; m_{max}]_{des}$ Section Thickness (ST) - $[ST_{min}; ST_{max}]_{des}$ Batch size (B) - $[B_{min}; B_{max}]_{des}$ Tolerance (To) - $[To_{min}; To_{max}]_{des}$ Surface roughness (SR) - $[SR_{min}; SR_{max}]_{des}$

As described above for the manufacturing technologies, process constraints are also defined by characteristic physical attributes. Therefore, these constraints can be conveniently displayed as simple bar charts. As well as the binary matrices, they also provide the selection tools needed for the screening phase. In the production database, five types of bar charts are present (as already shown in **Table 6**):

- Component mass (m) range chart: plot where limits to the size/mass of component that a process can make are defined;
- Section thickness (ST) chart: chart of the ranges of section thickness of which each manufacturing process is capable. The minimum section thickness (the lower bound of range - ST_{min}) represents the limits imposed by the physics of the process;

- Economic batch size (B) chart: chart where each process presents an economic batch size that is found by experience to be competitive in cost;
- Process-tolerance (To) chart: it shows the characteristic ranges of process-tolerance of which processes are capable;
- Process-surface roughness (SR) chart: it shows the characteristic ranges of surface roughness of which processes are capable.

These bar charts are compared with the process constraints imposed by the designer: if the designer values fall within the physical ranges, the process considered will be feasible for product design; Instead, if the process constraints partially fall in the physical ranges, the analyzed process will be considered partially acceptable: the solution will be considered acceptable only for the part of the acceptability range (provided by designer) that is feasible from a technological point of view. Finally, if the constraints are out of the physical attribute bounds, the process will be rejected and not considered during the screening phase. An example for bar charts in the production database is shown in **Figure 11**.

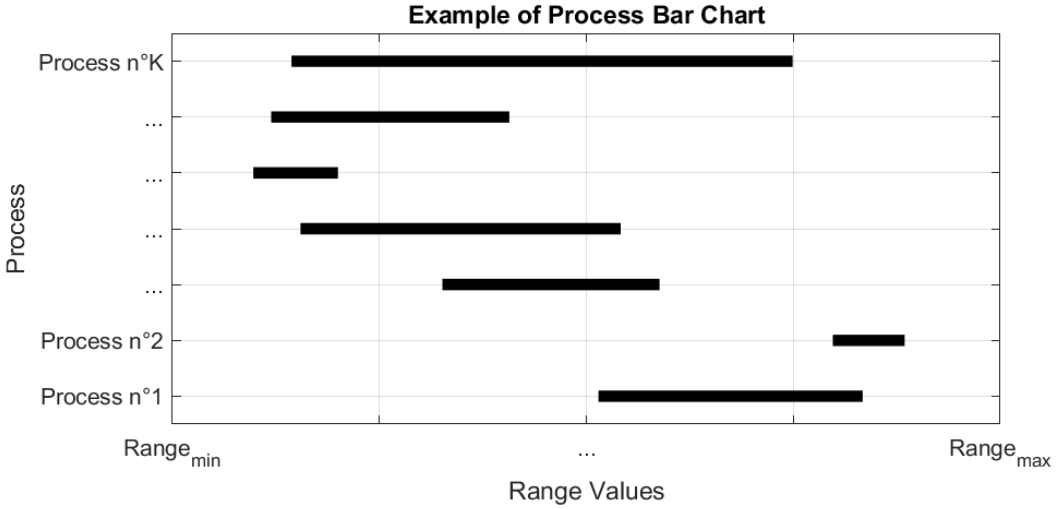

Figure 11. Example of bar charts in the production database.

Based on design constraints provided by the designer and material-shape-process compatibility provided by the production database, the screening of possible design solutions is carried out according to scheme in **Figure 12**: primary shape (chosen by the designer - constant input), materials and manufacturing processes (provided by production database – variable inputs) and process constraints (provided by the case study) are combined to perform the screening, thus obtaining all the feasible solutions.

The analytical modelling is carried out through MATLAB software, using the bar charts and binary matrices inserted in the production database. As a consequence, all the alternatives that do not meet the design requirements and/or are not technologically feasible are discarded, and the final output of the screening is the list of the feasible solutions, identified as a permitted "material-shape-process" combination. **Table 7** provides a scheme of the list of the feasible solutions S. **Figure A.2** in Annex A shows the graphic user interface (GUI) of the screening phase here described, developed using MATLAB App Designer.

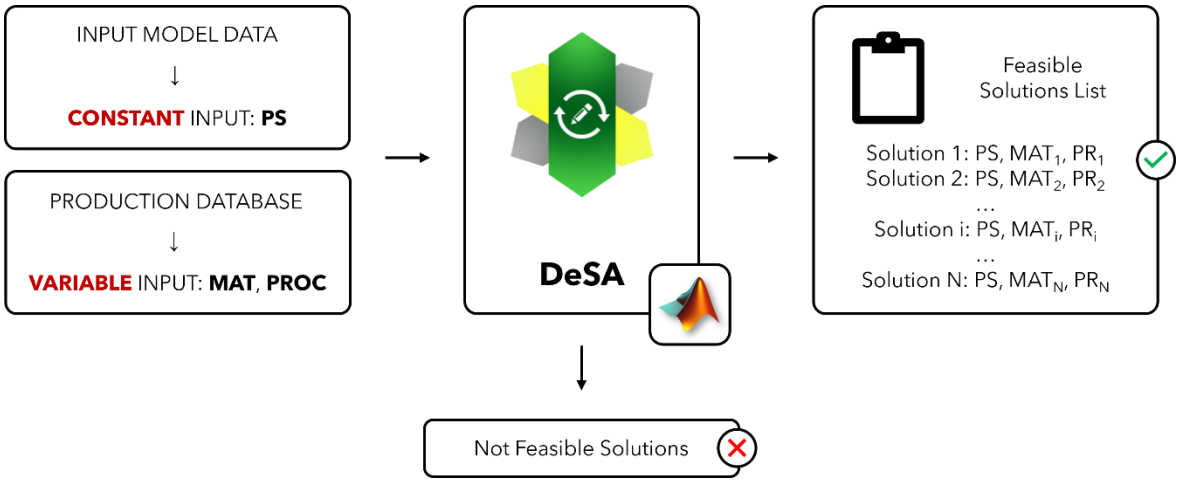

Figure 12. Screening phase framework.

Table 7. Representation of solutions list created by screening phase, where S_i is the generic i-th solution (combination of material (MAT), primary shape (PS) and process (PR)).

List of Feasible Solutions							
Sol.	**Mat.**	**Pr.**	**Shape**	**m**	**ST**	**…**	**SR**
S_1	MAT_1	PR_1	PS	$[m_{min}; m_{max}]_1$	$[ST_{min}; ST_{max}]_1$	…	$[SR_{min}; SR_{max}]_1$
S_2	MAT_2	PR_2	PS	$[m_{min}; m_{max}]_2$	$[ST_{min}; ST_{max}]_2$	…	$[SR_{min}; SR_{max}]_2$
…	…	…	…	…	…	…	…
S_i	MAT_i	PR_i	PS	$[m_{min}; m_{max}]_i$	$[ST_{min}; ST_{max}]_i$	…	$[SR_{min}; SR_{max}]_i$
…	…	…	…	…	…	…	…
S_N	MAT_N	PR_N	PS	$[m_{min}; m_{max}]_N$	$[ST_{min}; ST_{max}]_N$	…	$[SR_{min}; SR_{max}]_N$

2.2 Design and Sustainability analysis

This phase is aimed at evaluating the feasible design solutions obtained in the screening phase by means of an aggregated single-score indicator which performs a holistic assessment taking into account both design performance and sustainable profiles. The design and sustainability analysis is structured in three main sections which deal with design, environmental, and economic aspects respectively, as explained in the following.

2.2.1 Design analysis

The design analysis consists of a Finite Element Method (FEM) simulation modelling applied to all feasible solutions provided by the screening. The FEM analysis is aimed at assessing the design performance by means of a tailored indicator which quantifies the structural integrity provided by the different solutions. The FEM analysis is performed in terms of mechanical properties, and it provides as output a series of mechanical features which are used in the first and final classification phases (configuration of PSL).

In the following, the design analysis is described in detail divided into the following phases: design input data, FEM modelling and design performance.

2.2.1.1 Design input data. For the setting of FEM analysis, the framework requires that the designer characterizes the case study by providing the component Geometry (G) and the component Boundary Conditions (BCs). The framework provides that in this phase the designer develops the 3-D model of the component in CAD environment (e.g., SOLIDWORKS, CATIA, CREO) and exports it in IGES (i.e., Initial Graphics Exchange Specification) or STEP (i.e., Standard for the Exchange of Product Data) format to Altair Hypermesh software for pre-processing. The model meshing is done on the component geometry, and the designed loads and structural boundary constraints (i.e., BCs) are applied on the meshed model. Since G and BCs refer to the specific case study, they remain unaltered when passing from one solution to another. The other type of design inputs needed by the FEM modelling are the physical and mechanical properties that characterize materials of all feasible solutions. Material properties for linear, temperature-independent, and isotropic materials are considered; therefore, the chosen material properties (MAT) are density, Young modulus, Poisson ratio and yield strength. For the development of the design analysis phase, two approaches are defined in the methodology here described. These approaches vary depending on the information available to the designer:

1. Traditional approach (TRA): in the production database, the materials considered are specific. Therefore, physical, and mechanical properties are expressed by means of single (and constant) values.
2. Exploratory approach (EXA): the production database provides material classes (and not specific materials); thus, physical, and mechanical properties are expressed through variability ranges (min-max ranges).

Table 8 reports an overview of the required input data for the FEM analysis, considering both approaches here defined.

Table 8. Design Input data, with TR and EX approaches.

Design input data		
Component data (COMP)	**Material properties (MAT)**	
	Traditional Approach (TRA)	**Exploratory Approach (EXA)**
Component Geometry (G) Component Boundary Conditions (BCs)	Density (ρ); [ρ_{val}] Young modulus (E); [E_{val}] Poisson ratio (η); [η_{val}] Yield strength (σ); [σ_{val}]	Density (ρ); [ρ_{min}; ρ_{max}] Young modulus (E); [E_{min}; E_{max}] Poisson ratio (η); [η_{min}; η_{max}] Yield strength (σ); [σ_{min}; σ_{max}]

2.2.1.2 FEM modelling. Considering that FEM analysis needs single values to define material properties, the TR approach (TRA) is straightforward: specify the material properties in FE model and launch the simulation of generic i-th solution S_i (obtained as a feasible combination of material-shape-process in the screening phase).

Instead, EX approach (EXA) provides material properties in terms of variability ranges (see **Table 8**); thus, the framework explores the generic i-th solution S_i with N_i sub-solutions S_{ij} (j =1, …, N_i), each of which has to be modelled through a FEM simulation. The number of required FEM simulations strongly depends on the specific case study. To maximize the computational efficiency of the method, N_i is determined using the range sizes of different material properties (MAT). This approach guarantees an appropriate sampling of the solution domain space, thus considering the effective variability of each property. The analytical approach of EXA is described in **Equations 1-5** and **Figure 13**.

$$N_i = \frac{\lceil (x_i - 1) \cdot (n_{max} - n_{min}) \rceil}{(\delta - 1)} + n_{min} \quad (1)$$

$$\begin{bmatrix} \Omega^*_{i\,min} \\ \vdots \\ \Omega^*_i \\ \vdots \\ \Omega^*_{i\,max} \end{bmatrix} \rightarrow \begin{bmatrix} 1 \\ \vdots \\ x_i \\ \vdots \\ \delta \end{bmatrix} \quad (2)$$

$$[1 \ldots x_i \ \ldots \delta] \in \mathbb{N}$$

$$\Omega^*_i = \frac{\Omega_i}{(min\,(\Omega_i))} \quad (3)$$

$$\Omega_i = \prod_{k=1}^{4} \varphi_{ik} \quad (4)$$

$$\varphi_{ik} = \frac{(I_{ik\,max} - I_{ik\,min})}{I_{ik\,avg}} \quad (5)$$

Where:

δ = number of discretization steps of the adimensional domain space Ω^* for the i-th solution S_i, defined by the designer ($\delta > 2$);
k = k-th material property, where k = 1, …, 4 (number of material properties in **Table 8**);
x_i = conversion value of the i-th solution S_i ($x_i \in \mathbb{N}$);
n_{min} = minimum number of FEM simulation, provided by the designer;
n_{max} = maximum number of FEM simulation, provided by the designer;
Ω^*_i = adimensional domain space of the i-th solution Si;
$\Omega^*_{i\,min}$ = minimum value of adimensional domain space of the i-th solution S_i (with $\Omega^*_{i\,min} = \min(\Omega_i)/\min(\Omega_i) = 1$);
$\Omega^*_{i\,max}$ = maximum value of adimensional domain space of the i-th solution S_i (with $\Omega^*_{i\,max} = \max(\Omega_i)/\min(\Omega_i)$);
Ω_i = domain space of the i-th solution S_i;
I_{ik} = value of the k-th material property (e.g., density, young modulus) of the i-th solution S_i;
φ_{ik} = adimensional range size of the k-th material property (e.g., density, Young modulus, or Poisson ratio) of the i-th solution S_i;

$I_{ik\ max}$ = maximum value of range associated to k-th material property (associated to the i-th solution S_i) I_{ik} (see material properties reported in **Table 8**);
$I_{ik\ min}$ = minimum value of range associated to k-th material property (associated to the i-th solution S_i) I_{ik} (see material properties reported in **Table 8**);
$I_{ik\ avg}$ = average value of range associated to k-th material property (associated to the i-th solution S_i) I_{ik} (with $I_{ik\ avg} = (I_{ik\ max} + I_{ik\ min})/2$).

The starting point to determine N_i is the calculation of the domain space Ω_i (**Equation 4**) of the i-th solution S_i. Ω_i is calculated by multiplying dimensionless range sizes of the different material properties φ_{ik}, these latter calculated as the ratio between the property range size and its average value (**Equation 5**). Then the dimensionless value of the domain space (Ω^*_i, **Equation 3**) is determined by dividing Ω_i by the minimum domain space among all the alternatives S_i (i.e., min(Ω_i)). Ω^*_i is represented by means of dots in a Ω^*_i-Solution ID chart (red dots in **Figure 13**). Therefore, Ω^*_i is converted into a parameter x_i (**Equation 2** and **Figure 13**) whose value varies within a range [1, …, δ] ∈ ℕ, where δ is the number of discretization steps of the dimensionless domain space Ω^* and it is defined by the designer (with δ > 2). The conversion is performed with the line passing through the points (n_{min},1) and (n_{max}, δ). Finally, the number of simulations N_i is calculated rounding up the value obtained in **Equation 1**, according to parameters defined by the designer (n_{min}, n_{max} and δ).

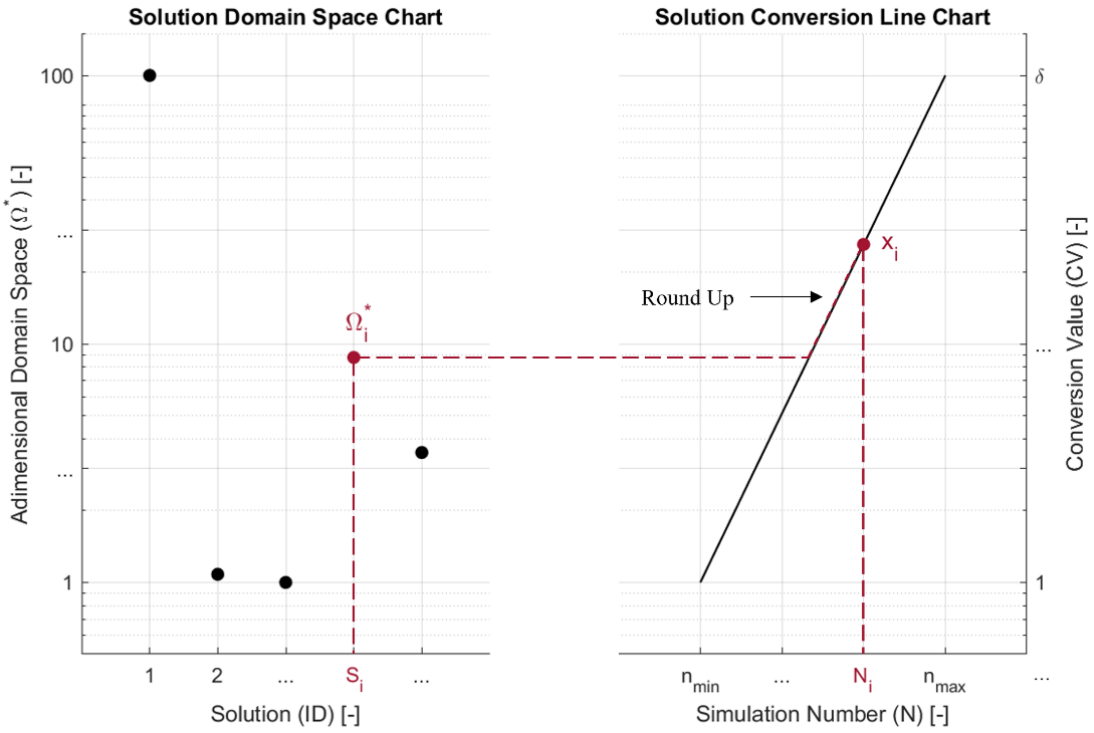

Figure 13. Domain space of design solutions and N_i calculation.

As an example, consider three solutions obtained from the screening phase with the following characteristics shown in **Table 9**.

Table 10 shows the material properties collected in the production database (for simplicity, only density (ρ) and yield strength (σ) are considered in the calculation); EXA is considered. **Equation 5** is used to calculate the adimensional range size (φ) of each material

property, calculating the ratio between the property range size (i.e., $I_{ik\ max}$ - $I_{ik\ min}$) and its average value ($I_{ik\ avg} = (I_{ik\ max} + I_{ik\ min})/2$).

Table 9. Solutions list used for the number of simulations N_i calculation.

List of Feasible Solutions			
Solution	**Shape**	**Material**	**ID Material**
S_1	Sheet-2D	Cast Iron (Ductile)	M1
S_2	Sheet-2D	High Carbon Steel	M2
S_3	Sheet-2D	Low Alloy Steel	M3

Table 10. Example of material data section in production database, used for the number of simulations (N_i) calculation.

Production Database				
Material Section (MAT)				
ID	**Material Class**	**Material Name**	**Density [kg/m^3]**	**Yield Strength [MPa]**
M1	Metals and Alloys	Cast Iron (Ductile)	7050-7250	250-680
M2	Metals and Alloys	High Carbon Steel	7800-7900	400-1160
M3	Metals and Alloys	Low Alloy Steel	7800-7900	400-1500

Considering the solution S_1, the material is Cast Iron (Ductile) (with ID = M1), thus the adimensional range size for density ($\varphi_{1\rho}$) and yield strength ($\varphi_{1\sigma}$) and the domain space (Ω_1) are calculated as follows (**Equations 6-8**):

$$\varphi_{1\rho} = \frac{(I_{1\rho\,max} - I_{1\rho\,min})}{I_{i\rho\,avg}} = \frac{7250 - 7050}{(7250 + 7050)/2} = 0.028 \tag{6}$$

$$\varphi_{1\sigma} = \frac{(I_{1\sigma\,max} - I_{1\sigma\,min})}{I_{1\sigma\,avg}} = \frac{680 - 250}{(680 + 250)/2} = 0.9247 \tag{7}$$

$$\Omega_1 = \prod_{k=1}^{2} \varphi_{1k} = \varphi_{1\rho} \cdot \varphi_{i\sigma} = 0.028 \cdot 0.9247 = 0.0259 \tag{8}$$

$$\Omega_1^* = \frac{\Omega_1}{\min(\Omega)} = \frac{\Omega_1}{\Omega_2} = \frac{0.0259}{0.0124} = 2.0877 \tag{9}$$

$$\Omega_1^* \rightarrow x_1 = 3$$

$$[1 \ldots x_i \ldots \delta] \in \mathbb{N} \rightarrow x_i = [1,2,3] \tag{10}$$

$$N_1 = \frac{[(x_1 - 1) \cdot (n_{max} - n_{min})]}{(\delta - 1)} + n_{min} = \frac{[(3 - 1) \cdot (5 - 3)]}{(3 - 1)} + 3 = 5 \tag{11}$$

Where:

Ω_1 = domain space of the solution S_1 (k = 2, number of material properties in **Table 10**));
$\varphi_{1\rho}$ = adimensional range size of the material property density of the solution S_1;
$\varphi_{1\sigma}$ = adimensional range size of the material property yield strength of the solution S_1;
$I_{1\rho\ max}$ = maximum value of range associated to material property density (ρ) of the solution S_1 (material property in **Table 10**);
$I_{1\rho\ min}$ = minimum value of range associated to material property density (ρ) of the solution S_1 (material property in **Table 10**);
$I_{1\rho\ avg}$ = average value of range associated to material property density (ρ) of the solution S_1 (material property in **Table 10**);
$I_{1\sigma\ max}$ = maximum value of range associated to material property yield strength (σ) of the solution S_1 (material property in **Table 10**);
$I_{1\sigma\ min}$ = minimum value of range associated to material property yield strength (σ) of the solution S_1 (material property in **Table 10**);
$I_{1\sigma\ avg}$ = average value of range associated to material property yield strength (σ) of the solution S_1 (material property in **Table 10**);

Table 11 reports the outcomes calculated for each solution; the dimensionless value of the domain space (Ω^*, see **Equation 3**) is determined by dividing Ω of each solution by the minimum domain space among all the alternatives S_i (in this case, Ω_2 = 0.0124). **Equation 9** shows the adimensional domain space of the solution S_1 calculation. In the next step, Ω* is converted into a parameter x (as shown in **Equation 2** and **Figure 13**) within a range [1, …, δ] ∈ N (with δ > 2); in this example the parameter δ is equal to 3. The conversion is performed with the line passing through the points (n_{min},1) and (n_{max}, δ), where n_{min} = 3, and n_{max} = 5. Finally, the number of simulations N is calculated for each solution rounding up the value obtained in **Equation 1**, according to parameters defined by the designer (i.e., n_{min}, n_{max} and δ). **Equations 10-11** report, for instance, the N_1 calculation of the first feasible solution S_1.

Table 11. Solutions outcomes obtained for the number of simulations N_i calculation.

List of Feasible Solutions							
Solution	**ID Material**	$\boldsymbol{\varphi_\rho}$	$\boldsymbol{\varphi_\sigma}$	**Ω**	**Ω***	**x**	**N**
S_1	M1	0.028	0.9247	0.0259	2.0877	3	5
S_2	M2	0.0127	0.9744	0.0124	1	1	3
S_3	M3	0.0127	1.1579	0.0147	1.1855	2	4

It follows from the above that S_{ij} depends on

- material properties (MAT_{ij}, see EXA properties in **Table 8**);
- component data (COMP, **Table 8**);
- setting parameters for the FEM modelling (N_i).

as provided by the following relations:

$$S_{ij} = S_{ij}(G, BC, MAT_{ij}, N_i)$$

$$N_i = N_i(MAT_i, n_{min}, n_{max}, \delta)$$

The sample of material properties (MAT_{ij}) is calculated through the Latin Hypercube Sampling (LHS) method (Viana, 2013; Helton & Davis, 2003). Such a method provides that the range of each material property (reported in **Table 8**) is partitioned into N_i non-overlapping intervals (depending on the design solution S_i) and one value from each interval is selected at random with respect to the probability density in the interval. Starting from the first material property, the N_i values obtained are paired in a random manner with the N_i values of the second property. This rule is applied to every range available in materials property, until a set of N_{ik}-tuples is formed (as said, k is the k-th material property, where k = 1, …, 4). However, if the interval of k-th material property considered has an adimensional range size (φ_{ik}) less than a threshold value imposed by the designer (in the methodology modelling, the threshold value is set to 0.05), the value sampled will be constant regardless of the sub-solutions and equal to the average value of the range itself (i.e., $I_{ik\ avg} = (I_{ik\ max} + I_{ik\ min})/2$). Such a set represents the sample used in FEM simulation for design solution S_i and sub-solutions S_{ij}. Resuming the example described above, the application of LH method to the solutions in **Table 9** (and considering the results of N_i calculation in **Table 11**) defines the material properties to be applied to the various sub-solutions S_{ij}.

Table 12 collects, as example, the material properties sampling of feasible solution; as said, the column of density (ρ) property present constant values, since the adimensional range size of the material property density (φ_ρ) of all solutions (see **Table 12**) is less than the arbitrary threshold value (in this methodology, equal to 0.05).

Table 12. Material properties sampling obtained by means of LH method (considering EXA).

Material Properties Sampling of Feasible Solutions					
Solution	**ID Material**	**N**	**Sub-Solution**	**Density [kg/m^3]**	**Yield Strength [MPa]**
S_1	M1	5	S_{11}	7150	266.73
			S_{12}	7150	535.47
			S_{13}	7150	596.09
			S_{14}	7150	392.40
			S_{15}	7150	266.73
S_2	M2	3	S_{21}	7850	625.26
			S_{22}	7850	951.54
			S_{23}	7850	1047.93
S_3	M3	4	S_{31}	7850	507.77
			S_{32}	7850	1379.16
			S_{33}	7850	685.65
			S_{34}	7850	998.70

2.2.1.3 <u>Design assessment</u>. For each solution S_i (with TR approach) or sub-solution S_{ij} (using EX approach) identified in the simulation modelling step, the design performance is assessed

by means of a tailored indicator which is representative of service levels accomplished by the product (such as structural integrity, stiffness, etc…). For this reason, the chosen indicator is the Performance Index (PI), defined as the ratio between the reference or arbitrary service levels (user-defined, depending on the case study) and the service levels on the component calculated through the FEM simulations. The design calculation is carried out according to the modeling framework reported in **Table 13** (**Equations 12-15**). The following points describe the peculiarities of the design assessment concerning the different design approaches (i.e., TRA and EXA as well as the reference or arbitrary service level):

Table 13. Design modelling.

Design Equations				
		Traditional Approach (TRA)	**Exploratory Approach (EXA)**	
Performance Index	**Arbitrary Scenario (ARB)**	$PI_i = \sum_{l=1}^{N_l} w_l \cdot \left(\frac{pi_i^{arb}}{pi_{FEMi}}\right)_l$	$PI_{ij} = \sum_{l=1}^{N_l} w_l \cdot \left(\frac{pi_{ij}^{arb}}{pi_{FEMij}}\right)_l$	(12)
	Reference Scenario (REF)	$PI_i = \sum_{l=1}^{N_l} w_l \cdot \left(\frac{pi^{ref}}{pi_{FEMi}}\right)_l$	$PI_{ij} = \sum_{l=1}^{N_l} w_l \cdot \left(\frac{pi^{ref}}{pi_{FEMij}}\right)_l$	(13)
Elasticity		$EL_i = PI_i - 1$	$EL_{ij} = PI_{ij} - 1$	(14)
Weights		$\sum_{l=1}^{N_l} w_l = 1$		(15)

Legend:
N_l = number of loadcases used for PI calculation (with l = 1, …, N_l) [-];
w_l = the weighting factor l-th loadcase for the design modelling [-];
pi^{arb}_{ij} = arbitrary (ARB) service level of the component for sub-solution S_{ij} in EX approach [*service-defined*];
pi^{ref} = reference (REF) service level of the component for reference solution in EX and TR approaches [*service-defined*];
pi_{FEMij} = service level on the component calculated through FEM simulation for sub-solution S_{ij} in EX approach [*service-defined*].
pi^{arb}_{i} = arbitrary (ARB) service level of the component for solution S_i in TR approach [*service-defined*];
pi_{FEMi} = service level on the component calculated through FEM simulation for solution S_i in TR approach [*service-defined*].
PI_{ij} = performance index for sub-solution S_{ij} in EX approach [-].
PI_i = performance index for solution S_i in TR approach [-].

- PI calculation: regardless of approach and scenario typology, PI is calculated considering the number of loadcases (N_l) available for the designer (**Equation 12**); moreover, the normalized data are systematically aggregated into a single score (i.e., PI_i or PI_{ij}) using the weights (w_l) associated to loadcases (with their sum equal to 1, see **Equation 15**). These weights are chosen by the designer, according to case study and know-how.

- Arbitrary scenario (ARB): in this scenario the solutions S_i (or sub-solutions S_{ij}) created during the FEM modelling are analyzed defining a designer-defined scenario.
- Reference scenario (REF): in this scenario the solutions S_i (or sub-solutions S_{ij}) created during the FEM modelling are analyzed using an existing reference scenario.
- To quantify the distance (or the over-dimensioning) of the generic solution S_i (or sub-solution S_{ij}) with respect to reference or arbitrary value (i.e., pi^{arb}, pi^{ref}, see **Table 13**), the analysis defines the Elasticity (EL) parameter, which expresses the potential to lighten a solution without compromising the design performance (**Equation 14**).

For example, consider the EX approach and ARB scenario, where the designer has the structural integrity as a unique service level ($N_l = 1$). In this case, the Performance Index (PI) will be defined as the ratio between the yield strength of the material and the maximum stress level on the component calculated through the FEM simulations (see **Equation 16**). In order to quantify the over-dimensioning of the generic sub-solution S_{ij} concerning the structural limit value, the EL parameter is calculated according to the design modelling (see **Equation 14** and **Equation 17**).

$$PI_{ij} = \frac{\sigma_{yij}}{\sigma_{FEMij}} \tag{16}$$

$$EL_{ij} = PI_{ij} - 1 = \frac{\sigma_{yij}}{\sigma_{FEMij}} - 1 \tag{17}$$

Where:
σ_{yij} = yield strength of the component material for the sub-solution S_{ij} (EX approach);
σ_{FEMij} = stress level on the component calculated through FEM simulations for the sub-solution S_{ij} (EX approach).

The methodology requires that the calculation of PI and EL is carried out for each design solution S_i or sub-solution S_{ij} through the combined use of MATLAB and Altair HyperWorks simulation software. The final output of the design analysis is the overall set of solution S_i or sub-solutions S_{ij} characterized in terms of PI and EL indexes:

$$PI \rightarrow \begin{cases} PI_i = f(G, BC, MAT_i) \quad TR\ Approach \\ PI_{ij} = f\left(G, BC, MAT_{ij}\right)\ EX\ Approach \end{cases}$$

$$EL \rightarrow \begin{cases} EL_i = f(PI_i) \quad TR\ Approach \\ EL_{ij} = f\left(PI_{ij}\right)\ EX\ Approach \end{cases}$$

2.2.2 Environmental analysis

In this phase the feasible solution S_i (or sub-solutions S_{ij}) provided by the design analysis are evaluated respect to the environmental profile. The chosen indicator is the Environmental Index (EI), which evaluation is carried out through the LCA methodology by means of the Climate Change (CC) indicator using the ILCD 1.09 Life Cycle Impact Assessment method (ILCD handbook, 2011) (see **Equation 33**). The CC is chosen as it is

the mostly representative impact category for the environmental burdens caused by passenger vehicles (Delogu et al., 2016; Del Pero et al., 2020). The CC is determined taking into account the overall component LC, defined according to the following main stages:

- materials, dealing with impacts from raw materials extraction and production up to the manufacturing of the semi-finished products;
- manufacturing, dealing with impacts of manufacturing processes required to convert the semi-finished products into the final component (no secondary and joining processes are considered);
- use, dealing with impacts due to both production of energy consumed during operation and exhaust air emissions during operation;
- EoL, dealing with impacts due to disposal of EoL components and materials, including credits from component reuse, recycling, or energy recovery.

2.2.2.1 Environmental Input data. The CC calculation framework involves an environmental characterization of all solutions S_i (or sub-solutions S_{ij}) obtained in the design analysis stage. Such a characterization is carried out by means of an environmental database which provides all the input data needed for the sustainability assessment. The environmental database is subdivided in two sections:

- setting parameters for the evaluation of the use stage (both internal combustion engine vehicles (ICEVs) and electric vehicles (EVs)) and EoL scenarios.
- specific impact values, providing mass-specific CC for each phase of component LC (expressed with respect to component mass).

Table 14 reports input data for the environmental analysis grouped according to the above classification, considering both design approaches (TRA, EXA). The tool envisages that the environmental database is filled in directly by the designer with inventory data coming from secondary LCI dataset (mass-specific CC parameters) and LC boundary conditions that characterize the case study.

2.2.2.2 Environmental modelling. The calculation of the environmental impact is carried out according to the modelling framework reported in **Table 15** (**Equations 18-34**). The following points describe the peculiarities of the environmental assessment with respect to the different LC stages:

- materials & manufacturing: the CC is assessed taking into account component reuse, that is the allocation of production impact to more than one vehicle LC (vehicle life-time assumed as reference for the assessment);
- use: the allocation of energy consumption and exhaust air emissions is carried out according to the inventory modelling framework provided by Delogu et al., 2016 and Del Pero et al. 2017, 2020;
- EoL disassembly: the component is assumed to be manually disassembled; therefore, the environmental impact is not considered;
- EoL shredding: the specific impact of the shredding is constant for all solution S_i (or sub-solutions S_{ij});

Table 14. Environmental database overview.

Environmental database		
	Traditional Approach (TRA)	**Exploratory Approach (EXA)**
LC setting parameters	mil_{veh} (vehicle model-based) CO_{2veh} (vehicle model-based) ρ_{fuel} (fuel type-based) m_{CO2} (fuel type-based) FRV (vehicle model-based) ERV (vehicle model-based)	
	SF_i (material-based) ϑ_i (material-based)	SF_{ij} (material-based) ϑ_{ij} (material-based)
Specific impact values	cc^{mat}_i (material-based) cc^{Shr}_i (material-based) cc^{Sep}_i (material-based) cc^{Enr}_i (material-based) cc^{Disp}_i (material-based) cc^{Man}_i (manufacturing process-based)	cc^{mat}_{ij} (material-based) cc^{Shr}_{ij} (material-based) cc^{Sep}_{ij} (material-based) cc^{Enr}_{ij} (material-based) cc^{Disp}_{ij} (material-based) cc^{Man}_{ij} (manufacturing process-based)
	cc_{fuel} (use-based) cc_{mix} (use-based)	

Legend:
cc^{mat}_i = mass-specific CC in material stage phase for solution S_i [kg CO_{2eq}/kg]
cc^{Shr}_i = mass-specific CC of shredding phase for solution S_i [kg CO_{2eq}/kg]
cc^{Sep}_i = mass-specific CC of separation phase for solution S_i [kg CO_{2eq}/kg]
cc^{Enr}_i = mass-specific CC of incineration with energy recovery for solution S_i (referred to plastic fraction) [kg CO_{2eq}/kg]
cc^{Disp}_i = mass-specific CC of disposal phase for solution S_i [kg CO_{2eq}/kg]
cc^{man}_i = mass-specific CC in manufacturing process phase for solution S_i [kg CO_{2eq}/kg]
cc^{mat}_{ij} = mass-specific CC in material stage phase for sub-solution S_{ij} [kg CO_{2eq}/kg]
cc^{Shr}_{ij} = mass-specific CC of shredding phase for sub-solution S_{ij} [kg CO_{2eq}/kg]
cc^{Sep}_{ij} = mass-specific CC of separation phase for sub-solution S_{ij} [kg CO_{2eq}/kg]
cc^{Enr}_{ij} = mass-specific CC of incineration with energy recovery for sub-solution S_{ij} (referred to plastic fraction) [kg CO_{2eq}/kg]
cc^{Disp}_{ij} = mass-specific CC of disposal phase for sub-solution S_{ij} [kg CO_{2eq}/kg]
cc^{man}_{ij} = mass-specific CC in manufacturing process phase for sub-solution S_{ij} [kg CO_{2eq}/kg]
cc_{fuel} = environmental impact of fuel production (for ICEVs) [kg CO2eq/kg]
cc_{mix} = environmental impact of electrical mix grid production (for EVs) [kg CO_{2eq}/kWh]
mil_{veh} = vehicle mileage [km]
CO_{2veh} = vehicle CO_2 emissions [kg CO_{2eq}/km]
ρ_{fuel} = fuel density [kg/l]
m_{CO2} = mass of CO_2 per liter of fuel [g/l]
FRV = fuel reduction value [l/100km*100kg]
ERV = energy reduction value [kWh/100km*100kg]
SF_i = recycling substitution factor of generic solution S_i (quota of avoided primary production impact due to recycling) [-]
ϑ_i = share of fibers for generic solution S_i (composite materials) [-]
SF_{ij} = recycling substitution factor of generic sub-solution S_{ij} (quota of avoided primary production impact due to recycling) [-]
ϑ_{ij} = share of fibers for generic sub-solution S_{ij} (composite materials) [-]

Table 15. Environmental modelling.

Life Cycle Equations				
Traditional Approach (TRA)			**Exploratory Approach (EXA)**	
Production	$CC_i^{Prod} = CC_i^{Mat} + CC_i^{Man}$		$CC_{ij}^{Prod} = CC_{ij}^{Mat} + CC_{ij}^{Man}$	(18)
	$CC_i^{Mat} = (1+R) \cdot m_i \cdot cc_i^{Mat}$		$CC_{ij}^{Mat} = (1+R) \cdot m_{ij} \cdot cc_{ij}^{Mat}$	(19)
	$CC_i^{Man} = (1+R) \cdot m_i \cdot cc_i^{Man}$		$CC_{ij}^{Man} = (1+R) \cdot m_{ij} \cdot cc_{ij}^{Man}$	(20)
Use	$CC_i^{Use} = CC_i^{WTT} + CC_i^{TTW}$		$CC_{ij}^{Use} = CC_{ij}^{WTT} + CC_{ij}^{TTW}$	(21)
	ICEVs	$CC_i^{WTT} = cc_{fuel} \cdot EC_{comp_i}$	$CC_{ij}^{WTT} = cc_{fuel} \cdot EC_{comp_{ij}}$	(22)
		$CC_i^{TTW} = (CO_{2veh} \cdot mil_{veh} \cdot EC_{comp_i})/EC_{veh}$	$CC_{ij}^{TTW} = (CO_{2veh} \cdot mil_{veh} \cdot EC_{comp_{ij}})/EC_{veh}$	(23)
		$EC_{comp_i} = (FRV \cdot \rho_{fuel} \cdot m_i \cdot mil_{veh})/10000$	$EC_{comp_{ij}} = (FRV \cdot \rho_{fuel} \cdot m_{ij} \cdot mil_{veh})/10000$	(24)
		$EC_{veh} = (EC_{100km} \cdot \rho_{fuel} \cdot mil_{veh})/100$		(25)
		$EC_{100km} = (CO_{2veh} \cdot 100)/m_{CO_2}$		(26)
	BEVs	$CC_i^{WTT} = cc_{mix} \cdot EC_{comp_i}$	$CC_{ij}^{WTT} = cc_{mix} \cdot EC_{comp_{ij}}$	(22)
		$CC_i^{TTW} = 0$	$CC_{ij}^{TTW} = 0$	(23)
		$EC_{comp_i} = (ERV \cdot m_i \cdot mil_{veh})/10000$	$EC_{comp_{ij}} = (ERV \cdot m_{ij} \cdot mil_{veh})/10000$	(24)
EoL	$CC_i^{EoL} = CC_i^{Dis} + CC_i^{Shr} + CC_i^{Sep} + CC_i^{Rec} + CC_i^{Enr} + CC_i^{Disp}$		$CC_{ij}^{EoL} = CC_{ij}^{Dis} + CC_{ij}^{Shr} + CC_{ij}^{Sep} + CC_{ij}^{Rec} + CC_{ij}^{Enr} + CC_{ij}^{Disp}$	(25)
	$CC_i^{Shr} = (1+R) \cdot m_i \cdot cc_i^{Shr}$		$CC_{ij}^{Shr} = (1+R) \cdot m_{ij} \cdot cc_{ij}^{Shr}$	(28)
	$CC_i^{Sep} = (1+R) \cdot m_i \cdot cc_i^{Sep}$		$CC_{ij}^{Sep} = (1+R) \cdot m_{ij} \cdot cc_{ij}^{Sep}$	(29)
	$CC_i^{Rec} = (1+R) \cdot \eta_{eff} \cdot m_i \cdot SF_i \cdot cc_i^{Mat}$		$CC_{ij}^{Rec} = (1+R) \cdot \eta_{eff} \cdot m_{ij} \cdot SF_{ij} \cdot cc_{ij}^{Mat}$	(30)
	$CC_i^{Enr} = (1+R) \cdot m_i \cdot cc_i^{Enr} \cdot (1-\vartheta_i)$		$CC_{ij}^{Enr} = (1+R) \cdot m_{ij} \cdot cc_{ij}^{Enr} \cdot (1-\vartheta_{ij})$	(31)
	$CC_i^{Disp} = \begin{cases} (1+R) \cdot m_i \cdot cc_i^{Disp} \cdot \vartheta_i \\ (1+R) \cdot (1-\eta_{eff}) \cdot m_i \cdot cc_i^{Disp} \end{cases}$		$CC_{ij}^{Disp} = \begin{cases} (1+R) \cdot m_{ij} \cdot cc_{ij}^{Disp} \cdot \vartheta_{ij} \\ (1+R) \cdot (1-\eta_{eff}) \cdot m_{ij} \cdot cc_{ij}^{Disp} \end{cases}$	(32)
LC	$CC_i^{LC} = CC_i^{Mat} + CC_i^{Man} + CC_i^{Use} + CC_i^{EoL}$		$CC_{ij}^{LC} = CC_{ij}^{Mat} + CC_{ij}^{Man} + CC_{ij}^{Use} + CC_{ij}^{EoL}$	(33)
	$EI_i = CC_i^{LC}$		$EI_{ij} = CC_{ij}^{LC}$	(34)

Legend:
CC^{Prod}_{i} = environmental impact of the production phase for solution S_i [kg CO_{2eq}].
CC^{Mat}_{i} = environmental impact of material stage phase for solution S_i [kg CO_{2eq}].
CC^{Man}_{i} = environmental impact of the manufacturing process phase for solution S_i [kg CO_{2eq}].
R = number of potential substitutions of the component (based on its durability) [-].
m_i = component mass for generic solution S_i [kg].
CC^{Use}_{i} = environmental impact of the use stage phase for solution S_i [kg CO_{2eq}].
CC^{WTT}_{i} = environmental impact of well-to-tank use stage phase for solution S_i [kg CO_{2eq}].
CC^{TTW}_{i} = environmental impact of tank-to-wheel use stage phase for solution S_i [kg CO_{2eq}].
EC_{veh} = energy consumption during operation of vehicle; [kg] for ICEVs, [kWh] for EVs.
EC_{comp} = energy consumption during operation of component; [kg] for ICEVs, [kWh] for EVs.
CC^{EoL}_{i} = environmental impact of the end-of-life phase for solution S_i [kg CO_{2eq}].
CC^{Dis}_{i} = environmental impact of component disassembly phase for solution S_i [kg CO_{2eq}].
CC^{Shr}_{i} = environmental impact of component shredding phase for solution S_i [kg CO_{2eq}].
CC^{Sep}_{i} = environmental impact of shredded material component separation phase for solution S_i [kg CO_{2eq}].
CC^{Rec}_{i} = environmental impact of separated material component recycling phase for solution S_i [kg CO_{2eq}].
CC^{Enr}_{i} = environmental impact of post-separation material component energy recovery phase for solution S_i [kg CO_{2eq}].
CC^{Disp}_{i} = environmental impact of residual component disposal phase for solution S_i [kg CO_{2eq}].
CC^{LC}_{i} = environmental impact of LC component for solution S_i [kg CO_{2eq}].
EI_i = environmental index of LC for solution S_i [kg CO_{2eq}].
CC^{Prod}_{ij} = environmental impact of the production phase for sub-solution S_{ij} [kg CO_{2eq}].
CC^{Mat}_{ij} = environmental impact of material stage phase for sub-solution S_{ij} [kg CO_{2eq}].
CC^{Man}_{ij} = environmental impact of the manufacturing process phase for sub-solution S_{ij} [kg CO_{2eq}].
m_{ij} = component mass for generic sub-solution S_{ij} [kg].
CC^{Use}_{ij} = environmental impact of the use stage phase for sub-solution S_{ij} [kg CO_{2eq}].
CC^{WTT}_{ij} = environmental impact of well-to-tank use stage phase for sub-solution S_{ij} [kg CO_{2eq}].
CC^{TTW}_{ij} = environmental impact of tank-to-wheel use stage phase for sub-solution S_{ij} [kg CO_{2eq}].
CC^{EoL}_{ij} = environmental impact of the end-of-life phase for sub-solution S_{ij} [kg CO_{2eq}].
CC^{Dis}_{ij} = environmental impact of component disassembly phase for sub-solution S_{ij} [kg CO_{2eq}].
CC^{Shr}_{ij} = environmental impact of component shredding phase for sub-solution S_{ij} [kg CO_{2eq}].
CC^{Sep}_{ij} = environmental impact of shredded material component separation phase for sub-solution S_{ij} [kg CO_{2eq}].
CC^{Rec}_{ij} = environmental impact of separated material component recycling phase for sub-solution S_{ij} [kg CO_{2eq}].
CC^{Enr}_{ij} = environmental impact of post-separation material component energy recovery phase for sub-solution S_{ij} [kg CO_{2eq}].
CC^{Disp}_{ij} = environmental impact of residual component disposal phase for sub-solution S_{ij} [kg CO_{2eq}].
CC^{LC}_{ij} = environmental impact of LC component [kg CO_{2eq}].
EI_{ij} = environmental index of LC for sub-solution S_{ij} [kg CO_{2eq}].

- EoL recycling: only metals materials are considered in this phase. The material substitution factor (SF) is assumed constant on the assumption of the same material. The environmental impact of recycling is multiplied by a factor (η_{sep}) which takes into account the separation efficiency in post-shredding phase (η_{sep} = 0.98 for metal materials, 0 otherwise);
- EoL energy recovery: the material percentage parameter is a non-zero value only for plastic composite materials and it depends on the quota of fibers within the material (ϑ_i, ϑ_{ij}); the parameter is null for plastic materials.
- EoL disposal: considering the metal materials, the environmental impact of disposal is multiplied by a factor (1 - η_{sep}) which takes into account the separation inefficiency in post-shredding phase (1- η_{sep} = 0.02 for metal materials);

The final output of the environmental analysis is the overall set of solution S_i (or sub-solutions S_{ij}) characterized in terms of Life-Cycle Climate Change (CC_{LC}):

$$EI \rightarrow \begin{cases} EI_i = CC_i^{LC} = f(G, MAT_i, MAN_i, USE_i, EoL_i) & TR\ Approach \\ EI_{ij} = CC_{ij}^{LC} = f\left(G, MAT_{ij}, MAN_{ij}, USE_{ij}, EoL_{ij}\right) & EX\ Approach \end{cases}$$

2.2.3 Economic analysis

In this last phase the feasible solution S_i (or sub-solutions S_{ij}) provided by the design analysis (and evaluated respect to environmental profile) are analyzed respect to the economic aspect. The chosen indicator is the Cost Index (CI), which evaluation is carried out through the LCC methodology by means of cost indicator (COST) using the environmental Life Cycle Costing (eLCC) method (Hunkeler et al. 2008) (**Equation 52**). The COST is chosen as it is the mostly representative of all costs associated with the LC of a product that are directly covered by any one or more of the actors in the product life cycle (e.g., supplier, manufacturer, user, consumer, or EoL actor). The COST is determined taking into account the overall component LC, defined according to the following main stages:

- materials, dealing with materials and feedstocks acquisition cost and production cost up to the manufacturing of the semi-finished products;
- manufacturing, dealing with manufacturing processes cost required to convert the semi-finished products into the final component (similar to the case of environmental modelling, no secondary and joining processes are considered);
- use, dealing with the contribution of propulsion system and the contribution of externalities as pollutant emissions (i.e., CO_2, NO_x) during operation;
- EoL, dealing with costs due to disposal of EoL components and materials, including credits from component reuse, recycling.

2.2.3.1 <u>Economic Input data</u>. The COST calculation framework involves an economic characterization of all solutions S_i (or sub-solutions S_{ij}) obtained in the design analysis stage. This characterization is performed through an economic database which provides all the input data needed for the assessment. The economic database is subdivided in three sections:

- setting parameters for the evaluation of the use stage (both internal combustion engine vehicles (ICEVs) and electric vehicles (EVs)) and EoL scenarios.
- manufacturing cost values,
- specific cost values, providing the specific COST for each phase of component LC (expressed with respect to component mass, batch size, etc…).

Table *16* reports input data for the economic analysis grouped according to the above classification, considering both design approaches (TRA, EXA). The tool provides that the economic database (as well as the environmental one) is filled in directly by the designer with inventory data coming from secondary LCI dataset (mass-specific COST parameters) and LC boundary conditions that characterize the case study.

2.2.3.2 Economic modelling. The calculation of the overall economic cost is carried out according to the modelling framework reported in **Table 17** (**Equations 35-53**). The following points describe the peculiarities of the economic assessment with respect to the different LC stages:

- materials & manufacturing: the COST is assessed taking into account component reuse, that is the allocation of production impact to more than one vehicle LC (as said in Environmental Analysis, the vehicle life-time assumed as reference for the assessment). The material cost is magnified by the factor $1/(1-f)$ where f is the scrap fraction - the fraction of the starting material that ends up as sprues, risers, turnings, rejects, or waste.
- use: the allocation of energy consumption is carried out on the basis of the environmental inventory modelling framework provided by Delogu et al., 2016 and Del Pero et al. 2017, 2020. As for the externalities ($COST^{ext}$), currently pollutants emissions costs are not borne by any actors (producer, consumer) but would be soon internalized so, according to the Code of Practice they should be included in the eLCC. Finally, the maintenance cost ($COST^{main}$) of the component was not included since it can be hardly estimated and depends on the given component;
- EoL disassembly: the component is assumed to be manually disassembled; however, the economic cost ($COST^{Dis}$) is not considered, because it can be hardly estimated and depends on the given component;
- EoL shredding and post-shredding: the specific consumption of the shredding and post-shredding (separation) is constant for all solutions S_i (or sub-solutions S_{ij});
- EoL recycling: only metals materials are considered in this phase. The material substitution factor (SF) is assumed constant on the assumption of the same material. The cost of recycling is multiplied by a factor (η_{sep}) which takes into account the separation efficiency in post-shredding phase (η_{sep} = 0.98 for metal materials, 0 otherwise);
- EoL energy recovery: the material percentage parameter is a non-zero value only for plastic composite materials and it depends on the quota of fibers within the material (ϑ_i, ϑ_{ij}); the parameter is null for plastic materials. The cost of energy recovery production is multiplied by lower heating value (LHV^{enr}) of material specified.

- EoL disposal: considering the metal materials, the economic cost of disposal is multiplied by a factor (1 - η_{sep}) which takes into account the separation inefficiency in post-shredding phase (1- η_{sep} = 0.02 for metal materials).

The final output of the economic analysis is the overall set of solution S_i (or sub-solutions S_{ij}) characterized in terms of Life-Cycle Cost ($COST_{LC}$):

$$CI \rightarrow \begin{cases} CI_i = COST_i^{LC} = f(G, MAT_i, MAN_i, USE_i, EoL_i) & TR\ Approach \\ CI_{ij} = COST_{ij}^{LC} = f(G, MAT_{ij}, MAN_{ij}, USE_{ij}, EoL_{ij}) & EX\ Approach \end{cases}$$

The overall design and sustainability phase is performed according to scheme reported in **Figure 14**, where the combination of MATLAB and Hyperworks allows the calculation of indexes previously defined (i.e., PI, EI, and CI) for each feasible solution S_i or S_{ij} obtained in the screening phase (see **Table 18**):

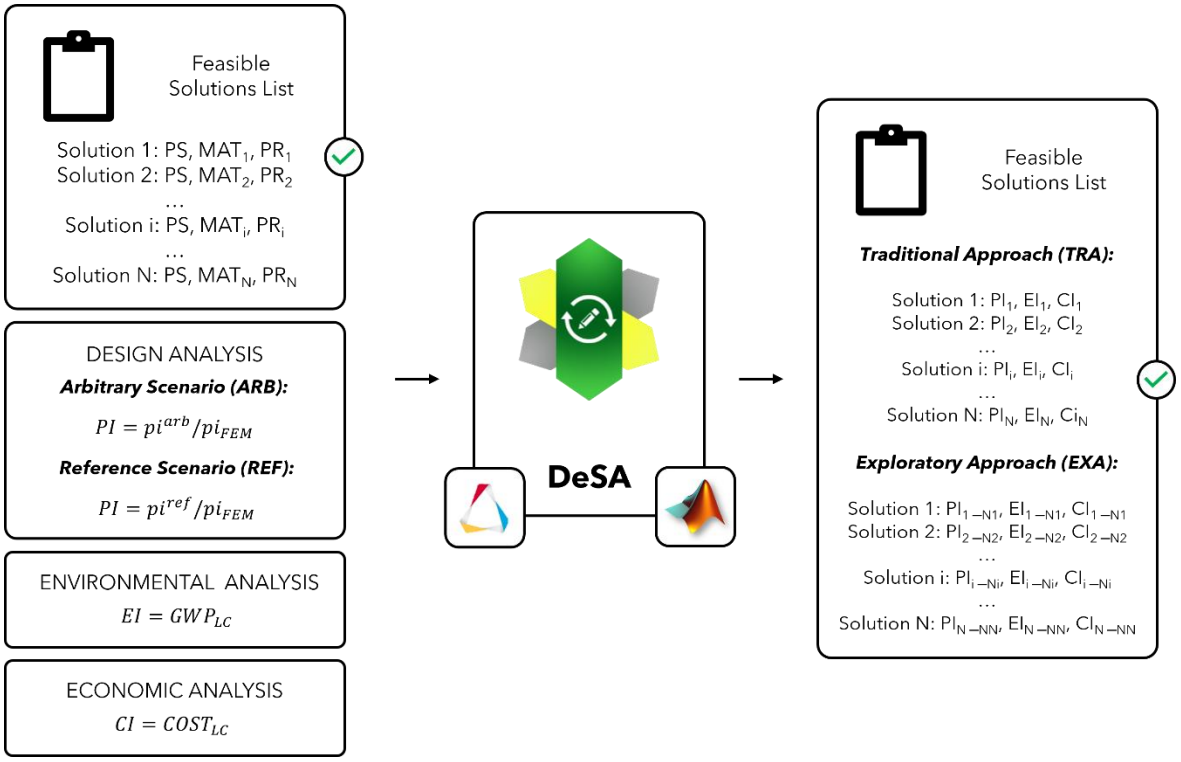

Figure 14. Design and Sustainability analysis phase framework.

Figure A.3, **Figure A.4**, and **Figure A.5** in the Appendix A show the GUI of the Design and Sustainability analysis phase described above (subdivided between Performance, Environmental, and Economic GUIs), developed by MATLAB App Designer software.

Table 16. Economic database overview.

Economic database		
	Traditional Approach (TRA)	**Exploratory Approach (EXA)**
LC setting parameters	mil_{veh} (vehicle model-based) ρ_{fuel} (fuel type-based) FRV (vehicle model-based) ERV (vehicle model-based) c_{fuel} (fuel type-based) c_{mix} (grid mix type-based)	
	SF_i (material-based) ϑ_i (material-based)	SF_{ij} (material-based) ϑ_{ij} (material-based)
Manufacturing cost values	f_i (manufacturing process-based) $c^{tool}{}_i$ (manufacturing process-based) $n^t{}_i$ (manufacturing process-based) n'_i (manufacturing process-based) $c^c{}_i$ (manufacturing process-based) L_i (manufacturing process-based) $t^{wo}{}_i$ (manufacturing process-based) $c^{or}{}_i$ (manufacturing process-based)	f_{ij} (manufacturing process-based) $c^{tool}{}_{ij}$ (manufacturing process-based) $n^t{}_{ij}$ (manufacturing process-based) n'_{ij} (manufacturing process-based) $c^c{}_{ij}$ (manufacturing process-based) L_{ij} (manufacturing process-based) $t^{wo}{}_{ij}$ (manufacturing process-based) $c^{or}{}_{ij}$ (manufacturing process-based)
Specific cost values	$c^{mat}{}_i$ (material-based) $c^{Disp}{}_i$ (material-based)	$c^{mat}{}_{ij}$ (material-based) $c^{Disp}{}_{ij}$ (material-based)
	$cons^{Shr}$ (material-based) $cons^{Sep}$ (material-based)	

Legend:
c^{mat}_i = mass-specific COST in material stage phase for solution S_i [EUR/kg]
$cons^{Shr}_i$ = mass-specific consumption of shredding phase for solution S_i [KWh/kg]
$cons^{Sep}_i$ = mass-specific consumption of separation phase for solution S_i [KWh /kg]
c^{Disp}_i = mass-specific COST of disposal phase for solution S_i [EUR/kg]
f_i = scrap fraction (the fraction of the starting material that ends up as sprues, risers, turnings, rejects, or waste) for solution S_i [-]
c^{tool}_i = COST of dedicated tooling applied to solution S_i [EUR]
n^{tool}_i = tool lifespan (number of units that a set of tooling can make before it has to be replaced) for solution S_i [-]
n'_i = production rate at which units are produced applied to solution S_i [pieces/h]
c^{cap}_i = Capital COST of equipment for solution S_i [EUR]
L_i = Load factor (the fraction of time for which the equipment is productive) for solution S_i [-]
t^{wo}_i = Capital write-off time for solution S_i [years]
c^{or}_i = Overhead rate (where the cost of labor, administration, general plant costs and energy are included) for solution S_i [EUR/h]
f_{ij} = scrap fraction (the fraction of the starting material that ends up as sprues, risers, turnings, rejects, or waste) for sub-solution S_{ij} [-]
c^{tool}_{ij} = Cost of dedicated tooling applied to sub-solution S_{ij} [EUR]
n^{tool}_{ij} = tool lifespan (number of units that a set of tooling can make before it has to be replaced) for sub-solution S_{ij} [-]
n'_{ij} = production rate at which units are produced applied to sub-solution S_{ij} [pieces/h]
c^{cap}_{ij} = Capital COST of equipment for sub-solution S_{ij} [EUR]
L_{ij} = Load factor (the fraction of time for which the equipment is productive) for sub-solution S_{ij} [-]
t^{wo}_{ij} = Capital write-off time for sub-solution S_{ij} [years]
c^{or}_{ij} = Overhead rate (where the cost of labor, administration, general plant costs and energy are included) for sub-solution S_{ij} [EUR/h]
c_{fuel} = fuel price (for ICEVs) [EUR/l]
c_{mix} = price of electrical mix grid production (for EVs) [EUR/kWh]
mil_{veh} = vehicle mileage [km]
ρ_{fuel} = fuel density [kg/l]
FRV = fuel reduction value [l/100km*100kg]
ERV = energy reduction value [kWh/100km*100kg]
SF_i = recycling substitution factor of generic solution S_i (quota of avoided primary production impact due to recycling) [-]
ϑ_i = share of fibers for generic solution S_i (composite materials) [-]
SF_{ij} = recycling substitution factor of generic sub-solution S_{ij} (quota of avoided primary production impact due to recycling) [-]
ϑ_{ij} = share of fibers for generic sub-solution S_{ij} (composite materials) [-]
c^{mat}_{ij} = mass-specific COST in material stage phase for generic sub-solution S_{ij} [EUR/kg]
$cons^{Shr}$ = mass-specific consumption of shredding phase [KWh/kg]
$cons^{Sep}$ = mass-specific consumption of separation phase [KWh /kg]
c^{Disp}_{ij} = mass-specific COST of disposal phase for generic sub-solution S_{ij} [EUR/kg]

Table 17. Economic modelling.

Life Cycle Equations				
		Traditional Approach (TRA)	**Exploratory Approach (EXA)**	
Production		$COST_i^{Prod} = COST_i^{Mat} + COST_i^{Man}$	$COST_{ij}^{Prod} = COST_{ij}^{Mat} + COST_{ij}^{Man}$	(35)
		$COST_i^{Mat} = (1+R) \cdot \frac{m_i \cdot c_i^{Mat}}{1-f_i}$	$COST_{ij}^{Mat} = (1+R) \cdot \frac{m_{ij} \cdot c_i^{Mat}}{1-f_{ij}}$	(36)
		$COST_i^{Man} = (1+R) \cdot \left(COST_i^{tool} + COST_i^{amm} + COST_i^{or}\right)$	$COST_{ij}^{Man} = (1+R) \cdot \left(COST_{ij}^{tool} + COST_{ij}^{amm} + COST_{ij}^{or}\right)$	(37)
		$COST_i^{tool} = \frac{c_i^{tool}}{n_i}\left\{int\left(\frac{n_i}{n_i^{tool}} + 0.51\right)\right\}$	$COST_{ij}^{tool} = \frac{c_{ij}^{tool}}{n_{ij}}\left\{int\left(\frac{n_{ij}}{n_{ij}^{tool}} + 0.51\right)\right\}$	(38)
		$COST_i^{amm} = \frac{1}{\dot{n}_i}\left(\frac{c_i^{cap}}{L_i \cdot t_i^{wo}}\right)$	$COST_{ij}^{amm} = \frac{1}{\dot{n}_{ij}}\left(\frac{c_{ij}^{cap}}{L_{ij} \cdot t_{ij}^{wo}}\right)$	(39)
		$COST_i^{or} = \frac{c_i^{or}}{\dot{n}_i}$	$COST_{ij}^{or} = \frac{c_{ij}^{or}}{\dot{n}_{ij}}$	(40)
Use		$COST_i^{Use} = COST_i^{prop} + COST_i^{ext} + COST_i^{main}$	$COST_{ij}^{Use} = COST_{ij}^{prop} + COST_{ij}^{ext} + +COST_{ij}^{main}$	(41)
	ICEVs	$COST_i^{prop} = \frac{EC_{comp_i} \cdot c_{fuel}}{\rho_{fuel}}$	$COST_{ij}^{prop} = \frac{EC_{comp_{ij}} \cdot c_{fuel}}{\rho_{fuel}}$	(42)
		$EC_{comp_i} = (FRV \cdot \rho_{fuel} \cdot m_i \cdot mil_{veh})/10000$	$EC_{comp_{ij}} = (FRV \cdot \rho_{fuel} \cdot m_{ij} \cdot mil_{veh})/10000$	(43)
	EVs	$COST_i^{prop} = EC_{comp_i} \cdot c_{mix}$	$COST_{ij}^{prop} = EC_{comp_{ij}} \cdot c_{mix}$	(42)
		$EC_{comp_i} = (ERV \cdot m_i \cdot mil_{veh})/10000$	$EC_{comp_{ij}} = (ERV \cdot m_{ij} \cdot mil_{veh})/10000$	(43)
		$COST_i^{ext} = 0$	$COST_{ij}^{ext} = 0$	(44)
		$COST_i^{main} = 0$	$COST_{ij}^{main} = 0$	(45)
EoL		$COST_i^{EoL} = COST_i^{Dis} + COST_i^{shr} + COST_i^{sep} + COST_i^{enr} + COST_i^{land} + COST_i^{rec}$	$COST_{ij}^{EoL} = COST_{ij}^{Dis} + COST_{ij}^{shr} + COST_{ij}^{sep} + COST_{ij}^{enr} + COST_{ij}^{land} + COST_{ij}^{rec}$	(46)
		$COST_i^{shr} = (1+R) \cdot m_i \cdot cons^{Shr} \cdot c_{mix}$	$COST_{ij}^{shr} = (1+R) \cdot m_{ij} \cdot cons^{Shr} \cdot c_{mix}$	(47)
		$COST_i^{sep} = (1+R) \cdot m_i \cdot cons^{Sep} \cdot c_{mix}$	$COST_{ij}^{sep} = (1+R) \cdot m_{ij} \cdot cons^{Sep} \cdot c_{mix}$	(48)
		$COST_i^{rec} = (1+R) \cdot \eta_{eff} \cdot m_i \cdot SF_i \cdot c_i^{Mat}$	$COST_{ij}^{rec} = (1+R) \cdot \eta_{eff} \cdot m_{ij} \cdot SF_{ij} \cdot c_{ij}^{Mat}$	(49)

Life Cycle Equations [CONTINUE]			
	Traditional Approach (TRA)	**Exploratory Approach (EXA)**	
EoL	$COST_i^{enr} = (1+R) \cdot m_i \cdot LHV^{enr} \cdot (1-\vartheta_i) \cdot c_{mix}$	$COST_{ij}^{enr} = (1+R) \cdot m_{ij} \cdot LHV^{enr} \cdot (1-\vartheta_{ij}) \cdot c_{mix}$	(50)
	$COST_i^{disp} = \begin{cases} (1+R) \cdot m_i \cdot c_i^{Disp} \cdot \vartheta_i \\ (1+R) \cdot (1-\eta_{eff}) \cdot m_i \cdot c_i^{Disp} \end{cases}$	$COST_{ij}^{disp} = \begin{cases} (1+R) \cdot m_i \cdot c_i^{Disp} \cdot \vartheta_i \\ (1+R) \cdot (1-\eta_{eff}) \cdot m_i \cdot c_i^{Disp} \end{cases}$	(51)
Life Cycle	$COST_i^{LC} = COST_i^{Mat} + COST_i^{Man} + COST_i^{Use} + COST_i^{EoL}$	$COST_{ij}^{LC} = COST_{ij}^{Mat} + COST_{ij}^{Man} + COST_{ij}^{Use} + COST_{ij}^{EoL}$	(52)
	$CI_i = COST_i^{LC}$	$CI_{ij} = COST_{ij}^{LC}$	(53)

Legend:
$COST^{Prod}_i$ = economic cost of the production phase for solution S_i [EUR].
$COST^{Mat}_i$ = economic cost of material stage phase for solution S_i [EUR].
$COST^{Man}_i$ = economic cost of the manufacturing process phase for solution S_i [EUR].
$COST^{tool}_i$ = economic cost of manufacturing tool for generic solution S_i [EUR].
$COST^{amm}_i$ = economic cost of amortization for generic solution S_i [EUR].
$COST^{or}_i$ = economic cost of overhead for generic solution S_i [EUR].
R = number of potential substitutions of the component (based on its durability) [-].
m_i = component mass for generic solution S_i [kg].
f_i = scrap fraction (the fraction of the starting material that ends up as sprues, risers, turnings, rejects, or waste) for solution S_i [-].
c^{tool}_i = Cost of dedicated tooling applied to solution S_i [EUR]
n^{tool}_i = tool lifespan (number of units that a set of tooling can make before it has to be replaced) for solution S_i [-]
n'_i = production rate at which units are produced applied to solution S_i [pieces/h]
c^{cap}_i = Capital COST of equipment for solution S_i [EUR]
L_i = Load factor (the fraction of time for which the equipment is productive) for solution S_i [-]
t^{wo}_i = Capital write-off time for solution S_i [years]
c^{or}_i = Overhead rate (where the cost of labor, administration, general plant costs and energy are included) for solution S_i [EUR/h]
$COST^{Use}_i$ = economic cost of the use stage phase for solution S_i [EUR].
$COST^{prop}_i$ = economic cost of propulsion system in the use stage phase for solution S_i [EUR].
$COST^{ext}_i$ = economic cost of externalities in use stage phase for solution S_i [EUR].
EC_{comp} = energy consumption during operation of component; [kg] for ICEVs, [kWh] for EVs.
$COST^{EoL}_i$ = economic cost of the end-of-life phase for solution S_i [kg CO_{2eq}].
$COST^{Dis}_i$ = economic cost of component disassembly phase for solution S_i [kg CO_{2eq}].
$COST^{Shr}_i$ = economic cost of component shredding phase for solution S_i [kg CO_{2eq}].

$COST^{Sep}_{i}$ = economic cost of shredded material component separation phase for solution S_i [kg CO_{2eq}].
$COST^{Rec}_{i}$ = economic cost of separated material component recycling phase for solution S_i [kg CO_{2eq}].
$COST^{Enr}_{i}$ = economic cost of post-separation material component energy recovery phase for solution S_i [kg CO_{2eq}].
LHV^{enr} = Lower heating value of post-separation material component [kWh].
$COST^{Disp}_{i}$ = economic cost of residual component disposal phase for solution S_i [kg CO_{2eq}].
$COST^{LC}_{i}$ = economic cost of LC component for solution S_i [EUR].
CI_i = cost index of LC for solution S_i [EUR].
$COST^{Prod}_{ij}$ = economic cost of the production phase for generic sub-solution S_{ij} [EUR].
$COST^{Mat}_{ij}$ = economic cost of material stage phase for generic sub-solution S_{ij} [EUR].
$COST^{Man}_{ij}$ = economic cost of the manufacturing process phase for generic sub-solution S_{ij} [EUR].
$COST^{tool}_{ij}$ = economic cost of manufacturing tool for generic sub-solution S_{ij} [EUR].
$COST^{amm}_{ij}$ = economic cost of amortization for generic sub-solution S_{ij} [EUR].
$COST^{or}_{ij}$ = economic cost of overhead for generic sub-solution S_{ij} [EUR].
m_{ij} = component mass for generic sub-solution S_{ij} [kg].
f_{ij} = scrap fraction (the fraction of the starting material that ends up as sprues, risers, turnings, rejects, or waste) for generic sub-solution S_{ij} [-].
c^{tool}_{ij} = Cost of dedicated tooling applied to sub-solution S_{ij} [EUR]
n^{tool}_{ij} = tool lifespan (number of units that a set of tooling can make before it has to be replaced) for sub-solution S_{ij} [-]
n'_{ij} = production rate at which units are produced applied to sub-solution S_{ij} [pieces/h]
c^{cap}_{ij} = Capital COST of equipment for sub-solution S_{ij} [EUR]
L_{ij} = Load factor (the fraction of time for which the equipment is productive) for sub-solution S_{ij} [-]
t^{wo}_{ij} = Capital write-off time for sub-solution S_{ij} [years]
c^{or}_{ij} = Overhead rate (where the cost of labor, administration, general plant costs and energy are included) for sub-solution S_{ij} [EUR/h]
$COST^{Use}_{ij}$ = economic cost of the use stage phase for sub-solution S_{ij} [EUR].
$COST^{Use}_{ij}$ = economic cost of the use stage phase for sub-solution S_{ij} [EUR].
$COST^{prop}_{ij}$ = economic cost of propulsion system in the use stage for sub-solution S_{ij} [EUR].
$COST^{ext}_{ij}$ = economic cost of externalities in use stage phase for sub-solution S_{ij} [EUR].
$COST^{EoL}_{ij}$ = economic cost of the end-of-life phase for sub-solution S_{ij} [kg CO_{2eq}].
$COST^{Dis}_{ij}$ = economic cost of component disassembly phase for sub-solution S_{ij} [kg CO_{2eq}].
$COST^{Shr}_{ij}$ = economic cost of component shredding phase for sub-solution S_{ij} [kg CO_{2eq}].
$COST^{Sep}_{ij}$ = economic cost of shredded material component separation phase for sub-solution S_{ij} [kg CO_{2eq}].
$COST^{Rec}_{ij}$ = economic cost of separated material component recycling phase for sub-solution S_{ij} [kg CO_{2eq}].
$COST^{Enr}_{ij}$ = economic cost of post-separation material component energy recovery phase for sub-solution S_{ij} [kg CO_{2eq}].
$COST^{LC}_{ij}$ = economic cost of LC component for generic sub-solution S_{ij} [EUR].
CI_{ij} = cost index of LC for generic sub-solution S_{ij} [EUR].

Table 18. Representation of solutions list created by screening phase, with PI, EL, EI, and CI indexes calculated for each solution S_i (or sub-solution S_{ij}).

List of Feasible Solutions						
Sol.	**Char.**	**N**	**Appr.**	**Design**	**Environment**	**Economy**
				PI, EL	**EI**	**CI**
S_1	MAT_1 PR_1 PS	N_1	TRA	PI_1 EL_1	EI_1	CI_1
			EXA	$[PI_{11}, \ldots, PI_{1N1}]$ $[EL_{11}, \ldots, EL_{1N1}]$	$[EI_{11}, \ldots, EI_{1N1}]$	$[CI_{11}, \ldots, CI_{1N1}]$
S_2	MAT_2 PR_2 PS	N_2	TRA	PI_2 EL_2	EI_2	CI_2
			EXA	$[PI_{21}, \ldots, PI_{2N2}]$ $[EL_{21}, \ldots, EL_{2N2}]$	$[EI_{21}, \ldots, EI_{2N2}]$	$[CI_{21}, \ldots, CI_{2N2}]$
…	…	…	…	…	…	…
S_i	MAT_i PR_i PS	N_i	TRA	PI_i EL_i	EI_i	CI_i
			EXA	$[PI_{i1}, \ldots, PI_{iNi}]$ $[EL_{i1}, \ldots, EL_{iNi}]$	$[EI_{i1}, \ldots, EI_{iNi}]$	$[CI_{i1}, \ldots, CI_{iNi}]$
…	…	…	…	…	…	…
S_N	MAT_N PR_N PS	N_N	TRA	PI_N EL_N	EI_N	CI_N
			EXA	$[PI_{N1}, \ldots, PI_{NNN}]$ $[EL_{N1}, \ldots, EL_{NNN}]$	$[EI_{N1}, \ldots, EI_{NNN}]$	$[CI_{N1}, \ldots, CI_{NNN}]$

Legend:
Sol. = list of solution (S) obtained from Screening phase;
Char. = main characteristics of generic solution S_i (i.e., material (MAT_i), manufacturing process (PR_i), and primary shape (PS);
N = Number of simulations for generic solution S_i, considered the EX approach
Appr. = Typology of approach used in Design and Sustainability analysis phase (i.e., Exploratory approach – EXA; Traditional approach - TRA)
PI = performance index for generic solution S_i (or sub-solution S_{ij}).
EL = elasticity for generic solution S_i (or sub-solution S_{ij}).
EI = environmental index of LC for generic solution S_i (or sub-solution S_{ij}).
CI = cost index of LC for generic solution S_i (or sub-solution S_{ij}).

2.3. First Classification

Once the Design and Sustainability analysis is performed for the solutions S_i (or sub-solutions S_{ij}), the first classification phase is carried out by means of the following steps: PSL calculation, elasticity screening and first ranking.

2.3.1 PSL calculation

The PSL index is calculated based on MCDA methods (Wang et al, 2009), which allows calculating a tailored overall efficiency score for each design alternative. The evaluation is performed on the basis of the relative importance of measurable data, and it is carried out by means of three main steps (i.e., normalization, weighting, and aggregation) according to the modelling framework reported in **Table 19** (**Equations 54-57**):

Table 19. PSL modelling.

PSL Equations				
		Traditional Approach (TRA)	**Exploratory Approach (EXA)**	
Product Sustainability Level		$PSL_i = K \cdot \sum_{p=1}^{N_p} \frac{w_p}{I_{Ni}^p}$	$PSL_{ij} = K \cdot \sum_{p=1}^{N_p} \frac{w_p}{I_{Nij}^p}$	(54)
Design and Sustainability Indexes Normalized	**Arbitrary Scenario (ARB)**	$I_{Ni}^p = I_i^p / I_i^{p(max)}$	$I_{Nij}^p = I_{ij}^p / I_{ij}^{p(max)}$	(55)
	Reference Scenario (REF)	$I_{Ni}^p = I_i / I^{p(ref)}$	$I_{Nij}^p = I_{ij} / I^{p(ref)}$	(56)
Weights		$\sum_{p=1}^{N_p} w_p = 1$		(57)

Legend:
PSL_i = Product Score Level for generic solution S_i [-].
PSL_{ij} = Product Score Level for sub-solution S_{ij} in EX approach [-].
N_p = number of pillars used for PSL calculation (i.e., design, environment, economy; p = 1, …, 3) [-];
K = PSL scale factor, chosen by the designer [-].
w_p = the weighting factor for p-th pillar for the PSL modelling (design, environment, economy) [-];
I^p_{Ni} = the normalized index for p-th pillar for generic solution S_i in TR approach [-].
I^p_{Nij} = the normalized index for p-th pillar for sub-solution S_{ij} in EX approach [-].
I^p_i = the index for p-th pillar for generic solution S_i modelling (i.e., design, environment and economy) in TR approach [-].
I^p_{ij} = the index for p-th pillar for sub-solution S_{ij} modelling (i.e., design, environment and economy) in EX approach [-].
$I^{p(max)}_i$ = the highest value of the p-th index for generic solution S_i in TR approach [-].
$I^{p(max)}_{ij}$ = the highest value of the p-th index for sub-solution S_{ij} in EX approach [-].
$I^{p(ref)}$ = the value of the p-th index for reference solution in TR and EX approach [-].

Physical data collected for each pillar cannot be summed up together directly, due to the inconsistency of units of measurements. Different indicators have different physical dimensions (units): then, the values of these indicators need to be scaled into dimensionless values such that they can be analyzed and compared. This process is called normalization; in general, there are different statistical methods that can be used for this phase, but in this context, two methods can be used. As described in the design analysis phase, two scenarios were defined in the methodology (i.e., ARB and REF), with four total combinations. Regardless of the type of design approach, in the arbitrary scenario (ARB) the normalization is performed through the "Max method" (Celen, 2014; Vafaei, 2016), which provides that design and sustainability indexes are normalized using the maximum value obtained from each index, according to **Equation 55**. Instead, in the reference scenario (REF) the normalization is performed through a method similar to the "Max method", where the design and sustainability indexes are normalized using the values coming from the existing reference solution, according to **Equation 56**.

As regards the weighting, several methods are commonly used, which are: equal weighting, subjective weighting (such as analytic hierarchy process (AHP)), and weighting

from analytical approaches. To compare the sustainability performance of several product solutions by mean of the proposed framework, an equal weight is assigned to all measurements, since it is assumed that all elements have the same level of importance (**Equation 57**). In the score aggregation step, the normalized data are systematically aggregated into a single score using the weights and the normalized indexes defined above (see **Equation 54**).

2.3.2 First Elasticity screening

The target of this step is identifying the list of acceptable design solutions (S^{acc}), defined as all solutions that at the same time satisfy elasticity requirements and are feasible from a technological point of view. The application of this phase varies depending on the information available to the designer, i.e., if the materials (as well as manufacturing process, etc…) considered in the production database are specific (TR approach) or ranges-defined (EX approach), and if the design scenario is designer- or reference-defined (ARB scenario and REF scenario, respectively).

Concerning the TR approach, this phase provides that the PSL, and EL of each solution S_i are defined through constant values obtained in Design and Sustainability phase (see the following model):

$$S_i \rightarrow \begin{Bmatrix} PSL_i \\ \\ EL_i \end{Bmatrix} TR\ Approach$$

Concerning the EX approach, this phase instead provides that the range of PSL and EL of each solution S_i is defined through the minimum and maximum values obtained for the sub-alternatives S_{ij}, according to the following model:

$$S_i \rightarrow \begin{Bmatrix} \{PSL_{i1}, \dots, PSL_{ij}\} \rightarrow PSL_i = [min(PSL_{ij}), max(PSL_{ij})] \\ \\ \{EL_{i1}, \dots, EL_{ij}\} \rightarrow EL_i = [min(EL_{ij}), max(EL_{ij})] \end{Bmatrix}$$

There are 4 combinations of the approaches/scenarios defined by the DeSA methodology and are shown in **Table 20**. The next subparagraphs will describe each combination.

Table 20. Combination of approaches (TRA, EXA) and scenarios (ARB, REF) defined in the proposed methodology.

Approaches/Scenarios Combinations		
	Arbitrary Scenario (ARB)	**Reference Scenario (REF)**
Traditional Approach (TRA)	[1] TRA - ARB	[2] TRA - REF
Explorative Approach (EXA)	[3] EXA - ARB	[4] EXA - REF

2.3.2.1 *TRA – ARB Combination*. Once PSL_i and EL_i are obtained according to the TR approach, the screening step envisages that:

- all solutions are represented through points in a PSL-EL "Point chart" (**Figure 15**);
- an ELasticity Value (ELV) is defined, which divides the point chart into two distinct zones (**Figure 15**): acceptable zone (A-zone), where EL is higher than ELV, and non-acceptable zone (B-zone), where EL is lower than ELV. The framework provides that ELV parameter is fixed by the designer, to leave the practitioner the possibility to set acceptability threshold values customized for the specific application or case study;
- the solutions that fall within the A-zone are considered as full acceptable solutions (S^{acc}_i) and they are considered in the first ranking step;
- the solutions that fall within the B-zone are considered as non-acceptable solutions and they are discarded since they do not fulfil the design requirements.

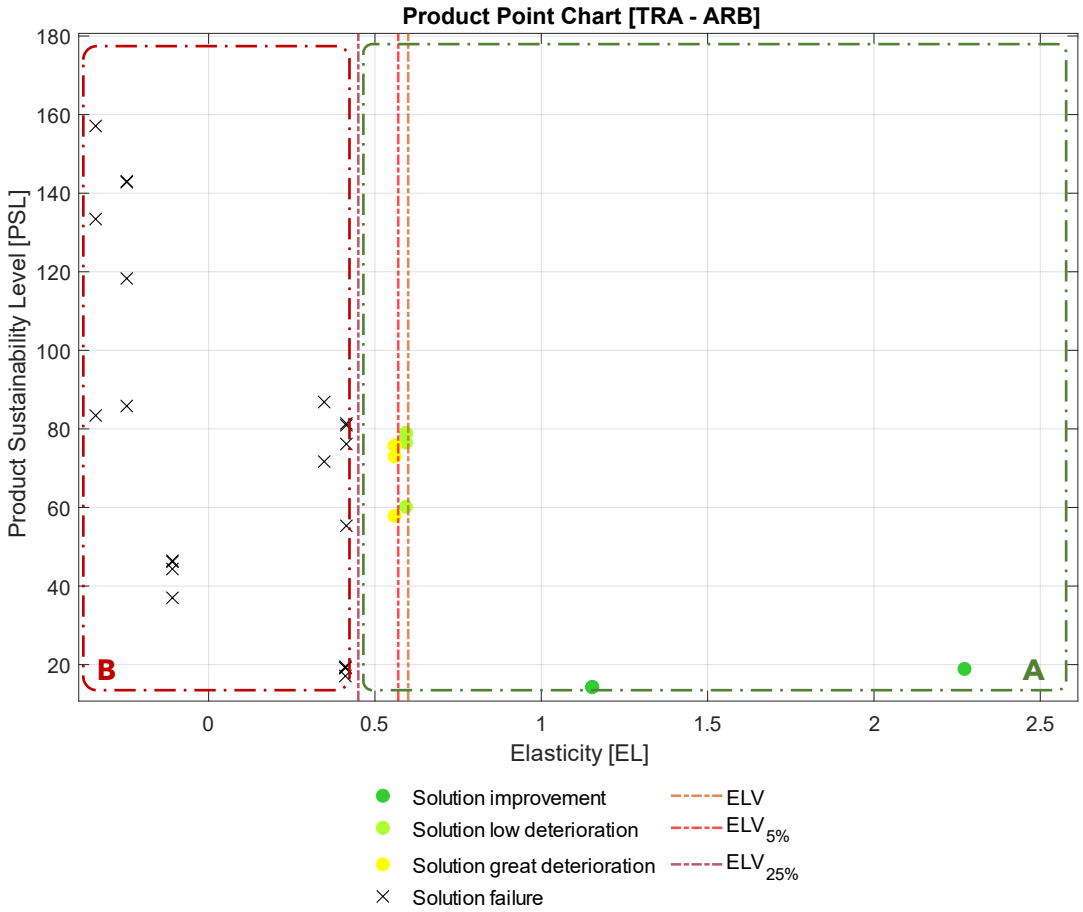

Figure 15. Example of point chart of design alternatives with ELV = 0.6; cross points represent discarded solutions.

If the generic solution S_i falls close to ELV, the solution is accepted or discarded depending on the acceptability threshold (AT), set by the designer. AT is defined by means of percentages compared to the ELV, according to scheme in **Table 21** (**Equations 58-61**):

- Solution failure (**Equation 58**): the solutions, whose EL_i is reduced by at least 25% compared to ELV, are discarded and they are not considered in the first ranking phase (cross points in **Figure 15**);
- Solution great deterioration (**Equation 59**): when the reduction of EL_i is between 5% and 25% respect to ELV, the solution is partially accepted and considered in the first ranking phase (yellow points in **Figure 15**).
- Solution low deterioration (**Equation 60**): when the reduction of EL_i is between 0% and 5% respect to ELV, the solution is accepted (since the solution's design performance is considered equal to the arbitrary limit imposed by the designer). Thus, the solution is evaluated during the first ranking phase (light green points plotted in **Figure 15**).
- Solution improvement (**Equation 61**): the solutions whose EL_i is close to ELV vertical line are accepted and evaluated during the first ranking phase (dark green points plotted in **Figure 15**).

Table 21. Acceptability threshold scheme in TRA-ARB combination.

Legend	AT Percentage Value	
Solution failure	$EL_i \leq ELV \cdot (1 - 0.25)$	(58)
Solution great deterioration	$ELV \cdot (1 - 0.25) < EL_i < ELV \cdot (1 - 0.05)$	(59)
Solution low deterioration (equal)	$ELV \cdot (1 - 0.05) < EL_i < ELV$	(60)
Solution improvement	$EL_i \geq ELV$	(61)

2.3.2.2 TRA – REF Combination. PSL_i and EL_i are obtained using the TR approach; thus, the screening phase provides that:

- all solutions are always represented through points in a PSL-EL "Point chart" (as shown in **Figure 16**);
- a Reference ELasticity Value (ELV^{ref}) is defined, which divides the point chart into two distinct zones (**Figure 16**): acceptable zone (A-zone), where EL is higher than ELV^{ref}, and non-acceptable zone (B-zone), where EL is lower than ELV^{ref}. The framework provides that ELV^{ref} parameter is obtained from the existing reference solution (automatically calculated by DeSA methodology);
- a Reference Product Sustainability Level Value ($PSLV^{ref}$) can be defined, which divides the point chart into two distinct zones (**Figure 16**): sustainable zone (C-zone), where PSL is higher than $PSLV^{ref}$, and non-sustainable zone (D-zone), where PSL is lower than $PSLV^{ref}$. The framework provides that $PSLV^{ref}$ parameter is automatically obtained by methodology from the existing reference solution;
- the solutions that fall within the A-zone are considered as full acceptable solutions (S^{acc}_i) and they are considered in the first ranking step;
- the solutions that fall within the B-zone are considered as non-acceptable solutions and they are discarded since they do not fulfil the design requirements.

Similar to the previous subparagraph, if the generic solution S_i falls close to ELV^{ref}, the solution is accepted or discarded depending on the acceptability threshold (AT).

However, the definition of these thresholds is obtained from the existing reference solution. Thus, AT is defined by means of percentages compared to the ELV^{ref}, according to the scheme in **Table *22*** (**Equations 62-65**):

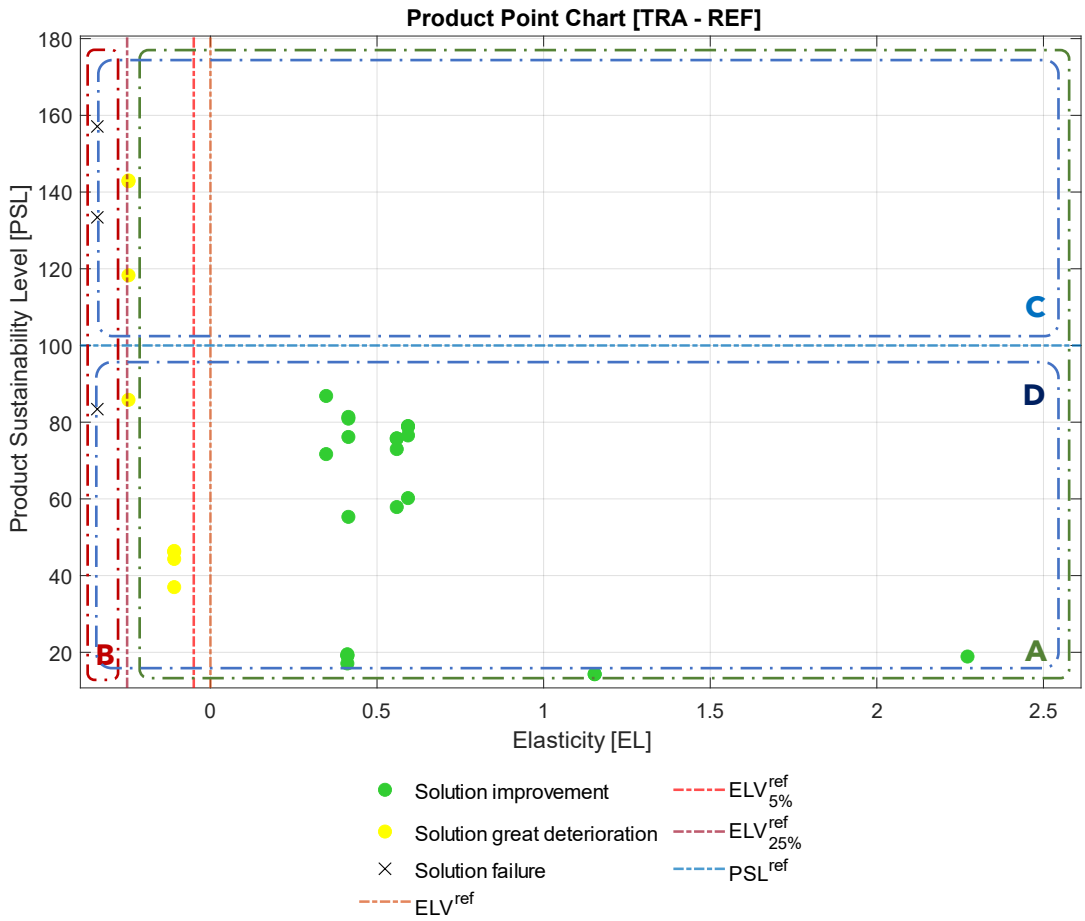

Figure 16. Example of point chart of design alternatives with $ELV^{ref} = 0$ and $PSL^{ref} = 100$; cross points represent discarded solutions.

- Solution failure (**Equation 62**): the solutions, whose EL_i is reduced by at least 25% compared to ELV^{ref}, are discarded and they are not considered in the first ranking phase (cross points in **Figure 16**);
- Solution great deterioration (**Equation 63**): when the reduction of EL_i is between 5% and 25% respect to ELV^{ref}, the solution is partially accepted and considered in the first ranking phase (yellow points in **Figure 16**).
- Solution low deterioration (**Equation 64**): when the reduction of EL_i is between 0% and 5% respect to ELV^{ref}, the solution is accepted (since the solution's design performance is considered equal to the reference solution). Thus, the solution is evaluated during the first ranking phase (light green points plotted in **Figure 16**).
- Solution improvement (**Equation 65**): the solutions whose EL_i is close to ELV^{ref} vertical line are accepted and evaluated during the first ranking phase (dark green points plotted in **Figure 16**).

Table 22. Acceptability threshold scheme in TRA-REF combination.

Legend	AT Percentage Value	
Solution failure	$EL_i \leq ELV^{ref} \cdot (1 - 0.25)$	(62)
Solution great deterioration	$ELV^{ref} \cdot (1 - 0.25) < EL_i < ELV^{ref} \cdot (1 - 0.05)$	(63)
Solution low deterioration (equal)	$ELV^{ref} \cdot (1 - 0.05) < EL_i < ELV^{ref}$	(64)
Solution improvement	$EL_i \geq ELV^{ref}$	(65)

2.3.2.3 EXA – ARB Combination. Once PSL_i and EL_i are obtained according to the EX approach, the screening phase envisages that:

- all solutions are represented through ellipses in a PSL-EL "bubble chart" (as shown in Figure *17.* Example of bubble chart of design alternatives with ELV = 0.6 and FL = 1 (in EXA – ARB combination). Dashed grey bubbles represent discarded solutions. **Figure 17** and **Figure 18**);
- an ELasticity Value (ELV) is defined, which divides the bubble chart into two distinct zones (**Figure 17**): acceptable zone (A-zone), where EL is higher than ELV, and non-acceptable zone (B-zone), where EL is lower than ELV. The framework provides that ELV parameter is fixed by the designer, to leave the practitioner the possibility to set acceptability threshold values customized for the specific application;
- the solutions that fall within the A-zone are considered as full acceptable solutions (S^{acc}_i) and they are considered in the first ranking step;
- the solutions that fall within the B-zone are considered as non-acceptable solutions and they are discarded since they do not fulfil the design requirements.

If the generic solution S_i falls in both zones, the solution is accepted or discarded depending on the filtering level (FL) set by the designer (**Equations 66-69**):

$$\%EL_i^{right} \gtreqless FL \tag{66}$$

$$\%EL_i^{right} = \frac{diff_i^{range}}{EL_i^{range}} \tag{67}$$

$$diff_i^{range} = \left(EL_{ij}\right) - \text{ELV} \tag{68}$$

$$EL_i^{range} = max\left(EL_{ij}\right) - min\left(EL_{ij}\right) \tag{69}$$

Where:
$\%EL^{right}_i$ = elasticity range percentage to the right of elasticity value (ELV) [-];
EL^{range}_i = elasticity range of solution Si [-];
$diff^{range}_i$ = elasticity range of solution Si to the right of elasticity value (ELV) [-];
FL = Filtering level (defined by the designer) [-];
ELV = Elasticity value (defined by the designer) [-].

- if EL^{right} < FL, the solutions whose bubble is crossed by ELV vertical line are discarded and they are not considered in the first ranking phase (see dashed grey bubbles shown in **Figure 17** and Figure *18*);
- if EL^{right} >= FL, the solutions whose bubble is crossed by ELV vertical line are accepted and considered in the first ranking phase (see green and yellow bubbles shown in **Figure 17** and Figure *18*);

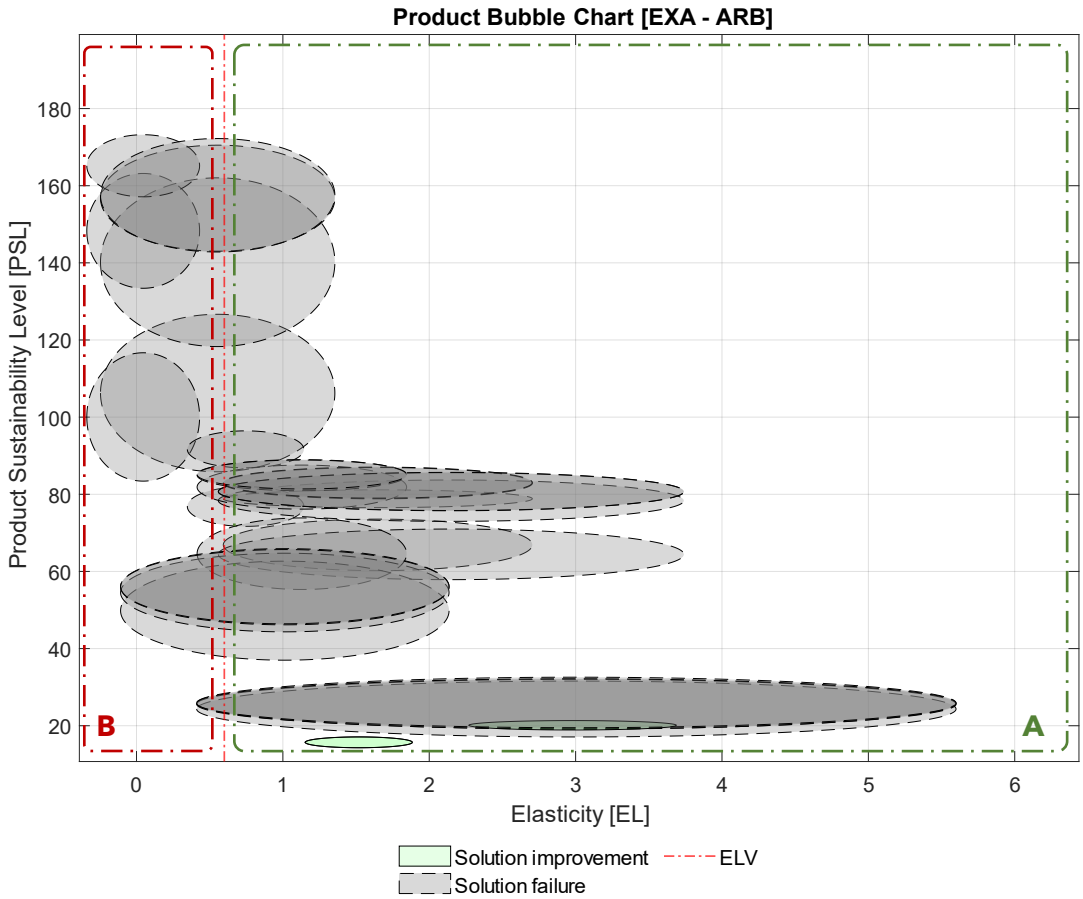

Figure 17. Example of bubble chart of design alternatives with ELV = 0.6 and FL = 1 (in EXA – ARB combination). Dashed grey bubbles represent discarded solutions.

Figure 17 and Figure *18* show an exemplifying case study where ELV is assumed equal to 0.5. Considering **Figure 17**, the FL value is assumed equal to 1 (i.e., 100%): in this case all solutions whose bubble is crossed by ELV vertical line are not considered. Whereas in the **Figure 18**, the FL value is assumed equal to 0.5 (i.e., 50%) and the solutions having at least half of the EL range to the right of ELV vertical line are accepted and they are considered in the next step of classification.

2.3.2.4 <u>EXA – REF Combination.</u> In this final typology, PSL_i and EL_i are obtained using the EX approach; thus, the screening step provides that:

- all solutions are represented through ellipses in a PSL-EL "bubble chart" (as shown in **Figure 19** and **Figure 20**);

- a Reference ELasticity Value (ELV^{ref}) is defined, which divides the bubble chart into two distinct zones (**Figure 19**): acceptable zone (A-zone), where EL is higher than ELV^{ref}, and non-acceptable zone (B-zone), where EL is lower than ELV^{ref}. The framework provides that ELV^{ref} parameter is obtained from the existing reference solution (automatically calculated by DeSA methodology);

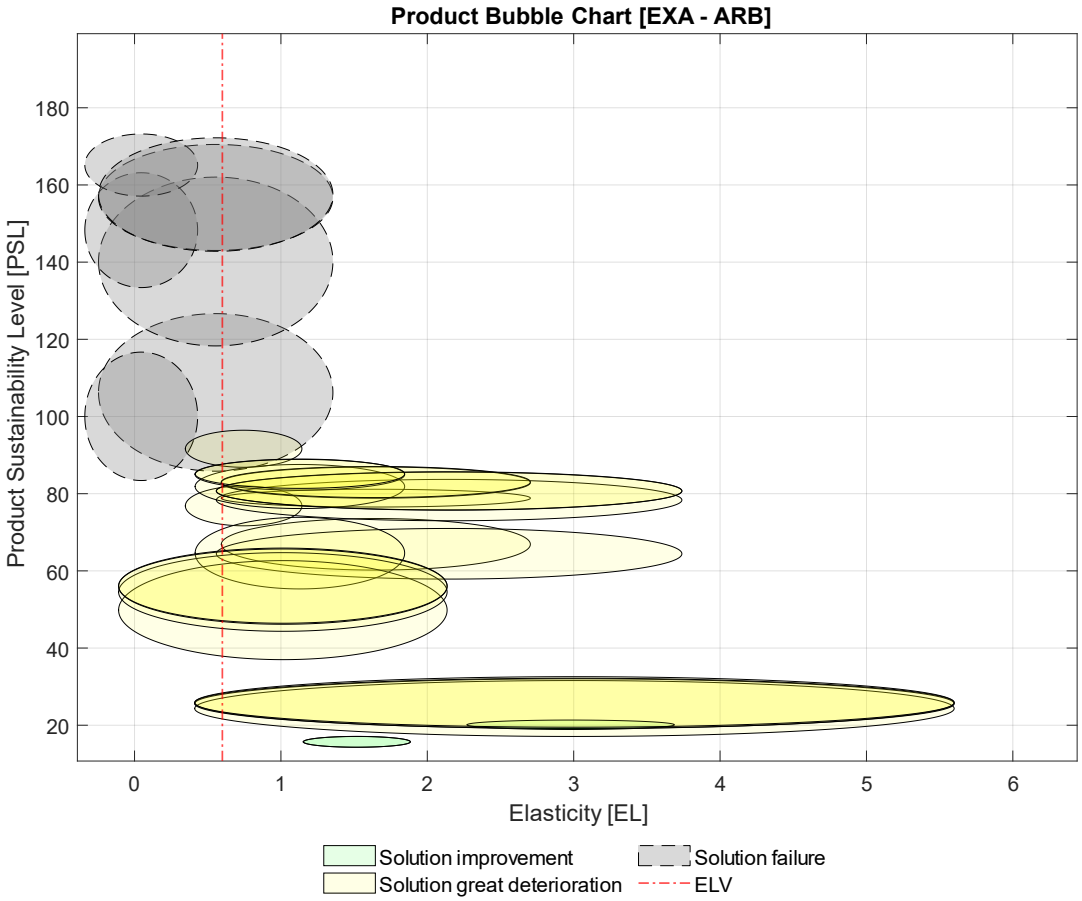

Figure 18. Example of bubble chart of design alternatives with ELV = 0.6 and FL = 0.5 (in EXA – ARB combination). Dashed grey bubbles represent discarded solutions.

- a Reference Product Sustainability Level Value ($PSLV^{ref}$) can be defined, which divides the bubble chart into two distinct zones (**Figure 19**): sustainable zone (C-zone), where PSL is higher than $PSLV^{ref}$, and non-sustainable zone (D-zone), where PSL is lower than $PSLV^{ref}$. The framework provides that $PSLV^{ref}$ parameter is automatically obtained by methodology from the existing reference solution;
- the solutions that fall within the A-zone are considered as full acceptable solutions (S^{acc}_i) and they are considered in the first ranking step;
- the solutions that fall within the B-zone are considered as non-acceptable solutions and they are discarded since they do not fulfil the design requirements.

Similar to the previous subparagraph, if the generic solution S_i falls in both zones, the solution is accepted or discarded depending on the FL set by the designer (**Equations 70-73**). However, the ELV^{ref} is used for the calculation (see **Equation 72**):

$$\%EL_i^{right} \lesseqgtr FL \tag{70}$$

$$\%EL_i^{right} = \frac{diff_i^{range}}{EL_i^{range}} \tag{71}$$

$$diff_i^{range} = \left(EL_{ij}\right) - ELV^{ref} \tag{72}$$

$$EL_i^{range} = max\left(EL_{ij}\right) - min\left(EL_{ij}\right) \tag{73}$$

Where:
$\%EL^{right}_i$ = elasticity range percentage to the right of elasticity value (ELV) [-];
EL^{range}_i = elasticity range of solution Si [-];
$diff^{range}_i$ = elasticity range of solution Si to the right of elasticity value (ELV) [-];
FL = Filtering level (defined by the designer) [-];
ELV^{ref} = Reference Elasticity value (defined by reference scenario) [-].

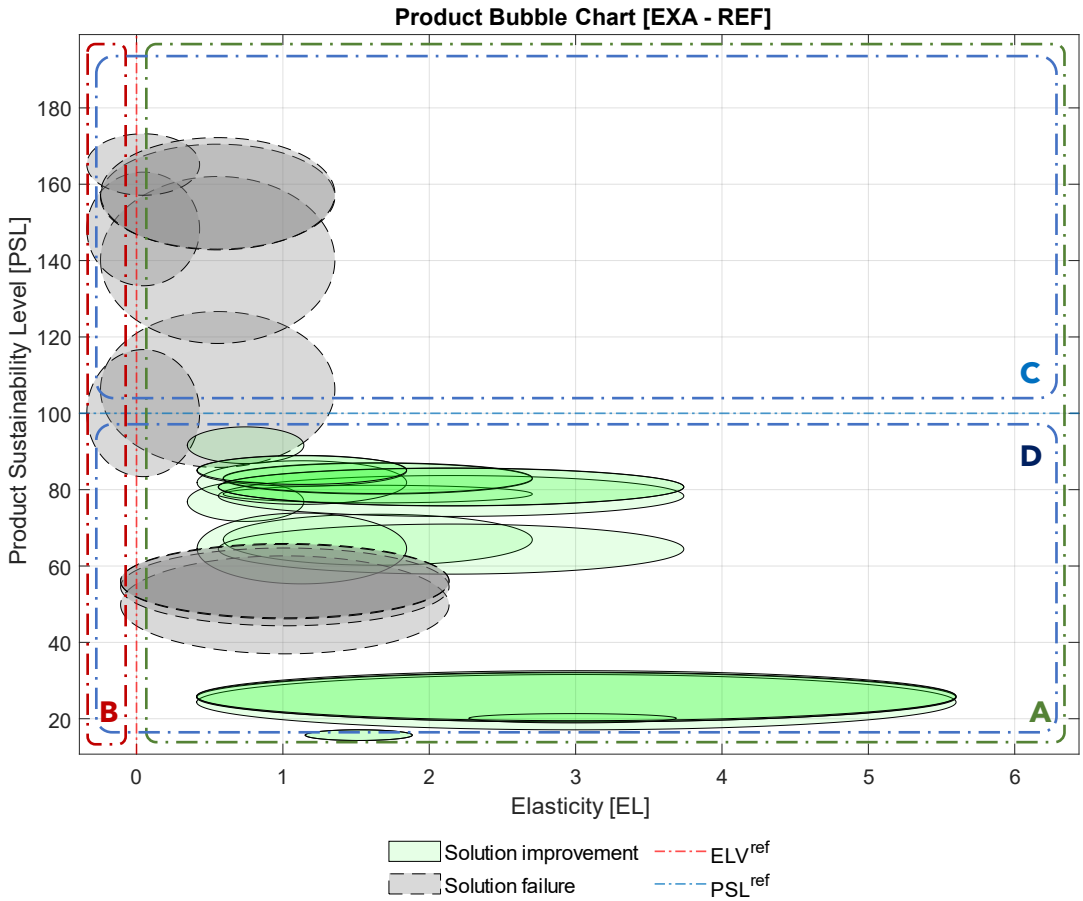

Figure 19. Example of bubble chart of design alternatives with ELV^{ref} = 0 and FL = 1 (in EXA – REF combination). Dashed grey bubbles represent discarded solutions.

- if EL^{right} < FL, the solutions whose bubble is crossed by ELV vertical line is discarded and it is not considered in the final ranking phase (see dashed grey bubbles shown in **Figure 19** and **Figure 20**);

- if EL^{right} >= FL, the solutions whose bubble is crossed by ELV vertical line is accepted and considered in the final ranking phase (see green and yellow bubbles shown in **Figure 19** and **Figure 20**).

Figure 19 and **Figure 20** show an exemplifying case study where ELV^{ref} is assumed equal to 0.5. Considering **Figure 19**, the FL value is assumed equal to 1 (i.e., 100%): in this case all solutions whose bubble is crossed by ELV^{ref} vertical line are not considered. Instead, the FL value is assumed equal to 0.5 (i.e., 50%) in **Figure 20**; thus, the solutions having at least half of the EL range to the right of ELV^{ref} vertical line are accepted and they are considered in the next step of classification.

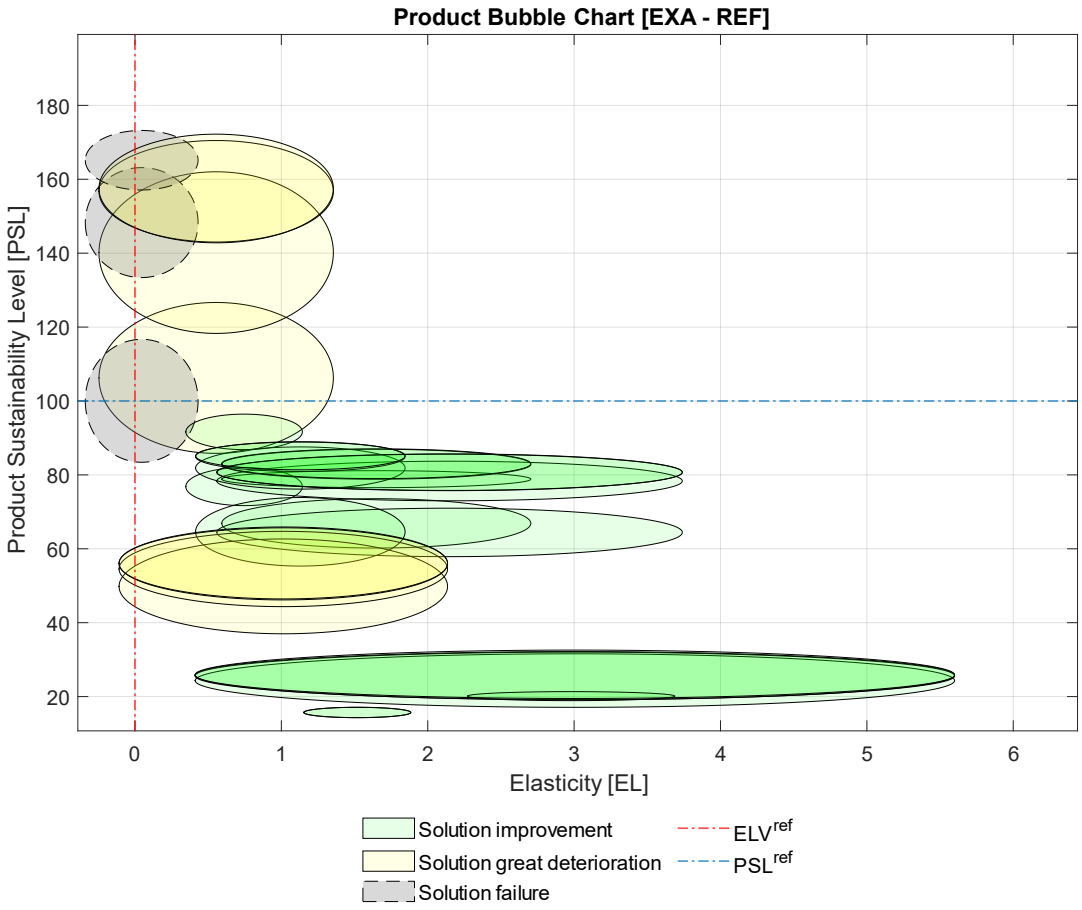

Figure 20. Example of bubble chart of design alternatives with ELV^{ref} = 0 and FL = 0.7 (in EXA – REF combination). Dashed grey bubbles represent discarded solutions.

The overall phase is performed according to overview reported in **Figure 21**, where MATLAB allows the screening of solutions thanks to one of above approaches, obtaining the acceptable solution S^{acc}_i (see Table *23*). The number of acceptable solution (N^{acc}) is comprised between:

$$0 \leq N^{acc} \leq N$$

Figure A.1 in the Appendix A shows the GUI of the Approaches/Scenarios setting phase described above, developed by MATLAB App Designer software; whereas **Figure A.6** shows the GUI of the first elasticity screening phase.

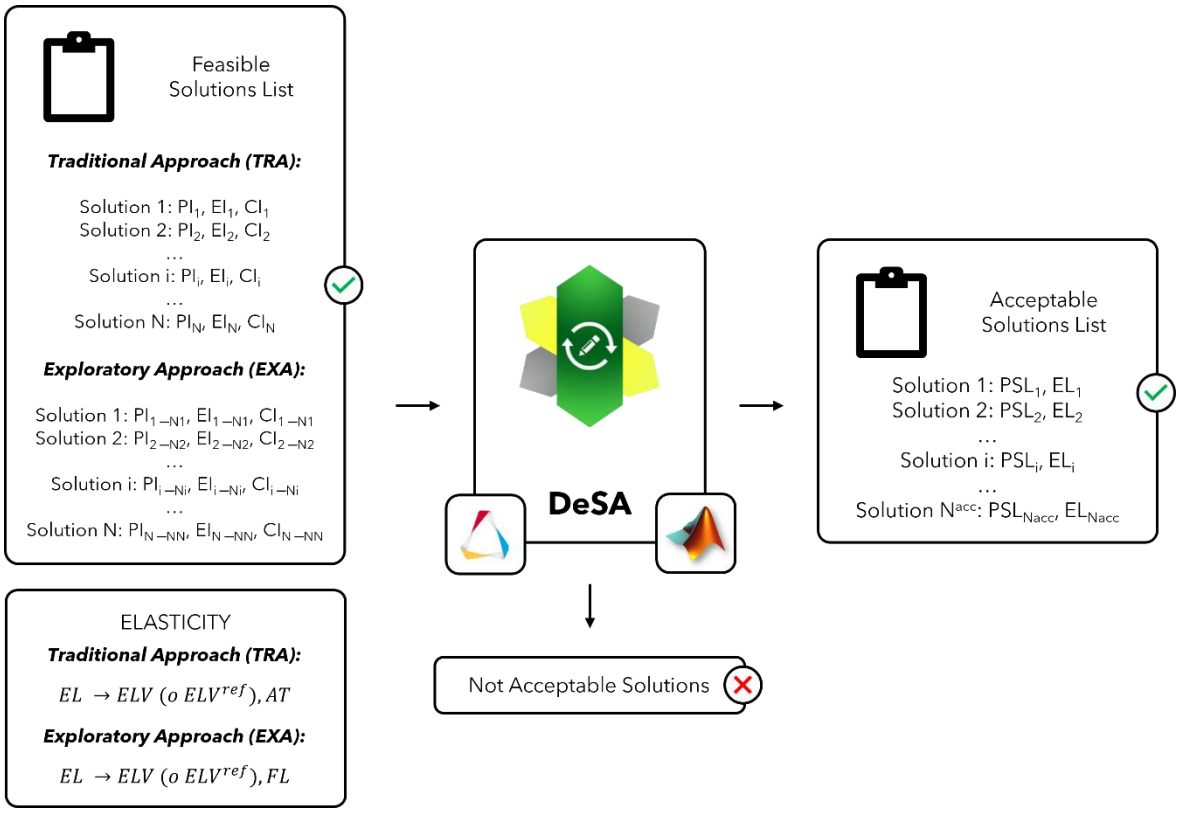

Figure 21. Overview of first elasticity screening phase.

Table 23. Representation of solutions list screening, with PSL, EL, and elasticity screening calculated for each solution S_i.

List of Solutions					
Sol.	**N**	**Appr.**	**PSL**	**EL**	**First Elasticity Screening**
S_1	N_1	TRA	PSL_1	EL_1	YES
		EXA	$[PSL_{11}, \ldots, PSL_{1N1}]$	$[EL_{11}, \ldots, EL_{1N1}]$	
S_2	N_2	TRA	PSL_2	EL_2	NO
		EXA	$[PSL_{21}, \ldots, PSL_{2N2}]$	$[EL_{21}, \ldots, EL_{2N2}]$	
…	…	…	…	…	NO
S_i	N_i	TRA	PSL_i	EL_i	YES
		EXA	$[PSL_{i1}, \ldots, PSL_{iNi}]$	$[EL_{i1}, \ldots, EL_{iNi}]$	
…	…	…	…	…	NO
S_N	N_N	TRA	PSL_N	EL_N	YES
		EXA	$[PSL_N, \ldots, PSL_{NNN}]$	$[EL_{N1}, \ldots, EL_{NNN}]$	

Legend:
Sol. = list of solution (S) obtained from Screening phase;
N = Number of simulations for generic solution S_i, considered the EX approach
Appr. = Typology of approach used in Design and Sustainability analysis phase (i.e., Exploratory approach – EXA; Traditional approach - TRA)
PSL = product sustainability level for generic solution S_i (or sub-solution S_{ij}).
EL = elasticity for generic solution S_i (or sub-solution S_{ij}).

2.3.3 First ranking

In the last phase, the PSL values of the acceptable solutions S^{acc}_i are compared, and the first ranking is compiled. As already mentioned, the solutions that do not pass the elasticity screening step are not taken into account in this phase.

The first ranking varies depending on the information available to the designer, i.e., if the data considered in the production database are specific- (TR approach) or ranges-defined (EX approach).

- Concerning the TR approach, the phase provides that the PSL of each solution is used directly; thus, the acceptable solutions $S^{acc}i$ are ranked from best to worst through their PSL value (see **Equation 74** in **Table 24**).
- Since in the EX approach each solution is characterized by a PSL range, the first ranking is done by means of the average value of such a range, as defined by **Equation 75** in **Table 24**. The acceptable solutions S^{acc}_i are finally ranked from best to worst through the value PSL^{rank} index calculated for each bubble.

Table 24. PSL ranking modelling.

PSL ranking equations		
Traditional Approach (TRA)	$PSL_i^{rank} = PSL_i$	(74)
Exploratory Approach (EXA)	$PSL_i^{rank} = mean(PSL_i) = \frac{(max(PSL_i) - min(PSL_i))}{2}$	(75)

Where:
PSL^{rank}_i = Product Sustainability Level for generic and acceptable solution S^{acc}_i evaluated for first ranking [-].

The first ranking phase is performed according to scheme reported in **Figure 22**, where MATLAB allows the classification of indexes previously defined (i.e., PSL^{rank}) for each acceptable solution S^{acc}_i obtained in the elasticity screening phase (see **Table 25**).

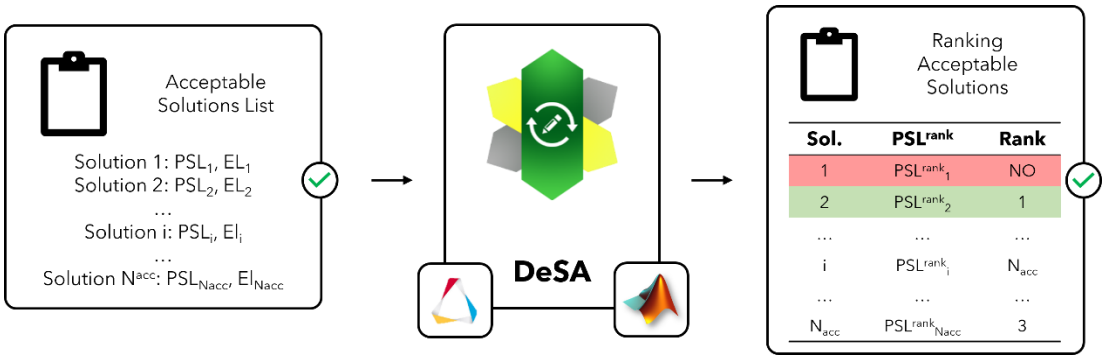

Figure 22. First ranking phase framework.

Table 25. Representation of acceptable solutions list ranking, with PSL, EL, and PSL^{rank} indexes calculated for each solution S^{acc}_i.

List of Acceptable Solutions						
Sol.	**N**	**Appr.**	**PSL**	**EL**	**PSL^{rank}**	**Ranking**
S^{acc}_1	N_1	TRA EXA	PSL_1 $[PSL_{11}, \ldots, PSL_{1N1}]$	EL_1 $[EL_{11}, \ldots, EL_{1N1}]$	PSL^{rank}_1	2
S^{acc}_2	N_2	TRA EXA	PSL_2 $[PSL_{21}, \ldots, PSL_{2N2}]$	EL_2 $[EL_{21}, \ldots, EL_{2N2}]$	PSL^{rank}_2	1
…	…	…	…	…	…	…
S^{acc}_i	N_i	TRA EXA	PSL_i $[PSL_{i1}, \ldots, PSL_{iNi}]$	EL_i $[EL_{i1}, \ldots, EL_{iNi}]$	PSL^{rank}_i	N_{acc}
…	…	…	…	…	…	…
S^{acc}_{Nacc}	N_{Nacc}	TRA EXA	PSL_{Nacc} $[PSL_{Nacc1}, \ldots, PSL_{NaccNNacc}]$	EL_{Nacc} $[EL_{Nacc1}, \ldots, EL_{NaccNNacc}]$	PSL^{rank}_{Nacc}	3

Legend:
Sol. = list of solution (S) obtained from Screening phase;
N = Number of simulations for generic solution S_i, considered the EX approach
Appr. = Typology of approach used in Design and Sustainability analysis phase (i.e., Exploratory approach – EXA; Traditional approach - TRA)
PSL = product sustainability level for generic solution S_i (or sub-solution S_{ij}).
EL = elasticity for generic solution S_i (or sub-solution S_{ij}).

2.4 Optimization

The main objective of the optimization phase is to take the acceptable solutions S^{acc}_i (or sub-solutions S^{acc}_{ij}) obtained from the first elasticity screening and optimize them, with the purpose of improving the product PSL, without compromising the mechanical performance of the analyzed design solutions. Depending on the type of primary shape (PS) chosen during the screening phase, the methodology will work on the solutions differently.

For the development of the optimization phase, two options are defined in the methodology here described:

1. Parameter Modification: option applied to mono- and bi-dimensional (1D/2D) shapes. Starting from a given design volume and the boundary condition data (loads, constraints, etc.), the methodology will accomplish the variation of one or more geometric parameters in order to obtain a solution that provides the best performance in relation to the user-defined objective.
2. Structural Optimization: option applied to three-dimensional (3D) shapes. Starting from a given design volume and the boundary condition data (loads, constraints, etc.), the numerical framework of structural optimization allows to obtain fully or partially automated design solution, that provides the best performance in relation with a user-defined goal and given design constraints (structural or manufacturing).

The following paragraphs explain these two options in detail.

2.4.1 1D/2D – Parameter Modification

Compared to 3D geometry (discussed in the following paragraphs), the optimization of 1D/2D geometry models is straightforward, because the methodology plays on the variation and modification of one or more geometric parameters of the analyzed component.

In this case, the geometry is directly modified when a geometric parameter chosen by the designer changes, in order to calculate the indexes described above (i.e., PI, EI, CI). Regardless of the design approach chosen by the user (TRA or EXA), the methodology works as follows.

- The considered geometric parameter (par) is defined by a user-defined range and subdivided into N_t values.
- Concerning the TR approach, each acceptable solution (S^{acc}_i) will be defined by several sub-solutions (S^{acc}_{it} with t = 1, ..., N_t - the number of subdivision of geometric parameter), where par is modified in solution geometry. It follows from the above that S^{acc}_{it} depends on material properties (MAT_i, see TRA properties in **Table 8**), modified geometry (G_t) and setting parameters for the parameter modification (N_t), as provided by the following relations:

$$S_{it}^{acc} = S_{it}^{acc}(G_t, BC, MAT_i, N_t)$$

$$N_t = user - defined$$

The simulations are launched and performed according to TR approach in Design and Sustainability Analysis phase (*2.2*); thus, the results are reported in a table (as shown in **Table 26**). Regardless of scenario considered (ARB, REF), all solutions are represented through points in a PSL-EL "Point chart" (see **Figure 15** and **Figure 16**); each point of a solution S^{acc}_i will have N_t points shown in the diagram. The results will be sent **DIRECTLY** to the final screening, since in this case, the geometry is already modified to obtain sustainability indexes.

Table 26. Parameter Modification Results in TRA approach.

1D/2D Optimization Results			
Acceptable Solution	**Geometric Parameter**		
	par_1	**…**	**par_{Nt}**
S^{acc}_1	$[PI^{par1}_1, EI^{par1}_1, CI^{par1}_1]$	…	$[PI^{parNt}_i, EI^{parNt}_i, CI^{parNt}_i]$
…	…	…	…
S^{acc}_i	$[PI^{par1}_i, EI^{par1}_i, CI^{par1}_i]$	…	$[PI^{parNt}_1, EI^{parNt}_1, CI^{parNt}_1]$
…	…	…	…
S^{acc}_{Nacc}	$[PI^{par1}_{Nacc}, EI^{par1}_{Nacc}, CI^{par1}_{Nacc}]$	…	$[PI^{parNt}_{Nacc}, EI^{parNt}_{Nacc}, CI^{parNt}_{Nacc}]$

- In the EX approach, each acceptable sub-solution (S^{acc}_{ij}) will be defined by several sub-solutions (S^{acc}_{ijt} with t = 1, ..., N_t - the number of subdivision of geometric parameter), where par is modified in solution geometry. It follows from the above that S^{acc}_{ijt} depends on material properties (MAT_{ij}, see EXA properties in **Table 8**), modified geometry (G_t) and setting parameters for the parameter modification (N_t), as provided by the following relations:

$$S_{ijt}^{acc} = S_{ijt}^{acc}(G_t, BC, MAT_{ij}, N_t)$$

$$N_t = user - defined$$

The simulations are launched and performed according to EX approach in Design and Sustainability Analysis phase (2.2); thus, the results are reported in a table (as shown in **Table 27**). Regardless of scenario considered (ARB, REF), all solutions are represented through bubbles in a PSL-EL "Bubble chart" (see **Figure 19** and **Figure 20**); each point of a sub-solution S^{acc}_{ij} will have N_t bubbles shown in the diagram. As said before, the results obtained will be sent **DIRECTLY** to the final screening, since the geometry is already modified to obtain sustainability indexes.

Table 27. Parameter Modification Results in EXA approach.

1D/2D Optimization Results			
Acceptable Solution	**Geometric Parameter**		
	par_1	**…**	**par_{Nt}**
S^{acc}_1	$[PI^{par1}_{11}, EI^{par1}_{11}, CI^{par1}_{11}]$ … $[PI^{par1}_{1N1}, EI^{par1}_{1N1}, CI^{par1}_{1N1}]$	…	$[PI^{parNt}_{i}, EI^{parNt}_{i}, CI^{parNt}_{i}]$ … $[PI^{parNt}_{1N1}, EI^{parNt}_{1N1}, CI^{parNt}_{1N1}]$
…	…	…	…
S^{acc}_i	$[PI^{par1}_{i}, EI^{par1}_{i}, CI^{par1}_{i}]$ … $[PI^{par1}_{1Ni}, EI^{par1}_{1Ni}, CI^{par1}_{1Ni}]$	…	$[PI^{parNt}_{1}, EI^{parNt}_{1}, CI^{parNt}_{1}]$ … $[PI^{parNt}_{1Ni}, EI^{parNt}_{1Ni}, CI^{parNt}_{1Ni}]$
…	…	…	…
S^{acc}_{Nacc}	$[PI^{par1}_{Nacc}, EI^{par1}_{Nacc}, CI^{par1}_{Nacc}]$ … $[PI^{par1}_{1NNacc}, EI^{par1}_{1NNacc}, CI^{par1}_{1NNacc}]$	…	$[PI^{parNt}_{Nacc}, EI^{parNt}_{Nacc}, CI^{parNt}_{Nacc}]$ … $[PI^{parNt}_{1NNacc}, EI^{parNt}_{1NNacc}, CI^{parNt}_{1NNacc}]$

2.4.2 3D – Structural Optimization

Structural optimization aims is to find optimal material distribution according to given design domain or space. An objective function, design variables and state variables needs to be introduced to formulate the structural optimization problem. The objective function (f) represents an objective that could either be minimized or maximized (for instance, maximize the stiffness or minimize the volume of a structure). The design variables (x) describe the design of the structure; thus, they represent the geometrical features. The state variables (y) represent the structural responses (which can be recognized as stress, strain, or displacement,

for instance); furthermore, the state variables depends on the design variables (i.e., y(x)). A state function g(y) that represents the state variables can be introduced and incorporated as a constraint to the optimization task, where it is usually formulated such that $g(y) \leq 0$. The objective function is subjected to the design and state variable constraints to address the optimization to a desired solution (see **Equation 76**).

$$\begin{cases} \min_x f(x) \\ subject\ to\ g(x) \leq 0 \end{cases} \tag{76}$$

Based on what geometrical feature (x) that is parametrized, the structural optimization problem can be classified into:

- Size optimization: the design variable x represents a structural element (such as a distributed thickness or a cross-sectional area of a truss model). During the optimization process these parameters can be modified by the algorithm to solve the optimization problem.
- Shape optimization: the design variable x represents the boundary of the state equation. In this case, the boundary of the considered domain x could vary such that some physical quantity is minimized; the shape of the structure, modeled through the finite element method, is modified by the node locations, obtaining a deformed geometry of the starting shape structure.
- Topology optimization: the design variable x represents the connectivity of the domain. It is a technique that determines the optimal material distribution within a given design space, by modifying the apparent material density considered as a design variable.

In the methodology proposed, Topology Optimization is chosen as structural optimization framework. Topology optimization is a mathematical technique that produces an optimized shape and material distribution for a structure within a given package space. By discretizing the domain into a finite element mesh, the FEM solver calculates material properties for each element. The solver algorithm alters the material distribution to optimize the user-defined objective under given constraints. The most implemented methodology to create a topology based on the structural analysis is *Simplified Isotropic Material with Penalization* (SIMP), where a ”equivalent” material density of each element (ρ_{el}) is defined and directly used as the design variable; it varies continuously between 0 and 1, representing the state of void and solid, respectively. The intermediate values of density represent fictitious material and it is assumed that material stiffness is linearly dependent on density. A penalization strategy is utilized to try to force intermediate density values in the final design toward values of either 1 or 0. In the following, the structural optimization is described in detail subdivided into the following phases: design optimization input data, FEM modelling & simulation, Outcomes & shape reconstruction.

2.4.1.1 Design optimization input data. As already explained in design input data (*2.2.1.1*), for the setting of FEM optimization, the framework always requires that the designer characterizes the case study by providing the component Geometry (G) and the component

Boundary Conditions (BCs). According to the framework, in this phase the designer develops the 3-D model of the component in CAD environment and exports it in IGES or STEP format to Altair Hypermesh software for pre-processing. The model meshing is done on the component geometry, and the designed loads and structural BCs are applied on the meshed model; regardless the case study, they remain unaltered when passing from one solution to another. In contrast to FEM analysis, the elements of the model are designated as falling within one of two categories (see an example reported in **Figure 23**):

- Design space (DS): the design space elements are those for which the element density (ρ_{el}) can vary within the topology optimization and may potentially be removed or altered for the final design (blue elements in **Figure 23**).
- Non-design space (NDS): the non-design space elements are those which remain unchanged during the optimization procedure, and are typically the locations where BCs, loads, or other constraints are applied (red elements in **Figure 23**).

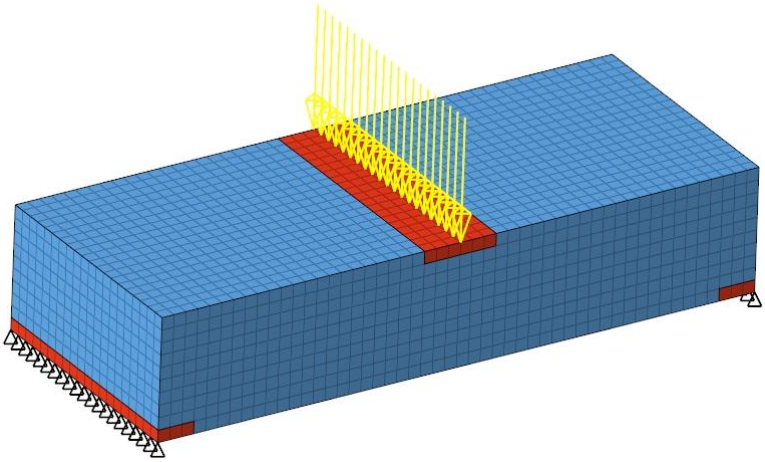

Figure 23. Representation of Design Space (DS) (see blue elements) and Non-Design Space (NDS) (see red elements).

The other type of inputs needed by the FEM modelling are the physical and mechanical properties that characterize materials of all acceptable solutions. These properties are already defined in the design analysis and, according to the information available to the designer, traditional (TR) or exploratory (EX) approach is chosen. **Table 28** reports an overview of the required input data for the FEM optimization, considering both approaches.

Table 28. Design optimization Input data, with TR and EX approaches.

Design optimization input data		
Component data (COMP)	**Material properties (MAT)**	
	Traditional Approach (TRA)	**Exploratory Approach (EXA)**
Component geometry (G) Design Space (DS) Non-Design Space (NDS) Component Boundary Conditions (BCs)	Density (ρ); [ρ_{val}] Young modulus (E); [E_{val}] Poisson ratio (η); [η_{val}] Yield strength (σ); [σ_{val}]	Density (ρ); [ρ_{min}; ρ_{max}] Young modulus (E); [E_{min}; E_{max}] Poisson ratio (η); [η_{min}; η_{max}] Yield strength (σ); [σ_{min}; σ_{max}]

2.4.1.2 FEM modelling & Simulation. Considering that also FEM optimization needs single values to define material properties, the TR approach (TRA) is straightforward: specify the material properties in FE model and launch the simulation of generic i-th acceptable solution S^{acc}_i. EX approach (EXA) provides material properties in terms of variability ranges (as shown in **Table 28**); thus, the framework explores the generic i-th acceptable solution S^{acc}_i with N_i sub-solutions S^{acc}_{ij} (j =1, …, N_i), each of which has to be modelled through a FEM simulation. The EX approach is already described in **Equations 1-5** and **Figure 13.**
The acceptable solution S^{acc}_i (or sub-solutions S^{acc}_{ij}) and number of required FEM simulations N^{acc}_i are already determined during FEM modelling in Design Analysis (2.2.1):

$$\begin{cases} S_i^{acc} = S_i = S_i(G, BC, MAT_i)\ TR\ Approach \\ S_{ij}^{acc} = S_{ij} = S_{ij}\left(G, BC, MAT_{ij}, N_i^{acc}\right)\ EX\ Approach \end{cases}$$

$$N_i^{acc} = N_i = N_i(MAT_i, n_{min}, n_{max}, \delta)$$

For each acceptable solution S^{acc}_i (with TR approach) or sub-solution S^{acc}_{ij} (using EX approach) already identified in the previous simulation modelling step, the optimization simulation is performed through the combined use of MATLAB and Altair HyperWorks simulation software; the solver used in this phase is Optistruct. The optimization problem for each solution is formulated according to the following strategy, reported in **Table 29**: the main objective of the topology optimization problem is the mass minimization, applying a strength constraint (as lower bound respect to yield strength (σ_y) of specific material).

Table 29. Optimization strategy used in the proposed methodology.

Optimization Strategy		
Optimization	**Goal/Response**	**Constraints**
Topology	Minimize Mass	$\sigma \leq \sigma_y$

2.4.1.3 Outcomes & Shape Reconstruction. After the optimization simulations are performed, the main steps are the outcomes extraction, thus the component shape reconstruction to use in the next and final methodology phase (i.e., Final Classification). Regardless of the approach (i.e., TRA and EXA) and scenario (i.e., ARB and REF), the main issue in this phase is the automatic reconstruction of the optimized shape from the acceptable solutions S^{acc}_i (or sub-solution S^{acc}_{ij}). The methodology envisages the following steps, according to the modelling framework reported in **Table 30** (**Equations 77-80**):

- Writing ".dens" and ".out" files for each acceptable solution (or sub-solution) submitted to the optimization phase. The ".dens" file presents the list of elements with the fictitious density value (ρ^{el}) obtained from the topology optimization. The ".out" file presents, in the form of a table, the percentage of elements having a specific density range.
- Extracting data from ".dens" and ".out" files just obtained.
- Writing density matrix (P) and calculating mean density vector ($\bar{\rho}$). The density matrix (P) is calculated from the ".dens" files by extracting the data for each solution

(or sub-solution) (see **Table 31**). Each column represents the list of density values of the elements within the solution (or sub-solution) considered; each row shows the density value of a specific element in all solutions (or sub-solutions). Therefore, the mean density vector ($\bar{\rho}$) is obtained by averaging the density values over the j-th element (see **Equation 77**).

Table 30. Shape Reconstruction Modelling.

Shape Reconstruction Equations		
	$\overline{\rho_j^{el}} = \frac{\sum_k^S (\rho_{jk}^{el})}{S}$	(77)
	$\overline{\tau_r^{el}} = \frac{\sum_k^S T_{rk}^{el}}{S}$	(78)
	$\sum_{r=1}^{10} \overline{\tau_r^{el}} = 1$	(79)
Traditional Approach (TRA)	$S = N_{acc}$	(80)
Exploratory Approach (EXA)	$S = \sum_{i=1}^{N_{acc}} N_i$	

Where:

N_{el} = Total number of elements constituting the (sub-)solution FEM model [-].
S = Total number of acceptable solutions (or sub-solutions) S^{acc} [-]
$\overline{\rho_e^{el}}$= Mean Density value for e-th element respect to all acceptable (sub-)solutions (with e=1, ..., N_{el}) [-]
ρ_{ek}^{el}= Density value for e-th finite element of k-th acceptable (sub-)solution (with k=1, …, S) [-]
$\overline{\tau_r^{el}}$= Mean percentage of finite elements included in r-th range respect to all acceptable (sub-) solutions (with r=1, …,10) [-]
T_{rk}^{el}= Percentage of finite elements included in r-th range of k-th acceptable (sub-) solution (with r=1, …,10 and k=1, …, S) [-]

Table 31. Density matrix and mean density vector representation.

ID Element	**Density Matrix (P)**					**Mean Density Vector ($\bar{\rho}$)**
	Solution 1	…	Solution k	…	Solution S	Avg Solution
1	ρ^{el}_{11}	…	ρ^{el}_{1k}	…	ρ^{el}_{1S}	$\overline{\rho_1^{el}}$
…	…	…	…	…	…	…
e	ρ^{el}_{e1}	…	ρ^{el}_{ek}	…	ρ^{el}_{eS}	$\overline{\rho_e^{el}}$
…	…	…	…	…	…	…
N_{el}	ρ^{el}_{Nel1}	…	ρ^{el}_{Nelk}	…	ρ^{el}_{NelS}	$\overline{\rho_{N_{el}}^{el}}$

- Writing density range matrix (T) and calculating mean range vector ($\bar{\tau}$) relative to density ranges. In this case, the density range matrix (T) is obtained from the ".out" files by extracting the data for each (sub-)solution; then, the average range vector ($\bar{\tau}$) is calculated as the mean of the percentage values over the density ranges (10 in total), according to the **Equation 78** (see **Table 32**). It is essential to highlight that the total sum of the components of the vector $\bar{\tau}$ is equal to 1 (or 100%), i.e., the totality of the elements constituting the FEM model.

Table 32. Density range matrix and mean range vector representation.

Density Range	**Density Range Matrix (T)**					**Mean Range Vector ($\bar{\tau}$)**
	Solution 1	…	Solution k	…	Solution S	Avg Solution
0 – 0.1	T^{el}_{11}	…	T^{el}_{1k}	…	T^{el}_{1S}	$\overline{\tau_1^{el}}$
0.1 – 0.2	T^{el}_{21}	…	T^{el}_{2k}	…	T^{el}_{2S}	$\overline{\tau_2^{el}}$
…	…	…	…	…	…	…
0.9 - 1.0	T^{el}_{101}	…	T^{el}_{10k}	…	T^{el}_{10S}	$\overline{\tau_{10}^{el}}$

- Setting a density threshold value (THR), chosen by the designer considering the mean range vector ($\bar{\tau}$) just calculated and using the following rule:

$$T_{des}^{el}\ such\ that: \sum_{r=1}^{r} \overline{\tau_r^{el}} \cong T_{des}^{el} \rightarrow r \rightarrow THR$$

  T^{el}_{des} represents the percentage of elements that the designer wants to remain in the optimized shape reconstruction; the methodology extracts the density range (r) for which the cumulative sum of the components of the vector $\bar{\boldsymbol{\tau}}$ is equal to T^{el}_{des} (as shown in **Equation 79**). Finally, THR is obtained considering the density range (r) extracted. For instance, if the designer imposes a elements percentage (T^{el}_{des}) equal to 75%, the density range will be that for which the sum of vector components equals T^{el}_{des}; therefore, THR = Density range so calculated.

- Output extraction, obtaining the elements that respect THR. The threshold obtained is compared with the values present in the mean density vector ($\bar{\rho}$); if the generic value of the vector is greater than THR, the e-th element respects the constraint imposed by the designer, otherwise the element is discarded and not considered in the shape reconstruction. as shown in **Table 33**.
  The elements thus obtained will be used to create a new FEM model following the optimization results. In this phase, the methodology, based on the results obtained from the data extraction phase, automatically reconstructs the component geometry. The designer will then have to redesign the model based on this new information and suggestions and re-prepare the FEM model; an example is shown in **Figure 24**. This model will be used in the final stage of the methodology, the final classification.

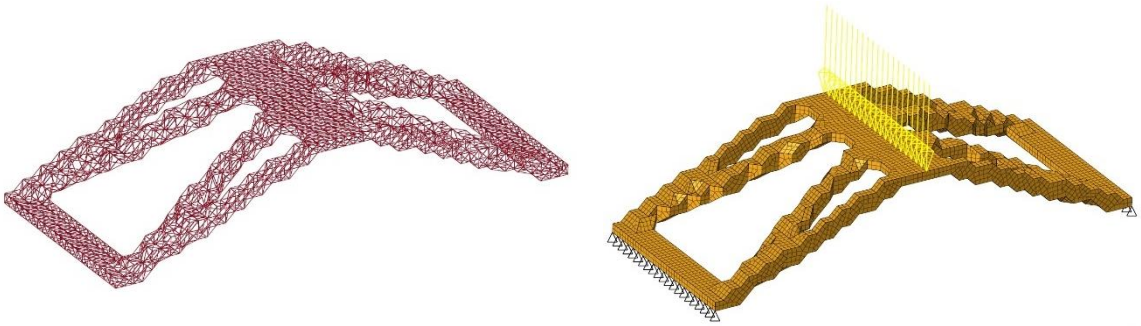

Figure 24. Example of shape reconstruction performed by DeSA methodology (left image) and redesign of a FEM model (right image).

Table 33. Representation of mean range vector subjected to THR screening.

ID Element	**Mean Density Vector ($\overline{\rho}$)** Avg Solution	**Screening** THR = Designer Value
1	$\overline{\rho_1^{el}}$	OK
…	…	…
e	$\overline{\rho_e^{el}}$	NO
…	…	…
N_{el}	$\overline{\rho_{N_{el}}^{el}}$	OK

Figure A.7 and **Figure A.8** in the Appendix A show the GUI of the Optimization and Shape Reconstruction phases described above, always developed by MATLAB App Designer software.

2.5 Final Classification

Once the Optimization is performed for the solutions S_i (or sub-solutions S_{ij}), the final classification phase is carried out by means of the following steps: Design and Sustainability Re-Analysis, final PSL calculation, final elasticity screening and final ranking.

2.5.1. Design and Sustainability Re-Analysis

This phase is aimed at evaluating the feasible and optimized design solutions obtained in the Optimization phase by means of the aggregated single-score indicator PSL, performing a holistic assessment where both design performance and sustainable profiles are considered. The design and sustainability re-analysis is structured in three main sections which deal with design, environmental, and economic aspects respectively, as explained in the following steps.

- The design re-analysis consists of a Finite Element Method (FEM) simulation modelling applied to all feasible and optimized solutions S^{opt}_i provided by the optimization. The FEM re-analysis is always aimed at assessing the design

performance by means of a tailored indicator which quantifies the service levels accomplished by the different solutions (structural integrity, stiffness, etc…). The FEM re-analysis is performed in terms of mechanical properties, and it provides as output a series of mechanical features which are used in the final classification phase (configuration of PSL). As already described in design analysis phase (*2.2.1*), the design re-analysis is divided into the following phases: design input data, FEM modelling and design performance.

Design input data. For the setting of FEM re-analysis, the framework always requires that the designer characterizes the case study by providing the component Geometry (G) and the component Boundary Conditions (BCs). The framework provides that in this phase the designer develops the model of the component in CAD environment and exports it in IGES or STEP format to Altair Hypermesh software for pre-processing. However, in this case G is obtained through the shape reconstruction step (performed in the Optimization phase). Thus, the model meshing is done on the new geometry (called G^{opt}), while the designed loads and structural boundary constraints (i.e., BCs) are applied on the meshed model. BCs, regardless of the specific case study, remain unaltered when passing from one solution to another. The other type of design inputs needed by the FEM modelling are the physical and mechanical properties that characterize materials of all solutions. Material properties (MAT) for linear, temperature-independent, and isotropic materials are considered (therefore, density, Young modulus, Poisson ratio and yield strength). As said in the design analysis phase (*2.2.1*), two approaches are defined in the methodology, depending on the information available to the designer (i.e., Traditional approach (TRA) and Exploratory approach (EXA)). **Table 6** reports an overview of the required input data for the FEM analysis, also considering both approaches here defined.

FEM modelling. Considering that FEM re-analysis needs single values to define material properties, the TR approach (TRA) is straightforward: specify the material properties in FE model and launch the simulation of generic i-th solution S^{opt}_i. Instead, EX approach (EXA) provides material properties in terms of variability ranges (as shown in **Table 6**); thus, the framework explores the generic i-th solution S^{opt}_i with N_i sub-solutions S^{opt}_{ij} (j =1, …, N_i), each of which has to be modelled through a FEM simulation. The analytical approach of EXA is described in **Equations 1-5** and **Figure 13**. The number of required FEM simulations N_i was already determined in the design analysis phase, using the range sizes of different material properties (MAT) and several parameters defined by the designer (n_{min}, n_{max} and δ). The sample of material properties (MAT_{ij}) is still calculated through the LHS method (described in detail in the Appendix B) and used in FEM simulation for design solution S^{opt}_i and sub-solutions S^{opt}_{ij}.

Design assessment. For each solution S^{opt}_i (with TR approach) or sub-solution S^{opt}_{ij} (using EX approach) identified in the simulation modelling step, the design performance is assessed by the Optimized Performance Index (PI^{opt}), defined as the ratio between the reference or arbitrary service levels (user-defined, depending on the case study) and the service levels on the component (with the optimized geometry) calculated through the new FEM simulations. To quantify the distance (or the over-dimensioning) of the generic solution S^{opt}_i (or S^{opt}_{ij}) with respect to reference (REF scenario) or arbitrary (ARB scenario) value, the analysis defines the Optimized

Elasticity (EL^{opt}) parameter, which expresses the potential to lighten a solution without compromising the design performance (**Equation 14**). The design calculation is carried out according to the modeling framework reported in **Table 13** (**Equations 12-15**), except that the service level on the component calculated through FEM simulation (pi_{FEM}) is referred to the optimized geometry (i.e., $pi_{FEM} \rightarrow pi^{opt}_{FEM}$). The calculation of PI^{opt} and EL^{opt} is carried out for each design solution S^{opt}_{i} (or sub-solution S^{opt}_{ij}) through the combined use of MATLAB and Altair HyperWorks simulation software. The final output of the design analysis is the overall set of PI^{opt} and EL^{opt} indexes:

$$PI^{opt} \rightarrow \begin{cases} PI_i^{opt} = f(G^{opt}, BC, MAT_i) \quad TR\ Approach \\ PI_{ij}^{opt} = f\left(G^{opt}, BC, MAT_{ij}\right) EX\ Approach \end{cases}$$

$$EL^{opt} \rightarrow \begin{cases} EL_i^{opt} = f\left(PI_i^{opt}\right) \quad TR\ Approach \\ EL_{ij}^{opt} = f\left(PI_{ij}^{opt}\right) EX\ Approach \end{cases}$$

- In <u>environmental re-analysis,</u> the optimized solution S^{opt}_{i} (or sub-solutions S^{opt}_{ij}) provided by the design re-analysis are evaluated respect to the environmental profile. The chosen indicator is the Optimized Environmental Index (EI^{opt}), which evaluation is always carried out through the LCA methodology by means of the CC indicator using the ILCD 1.09 LCIA method. The CC is determined taking into account the overall component LC, defined according to the main stages (materials, manufacturing, use, EoL). As already described in environmental analysis (2.2.2), the environmental re-analysis is divided into the two following phases: environmental input data and environmental modelling.

  <u>Environmental Input data</u>. The CC calculation framework involves an environmental characterization of all solutions S^{opt}_{i} (or sub-solutions S^{opt}_{ij}) obtained in the design re-analysis stage. Such a characterization is carried out by means of the environmental database which provides all the input data needed for the sustainability assessment (**Table 14**). The environmental database reports the setting parameters for the evaluation of the use stage (both ICEVs and EVs) and EoL scenarios, and the specific impact values, providing mass-specific CC for each phase of component LC.

  <u>Environmental modelling.</u> For each solution S^{opt}_{i} (with TR approach) or sub-solution S^{opt}_{ij} (using EX approach) identified in the previous simulation modelling step, the environmental performance is assessed by the Optimized Environmental Index (EI^{opt}), defined as the component LC CC (with the optimized geometry). The calculation of the environmental impact is carried out according to the modelling framework reported in **Table 15** (**Equations 18-34**), except that the component mass (m) calculated through FEM simulations is referred to the optimized geometry (i.e., $m \rightarrow m^{opt}$). The final output of the environmental re-analysis is the overall set of design solution S^{opt}_{i} (or sub-solution S^{opt}_{ij}) characterized in terms of Optimized Life-Cycle Climate Change ($CC^{opt}_{LC} = EI^{opt}$, see **Equation 34**):

$$EI^{opt} \rightarrow \begin{cases} EI_i^{opt} = CC_i^{opt(LC)} = f(G^{opt}, MAT_i, MAN_i, USE_i, EoL_i) & TR\ Approach \\ EI_{ij}^{opt} = CC_{ij}^{opt(LC)} = f\left(G^{opt}, MAT_{ij}, MAN_{ij}, USE_{ij}, EoL_{ij}\right) & EX\ Approach \end{cases}$$

- In economic re-analysis phase, the optimized solution S^{opt}_i (or sub-solutions S^{opt}_{ij}) provided by the design re-analysis (and evaluated respect to environmental profile) are analyzed respect to the economic aspect. The chosen indicator is the Optimized Cost Index (CI^{opt}), which evaluation is carried out through the LCC methodology by means of cost indicator (COST) using the eLCC method (see **Equation 52**). The COST is determined taking into account the overall costs associated with the LC of a product that are directly covered by any one or more of the actors in the product life cycle (e.g., supplier, manufacturer, user, or consumer, or EoL actor). As already described in economic analysis (2.2.3), the economic re-analysis is divided into the two following phases: economic input data and economic modelling.

  Economic Input data. The COST calculation framework involves an economic characterization of all solutions S^{opt}_i (or sub-solutions S^{opt}_{ij}) obtained in the design re-analysis stage. Such a characterization is carried out by means of the economic database with all the input data needed for the sustainability assessment (see **Table 16**). The economic database collects the setting parameters for the evaluation of the use stage cost (both ICEVs and EVs) and EoL scenarios, manufacturing cost values, and the specific cost values, providing the specific COST for each phase of component LC (expressed with respect to component mass, batch size, …).

  Economic modelling. For each solution S^{opt}_i (with TR approach) or sub-solution S^{opt}_{ij} (using EX approach) identified in the previous simulation modelling step, the economic performance is assessed by the Optimized Cost Index (CI^{opt}), defined as the component LC COST (with the optimized geometry). The calculation of the overall economic cost is carried out according to the modelling framework reported in **Table 17** (**Equations 35-53**), but the component mass (m) calculated through FEM simulations is referred to the optimized geometry (i.e., m → m^{opt}). The final output of the economic re-analysis is the overall set of design solution S^{opt}_i (or sub-solution S^{opt}_{ij}) characterized in terms of Optimized Life-Cycle Cost ($COST^{opt}_{LC}$ = CI^{opt}, see **Equation 52**):

$$CI^{opt} \rightarrow \begin{cases} CI_i^{opt} = COST_i^{opt(LC)} = f(G^{opt}, MAT_i, MAN_i, USE_i, EoL_i) & TR\ Approach \\ CI_{ij}^{opt} = COST_{ij}^{opt(LC)} = f\left(G^{opt}, MAT_{ij}, MAN_{ij}, USE_{ij}, EoL_{ij}\right) & EX\ Approach \end{cases}$$

The overall design and sustainability re-analysis phase is performed according to scheme reported in **Figure 25**, where the combination of MATLAB and Hyperworks allows the calculation of indexes previously defined (i.e., PI^{opt}, EI^{opt}, and CI^{opt}) for each optimized solution S_i or S_{ij} obtained in the Optimization phase (see **Table 34**).

Figure A.9 in Appendix A show the GUI of the design and sustainability re-analysis phase described above, which is developed by MATLAB App Designer software.

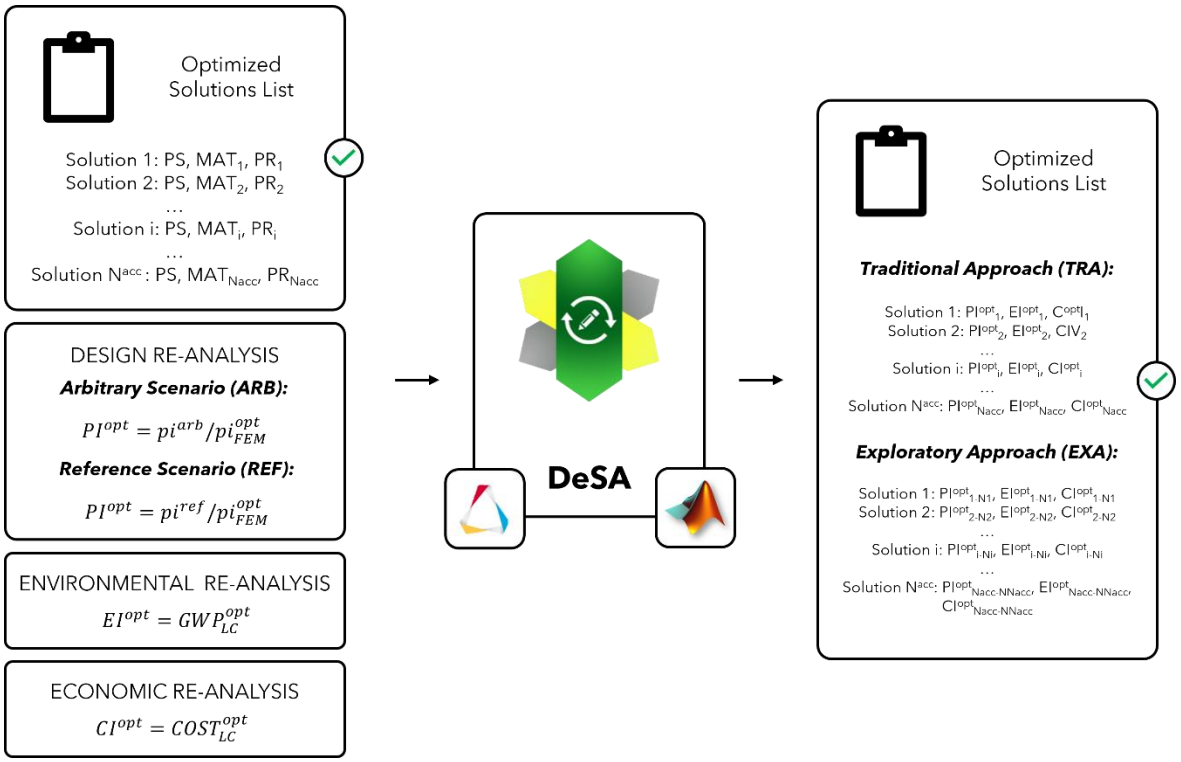

Figure 25. Design and Sustainability re-analysis phase framework.

2.5.2 Final PSL calculation

Once the Design and Sustainability re-analysis is performed for the solution S^{opt}_i (or sub-solution S^{opt}_{ij}), in the PSL calculation step, The optimized PSL index (named PSL^{opt}) is calculated based on MCDA methods, thus calculating a tailored overall efficiency score for each design optimized alternative. The evaluation is carried out by means of three main steps (normalization, weighting, and aggregation) according to the modelling framework reported in **Table 35** (see **Equations 76-79**).

Concerning the normalization phase, two methods can be used (i.e., ARB and REF scenarios). Regardless of the type of design approach, in the arbitrary scenario (ARB) the normalization is performed through the "Max method", which provides that design and sustainability indexes are normalized using the maximum value obtained from each index during the design and sustainability phase (2.2), according to **Equation 77**. Instead, in the reference scenario (REF) the normalization is performed through a method similar to the "Max method", where the design and sustainability indexes are normalized using the values coming from the existing reference solution (without the optimization phase), according to **Equation 78.** As regards the weighting, to compare the sustainability performance of optimized solutions by mean of the proposed framework, an equal weight is assigned to all measurements, since it is assumed that all elements have the same level of importance (**Equation 79**). In the score aggregation step, the optimized normalized data are systematically aggregated into a single score using the weights and the normalized indexes defined above (see **Equation 76**).

Table 34. Representation of solutions list obtained by optimization phase, with PI^{opt}, EL^{opt}, EI^{opt}, and CI^{opt} indexes calculated for each solution S^{opt}_i (or sub-solution S^{opt}_{ij}).

List of Optimized Solutions						
Sol.	**Char.**	**N**	**Appr.**	**Design**	**Environment**	**Economy**
				PI, EL	**EI**	**CI**
S^{opt}_1	MAT_1 PR_1	N_1	TRA	PI^{opt}_1 EL^{opt}_1	EI^{opt}_1	CI^{opt}_1
			EXA	$[PI^{opt}_{11}, \ldots, PI^{opt}_{1N1}]$ $[EL^{opt}_{11}, \ldots, EL^{opt}_{1N1}]$	$[EI^{opt}_{11}, \ldots, EI^{opt}_{1N1}]$	$[CI^{opt}_{11}, \ldots, CI^{opt}_{1N1}]$
S^{opt}_2	MAT_2 PR_2	N_2	TRA	PI^{opt}_2 EL^{opt}_2	EI^{opt}_2	CI^{opt}_2
			EXA	$[PI^{opt}_{21}, \ldots, PI^{opt}_{2N2}]$ $[EL^{opt}_{21}, \ldots, EL^{opt}_{2N2}]$	$[EI^{opt}_{21}, \ldots, EI^{opt}_{2N2}]$	$[CI^{opt}_{21}, \ldots, CI^{opt}_{2N2}]$
…	…	…	…	…	…	…
S^{opt}_i	MAT_i PRi	N_i	TRA	PI^{opt}_i EL^{opt}_i	EI^{opt}_i	CI^{opt}_i
			EXA	$[PI^{opt}_{i1}, \ldots, PI^{opt}_{iNi}]$ $[EL^{opt}_{i1}, \ldots, EL^{opt}_{iNi}]$	$[EI^{opt}_{i1}, \ldots, EI^{opt}_{iNi}]$	$[CI^{opt}_{i1}, \ldots, CI^{opt}_{iNi}]$
…	…	…	…	…	…	…
S^{opt}_{Nacc}	MAT_{Nacc} PR_{Nacc}	N_{Nacc}	TRA	PI^{opt}_{Nacc} EL^{opt}_{Nacc}	EI^{opt}_{Nacc}	CI^{opt}_{Nacc}
			EXA	$[PI^{opt}_{Nacc1}, \ldots, PI^{opt}_{NaccNacc}]$ $[EL^{opt}_{Nacc1}, \ldots, EL^{opt}_{NaccNacc}]$	$[EI^{opt}_{Nacc1}, \ldots, EI^{opt}_{NaccNacc}]$	$[CI^{opt}_{Nacc1}, \ldots, CI^{opt}_{NaccNacc}]$

Legend:
Sol. = list of solution (S^{opt}) obtained from optimization phase;
Char. = Characteristics of generic solution S^{opt}_i (i.e., material (MAT_i) and manufacturing process (PR_i))
N = Number of simulations for generic solution S^{opt}_i, considered the EX approach
Appr. = Typology of approach used in Design and Sustainability re-analysis phase (i.e., Exploratory approach – EXA; Traditional approach - TRA)
PI = performance index for generic solution S^{opt}_i (or sub-solution S^{opt}_{ij}).
EL = elasticity for generic solution S^{opt}_i (or sub-solution S^{opt}_{ij}).
EI = environmental index of LC for generic solution S^{opt}_i (or sub-solution S^{opt}_{ij}).
CI = cost index of LC for generic solution S^{opt}_i (or sub-solution S^{opt}_{ij}).

Table 35. PSL^{opt} modelling.

PSL^{opt} Equations			
		Traditional Approach (TRA)	**Exploratory Approach (EXA)**
Optimized Product Sustainability Level		$PSL_i^{opt} = \sum_{p=1}^{N_p} \frac{w_p}{I_{Ni}^{p(opt)}}$	$PSL_{ij}^{opt} = \sum_{p=1}^{N_p} \frac{w_p}{I_{Nij}^{p(opt)}}$ (76)
Optimized Design and Sustainability Indexes Normalized	**Arbitrary Scenario (ARB)**	$I_{Ni}^{p(opt)} = I_i^{p(opt)} / I_i^{p(max)}$	$I_{Nij}^{p(opt)} = I_{ij}^{p(opt)} / I_{ij}^{p(max)}$ (77)
	Reference Scenario (REF)	$I_{Ni}^{p(opt)} = I_i^{p(opt)} / I_i^{p(ref)}$	$I_{Nij}^{p(opt)} = I_{ij}^{p(opt)} / I_{ij}^{p(ref)}$ (78)
Weights		$\sum_{p=1}^{N_p} w_p = 1$ (79)	

Legend:
PSL^{opt}_i = Product Score Level for generic optimized solution S_i in TR approach[-].
PSL^{opt}_{ij} = Product Score Level for optimized sub-solution S_{ij} in EX approach [-].
N_p = number of pillars used for PSL calculation (design, environment, economy; with p = 1, …, 3) [-];
K = PSL scale factor, chosen by the designer [-].
w_p = the weighting factor for p-th pillar for the PSL modelling (design, environment, economy) [-];
$I^{p(opt)}_{Ni}$ = the normalized index for p-th pillar for generic optimized solution S_i in TR approach [-].
$I^{p(opt)}_{Nij}$ = the normalized index for p-th pillar for optimized sub-solution S_{ij} in EX approach [-].
$I^{p(opt)}_{i}$ = the index for p-th pillar for generic optimized solution S_i modelling (i.e., design, environment and economy) in TR approach [-].
$I^{p(opt)}_{ij}$ = the index for p-th pillar for optimized sub-solution S_{ij} modelling (i.e., design, environment and economy) in EX approach [-].
$I^{p(max)}_{i}$ = the highest value of the p-th index for generic solution S_i in TR approach [-].
$I^{p(max)}_{ij}$ = the highest value of the p-th index for sub-solution S_{ij} in EX approach [-].
$I^{p(ref)}_{i}$ = the value of the p-th index for reference solution S_i in TR approach [-].
$I^{p(ref)}_{ij}$ = the value of the p-th index for reference sub-solution S_{ij} in EX approach [-]

2.5.3 Final Elasticity screening

The target of this step is identifying the list of acceptable and optimized design solutions ($S^{acc(opt)}$), defined as all optimized solutions that at the same time satisfy elasticity requirements and are feasible from a technological point of view. As said in the first elasticity screening, the application of this phase varies depending on the information available to the designer, i.e., if the data considered in the production database are specific (TR approach) or ranges-defined (EX approach), and if the design scenario is designer- (ARB scenario) or reference-defined (REF scenario).

Concerning the TR approach, this phase provides that the PSL^{opt}, and EL^{opt} of each solution S^{opt}_i are defined through constant values obtained in Design and Sustainability re-phase (see the following model):

$$S_i^{opt} \rightarrow \begin{Bmatrix} PSL_i^{opt} \\ \\ EL_i^{opt} \end{Bmatrix}$$

Instead, in the EX approach this phase provides that the range of PSL^{opt} and EL^{opt} of each solution S_i is defined through the minimum and maximum values obtained for the optimized sub-alternatives S^{opt}_{ij}, according to the following model:

$$S_i^{opt} \rightarrow \begin{Bmatrix} \left\{PSL_{i1}^{opt}, \dots, PSL_{ij}^{opt}\right\} \rightarrow \ PSL_i^{opt} = \left[min\left(PSL_{ij}^{opt}\right), max\left(PSL_{ij}^{opt}\right)\right] \\ \\ \left\{EL_{i1}^{opt}, \dots, EL_{ij}^{opt}\right\} \rightarrow \ EL_i^{opt} = \left[min\left(EL_{ij}^{opt}\right), max\left(EL_{ij}^{opt}\right)\right] \end{Bmatrix}$$

As already shown in **Table 20**, there are four combinations of the approaches/scenarios defined by the DeSA methodology, described below.

1. TRA – ARB Combination. Once PSL^{opt}_i and EL^{opt}_i are obtained according to the TR approach, the screening step envisages that all solutions are represented through points in a PSL-EL "Point chart" (as shown in **Figure 15**). The ELasticity Value (ELV) is defined, and it divides the chart into two distinct zones: acceptable zone (A-zone), with EL^{opt} higher than ELV, and non-acceptable zone (B-zone), with EL^{opt} lower than ELV. The framework provides that ELV parameter is fixed by the designer, in order to set acceptability threshold values customized for the specific application. The solutions that fall within the A-zone are considered as full acceptable and optimized solutions ($S^{acc(opt)}_i$) and they are considered in the final ranking step; instead, the solutions that fall within the B-zone are considered as non-acceptable optimized solutions and they are discarded since they do not satisfy the design requirements. If the generic solution S^{opt}_i falls close to ELV, the solution is accepted or discarded depending on the acceptability threshold (AT), set by the designer and defined by means of percentages compared to the ELV (see the scheme in **Table 21**, **Equations 58-61**).
2. TRA – REF Combination. PSL^{opt}_i and EL^{opt}_i are obtained using the TR approach; thus, the screening phase provides that all solutions are always represented through points in a PSL-EL "Point chart" (see **Figure 16**). The Reference ELasticity Value

(ELV^{ref}) is defined, which divides the point chart into two distinct zones: acceptable zone (A-zone), where EL^{opt} is higher than ELV^{ref}, and non-acceptable zone (B-zone), where EL^{opt} is lower than ELV^{ref}. In this case, the framework provides that ELV^{ref} parameter is obtained from the existing reference solution. Moreover, the Reference Product Sustainability Level Value ($PSLV^{ref}$) can be defined, dividing the point chart into two distinct zones: sustainable zone (C-zone), where PSL^{opt} is higher than $PSLV^{ref}$, and non-sustainable zone (D-zone), where PSL^{opt} is lower than $PSLV^{ref}$. The framework provides that $PSLV^{ref}$ parameter is obtained always from the existing reference solution. The solutions that fall within the A-zone are considered as full acceptable and optimized solutions ($S^{acc(opt)}_i$) and they are considered in the final ranking step; the solutions that fall within the B-zone are considered as non-acceptable optimized solutions and they are discarded since they do not fulfil the design requirements. Similar to the previous combination, if the generic solution S_i falls close to ELV^{ref}, the solution is accepted or discarded depending on the acceptability threshold (AT). However, the definition of these thresholds is automatically obtained by methodology from the existing reference solution, according to the scheme in **Table 22** (**Equations 62-65**).

3. EXA – ARB Combination. In this combination, PSL_i and EL_i are obtained from the data ranges according to the EX approach. Therefore, the screening phase envisages that all solutions are represented through ellipses in a PSL-EL "bubble chart" (as shown in **Figure 17** and **Figure 18**); the ELasticity Value (ELV) is defined, and it divides the bubble chart into two distinct zones: acceptable zone (A-zone), with EL^{opt} higher than ELV, and non-acceptable zone (B-zone), with EL^{opt} lower than ELV. The ELV parameter is fixed by the designer, leaving the practitioner the possibility to set acceptability threshold values customized for the specific application. If the solutions fall within the A-zone, they are considered as full acceptable and optimized solutions ($S^{acc(opt)}_i$) and used in the final ranking step; instead, the solutions that fall within the B-zone are considered as non-acceptable solutions and they are discarded since they do not fulfil the design requirements. If the generic solution S_i falls in both zones, the solution is accepted or discarded depending on the filtering level (FL) set by the designer (**Figure 17** and **Figure 18**); the FL calculation is carried out according to the modeling framework reported in **Equations 66-69**, except that the EL is referred to the optimized solution (i.e., $EL^{range} \rightarrow EL^{range(opt)}$). If $EL^{right} < FL$, the solutions whose bubble is crossed by ELV vertical line is discarded and it is not considered in the final ranking phase; if $EL^{right} >= FL$, the solutions whose bubble is crossed by ELV vertical line is accepted and considered in the final ranking phase.
4. EXA – REF Combination. In this final combination, PSL_i and EL_i are obtained from the data ranges according to the EX approach; thus, the screening step provides that all solutions are represented through ellipses in a PSL-EL "bubble chart" (see **Figure 19** and **Figure 20**). The Reference ELasticity Value (ELV^{ref}) is defined, which divides the bubble chart into two distinct zones: acceptable zone (A-zone), where EL^{opt} is higher than ELV^{ref}, and non-acceptable zone (B-zone), where EL^{opt} is lower than ELV^{ref}. The ELV^{ref} parameter is obtained from the existing reference solution. Moreover, the Reference Product Sustainability Level Value ($PSLV^{ref}$) can be defined, which divides the bubble chart into two distinct zones: sustainable zone (C-zone), where PSL^{opt} is higher than $PSLV^{ref}$, and non-sustainable zone (D-zone), where PSL^{opt} is lower than $PSLV^{ref}$. The $PSLV^{ref}$ parameter is obtained always from

the existing reference solution. If the solutions fall within the A-zone, they are considered as full acceptable and optimized solutions ($S^{acc(opt)}_i$) and they are considered in the final ranking step; instead, the solutions that fall within the B-zone are considered as non-acceptable optimized solutions and they are discarded. Similar to the previous combination, if the generic solution S_i falls in both zones, the solution is accepted or discarded depending on the filtering level (FL) set by the designer (see **Figure 19** and **Figure 20**). the FL calculation is carried out according to the modeling framework reported in **Equations 70-73**, except that the EL is referred to the optimized solution (i.e., $EL^{range} \rightarrow EL^{range(opt)}$) and the ELV^{ref} is used for the calculation. When $EL^{right} < FL$, the solutions whose bubble is crossed by ELV vertical line is discarded and it is not considered in the final ranking phase; when $EL^{right} >= FL$, the solutions whose bubble is crossed by ELV vertical line is accepted and considered in the final ranking phase.

The overall phase is performed according to overview reported in **Figure 26**, where MATLAB allows the screening of optimized solutions thanks to one of above approaches, obtaining the acceptable and optimized solution $S^{acc(opt)}_i$ (see **Table 36**). The number of acceptable and optimized solution ($N^{acc(opt)}$) is comprised between:

$$0 < N^{acc(opt)} < N^{acc}$$

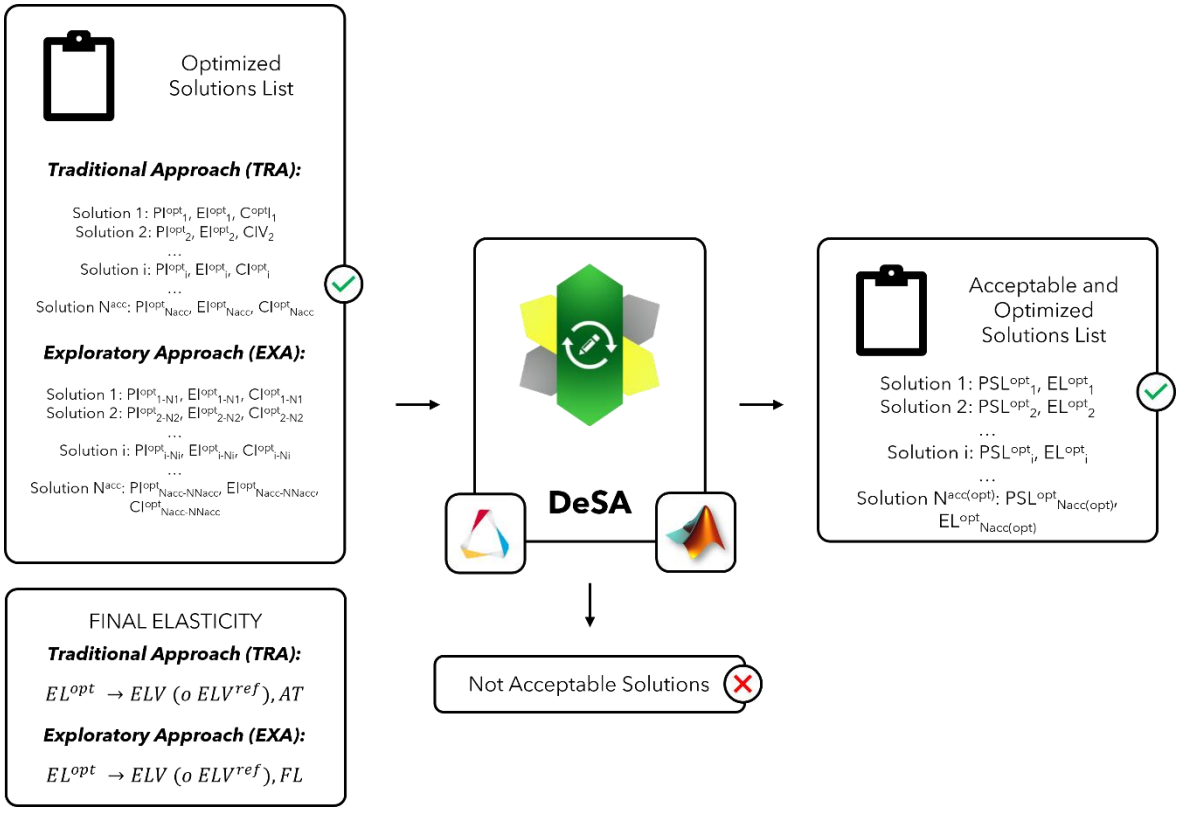

Figure 26. Overview of final elasticity screening phase.

Table 36. Representation of solutions list screening, with PSL^{opt}, EL^{opt}, and final elasticity screening calculated for each optimized solution S^{opt}_i.

List of Optimized Solutions					
Sol.	**N**	**Appr.**	**PSL^{opt}**	**EL^{opt}**	**Final Elasticity Screening**
S^{opt}_1	N_1	TRA EXA	PSL^{opt}_1 $[PSL^{opt}_{11}, \ldots, PSL^{opt}_{1N1}]$	EL^{opt}_1 $[EL^{opt}_{11}, \ldots, EL^{opt}_{1N1}]$	YES
S^{opt}_2	N_2	TRA EXA	PSL^{opt}_2 $[PSL^{opt}_{21}, \ldots, PSL^{opt}_{2N2}]$	EL^{opt}_2 $[EL^{opt}_{21}, \ldots, EL^{opt}_{2N2}]$	YES
…	…	…	…	…	NO
S^{opt}_i	N_i	TRA EXA	PSL^{opt}_i $[PSL^{opt}_{i1}, \ldots, PSL^{opt}_{iNi}]$	EL^{opt}_i $[EL^{opt}_{i1}, \ldots, EL^{opt}_{iNi}]$	YES
…	…	…	…	…	NO
S^{opt}_{Nacc}	N_{Nacc}	TRA	PSL^{opt}_{Nacc}	EL^{opt}_{Nacc}	YES

Legend:
Sol. = list of solution (S^{opt}) obtained from optimization phase;
N = Number of simulations for generic solution S^{opt}_i, considered the EX approach
Appr. = Typology of approach used in Design and Sustainability re-analysis phase (i.e., Exploratory approach – EXA; Traditional approach - TRA)
PSL^{opt} = performance index for generic optimized solution S^{opt}_i (or sub-solution S^{opt}_{ij}).
EL^{opt} = elasticity for generic optimized solution S^{opt}_i (or sub-solution S^{opt}_{ij}).

Figure A.9 in Appendix A shows the GUI of the final elasticity screening phase, developed by MATLAB App Designer software.

2.5.4 Final ranking

In this last phase, PSL^{opt} values of the acceptable and optimized solutions $S^{acc(opt)}_i$ are compared, and the final ranking is compiled. As already mentioned, the solutions that do not pass the final elasticity screening step are not taken into account in this phase.
The final ranking varies depending on the information available to the designer, i.e., if the data considered in the production database are specific (TR approach) or ranges-defined (EX approach).

- Concerning the TR approach, the phase provides that the PSL^{opt} of each solution is used directly; thus, the acceptable and optimized solutions $S^{acc(opt)}i$ are ranked from best to worst through their PSL value (see **Equation 80** in **Table 37**).
- Since in the EX approach each solution is characterized by a PSL range, the final ranking is done by means of the average value of such a range, as defined by **Equation 81** in **Table 37**. The acceptable and optimized solutions $S^{acc(opt)}_i$ are ranked from best to worst through the value $PSL^{rank(opt)}$ index calculated for each bubble.

Moreover, the methodology proposed calculates the improvement (or worsening) of each acceptable solution S^{acc} obtained during the first classification and further analyzed in Optimization and Final Classification phases. The **Equation 82** defines the percentage variation between the initial condition of solution (i.e., before the optimization - PSL^{rank}) and the optimized one (i.e., after optimization - $PSL^{rank(opt)}$).

Table 37. PSL^{opt} ranking modelling.

PSL^{opt} ranking equations		
Traditional Approach (TRA)	$PSL_i^{rank(opt)} = PSL_i^{opt}$	(80)
Exploratory Approach (EXA)	$PSL_i^{rank(opt)} = mean(PSL_i^{opt}) = \frac{\left(max(PSL_i^{opt}) - min(PSL_i^{opt})\right)}{2}$	(81)
Arbitrary Scenario (ARB)	$\%PSL^{rank} = 100 \cdot \left(\frac{PSL_i^{rank(opt)} - PSL_i^{rank}}{PSL_i^{rank}}\right)$	(82)
Reference Scenario (REF)	$\%PSL^{rank} = 100 \cdot \left(\frac{PSL_i^{rank(opt)} - PSL^{rank(ref)}}{PSL^{rank(ref)}}\right)$	

Where:
PSL^{rank}_i = Product Sustainability Level for generic acceptable solution S^{acc}_i calculated during first ranking [-].
$PSL^{rank(opt)}_i$ = Product Sustainability Level for generic acceptable and optimized solution $S^{acc(opt)}_i$ defined in final ranking [-].
$\%PSL^{rank}$ = Percentage variation of Product Sustainability Level for generic acceptable solution S^{acc}_i calculated in final ranking [-].
$PSL^{rank(ref)}$ = Product Sustainability Level for reference solution defined for case study [-].

The final ranking phase is performed according to scheme reported in **Figure 27**, where MATLAB allows the classification of indexes previously defined (i.e., $PSL^{rank(opt)}$) for each acceptable and optimized solution $S^{acc(opt)}_i$ obtained in the final elasticity screening phase (see **Table 38**) .

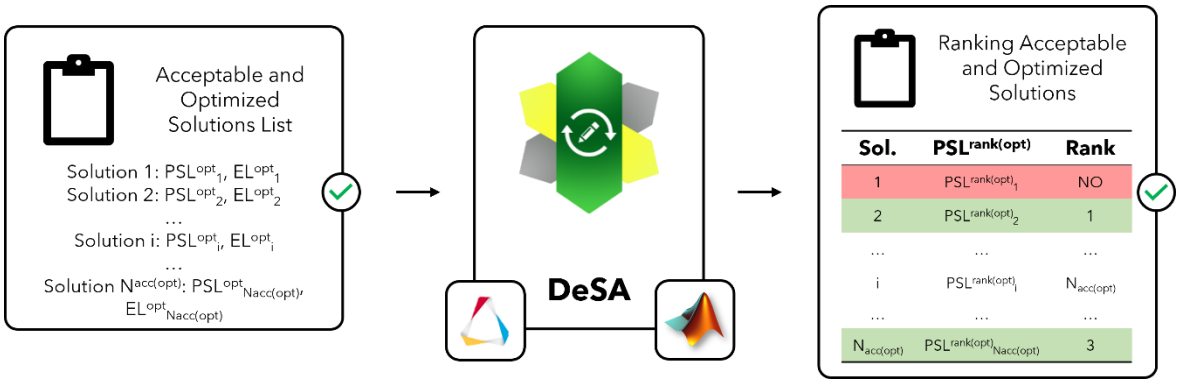

Figure 27. Final ranking phase framework.

Table 38. Representation of acceptable and optimized solutions list ranking, with $PSL^{rank(opt)}$ index calculated for each solution $S^{acc(opt)}_i$.

List of Acceptable and Optimized Solutions							
Sol.	**N**	**Appr.**	**PSL^{rank}**	**$PSL^{rank(opt)}$**	**$\%PSL^{rank}$**	**First Ranking**	**Final Ranking**
$S^{acc(opt)}_1$	N_1	TRA EXA	PSL^{rank}_1	$PSL^{rank(opt)}_1$	$\%PSL^{rank}_1$	1	2
$S^{acc(opt)}_2$	N_2	TRA EXA	PSL^{rank}_2	$PSL^{rank(opt)}_2$	$\%PSL^{rank}_2$	2	1
…	…	…	…	…	…	…	…
$S^{acc(opt)}_i$	N_i	TRA EXA	PSL^{rank}_i	$PSL^{rank(opt)}_i$	$\%PSL^{rank}_i$	3	$N_{acc(opt)}$
…	…	…	…	…	…	…	…
$S^{acc(opt)}_{Nacc(opt)}$	$N_{Nacc(opt)}$	TRA EXA	PSL^{rank}_{Nacc}	$PSL^{rank(opt)}_{Nacc(opt)}$	$\%PSL^{rank}_{Nacc(opt)}$	N_{acc}	3

Legend:
Sol. = list of solution (S) obtained from Screening phase;
N = Number of simulations for generic solution S_i, considered the EX approach
Appr. = Typology of approach used in Design and Sustainability analysis phase (i.e., Exploratory approach – EXA; Traditional approach - TRA)
PSL = product sustainability level for generic solution S_i (or sub-solution S_{ij}).
PSL^{rank} = Product Sustainability Level for generic acceptable solution S^{acc}_i (or sub-solution S^{acc}_{ij}) calculated during first ranking [-].
$PSL^{rank(opt)}_i$ = Product Sustainability Level for generic acceptable and optimized solution $S^{acc(opt)}_i$ (or sub-solution $S^{acc(opt)}_{ij}$) defined in final ranking [-].
$\%PSL^{rank}$ = Percentage variation of Product Sustainability Level for generic acceptable solution S^{acc}_i calculated in final ranking [-].

3. Results and Discussion

As already shown in "First Elasticity screening" paragraph (*2.3.2*, see **Table 20**), there are four combinations of the approaches/scenarios defined by the DeSA methodology. For this reason, four case studies will be presented and discussed, varying in primary shape (PS: 1D, 2D, and 3D), approach (i.e., TR and EX approaches), and scenario (i.e., ARB and REF scenarios); they are reported in **Table 39**.

Table 39. Case Studies features: combination of shapes (1D, 2D, and 3D), approaches (TRA, EXA) and scenarios (ARB, REF) defined in the proposed methodology.

Case Studies Features			
Case Study	**Primary Shape**	**Approach**	**Scenario**
Torsion Bar (TB)	1D	EXA	REF
Top Roof (TRF)	2D	TRA	REF
Front Lower Control Arm (FLCA)	3D	EXA	ARB
Engine Mounting Bracket (EMB)	3D	TRA	ARB

The following subparagraphs show the application of the framework to the case studies defined above, strictly closed to theoretical approach presented in previous sections.

3.1 1D | EXA-REF Case Study: Torsion Bar (TB)

The suspension system is a significant and acute element of a vehicle's design. Regardless of the design and components (such as cross-members, axles, knuckles, etc…), all suspension systems do the same functions: keep the tires in contact with the surface of the road, upkeep the weight of a vehicle, absorb the forces produced by the movement and motion of the vehicle and control the vehicle's direction of travel.

The torsion bar (TB) is a suspension system usually used in vehicles such as cars, trucks, and vans. The resistance is the basic principle behind this type of suspension system: the forces made by the vehicle's motion produce a torque on the bar, which turns it along its axis; the torsion bar will resist the twisting effect and return to its normal state, thus counteracting the torque. By doing so, the suspension supplies a level of resistance to the forces generated by the movement of the vehicle, fulfilling its function. In this context, the torsion bar (TB) is chosen as an applicative mono-dimensional (1D) case study and Functional Unit (FU) for DeSA methodology.

3.1.1 Screening

Starting point of the screening phase is primary shape design constraint choice (see **Table 6**). For this case study, mono-dimensional (1D) shape is chosen; **Figure 28** illustrates the initial FEM model of TB.

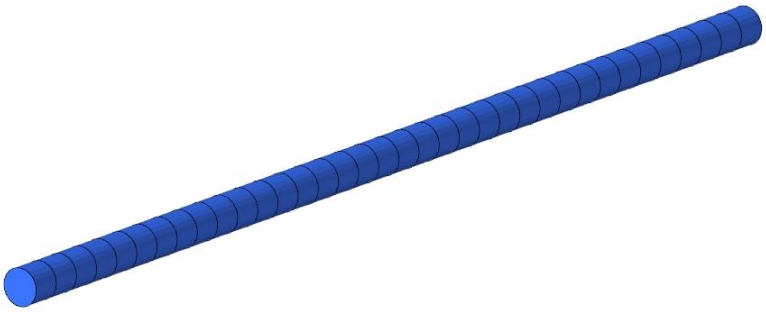

Figure 28. TB FEM model.

Then, the creation of the production database is performed, defined by materials and manufacturing processes available to the designer. Exploratory approach (EXA) is considered, i.e., the production database provides physical and mechanical properties through variability ranges (min-max ranges). For the TB component, the list of available materials (MAT) is made of metals and alloys and composites (in the hybrids material class): each material is defined by a material ID (MAT_{ID}), mechanical (i.e., density, Young modulus, etc.), environmental (i.e., climate change), and economic properties (i.e., cost). **Table 40** presents the list of materials chosen, while Appendix B reports all materials properties used for the analysis.

Table 40. List of available materials and processes in TB production database.

Production Database				
Material Section (MAT)				
	Material ID	**Material Class**	**Material Subclass**	**Material Name**
Materials	M1	Metals and Alloys	Ferrous	Cast Iron (Ductile)
	M2	Metals and Alloys	Ferrous	High Carbon Steel
	M3	Metals and Alloys	Ferrous	Stainless Steel
	M4	Metals and Alloys	Non-Ferrous	Age-Hardening Wrought Al-Alloys
	M5	Metals and Alloys	Non-Ferrous	Titanium Alloys
	H1	Hybrids	Composites	Carbon Fiber Reinforced Polymer (CFRP)
	H2	Hybrids	Composites	Glass Fiber Reinforced Polymer (GFRP)
Manufacturing Technologies Section (MAN)				
	Process ID	**Process Class**	**Process Subclass**	**Process Name**
Processes	CA1	Casting	Die Casting Processes	High Pressure Die casting
	CA2	Casting	Investment Casting Processes	Investment Casting
	DE1	Deformation	Bulk Deformation Processes	Extrusion
	CO1	Composite Forming	Advanced Composite Forming Processes	Resin Transfer Molding (RTM)
	CO2	Composite Forming	Conventional Composite Forming Processes	Lay-Up Methods

As shown in **Table 40**, the list of allowable processes (MAN) is made of manufacturing technologies able to generate mono-dimensional (1D) shapes: each process is defined by a process ID (PR_{ID}), mechanical, environmental, and economic features. Appendix B also reports all processes data used for the TB case study.

The second step of screening is the application of design constraints (directly provided by the designer). The unique physical constraints applied to the case study is the process constraint Batch size (B) (see **Table 6**), with the objective to explore all possible combinations generated by the proposed methodology with an economic batch limitation.

The final step of the screening is determining all design solutions that satisfy the design requirements (imposed by the designer) and are feasible from a technical point of view. Several solutions are automatically generated thanks to applying design constraints and design choices regarding geometry, materials, and processes. As provided by the theoretical background reported in previous paragraphs, all combinations that do not meet the above requirements are not inserted into the feasible solutions list.

3.1.2 Design and Sustainability analysis

In this phase, the design and sustainability performances of TB alternative design solutions (obtained in the screening step) are analyzed and compared over its whole LC.

In design analysis step, FEM simulation modelling of all feasible solutions is performed (**Figure 4**). The reference scenario (REF) is chosen; thus, the analysis of this case study is performed based on of two loadcases provided by the generic alternative:

- structural integrity, as ratio between the stress level on the reference scenario and the maximum stress level on the TB component calculated through the FEM simulations (as shown in **Equation 16**);
- deformation level, as ratio between the maximum deformation on the reference scenario and the maximum deformation on the TB component calculated through the FEM simulations.

The first load case is obtained from linear static analysis, using a twisting moment applied to the torsion bar axis (see the red arrow in **Figure 29**). At the same time, the second load case is defined from the torsional deflection of the entire TB, always calculated from linear static analysis.

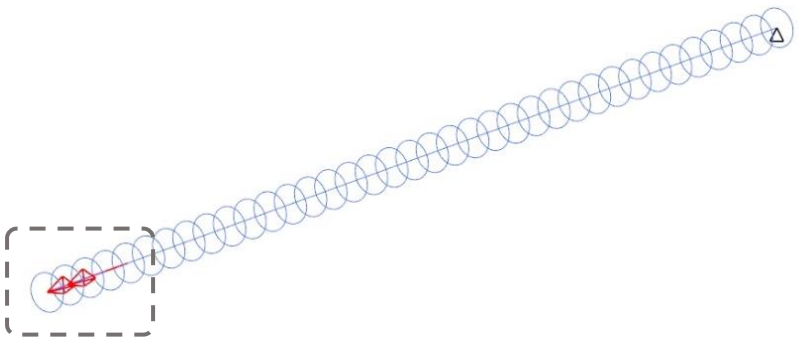

Figure 29. Moment (represented as red arrow) applied to TB axis for linear static analysis.

As shown in **Equation 13**, the weighting factors for two loadcases (w_l), used for the design modelling, are defined to calculate the performance level PI; an equal weight is

assigned to two loadcases ($w_{l1} = w_{l2} = 0.5$), since it is assumed that they have the same level of importance. **Figure 30** shows the BCs of the TB: the surface linked with the lever (i.e., the torsion key) mounted perpendicular to the bar itself and attached to a suspension arm, and the connection with the chassis are defined by zones A and B, respectively.

Figure 30. TB BCs nodes.

The load is applied to node A as a moment vector around TB axis (i.e., the z-direction, according to the global system reported in **Figure 30**). By assumption, the twisting moment is calculated considering the force defined through a static distribution of the vehicle mass (as shown in **Table 41**) on each wheel (F_{wheel}) and multiplying this result by the lever arm (l_{arm}) chosen for the case study (**Equations 83-84**):

$$m_{veh} = 1440\ kg \rightarrow\ F_{wheel} = (m_{veh} \cdot g)/4 \approx 3600\ N \tag{83}$$

$$M_z = F_{wheel} \cdot l_{arm} = 3600 \cdot 100 = 3.6 \times 10^5\ Nmm \tag{84}$$

Table 41. TB Case Study - Vehicle features inputs.

Vehicle Features Inputs	
Feature	**Value**
Vehicle Mass	1440 [kg]
Vehicle Lifetime	200000 [km]
Vehicle Class	C
Powertrain	BEV
Driving Cycle	Worldwide Harmonized Light Vehicles Test Procedure (WLTP)
Electric Grid Mix	EU-28

Finally, node B (the connection between chassis and torsion bar) is fixed and no translational motion in x, y and z-directions is allowed, as well as x, y and z-rotational motion.

Considering that data characterizing the generic solution S_i are provided in terms of ranges (i.e., EX approach), the LH method is applied to implement such data in the FEM simulations. For this case study a number of simulations (n_{sim}) variable between 3 and 5 is assumed; this variability mainly depends on solution's data (see **Figure 13** and **Equations 1**

- 5). **Table B.1** and **Table B.2** in Appendix B show design data of materials and processes available for this case study (as well as the material/shape/process compatibility matrices).

The environmental analysis step performs the LCA of all feasible sub-simulations S_{ij} obtained from the design analysis, calculating the environmental level EI. The reference vehicle on which the FU (i.e., TB) is assumed to be installed is the VOLKSWAGEN e-Golf with electric battery, with a life-distance of 200,000 km. The component lifetime is assumed equal to the one of the vehicle: no substitution during operation is assumed. As described in a previous section (*2.2.2 - Environmental modelling*) the system boundaries include the following life cycle phases: materials production, component manufacturing, use stage, and EoL treatments. **Table 41** provides the electric car technical features, whereas **Table B.3** and **Table B.4** in Appendix B show the environmental impacts of materials and processes available for this case study.

The economic analysis step performs the LCC of all feasible sub-simulations S_{ij} obtained from the design analysis and assessed in environmental analysis, calculating the economic level CI. As described in a previous section (*2.2.3 - Economic modelling*), the system boundaries include the same life cycle phases reported in the environmental step: overall production (comprising materials and manufacturing stages), use phase, and EoL.

The economic batch size (B) chosen for FU is 5000 pieces, and the fraction of time for which the equipment is productive (i.e., the load factor (L)) is set to 50%, fixed for all processes available in the production database. In the same way, the capital write-off time is equal for all processes. **Table 42** provides economic features, instead **Table B.5** and **Table B.6** (in Appendix B) show economic costs of materials and manufacturing processes available for TB case study.

Table 42. TB Case Study - Economic features inputs.

Economic Features Inputs	
Feature	**Value**
Batch Size	5000 [pc.]
Load Factor	50 [%]
Capital Write-off Time	5 [yr.]
EoL Grid-Mix	EU-28
Electric Grid Mix	EU-28

3.1.3 First Classification

Design and Sustainability analysis is performed for the design alternatives; then, the PSL is calculated through indexes (i.e., PI, EI, and CI). After the first elasticity screening is performed, the first ranking of the acceptable solutions is occurred.

The PSL calculation step performs the calculation of the PSL by a weighted sum formula to combine the weights of criteria with the performance/sustainability scores for each design alternative (see section *2.3.1 – PSL calculation*). The PSL scale factor (K) assumed for the case study is 10.

The first elasticity screening step identifies all design solutions that are acceptable from an elasticity perspective. Since the TB case study is defined considering an EX

approach with REF scenario, such a screening is performed by means of ELV^{ref} and FL parameters. **Table 43** shows the reference scenario chosen for TB case study.

Table 43. TB Case Study – Reference Scenario Data.

Reference Scenario Data			
Material Section (MAT)			
Material ID	**Material Class**	**Material Subclass**	**Material Name**
M^{ref}	Metals and Alloys	Ferrous	Stainless Steel
Manufacturing Technologies Section (MAN)			
Process ID	**Process Class**	**Process Subclass**	**Process Name**
CA^{ref}	Casting	Investment Casting Processes	Investment Casting
Sustainability Indexes Section (IND)			
Reference Stress (σ^{ref})		200 [MPa]	
Reference Angular Deflection (ϑ^{ref})		5 [°]	
Reference Climate Change (CC^{ref})		160 [$kgCO_{2eq}$]	
Reference Cost ($COST^{ref}$)		300 [EUR]	

In this context, ELVref is calculated automatically from this scenario, and it is set equal to 0 (that means a structural integrity level (PI) equal to 1). Whereas FL is assumed by the designer equal to 0.5, all alternatives with less than 50% of EL range to the right of ELV^{ref} vertical line are rejected and are not considered in the first ranking. The Reference Product Sustainability Level Value ($PSLV^{ref}$) is also defined and equal to scale factor K. The ranking step provides that the PSL values related to the acceptable solutions are compared; such a ranking is performed by means of the average value of the PSL range (i.e., PSL_{ss}), according to explorative approach (see **Equation 75**).

3.1.4 Optimization

The main objective of the optimization phase is to take the acceptable solutions S^{acc}_{i} (as well as sub-solutions S^{acc}_{ij}, in the EX approach) obtained from the first elasticity screening and optimize them, to improve the PSL of TB alternatives, without compromising the mechanical performance (in this case, structural integrity and deformation level) of the analyzed design solutions. Since the type of primary shape (PS) chosen during the screening phase is mono-dimensional (1D), the methodology will work on the (sub-)solutions using the Parameter Modification: starting from given TB volume and the boundary condition data (loads, constraints, etc., as shown in **Figure 29** and **Figure 30**), the methodology will accomplish the variation of one or more geometric parameters in order to obtain the solutions that provides the best performance in relation to the user-defined objective. In this context, the TB geometry is directly modified when a unique geometric parameter chosen by the designer changes, in order to calculate the indexes described in the DeSA methodology.

Since the design approach chosen by the designer is "Exploratory" (EXA), the methodology works as follows:

- The geometric parameter (par) defined for this case study is the inner radius (r_{inn}) of the circular section used for the TB. The user-defined range is chosen subdivided into following values (with $N_t = 5$):

$$r_{inn} = [0, \dots, x]\ mm \rightarrow \begin{bmatrix} 0 \\ 2.5 \\ 5 \\ 7.5 \\ 10 \end{bmatrix} mm$$

- In the EX approach, each acceptable sub-solution (S^{acc}_{ij}) will be defined by several sub-solutions (S^{acc}_{ijt} with t = 1, ..., 5 - the number of subdivision of the inner radius (r_{inn})), where par is modified in each solution geometry. It follows from the above that S^{acc}_{ijt} depends on material properties (MAT_{ij}, see EXA properties in **Table B.1** in Appendix B), modified geometry (G_t) and setting parameters for the parameter modification (N_t), as provided by the following relations:

$$S^{acc}_{ijt} = S^{acc}_{ijt}(G_t, BC, MAT_{ij}, N_t)$$

$$N_t = 5 \rightarrow r_{inn} = [0, 2.5{,}5{,}7.5{,}10]\ mm$$

  The simulations are launched and performed according to EX approach in Design and Sustainability Analysis phase (*2.2*); thus, the results are reported in a table (as already shown in **Table 27**). All solutions are represented through bubbles in a PSL-EL "Bubble chart" (see **Figure 17** and **Figure 18**); each bubble of a sub-solution S^{acc}_{ij} will have 5 bubbles shown in the diagram. Finally, the results obtained will be sent **DIRECTLY** to the final screening, since in this case, the TB geometry is already modified to obtain sustainability indexes.

3.1.5 Final classification

Once the Optimization is performed for the acceptable sub-solutions S_{ij}, the final classification phase is carried out by means of the following steps: Design and Sustainability Re-Analysis and final PSL calculation. After the final elasticity screening, the final ranking of the acceptable and optimized alternatives is occurred.

The final PSL calculation step performs the calculation of the PSL always using a weighted sum formula to combine the weights of criteria with the performance/sustainability scores for each design alternative (as already shown in section *3.3.1*). The PSL scale factor (K) assumed for the case study is the same used in the previous paragraphs, equal to 10.

The final elasticity screening step identifies all optimized solutions that are acceptable from an elasticity perspective. Since the TB case study is defined considering an EX approach with REF scenario, the screening is performed by means of ELV^{ref} and FL parameters already defined previously: ELV^{ref} is assumed equal to 0, and FL is assumed equal to 0.5. As shown in **Table 43,** the reference scenario is still used for final classification.

The final ranking step provides that the PSL values related to the acceptable and optimized sub-solutions are compared; such a ranking is performed by means of the average value of the PSL range (i.e., $PSL^{rank(opt)}$), according to explorative approach (see **Equation 81**). Finally, the methodology calculates the improvement (or worsening) of each acceptable solution S^{acc} obtained during the first classification and further analyzed in Optimization and Final Classification phases (see **Equation 82**).

3.1.6 Results & Discussion

Table 44 reports the 7 solutions generated in the screening stage that satisfy both design requirements (imposed by designer) and are feasible from a technical perspective.

Table 44. TB Case Study - List of solutions created in the first screening phase (IN); outcomes obtained through First Elasticity Screening and First Ranking.

TB Solutions List – BEFORE OPTIMIZATION						
ID	**Design Solution ID**	**PSL^{IN}_{range}**	**EL^{IN}_{range}**	**PSL^{IN}_{rank}**	**First Elasticity Screening**	**First Ranking**
2	2_Circular_M1_CA2	[15.13, 29.09]	[2.28, 3.14]	22.11	OK	3
3	3_Circular_M2_CA2	[16.31, 27.45]	[3.45, 4.74]	21.88	OK	4
4	4_Circular_M3_CA2	[10.83, 15.13]	[2.57, 4.37]	12.98	OK	6
5	5_Circular_M4_CA2	[16.86, 38.51]	[0.52, 1.49]	27.68	OK	2
6	6_Circular_M4_DE1	[25.79, 67.85]	[0.52, 1.49]	46.81	OK	1
8	8_Circular_H1_CO1	[18.24, 19.60]	[1.93, 3.22]	18.92	OK	5
9	9_Circular_H2_CO1	[37.34, 39.66]	[-0.42, -0.22]	38.50	NO	No Rank

A Design Solution ID is defined for generic design alternative as a combination of shape (primary component shape defined by the designer – 1D, 2D, or 3D), material (MAT_{ID}, see **Table 40**), and process (PR_{ID}, see **Table 40**).

Considering that generic i-th solution S_i is defined in terms of material intervals (i.e., EX approach, see **Table 8**), it is explored with N_i sub-solutions S_{ij} (j =1, …, N_i), each of which is modelled through a FEM simulation. The number of required FEM simulations N_i is determined using the range sizes of different material properties (**Table B.1** in Appendix D) and number of simulations (n_{sim}) variable between 3 and 5 (assumed by the designer). With these assumptions, the LH method provides 6 simulations, defined on the basis of material types reported in **Table 40**, with a total of 26 sub-simulations. **Table 45** reports simulations created by LH method and the N_i associated by the generic solution.

Table 45. TB Case Study - List of simulations created by LH method.

ID	LH Simulation ID	Number of Sub-simulations
1	M4	5
2	H1	3
3	M1	5
4	H2	3
5	M2	5
6	M3	5
	Total Sub-simulations	26

Looking at the list of solutions, High Pressure Die casting (ID: CA1) is not compatible with any of the available material. Therefore, no solution made with the specific process is generated. Moreover, Titanium Alloys (ID: M5) are not compatible with any of the available process; thus, no solution made with the titanium is created. 6 out of 7 solutions (≈ 86%) comply with the first elasticity screening, reported in a unique group:

- full-acceptable solutions, that present EL range always greater than ELV (see green lines in **Table 45**).

All solutions analyzed in the design and sustainability analysis phase can be represented through ellipses in the PSL-EL bubble chart, shown in **Figure 31**.

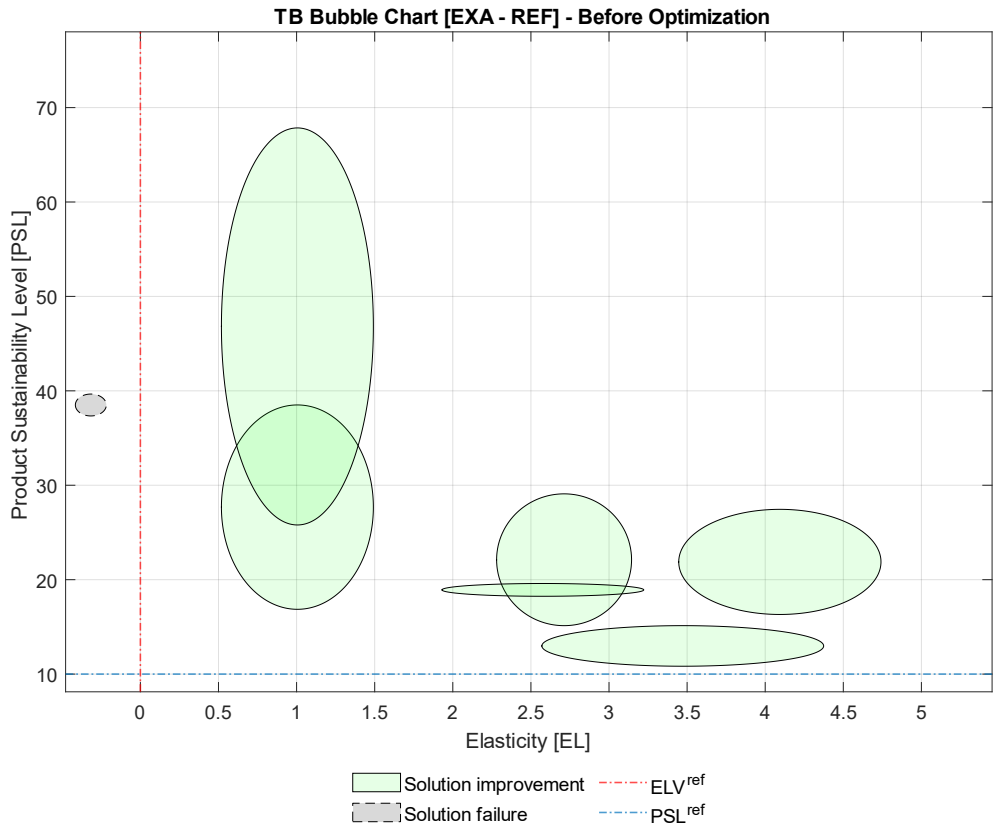

Figure 31. TB bubble chart (with FL = 0.5), before the Optimization phase. Dashed bubbles represent discarded solutions.

The full-acceptable solutions S^{acc}_i are those identified by bubbles (in green in **Figure 31**) whose area is entirely to the right of the ELV line. On the other hand, the FL-acceptable solutions S^{acc}_i are those identified by bubbles whose area is to the right of the ELV line by more than 50%; however, no solution is present in this typology. The solutions with more than half of the surface to the left of the ELV line are non-acceptable, therefore, rejected. In this case, the only solution that has not passed the first screening phase is the solution defined by the Glass Fiber Reinforced Polymer (GFRP) material (ID = H2).
Finally, **Table 45** reports PSL_{rank} for all acceptable design options, also including the first ranking, from which the best acceptable solution results to be the one identified by ID = 6 (highest value of PSL^{IN}_{rank}), made of Age-Hardening Wrought Al-Alloys and shaped trough extrusion process.

Next, the acceptable solutions S^{acc}_i (therefore, the sub-solutions S^{acc}_{ij}) obtained from the first elasticity screening will be optimized to improve the PSL, without compromising the mechanical performance of the analyzed design solutions. The type of primary shape chosen during the screening phase is mono-dimensional (1D); thus, the methodology will work on the (sub-)solutions S^{acc}_{ij} using the Parameter Modification. After the optimization simulations are performed, the results will be sent **DIRECTLY** to the final screening, since the geometry is already modified to obtain sustainability indexes described in the DeSA (i.e., PI^{opt}, EL^{opt}, EI^{opt}, and CI^{opt}) and used for final PSL calculation (according to the modelling framework reported in **Table 27**). **Table 46** shows the results obtained from Parameter Modification in EX approach.

Table 46. TB Case Study - List of solutions after the Parameter Modification phase; outcomes obtained through geometric parameter (par) modification.

TB Solutions List – AFTER PARAMETER MODIFICATION						
ID	**Geometric Parameter**					
	Index	**r_{inn} = 0 [mm]**	**r_{inn} = 2.5 [mm]**	**r_{inn} = 5 [mm]**	**r_{inn} = 7.5 [mm]**	**r_{inn} = 10 [mm]**
2	PSL_{range}	[15.13, 29.09]	[15.30, 29.34]	[15.83, 30.14]	[16.86, 31.63]	[18.66, 34.14]
	EL_{range}	[2.28, 3.14]	[2.28, 3.14]	[2.27, 3.13]	[2.23, 3.09]	[2.12, 2.98]
3	PSL_{range}	[16.31, 27.45]	[16.48, 27.69]	[16.99, 28.46]	[17.97, 29.87]	[19.67, 32.23]
	EL_{range}	[3.45, 4.74]	[3.45, 4.74]	[3.43, 4.73]	[3.38, 4.68]	[3.25, 4.56]
4	PSL_{range}	[10.83, 15.13]	[10.96, 15.30]	[11.36, 15.84]	[12.13, 16.84]	[13.48, 18.56]
	EL_{range}	[2.57, 4.37]	[2.57, 4.37]	[2.56, 4.36]	[2.51, 4.31]	[2.38, 4.18]
5	PSL_{range}	[16.86, 38.51]	[17.06, 38.80]	[17.69, 39.71]	[18.89, 41.40]	[21.02, 44.23]
	EL_{range}	[0.52, 1.49]	[0.52, 1.49]	[0.51, 1.49]	[0.50, 1.47]	[0.45, 1.42]
6	PSL_{range}	[25.79, 67.85]	[26.01, 68.56]	[26.70, 70.79]	[28.01, 74.89]	[30.26, 81.62]
	EL_{range}	[0.52, 1.49]	[0.52, 1.49]	[0.51, 1.49]	[0.50, 1.47]	[0.45, 1.42]
8	PSL_{range}	[18.24, 19.60]	[18.50, 19.88]	[19.33, 20.80]	[20.91, 22.55]	[23.63, 25.60]
	EL_{range}	[1.93, 3.22]	[1.93, 3.22]	[1.93, 3.22]	[1.90, 3.19]	[1.84, 3.11]

Table 47 reports the 6 solutions analyzed in the Optimization phase and assessed through the final screening, satisfying both design requirements and technically feasible.

Table 47. TB Case Study - List of solutions created after the Optimization phase (OPT); outcomes obtained through Final Elasticity Screening and Final Ranking.

TB Solutions List – AFTER OPTIMIZATION						
ID	**Design Solution ID**	**PSL^{OPT}_{range}**	**EL^{OPT}_{range}**	**PSL^{OPT}_{rank}**	**Final Elasticity Screening**	**Final Ranking**
2	2_Circular_M1_CA2	[18.66, 34.14]	[2.12, 2.98]	26.40	OK	3
3	3_Circular_M2_CA2	[19.67, 32.23]	[3.25, 4.56]	25.95	OK	4
4	4_Circular_M3_CA2	[13.48, 18.56]	[2.38, 4.18]	16.02	OK	6
5	5_Circular_M4_CA2	[21.02, 44.23]	[0.45, 1.42]	32.63	OK	2
6	6_Circular_M4_DE1	[30.26, 81.62]	[0.45, 1.42]	55.94	OK	1
8	8_Circular_H1_CO1	[23.63, 25.60]	[1.84, 3.11]	24.61	OK	5

Considering that generic i-th solution S^{acc}_i is defined in terms of material variability range (EX approach in **Table 8**), it is explored with (N^{acc}_i x N_t) sub-solutions S^{acc}_{ijt} (where j =1, …, N^{acc}_i and t = 1, ..., N_t - the number of subdivision of geometric parameter), each of which was modelled through a FEM simulation. The number of required FEM simulations N^{acc}_i is already determined during FEM modelling in Design Analysis (**Table 45**).

Therefore, all solutions - 100% respect the total number of design alternatives - comply with the final elasticity screening, reported in a unique group:

- full-acceptable and optimized solutions, that present EL range always greater than ELV^{ref} (**Table 47** and **Table 48**).

Table 48. TB Case Study - List of solutions compared before (IN) and after (OPT) the Optimization phase.

TB Solutions List – COMPARISON BEFORE/AFTER OPTIMIZATION					
ID	**Design Solution ID**	**PSL^{IN}_{rank}**	**PSL^{OPT}_{rank}**	**$\%PSL_{rank}$**	**Final Ranking**
2	2_Circular_M1_CA2	22.11	26.40	19.40%	3
3	3_Circular_M2_CA2	21.88	25.95	18.60%	4
4	4_Circular_M3_CA2	12.98	16.02	23.42%	6
5	5_Circular_M4_CA2	27.68	32.63	17.88%	2
6	6_Circular_M4_DE1	46.81	55.94	19.50%	1
8	8_Circular_H1_CO1	18.92	24.61	30.07%	5

All solutions analyzed in the design and sustainability re-analysis phase are represented through ellipses in the PSL-EL bubble chart of **Figure 32**.

The full-acceptable and optimized solutions $S^{acc/opt}_i$ are those identified by bubbles whose surface is entirely to the right of the ELV^{ref} line – green bubbles in **Figure 32**). On the other hand, the FL-acceptable and optimized solutions $S^{acc/opt}_i$ are always those identified by bubbles whose area is to the right of the ELV^{ref} line by more than 50% (in yellow); however, despite the optimization no solution is present in this typology. The other solutions (those that have more than half of the bubble area to the left of the ELV^{ref} line) are not acceptable and therefore they are rejected.

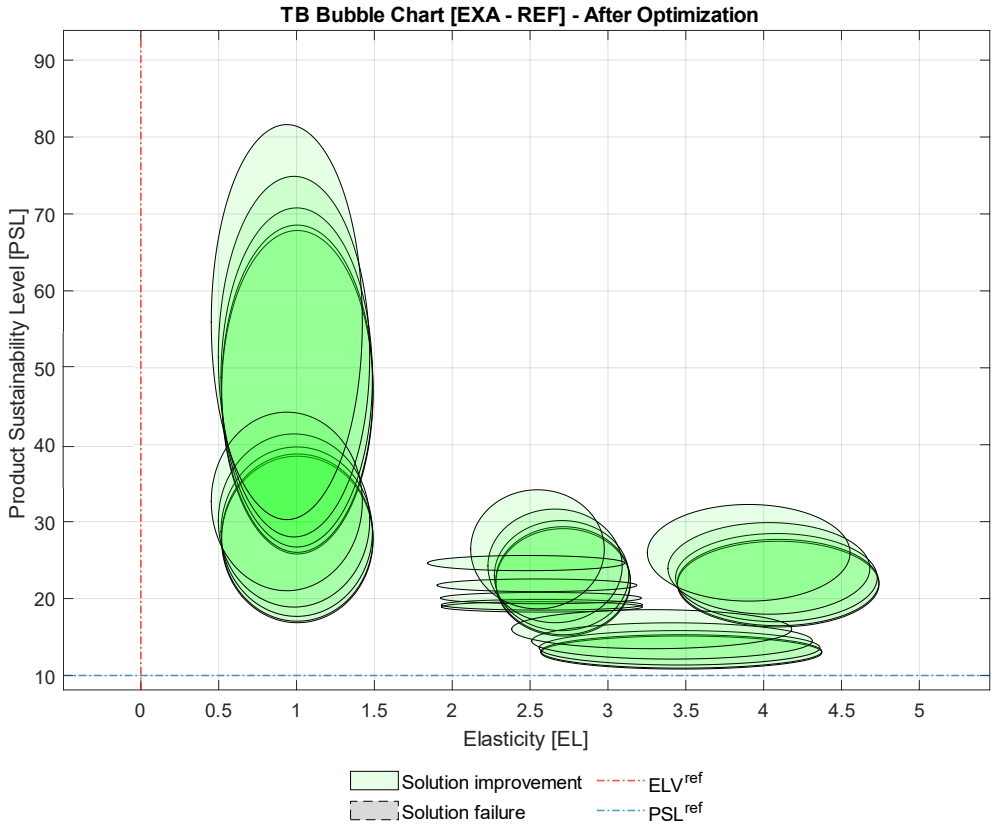

Figure 32. Torsion Bar bubble chart (with FL = 0.5), after the Optimization phase. Dashed bubbles represent discarded solutions.

Moreover, **Table 48** reports PSL_{rank} for all acceptable and optimized design alternatives, including the final ranking; assuming that, regardless of the variation of the geometric parameter r_{inn}, all solutions are considered acceptable for elasticity phase, the calculation of PSL^{OPT}_{rank} considers the solutions with r_{inn} = 10 mm. Thus, the best acceptable and optimized solution results to be the one identified by ID = 6, made of aluminium shaped by extrusion process. This solution is the same as before optimization, with the highest value of PSL^{OPT}_{rank}.

The methodology finally calculates the improvement (or worsening) of each acceptable solution S^{acc} obtained during the first classification and further analyzed in Optimization and Final Classification phases (see **Table 48** and **Equation 82**).

The analyzed solutions' improvement is between 17% and 30%; the elasticity (EL_{range}) presents rather high values compared to the reference value (ELV^{ref} = 0, see **Table 47**). This implies that the acceptable design alternatives S^{acc} can be further optimised to increase their PSL without compromising the performance (structural integrity and torsion angle).

The solutions analysis is based on an integrated single score index (PSL), as well as the specific sustainability indexes (PI, EI, and CI).

Regarding the Sustainability Level, **Figure 33** (*left*) shows the variability range of PSL^{IN} for all TB solutions considered acceptable during the first ranking.

Figure 33. TB Case Study – PSL of all best solutions, before (IN) and after (OPT) the Optimization.

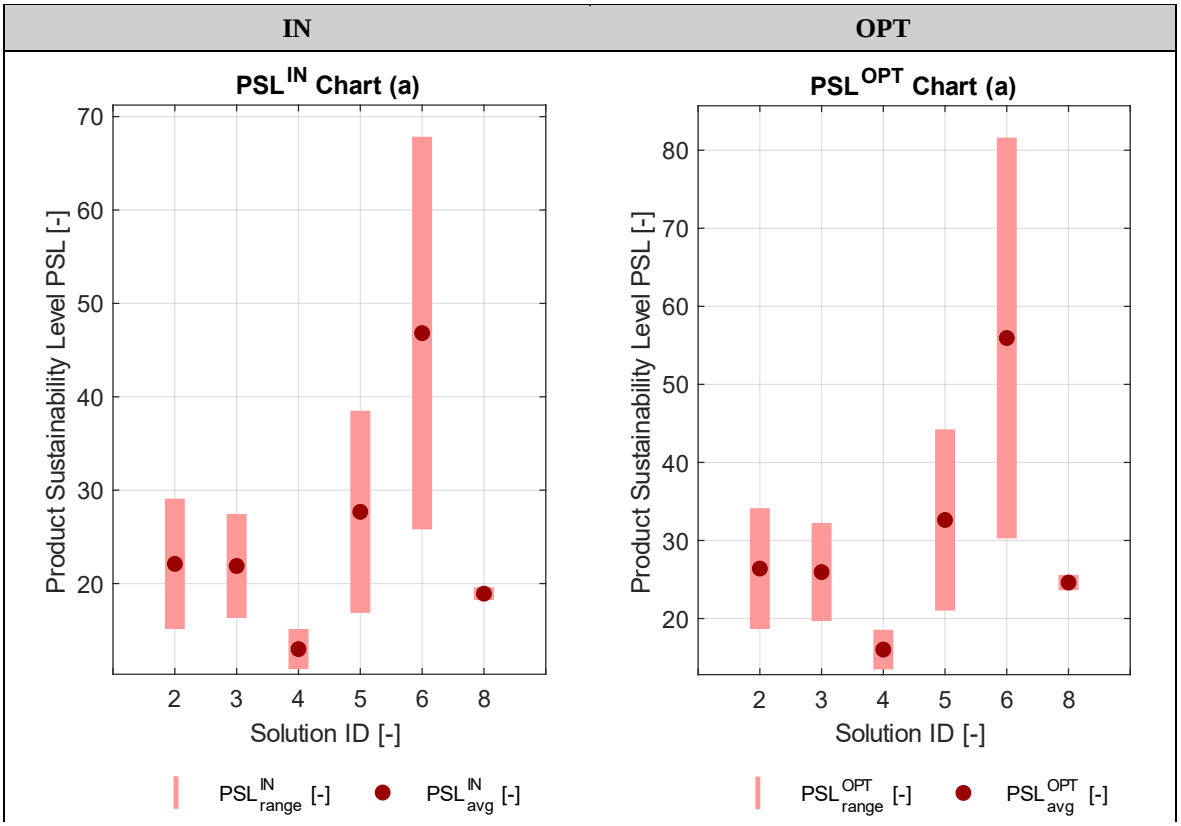

It is interesting to stress that the best design option (made of aluminium shaped by extrusion process - ID = 6) results preferably when considering the minimum value of the range (minimum value higher respect the other solutions, except for the solution with ID = 5 - second in the first ranking). Moreover, 5 out of 6 solutions present a PSL^{IN} value much higher than the value of the reference solution ($PSLV^{ref}$ = 10, see blue dotted line in **Figure 31** and **Figure 32**). Whereas the design alternative made by Stainless Steel (ID = 4), since it is defined by the same family of materials to which the reference solution belongs (e.g., M3), presents a PSL value comparable to that of the reference scenario.

Another relevant outcome of the TB case study is that all acceptable solutions have high PI ranges, which clearly indicates a significant margin for improvement in the lightweight perspective (starting point for the Optimization phase). Indeed, reducing component mass would certainly provide beneficial effects not only on the environment (decrease of CC in all LC stages, according to **Equations 8-23**), but also in terms of the overall sustainability level (an increase of PSL_{rank}).

Figure 33 (*right*) shows instead the variability range of PSL^{OPT} for all TB solutions considered acceptable during the final ranking. It is interesting to stress that the best design option is always the solution identified made of aluminium (ID = 6), preferably when considering the minimum value of the range (minimum value higher respect the other solutions, except for the solution with ID = 5 - second in the final ranking) even after the optimization. It sees that 5 out of 6 solutions present a PSL^{OPT} value much higher than the value of the reference solution ($PSLV^{ref}$ = 10). Also, the design alternative made by Stainless Steel (ID = 4), even if it is defined by the same family of materials ascribed to the reference solution, presents a PSL slightly higher than the reference, thanks to the optimization.

All acceptable and optimized solutions have still high PI ranges, which clearly indicates a further margin for improvement in the lightweight perspective; thus, still reducing the TB mass would certainly provide other beneficial effects on the environment (decrease of CC^{OPT}) and in terms of the overall sustainability level (an increase of $PSL_{rank(opt)}$).

On the contrary, the outcomes of the study strongly change when taking into account separately design, environmental and economic points of view, that is analyzing separately PI, EI and CI indexes. In this respect, **Figure 34** reports the bar charts for PI before and after the Optimization phase.

Figure 34. TB Case Study – PI of all best solutions, before (IN) and after (OPT) the Optimization.

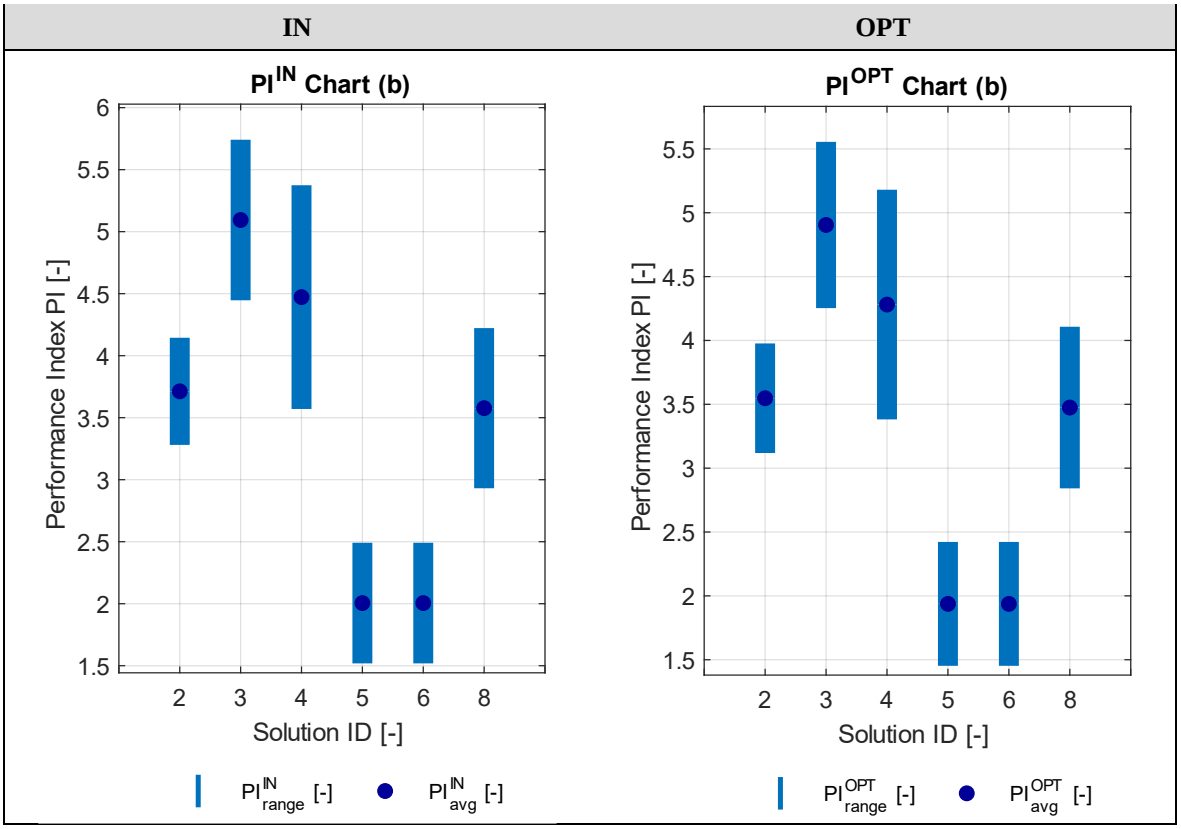

Before the Optimization, it sees that all six solutions present a range for PI^{IN} which is entirely above the ELV^{ref} automatically imposed by the reference scenario (see red dotted line in **Figure 31** and **Figure 32**), thus resulting the fully-acceptable design options. Interestingly, the solution with ID = 3 (the fourth in the first ranking of **Table 44**) presents a range for PI which is entirely above the best acceptable solution in PSL perspective (see solution with ID = 6 in **Figure 34** (*left*)), thus resulting the design option with the highest PI level, even when basing the assessment on the minimum value of the range. As a consequence, where the TB case study is carried out according to a traditional design perspective, the higher average value of PI and the contained variability of PI make that solution with ID = 3 appears to be definitely the most profitable one. It is worthy to be noticed that such a solution results over-dimensioned when being evaluated through the DeSA, thus resulting in a lower value of PSL^{IN}_{rank} (**Table 44**).

After the Optimization phase, all six solutions present a range for PI^{OPT} slightly smaller than the PI^{IN} ranges, but still entirely above the ELV^{ref} automatically imposed by the reference scenario. Interestingly, the solution with ID = 3 (the fourth in the final ranking of **Table 47**)

still presents PI range entirely above the best acceptable and improved solution in PSL perspective, thus resulting the design option with the highest PI level, even when basing the assessment on the minimum value of the range. As already discussed, according to a traditional design perspective, the higher average value of PI^{OPT} and the contained PI variability make that solution with ID = 3 the most profitable one after the optimization. It is worthy to be noticed that such a solution results still over-dimensioned when being evaluated through the DeSA, thus resulting in a lower value of $PSL^{OPT}{}_{rank}$ (**Table 47**).

Figure 35.a reports the bar charts for EI before and after the Optimization phase; whereas **Figure 35.b** shows all LC phases in environmental perspective (i.e., raw material, manufacturing, use, EoL).

Figure 35. TB Case Study – EI(a) and LC(b) phases of all best solutions, before (IN) and after (OPT) the Optimization.

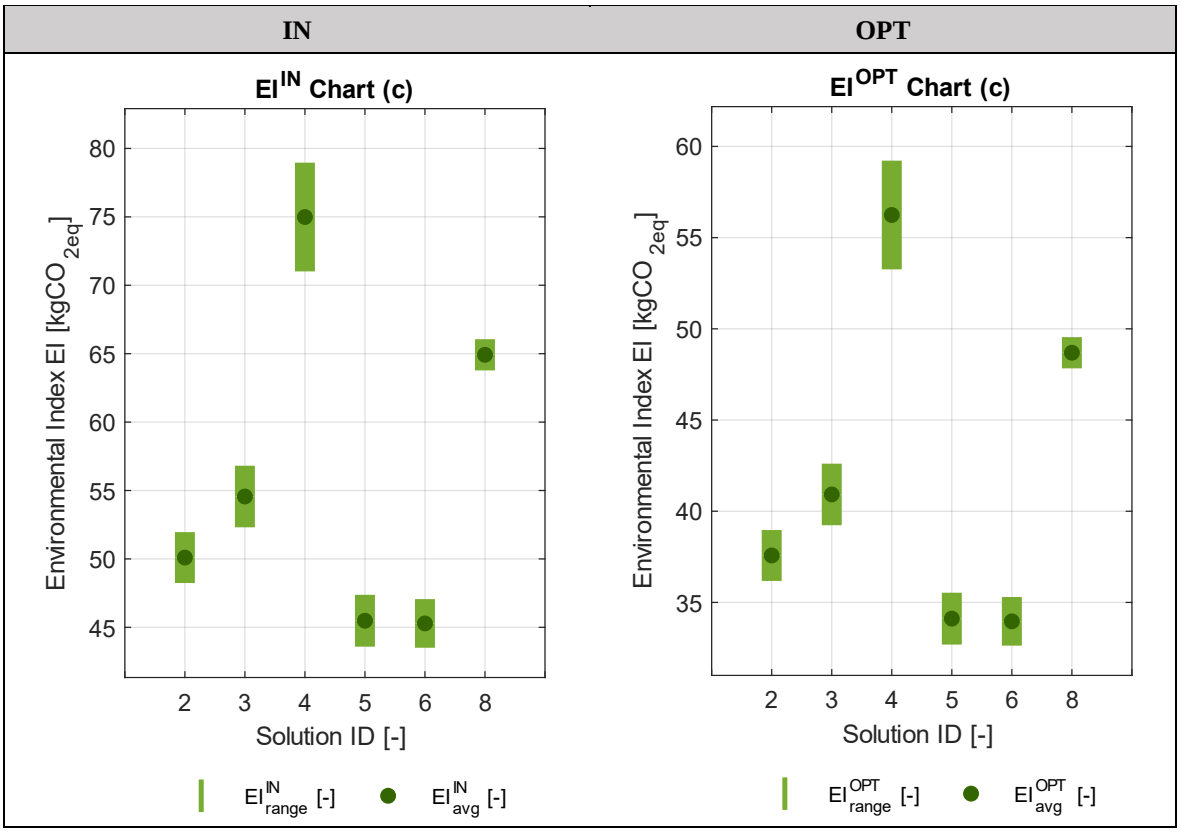

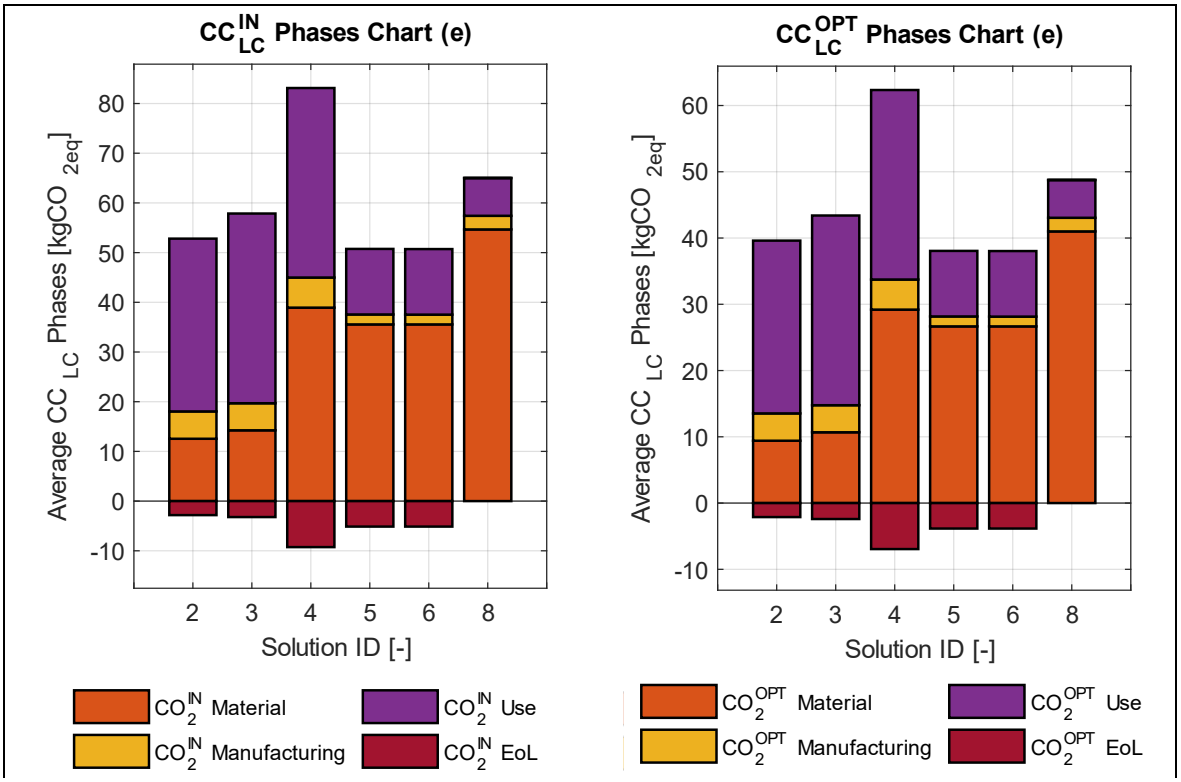

Before the Optimization phase, the solutions with ID = 2, 3, 5, and 6 provide the best environmental performances, as shown in **Figure 35.a** (*left*). In this regard, the critical discussion of EI^{IN} values stresses two main key-points. The first one is that EI^{IN} varies moderately when passing from one solution to another (range: 43 $kgCO_{2eq}$ < EI^{IN} < 57 $kgCO_{2eq}$); the second point is that the variability range that characterizes the four solutions considered is limited (less than ± 3 for all options). The main reasons are reported below:

- Considering the solutions with ID = 2 and 3, the use stage covers the vast majority of total CC_{LC} (approximately 70%), and the impact is the almost the same for the alternatives (35-38 $kgCO_{2eq}$), since the base material being steel (i.e., Cast Iron (Ductile) and High Carbon Steel) for each of those (use stage modelled on a mass basis, as provided by section *2.2 – Environmental Modeling*). This implies that also CC_{EoL} is more or less the same for all options (see the red bars in **Figure 35.b** (*left*)). Moreover, the variability of EI^{IN} is due to materials and manufacturing phases, but the lower variability in CC inventory data and the relatively lesser influence on total CC_{LC} (it does not exceed 30% of total for alternatives) making the final range for EI^{IN} small (**Figure 35.b** (*left*)).
- Considering the solutions with ID = 5 and 6, the use stage covers the minority of total CC_{LC} (approximately 30%), and the impact is the almost the same for the alternatives (12-13 $kgCO_{2eq}$), since the base material being aluminium for each of those. According to the use stage modelled on a mass basis (*2.2 – Environmental Modeling*), the lower impact in the use stage is due to the lower density of the material considered. This implies that also CC_{EoL} is more or less the same for all options (see the red bars in **Figure 35.b** (*left*)). However, the variability of EI^{IN} is also due to materials and manufacturing phases, but in this case the vast variability in CC inventory data and the relatively greater influence on total CC_{LC} (it takes

almost the 70% of total for alternatives) make that the final range for EI^{IN} comparable to the previous solutions analyzed (**Figure 35.b** (*left*)).

The solutions with Stainless Steel and CFRP (ID = 4 and 8, respectively) represent the exception. The former has a high impact on both the use stage and the materials phase, since it is made of stainless steel, which not only has a high density (affecting the use and materials stage) but also a high specific impact (see material in **Table B.3**). The latter instead presents a high impact on only the materials phase since it is made by Carbon Fiber Reinforced Polymer (CFRP), which has a vast specific impact, consequently affecting the materials stage (see material in **Table B.3**).
After the Optimization, it sees that all six solutions present a range for EI^{OPT} smaller than the EI^{IN} ranges, highlighting the reduction of environmental impact through optimization of the solutions considered. The optimized solutions with ID = 2, 3, 5, and 6 provide the best environmental performances, as shown in **Figure 35.b** (*right*). The critical discussion of EI^{OPT} values stresses two main key-points. The first one is that EI^{OPT} varies moderately when passing from one solution to another (range: 33 $kgCO_{2eq}$ < EI^{OPT} < 43 $kgCO_{2eq}$); the second point is that the variability range that characterizes the four solutions considered is more limited respect to EI^{IN} ranges (less than ± 2 for all options). The reasons are:

- Considering the solutions with ID = 2 and 3, the use stage always covers the vast majority of total CC_{LC} (approximately 70%), and the impact is the almost the same for the alternatives (26-28 $kgCO_{2eq}$), since the base material being steel (i.e., Cast Iron (Ductile) and High Carbon Steel) for each of those (use stage modelled on a mass basis, always provided by section *2.2 – Environmental Modeling*). This implies that the environmental impact of use stage ($CO^{OPT}{}_{2eq}$ Use) is reduced approximately of 26% respect to impact before the optimization. Moreover, this means that also CC_{EoL} is more or less the same for all options but reduced since the solutions have minor mass (see the red bars in **Figure 35.b** (*right*)). Finally, the variability of EI^{OPT} is also due to materials and manufacturing phases, but the lower variability in CC inventory data and the relatively lesser influence on total CC_{LC} (it does not exceed 30% of total for alternatives) – as well as the mass reduction obtained during the optimization - make that the final range for EI^{OPT} is small (**Figure 35.b** (*right*)).
- Considering the solutions with ID = 5 and 6, the use stage still covers the minority of total CC_{LC} (approximately 30%), and the impact is the almost the same for the alternatives (9-10 $kgCO_{2eq}$), since the base material being aluminium for each of those. This implies that the environmental impact of use stage ($CO^{OPT}{}_{2eq}$ Use) is reduced approximately of 25% respect to impact before the optimization. According to the use stage modelled on a mass basis (*2.2 – Environmental Modeling*), the lower impact in the use stage is also due to the lower density of the material considered. The CC_{EoL} is more or less the same for all options but reduced since the solutions have minor mass (red bars in **Figure 35.b** (*right*)). Finally, the variability of EI^{OPT} is also due to materials and manufacturing phases, but in this case the vast variability in CC inventory data and the relatively greater influence on total CC_{LC} (it takes almost the 70% of total for alternatives) – even if the mass reduction is obtained during the optimization - make that the final range for EI^{OPT} comparable to the previous solutions analyzed (**Figure 35.b** (*right*)).

Despite the reduction of the environmental impact due to optimisation, the solutions with ID = 4 and 8 still represent the exception respect to the other ones. The former has still a high impact on both the use stage and the materials phase, since it is made of stainless steel (M3) (high density - affecting the use and materials stage – and a high specific impact - consequently affecting the materials stage (see **Table B.3**)). The latter one presents a high impact on only the materials phase since it is made by Carbon Fiber Reinforced Polymer (CFRP) (H1), which has a vast specific impact (see material properties in **Table B.3**).

Finally, **Figure 36.a** shows the bar charts for CI before and after the Optimization; **Figure 36.b** reports instead all LC phases in economic perspective (raw material, manufacturing, use, EoL, respectively).

Figure 36. TB Case Study – CI(a) and LC(b) phases of all best solutions, before (IN) and after (OPT) the Optimization.

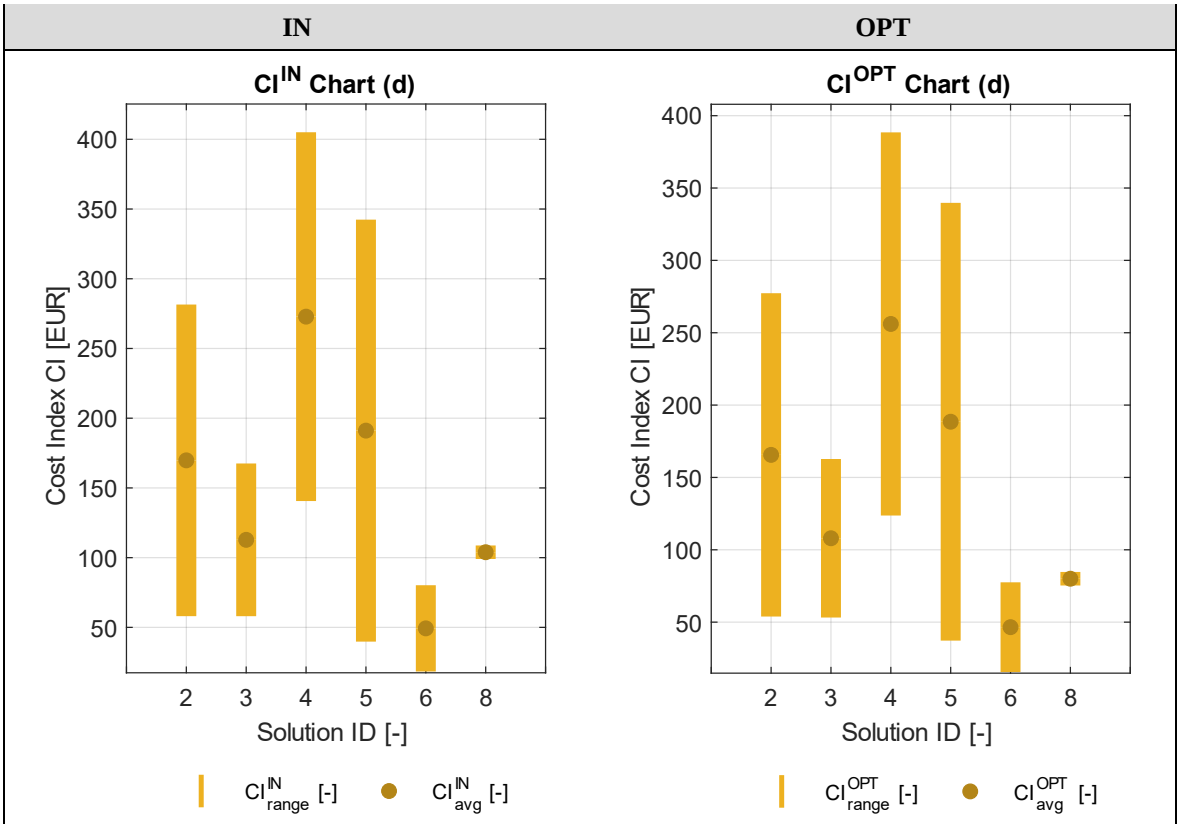

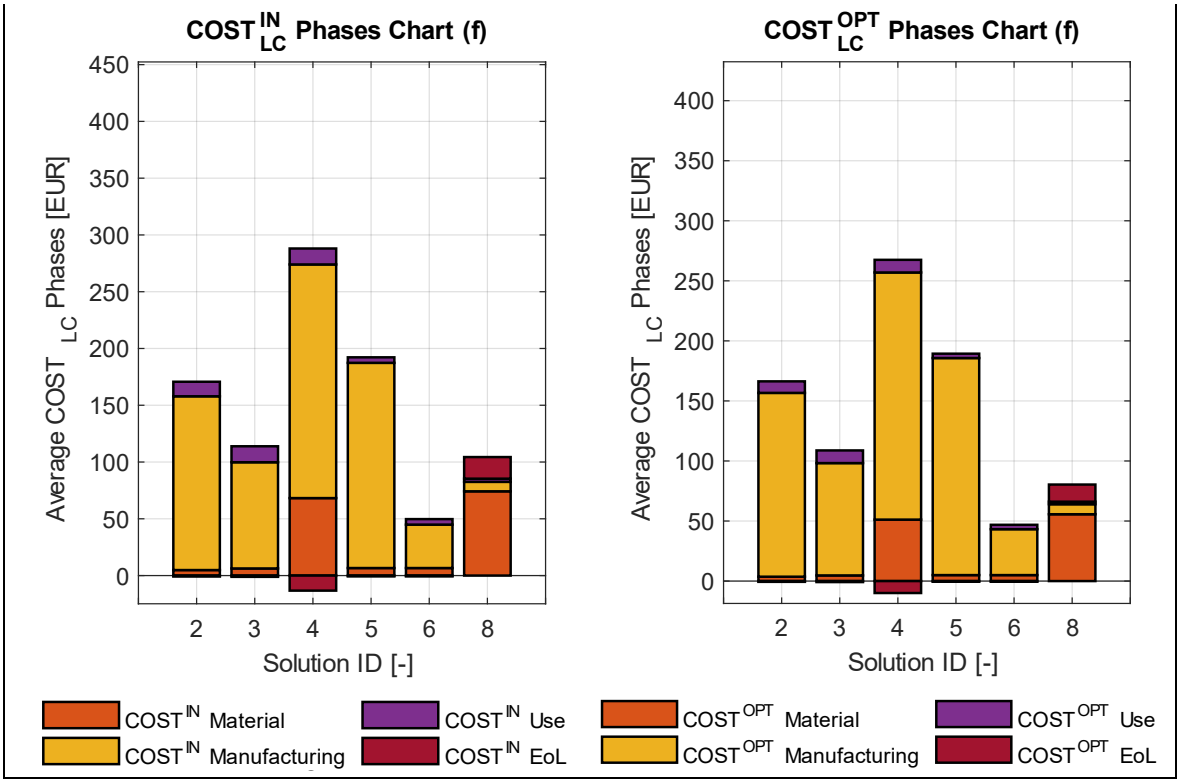

Before the Optimization, it sees that the solutions with ID = 3, 6, and 8 provide the best economic performances, as shown in **Figure 36.a** (*left*). In this regard, the critical discussion of CI^{IN} values stresses two main key-points. The first one is that CI^{IN} varies significantly when passing from one solution to another (range: 20 EUR < CI^{IN} < 170 EUR); the second point is that the variability range that characterizes the four solutions considered is high (between ± 4 and ± 81). The main reasons for this are reported below:

- Considering the solutions with ID = 3 and 6, the manufacturing stage covers the vast majority of total $COST_{LC}$ (between 71-85%), and the cost is different for the alternatives (27-111 EUR), since the base manufacturing process being Investment Casting (CA2) and Extrusion (DE1), respectively (production stage modelled provided by section *2.3 – Economic Modeling*). Moreover, the variability of CI^{IN} is due to materials and use phases, but the lower variability in COST inventory data and the relatively lesser influence on total $COST_{LC}$ (it does not exceed 15-29% of total for alternatives) make that the final range for CI^{IN} is manufacturing-based (**Figure 36.b** (*left*)). Finally, since the base material being metals (i.e., High Carbon Steel (M2) and Age-Hardening Wrought Al-Alloys (M4)) for each of solutions, it implies that the $COST_{EoL}$ is more or less the same for all options and near to zero, according to **Table B.5** (red bars in **Figure 36.b** (*left*)).
- Considering the solution with ID = 8, the manufacturing stage covers the minority of total CC_{LC} (approximately 7%), and the cost is low (approximately 7 EUR), since the base manufacturing process being Lay-Up Methods (CO1). According to the production stage (*2.3 – Economic Modeling*), the lower cost in the manufacturing stage is due to the lower cost of the process considered. However, the variability of CI^{IN} is also due to materials and EoL phases, but in this case the vast variability in COST inventory data and the relatively greater influence on total $COST_{LC}$ (it takes

almost the 90% of total) make that the final range for CI^{IN} comparable to the previous solution analyzed with ID = 3 (**Figure 36.b** (*left*)).

The solutions with ID = 2, 4, and 5 represent the exception (see **Figure 36.b** (*left*)): they have a high impact on the manufacturing phase, since they are processed by means of Investment Casting (CA2), which has a vast specific impact cost (see process in **Table B.6**). Moreover, the solution with ID = 4 presents a high impact on the materials phase since it is made by stainless steel (M3), which has a high specific cost, consequently affecting the materials stage (see material in **Table B.5**).
After the Optimization, all six solutions present a range for CI^{OPT} smaller than the CI^{IN} ranges, highlighting the reduction of economic cost through optimization of the solutions considered. In this context, the optimized solutions with ID = 3, 6, and 8 provide the best economic performances, as shown in **Figure 36.b** (*right*). In this regard, the critical discussion of CI^{OPT} values stresses two main key-points. The first one is that CI^{OPT} varies significantly when passing from one solution to another (range: 15 EUR < CI^{OPT} < 162 EUR); the second point is that the variability range that characterizes the four solutions considered is high (between ± 4 and ± 80). The main reasons for this are reported below:

- Considering the solutions with ID = 3 and 6, the manufacturing stage always covers the vast majority of total $COST_{LC}$ (between 71-85%), and the cost is different for the alternatives (27-111 EUR), since the base manufacturing process being Investment Casting (CA2) and Extrusion (DE1), respectively (production stage modelled provided by section *2.3 – Economic Modeling*). This implies that the economic cost of manufacturing stage ($COST^{OPT}$ Man) is constant respect to cost before the optimization. Moreover, the variability of CI^{OPT} is due to materials and use phases, but the lower variability in COST inventory data and the relatively lesser influence on total $COST_{LC}$ (it does not exceed 15-29% of total for alternatives) make that the final range for CI^{OPT} is manufacturing-based (**Figure 36.b** (*right*)). Finally, since the base material being metals (i.e., High Carbon Steel (M2) and Age-Hardening Wrought Al-Alloys (M4)) for each of solutions, it implies that the $COST_{EoL}$ is more or less the same for all options and near to zero, according to **Table B.5** (see the red bars in **Figure 36.b** (*right*)).
- Considering the solution with ID = 8, the manufacturing stage always covers the minority of total CC_{LC} (approximately 4%), and the cost is low (approximately 7 EUR), since the base manufacturing process being Lay-Up Methods (CO1). This implies that the economic cost of manufacturing stage ($COST^{OPT}$ Man) is constant respect to cost before the optimization. According to the production stage (*2.3 – Economic Modeling*), the lower cost in the manufacturing stage is due to the lower cost of the process considered. However, the variability of CI^{OPT} is also due to materials and EoL phases, but in this case the vast variability in COST inventory data and the relatively greater influence on total $COST_{LC}$ (it takes almost the 90% of total) – even if the mass reduction is obtained during the optimization - make that the final range for CI^{OPT} comparable to the previous solution analyzed with ID = 3.

Despite the reduction of the economic cost due to optimisation, the solutions with ID = 4 and 8 represent the exception respect to the other ones (see **Figure 36.b** (*right*)): they have

a high impact on the manufacturing phase, since they are processed by means of Investment Casting (CA2), which has a vast specific impact cost (consequently affecting the manufacturing stage) (see process in **Table B.6**). Moreover, the solution with ID = 4 presents a high impact on the materials phase since it is made by stainless steel, which has a high specific cost (consequently affecting the materials stage) (see material in **Table B.5**).

3.2 2D | TRA-REF Case Study: Top Roof (TRF)

The automotive body-in-white (BiW) can be differentiated into the main structure, "body-less-doors", and the "bolt-on" (or skin) assemblies. In turn, each of these skin assemblies can be broken down into the inner panels, usually made by deep drawn to provide bulk shape and rigidity, and the shallow skin panels, which provide the outer contour of the body shape and require more aesthetic properties (smooth blemish-free surface and scuff) and dent resistance. Thus, the requirements of each part change depending on the part itself.

The top roof (TRF) is a type of outer panel in vehicle body, where its principal performance criteria are stiffness, oil canning (or critical buckling load), and dent resistance. Stiffness is a fundamental concern for the perceived quality of a body panel (i.e., rigidity); oil canning (the 'popping' of a panel when pressed) determines how the panel 'feels' to a customer (i.e., aesthetic properties). Finally, dent resistance is important to avoid panel damage in-plant and to minimize dents and dings on external parts in-service. In this context, the automotive top roof (TRF) is chosen as applicative bi-dimensional (2D) case study and Functional Unit (FU) for DeSA methodology.

3.2.1 Screening

As shown in **Table 6**, the starting point of the screening phase is primary shape design constraint choice. **Figure 37** illustrates the initial FEM model of the TRF; for this reason, bi-dimensional (2D) shape is chosen. Then, the production database is created, with materials and manufacturing processes available to the designer/case study. In this context, Traditional approach (TRA) is considered, thus, the production database provides physical and mechanical properties through constant values.

Figure 37. TRF FEM model.

Concerning the possible TRF materials, the list of available materials is made of metals and alloys and composites (hybrids), always defining each material by a material ID (MAT_{ID}), mechanical (i.e., density, Poisson ratio, etc.), environmental (i.e., climate change), and economic properties (i.e., cost). In turn, the list of allowable processes is made of manufacturing technologies able to generate sheet (2D) shapes: each process is defined by a process ID (PR_{ID}), mechanical, environmental, and economic features. **Table 49** presents

the list of materials and processes chosen, while Appendix D reports all properties used for the TRF case study.

Table 49. List of available materials and processes in TRF production database.

Production Database				
Material Section (MAT)				
Material ID		**Material Class**	**Material Subclass**	**Material Name**
Materials	M1	Metals and Alloys	Ferrous	Stainless Steel
	M2	Metals and Alloys	Non-Ferrous	Age-Hardening Wrought Al-Alloys
	H1	Hybrids	Composites	Carbon Fiber Reinforced Polymer (CFRP)
	H2	Hybrids	Composites	Natural Fiber Reinforced Polymer (NFRP)
Manufacturing Technologies Section (MAN)				
Process ID		**Process Class**	**Process Subclass**	**Process Name**
Processes	DE1	Deformation	Sheet Deformation Processes	Sheet Stamping Drawing and Blanking
	CO1	Composite Forming	Advanced Composite Forming Processes	Resin Transfer Molding (RTM)
	MO1	Thermoplastic Molding	Thermoforming	Molding

The second step of screening is the application of design constraints: only the process constraint Batch size (B) is applied to the case study as physical constraint. The main objective is to explore all possible combinations generated by the methodology, but with economic batch limitation.

The determination of all design solutions that satisfy the design requirements and that are feasible from a technical point of view is the final step of the screening. The application of design constraints and design choices in terms of geometry, materials, and processes automatically generates several design solutions. As already said by theoretical background reported in previous paragraphs, all combinations that do not meet the above requirements are discarded and not inserted in the list of feasible solutions.

3.2.2 Design and Sustainability analysis

In this phase the design and sustainability performances of TRF alternative design solutions (obtained in the screening step) are analyzed and compared over its whole LC.

In design analysis step, FEM simulation modelling of all feasible solutions is performed (**Figure 4**). The reference scenario (REF) is chosen; thus, the analysis of this case study is performed on the basis of two loadcases provided by the generic design alternative:

- deformation level, as ratio between the maximum deformation on the reference scenario and the maximum deformation on the TRF component calculated through the FEM simulations.

- torsion level, as ratio between the compliance evaluated from the reference scenario and the maximum compliance (related to the presence of TRF component) calculated through the FEM simulations.

The first load case is obtained from static dent resistance analysis, using an indenter placed in the centerline of the top roof (see the red circle in **Figure 38** (*left*)); instead, the second load case is defined from the torsional stiffness analysis of the entire vehicle body on which the TRF is supposed to be mounted (i.e., BiW, see **Figure 38** (*right*)).

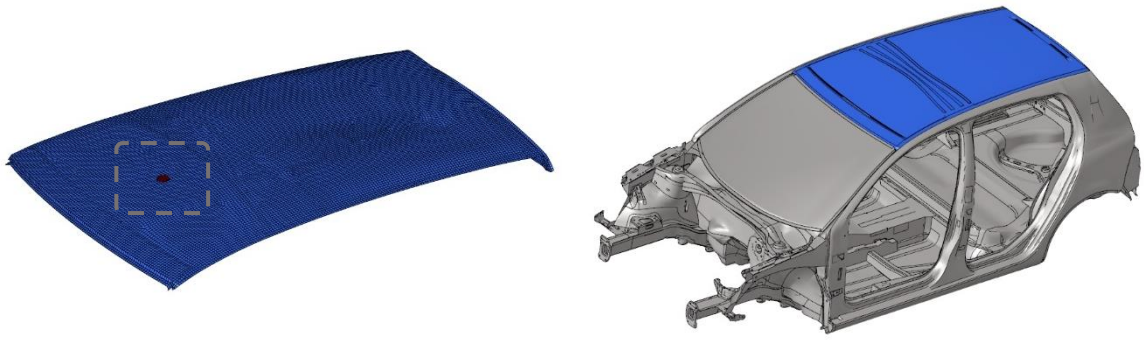

Figure 38. Indenter positioned in the TRF for dent resistance (see dotted grey square in left image); Vehicle BiW where TRF is mounted for torsional stiffness analysis (right image).

As shown in **Equation 13**, the weighting factors for two loadcases (w_l) are used for the performance modelling and defined to calculate the performance level PI. An equal weight is assigned to two loadcases (i.e., $w_{l1} = w_{l2} = 0.5$), since it is assumed that they have the same level of importance. **Figure 39** shows the BCs of the top roof component: the connection with the rest of the BiW, the indenter application surface, and front suspension struts are tied to zones A, B and C, respectively.

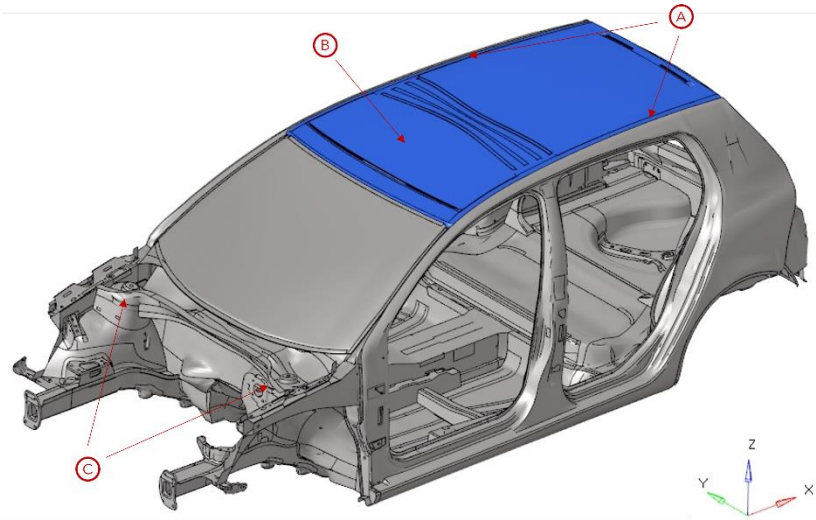

Figure 39. TRF BCs zones.

Considering the static dent resistance analysis, the load (connected to the indenter, see **Figure 38** and **Figure 39**) is applied to zone B as force vector (according to the global system reported in **Figure 39**); the only component is in z-direction (vertical). In this context, the force is applied in time steps (from 0 to 250 N) to simulate the contact between the indenter and the surface (so as to study the contact force-deformation pattern in detail during the simulation). The time range (t_{frame}) is set equal to [0,1]s; the maximum force (F_{dent}) is set equal to 250 N. The deformation of TRF ε_{FEM} is obtained from force-deflection contact diagram; when $F_{cont} = F_{dent}$ during the t_{frame}, the deformation is extracted; otherwise, ε_{FEM} is equal to a threshold value (ε_{Fail}) that defines the failure of the solution (**Equations 85-86**):

$$\begin{matrix} F_{dent} = 250\ N \\ t_{frame} = [0,1]s \end{matrix} \tag{85}$$

$$\varepsilon_{FEM} = \begin{cases} \varepsilon\ when\ F_{cont} = F_{dent} = 250N\ during\ t_{frame} \\ \\ \varepsilon_{Fail}\ otherwise \end{cases} \tag{86}$$

In torsional stiffness analysis, the load is applied to zone C (the front strut attachment points) as opposite force vectors (according to the global system reported in **Figure 39**); the only component is in z-direction (vertical). These forces are defined on each suspension strut (F_{strut}), equal to 2000 N; the twist moment (M_x) is calculated multiplying F_{strut} by lever arm (l_{arm}) chosen for the case study. The torsion of BiW T_{FEM} and the compliance C_{FEM} (related to the presence or absence of TRF) are obtained as a ratio between twist moment and angular deflection and reverse ratio, respectively (see **Equations 87-90**):

$$\begin{matrix} F_{strut} = 2000\ N \\ l_{arm} = 570\ mm \end{matrix} \tag{87}$$

$$M_x = F_{strut} \cdot l_{arm} = 2000 \cdot 570 = 1.135 \times 10^6 Nmm \tag{88}$$

$$T_{FEM} = \frac{M_x}{\theta_{FEM}} \rightarrow\ C_{FEM} = (T_{FEM})^{-1} \tag{89}$$

$$\theta_{FEM} = \frac{360}{2\pi} \cdot arctg\left(\frac{\delta_{FEM}}{l_{arm}}\right) \tag{90}$$

Finally, zone A (the connection between BiW and TRF) is fixed and no translational motion in x, y and z-directions is allowed, as well as x, y and z-rotational motion.

According to the loadcases description, the performance level PI is calculated as follows (**Equations 91-92**):

$$PI = w_{l1} \cdot \frac{\varepsilon_{FEM}^{ref}}{\varepsilon_{FEM}} + w_{l2} \cdot \frac{C_{FEM}^{ref}}{C_{FEM}} \tag{91}$$

$$w_{l1} = w_{l2} = 0.5 \tag{92}$$

Considering that data characterizing the generic solution S_i are provided in terms of single values (according to the TR approach), the methodology applies such data in the FEM simulations straightforwardly. **Table B.7** and **Table B.8** in Appendix D show design data of

materials and processes available for TRF case study (as well as the material, shape, & process compatibility matrices).

The environmental analysis step performs the LCA of all feasible simulations S_i obtained from the design analysis, calculating the environmental level EI. The reference vehicle on which the FU (i.e., TRF) is assumed to be installed is the VOLKSWAGEN e-Golf with electric battery, with a life-distance of 150,000 km; the component lifetime is assumed equal to the one of the vehicle (no substitution during operation is assumed). As described in a previous section (*2.2.2 - Environmental modelling*) the system boundaries include the following life cycle phases: materials production, component manufacturing, use stage and EoL treatments. **Table 50** provides the electric car technical features, instead **Table B.9** and **Table B.10** in Appendix D show environmental impacts of materials and processes available for this case study.

Table 50. TRF Case Study - Vehicle features inputs.

Vehicle Features Inputs	
Feature	**Value**
Vehicle Mass	1440 [kg]
Vehicle Lifetime	150000 [km]
Vehicle Class	C
Powertrain	BEV
Driving Cycle	Worldwide Harmonized Light Vehicles Test Procedure (WLTP)
Electric Grid Mix	EU-28

The economic analysis step performs the LCC of all feasible simulations S_i obtained from the design analysis and assessed in environmental analysis, calculating the economic level CI. As described in a previous section (*2.2.3 - Economic modelling*), the system boundaries include the following life cycle phases: materials production, component manufacturing, use stage and EoL treatments. The economic batch size (B) chosen for FU is 7500 pieces, and the fraction of time for which the equipment is productive (i.e., the load factor (L)) is set to 50%, fixed for all processes available in the production database. In the same way, the capital write-off time is equal for all processes. **Table 51** provides economic features, instead **Table B.11** and **Table B.12** in Appendix D show economic impacts of materials and processes available for this case study.

Table 51. TRF Case Study - Economic features inputs.

Economic Features Inputs	
Feature	**Value**
Batch Size	7500 [pc.]
Load Factor	50 [%]
Capital Write-off Time	5 [yr.]
EoL Grid-Mix	EU-28
Electric Grid Mix	EU-28

3.2.3 First Classification

Design and Sustainability analysis is performed for the design solutions, thus, the PSL is calculated through indexes (i.e., PI, EI, and CI). After the first elasticity screening is performed, the first ranking of the acceptable alternatives is occurred.

The PSL calculation step performs the calculation of the PSL by a weighted sum formula to combine the weights of criteria with the performance/sustainability scores for each design alternative (see section *2.3.1 – PSL calculation*). The PSL scale factor (K) assumed for the case study is 10.

The first elasticity screening step identifies all solutions that are acceptable from an elasticity perspective. Since the TRF case study is defined considering a TR approach with REF scenario, the elasticity screening is performed using ELV^{ref} and acceptability threshold (AT). Indeed, **Table 52** shows the reference scenario chosen for TRF case study.

Table 52. TRF Case Study – Reference Scenario Data.

Reference Scenario Data			
Material Section (MAT)			
Material ID	**Material Class**	**Material Subclass**	**Material Name**
M^{ref}	Metals and Alloys	Ferrous	Stainless Steel
Manufacturing Technologies Section (MAN)			
Process ID	**Process Class**	**Process Subclass**	**Process Name**
DE^{ref}	Deformation	Sheet Deformation Processes	Sheet Stamping Drawing and Blanking
Sustainability Indexes Section (IND)			
Reference Compliance (C^{ref})		$4.9577 \cdot 10^{-5}$ [°/Nm]	
Reference Deformation (ε^{ref})		15.71 [mm]	
Reference Climate Change (CC^{ref})		74.88 [$kgCO_{2eq}$]	
Reference Cost ($COST^{ref}$)		101.40 [EUR]	

For this reason, ELV^{ref} is calculated automatically from the reference scenario, and it is set equal to 0 (that means a performance level (PI) equal to 1), while AT is calculated according to **Table 22** (**Equations 62-65**), that is, all alternatives that have less than 25% of ELV^{ref} vertical line are rejected and they are not considered in the first ranking.

The first ranking step provides that the PSL values related to the acceptable solutions are compared; such a ranking is performed directly by means of the value of PSL of each solution, according to traditional approach (see **Equation 74**).

3.2.4 Optimization

The main objective of this phase is to take the acceptable solutions S^{acc}_i (considering the TR approach) obtained from the first elasticity screening and optimize them, to improve

the PSL of the top roof, without compromising the mechanical performance (in this case, deformation level and torsion level) of the analyzed design solutions. The typology of primary shape (PS) chosen during the screening phase is bi-dimensional (2D); thus, the methodology will work on the solutions using the Parameter Modification. Starting from given TRF volume and the boundary condition data (loads, constraints, etc., as shown in **Figure 39)**, the methodology will perform the variation of one or more geometric parameters to obtain the solutions that provide the best performance concerning the user-defined objective. In this context, the TR geometry is directly modified when a unique geometric parameter chosen by the designer changes, in order to calculate the sustainability indexes described in the DeSA. Since the design approach chosen by the designer is "Traditional" (TRA), the methodology works as follows:

- The geometric parameter (par) defined for this case study is the thickness (t) of the sheet used for the TRF. The user-defined range is chosen subdivided into following values (with N_t equal to 5):

$$t = [0.75, \dots, 2.5]\ mm \rightarrow \begin{bmatrix} 0.75 \\ 1.1875 \\ 1.625 \\ 2.0625 \\ 2.5 \end{bmatrix} mm$$

- In the TR approach, each acceptable solution (S^{acc}_i) will be defined by several sub-solutions (S^{acc}_{it} with t = 1, ..., 5 - the number of subdivision of the TRF thickness (t)), where par is modified in each solution geometry. It follows from the above that S^{acc}_{it} depends on material properties (MAT_i, see TRA properties in **Table B.7** in Appendix D), modified geometry (G_t) and setting parameters for the parameter modification (N_t), as provided by the following relations:

$$S_{it}^{acc} = S_{it}^{acc}(G_t, BC, MAT_i, N_t)$$

$$N_t = 5 \rightarrow\ t = [0.75, 1.1875, 1.625, 2.0625, 2.5]\ mm$$

  The simulations are launched and performed according to TR approach in Design and Sustainability Analysis phase (*2.2*); thus, the results are reported in a table (as already shown in **Table 26**). All solutions are represented through points in a PSL-EL "Point chart" (see **Figure 15** and **Figure 16**); each point of solution S^{acc}_i will have 5 points, shown in the chart. Finally, the results obtained will be sent **DIRECTLY** to the final screening, since in this case, the TRF geometry is already modified to obtain sustainability indexes.

3.2.5 Final classification

Once the Optimization is performed for the acceptable solutions S_i of the TRF, the final classification phase is carried out by means of the following steps: Design and

Sustainability Re-Analysis and final PSL calculation. After the final elasticity screening, the final ranking of the acceptable and optimized alternatives is occurred.

The final PSL calculation step performs the calculation of the PSL using a weighted sum formula to combine the weights of criteria with the performance/sustainability scores for each design alternative (as already shown in section *2.3.1 – PSL Calculation*). The PSL scale factor (K) for the case study is the same used in the previous paragraphs, equal to 10.

The final elasticity screening step identifies all design and optimized solutions that are acceptable from an elasticity perspective. Since the TRF case study is defined considering a TR approach with REF scenario, the screening is performed by means of ELV^{ref} and acceptability threshold (AT) already defined previously: ELV^{ref} is assumed equal to 0 (that means a performance level (PI) equal to 1), while AT is calculated according to **Table 22** (**Equations 62-65**), that is, all alternatives that have less than 25% of ELV vertical line are rejected and they are not considered in the final ranking. **Table 52** shows the reference scenario chosen for TRF case study and used also for final classification.

The final ranking step provides that the PSL values related to the acceptable and optimized sub-solutions are compared; such a ranking is performed by means of value of the PSL (i.e., $PSL^{rank(opt)}$), according to traditional approach (see **Equation 80**). Finally, the methodology calculates the improvement (or worsening) of each acceptable solution S^{acc} obtained during the first classification and further analyzed in Optimization and Final Classification phases (see **Equation 82**).

3.2.6 Results & Discussion

Table 53 reports the 4 solutions generated in the screening phase that satisfy both design requirements (imposed by designer) and are technically feasible.

Table 53. TRF Case Study - List of solutions created in the first screening phase (IN); outcomes obtained through First Elasticity Screening and First Ranking.

TRF Solutions List – BEFORE OPTIMIZATION						
ID	**Design Solution ID**	**PSL^{IN}**	**EL^{IN}**	**PSL^{IN}_{rank}**	**First Elasticity Screening**	**First Ranking**
1	1_Flat_M1_DE1	9.90	0	9.90	OK [Reference]	4
2	2_Flat_M2_DE1	33.00	-0.13	33.00	OK, with AT	1
3	3_Flat_H1_CO1	11.22	-0.13	11.22	OK, with AT	3
4	4_Flat_H2_MO1	29.55	-0.16	29.55	OK, with AT	2

As always, a Design Solution ID is defined for generic design alternative as a combination of shape (primary component shape defined by the designer – 1D, 2D, or 3D), material (MAT_{ID}), and process (PR_{ID}) (see **Table 49**).

Considering that generic i-th solution S_i is defined in terms of material single values (i.e., TR approach, see **Table 8**), it is explored straightforwardly through a FEM simulation. Looking at the list of solutions, all solutions (100% respect the total number of design alternatives) comply with the first elasticity screening, subdivided in two main groups:

- Solutions with great deterioration, that present the reduction of EL_i between 5% and 25% respect to ELV^{ref} (see yellow lines in **Table 53**);

- Solution with improvement, that present EL_i greater than ELV^{ref} (see green lines reported in **Table 53**);

The solutions analyzed in the design and sustainability analysis phase are represented through points in the PSL-EL point chart of **Figure 40**.

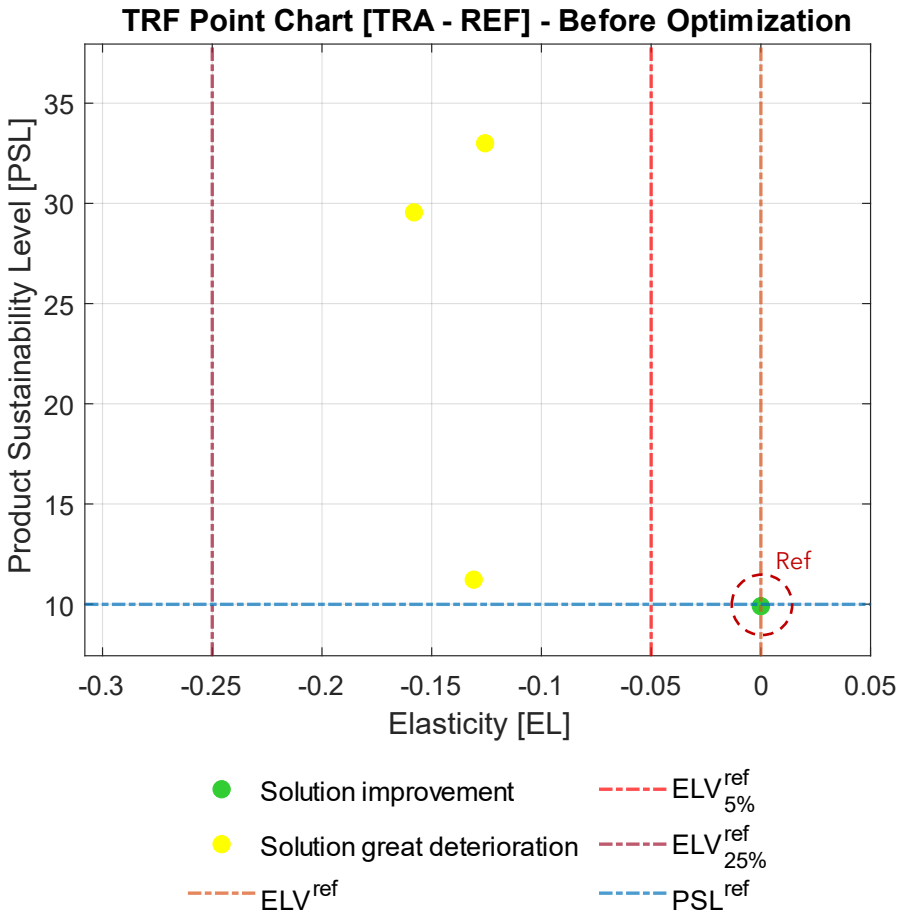

Figure 40. Top Roof point chart (with AT) before the Optimization phase. Cross points represent discarded solutions.

The full-acceptable solutions S^{acc}_i (or solutions with improvement) are those identified by points whose area is entirely to the right of the ELV^{ref} line - in green in **Figure 40**). In this context, the unique full-acceptable solution is the reference scenario (**Table 52**): indeed, the green point is centered respect to ELV^{ref} and PSL^{ref} (see the dotted red circle in the figure itself). On the other hand, the partially-acceptable solutions S^{acc}_i (or solutions with great deterioration) are those identified by points whose area is between -5% and -25% lines of reduction – according to **Table 22** - respect to ELV^{ref} (in yellow in **Figure 40**). The other solutions (those that have the point area to the left of the -25% line of reduction respect to ELV^{ref}) are not acceptable and therefore they are rejected. In this case, no solution is present in this typology. Moreover, **Table 53** reports PSL_{rank} for all acceptable design options, also including the first ranking, from which the best acceptable solution results to be the one identified by ID = 2 (highest value of PSL^{IN}_{rank}).

Next, the acceptable solutions S^{acc}_i obtained from the first elasticity screening will be optimized to improve PSL, without compromising the mechanical performance of the

analyzed design solutions. The type of primary shape (PS) chosen during the screening phase is bi-dimensional (2D); thus, the methodology will work on the solutions S^{acc}_i using the Parameter Modification.

After the optimization simulations are performed, the results will be sent **DIRECTLY** to the final screening, since the geometry is already modified to obtain sustainability indexes described in the DeSA (i.e., PI^{opt}, EL^{opt}, EI^{opt}, and CI^{opt}) and used for final PSL calculation (according to the modelling framework reported in **Table 26**). **Table 54** shows the results obtained from Parameter Modification in TR approach.

Table 54. TRF Case Study - List of solutions after the Parameter Modification phase; outcomes obtained through geometric parameter (par) modification.

TRF Solutions List – AFTER PARAMETER MODIFICATION						
ID	**Geometric Parameter**					
	Index	**t = 0.75 [mm]**	**t = 1.1875 [mm]**	**t = 1.625 [mm]**	**t = 2.0625 [mm]**	**t = 2.5 [mm]**
1	PSL	9.90	5.65	3.49	2.72	2.20
	EL	0	1.19	7.29	13.51	19.91
2	PSL	33.00	21.69	15.50	11.71	9.23
	EL	-0.13	0.04	0.49	2.59	5.79
3	PSL	11.22	8.40	6.19	4.55	3.14
	EL	-0.13	-0.1	0.23	0.85	2.84
4	PSL	29.55	20.41	15.88	13.14	10.91
	EL	-0.16	-0.14	-0.14	-0.09	0.09

Table 54 and **Table 55** report the 4 solutions analyzed in the Optimization phase and assessed through the final screening stage, satisfying design requirements (imposed by the designer) and feasible from a technical perspective.

Table 55. TFR Case Study - List of solutions compared before (IN) and after (OPT) the Optimization phase.

TRF Solutions List – COMPARISON BEFORE/AFTER OPTIMIZATION						
ID	**Design Solution ID**	**t [mm]**	**PSL^{IN}_{rank}**	**PSL^{OPT}_{rank}**	**$\%PSL_{rank}$**	**Final Ranking**
1	1_Flat_M1_DE1	0.75	9.90	9.90	0%	4
2	2_Flat_M2_DE1	1.1875	33.00	21.69	119.09%	1
3	3_Flat_H1_CO1	1.625	11.22	6.19	-37.47%	3
4	4_Flat_H2_MO1	2.5	29.55	10.91	10%	2

Considering that generic i-th solution S^{acc}_i is defined in terms of material single values (TR approach, see **Table 8**), it is explored with N_t sub-solutions S^{acc}_{it} (where t = 1, ..., N_t - the number of subdivision of geometric parameter) modelled through a FEM simulation.

Table 56. TFR Case Study - List of solutions created after the Optimization phase (OPT); outcomes obtained through Final Elasticity Screening and Final Ranking.

TRF Solutions List – AFTER OPTIMIZATION							
ID	**Design Solution ID**	**t [mm]**	**PSL^{OPT}**	**EL^{OPT}**	**PSL^{OPT}_{rank}**	**Final Elasticity Screening**	**Final Ranking**
1	1_Flat_M1_DE1	0.75	9.90	0	9.90	OK [Reference]	11
		1.1875	5.65	1.19	5.65	OK	15
		1.625	3.49	7.29	3.49	OK	17
		2.0625	2.72	13.51	2.72	OK	19
		2.5	2.20	19.91	2.20	OK	20
2	2_Flat_M2_DE1	0.75	33.00	-0.13	33.00	OK, with AT	1
		1.1875	21.69	0.04	21.69	OK	3
		1.625	15.50	0.49	15.50	OK	6
		2.0625	11.71	2.59	11.71	OK	8
		2.5	9.23	5.79	9.23	OK	12
3	3_Flat_H1_CO1	0.75	11.22	-0.13	11.22	OK, with AT	9
		1.1875	8.40	-0.1	8.40	OK, with AT	13
		1.625	6.19	0.23	6.19	OK	14
		2.0625	4.55	0.85	4.55	OK	16
		2.5	3.14	2.84	3.14	OK	18
4	4_Flat_H2_MO1	0.75	29.55	-0.16	29.55	OK, with AT	2
		1.1875	20.41	-0.14	20.41	OK, with AT	4
		1.625	15.88	-0.14	15.88	OK, with AT	5
		2.0625	13.14	-0.09	13.14	OK, with AT	7
		2.5	10.91	0.09	10.91	OK	10

Therefore, all solutions - 100% respect the total number of design alternatives - comply with the final elasticity screening, subdivided in two main groups:

- Solutions with great deterioration, that present the reduction of EL_i between 5% and 25% respect to ELV^{ref} (see yellow lines in **Table 55** and **Table 56**).
- Solution with improvement, that present EL_i greater than ELV^{ref} (see green lines reported in **Table 55** and **Table 56**);

All solutions analyzed in the design and sustainability re-analysis phase are represented again through points in the PSL-EL point chart of **Figure 41**.

The full-acceptable and optimized solutions $S^{acc/opt}_i$ (or solutions with improvement – in green) are those identified by points whose area is entirely to the right of the ELV^{ref}. On the other hand, the partially-acceptable and optimized solutions $S^{acc/opt}_i$ (or solutions with great deterioration – in yellow) are those identified by points whose area is between -5% and -25% lines of reduction – according to **Table 22** - respect to ELV^{ref}.

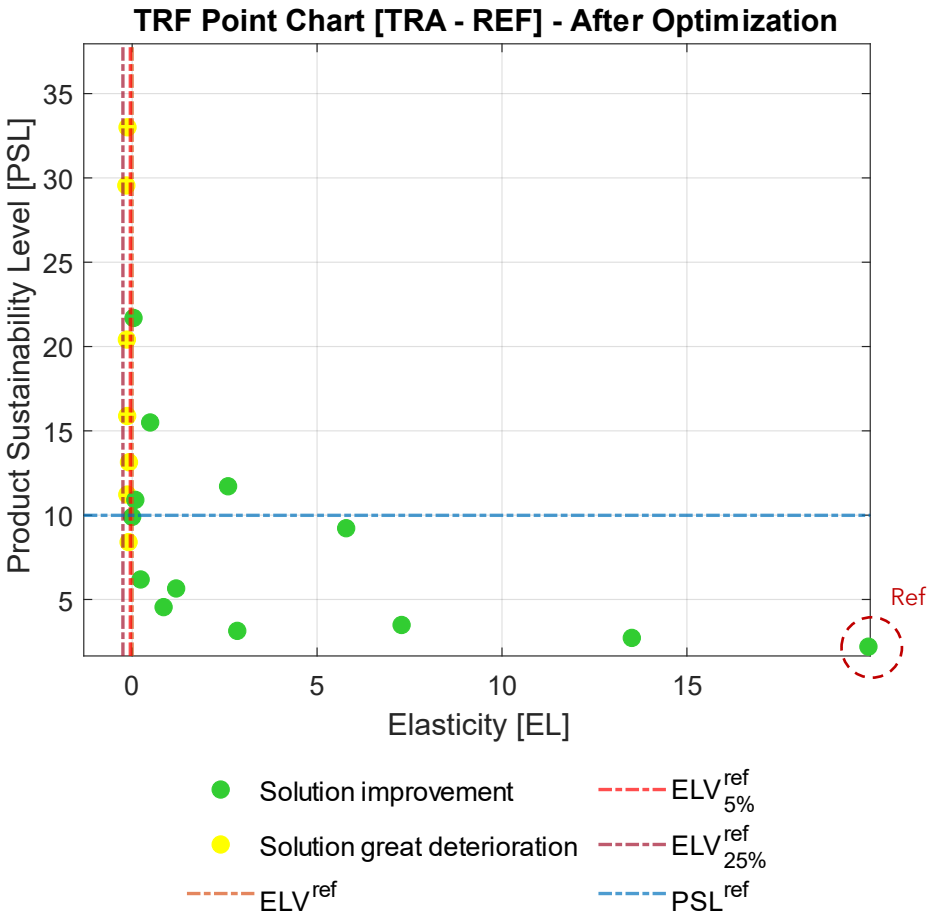

Figure 41. Top roof point chart (with AT), after the Optimization phase. Cross points represent discarded solutions.

The other solutions (those that have the point area to the left of the -25% line of reduction respect to ELV^{ref}) are not acceptable and therefore they are rejected. However, despite the optimization no solution is present in this typology. Moreover, **Table 56** reports PSL_{rank} for all acceptable and optimized design alternatives, including the final ranking; assuming that, regardless of the variation of the geometric parameter t, all solutions are considered acceptable for elasticity (green and yellow points in **Figure 41**), the calculation of PSL^{OPT}_{rank} will consider solutions with PSL greater than reference scenario sustainability level and considered full-acceptable at the same time. For this reason, the best acceptable and optimized solution results to be the one identified by ID = 2 (the same as before optimization) with the highest value of PSL^{OPT}_{rank}.

The methodology finally calculates the improvement (or worsening) of each acceptable solution S^{acc} obtained during the first classification and further analyzed in Optimization and Final Classification phases (see **Table 55** and **Equation 82**). We see that the analyzed solutions' improvement is between -37% and 120%; moreover, the elasticity (EL) presents values greater than the reference value (ELV^{ref} = 0). This implies that several acceptable and optimized design alternatives S^{acc} presented a reduction of PSL, without compromising their mechanical performance (i.e., deformation and compliance).

The solutions analysis is based on the integrated single score index PSL, as well as the specific sustainability indexes (PI, EI, and CI).

Regarding the Sustainability Level, **Figure 42** (*left*) shows the outcomes of PSL^{IN} for all TRF solutions considered acceptable during the first ranking.

Figure 42. TRF Case Study - PSL of all best solutions, before (IN) and after (OPT) the Optimization phase.

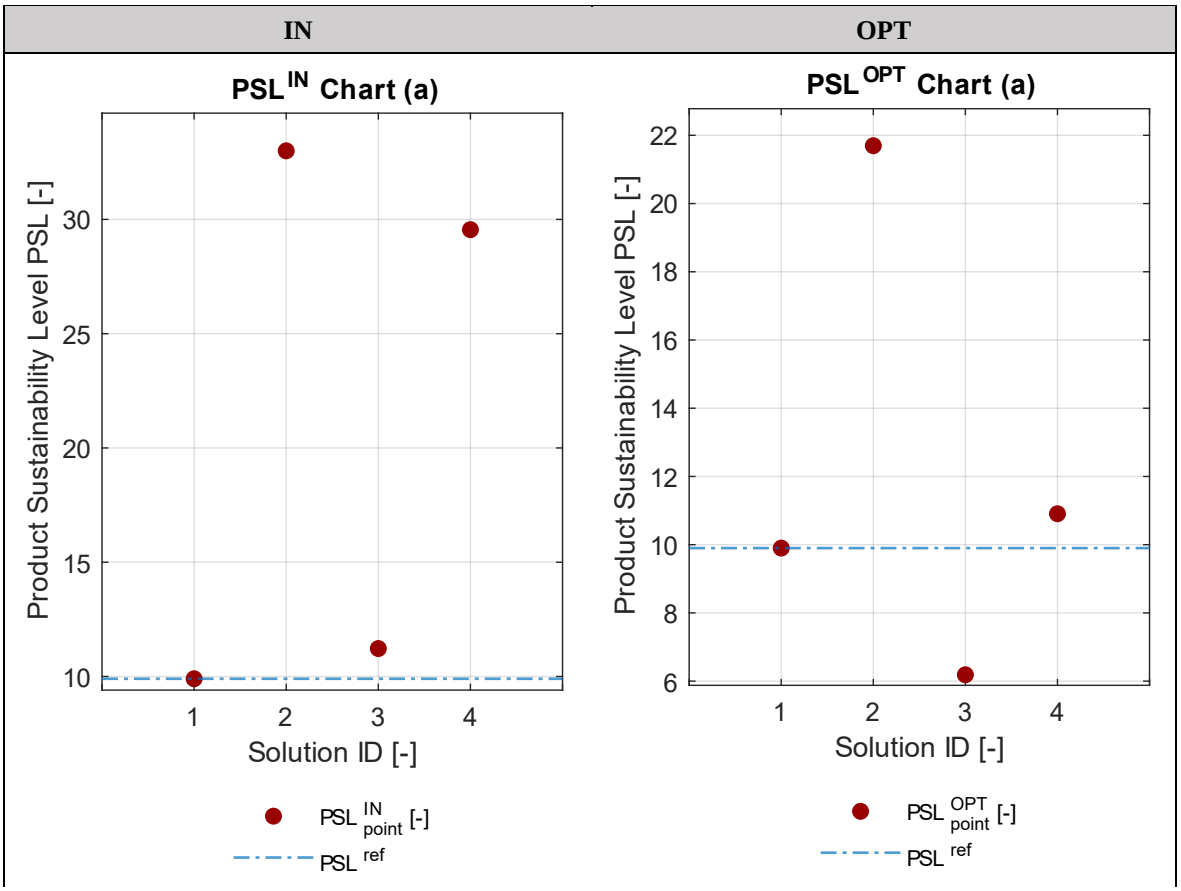

It is interesting to stress that the best design option (with ID = 2) results preferably when considering the value of the range (higher respect the other solutions). Moreover, 3 out of 4 solutions present a PSL^{IN} value greater than the value of the reference solution ($PSLV^{ref}$ = 10, see blue dotted line in **Figure 40**, **Figure 41**, and **Figure 42** *(left)*). Whereas the design alternative with ID = 1 represents the reference scenario - it is defined by the material reported in **Table 52** (Stainless Steels – M1) - presents a PSL value centered to PSL^{ref}.

Another relevant outcome of the TRF case study is that all acceptable solutions have PI values less than reference condition's performance level, which clearly indicates that the initial thickness value used for the TRF (i.e., t = 0.75 mm) implies a worsening of the mechanical performance. For this reason, as starting point for the Optimization phase, rising the component mass (without exceeding the reference solution mass value) would provide always beneficial effects not only on the environment (decrease of CC in all LC stages, according to **Equations 8-23**), but also in terms of the overall sustainability level (an increase of PSL_{rank}) A significant margin for improvement in the lightweight perspective must be maintained.

Figure 42 (*right*) shows the outcomes of PSL^{OPT} for all TFR solutions considered acceptable during the final ranking. It is interesting to stress that the best design option (solution identified by ID = 2) results preferably when considering the value of the range (higher

respect the other solutions) even after the optimization. Moreover, 2 out of 4 solutions present a PSL^{OPT} value much greater than the value of the reference solution ($PSLV^{ref}$ = 10, see blue dotted line in **Figure 40**, **Figure 41**, and **Figure 42** *(right)*). Whereas the design alternative with ID = 1 represents the reference scenario - it is defined by the material reported in **Table 52** (Stainless Steels – M1) - presents a PSL value centered to PSL^{ref}. However, due to the optimization, the design alternative with ID = 3 presents an optimized PSL value significantly lower than the reference scenario.
Another relevant outcome of the TRF case study is that all optimized and acceptable solutions have PI values improved respect to reference condition's performance level, which indicates that the new thickness values used for the TRF involve an improvement of the mechanical performance.

On the contrary, the outcomes of the study change considering design, environmental and economic points of view, separately (PI, EI and CI indexes). In this respect, **Figure 43** reports the point charts for PI before and after the Optimization phase.

Figure 43. TRF Case Study - PI of all best solutions, before (IN) and after (OPT) the Optimization phase.

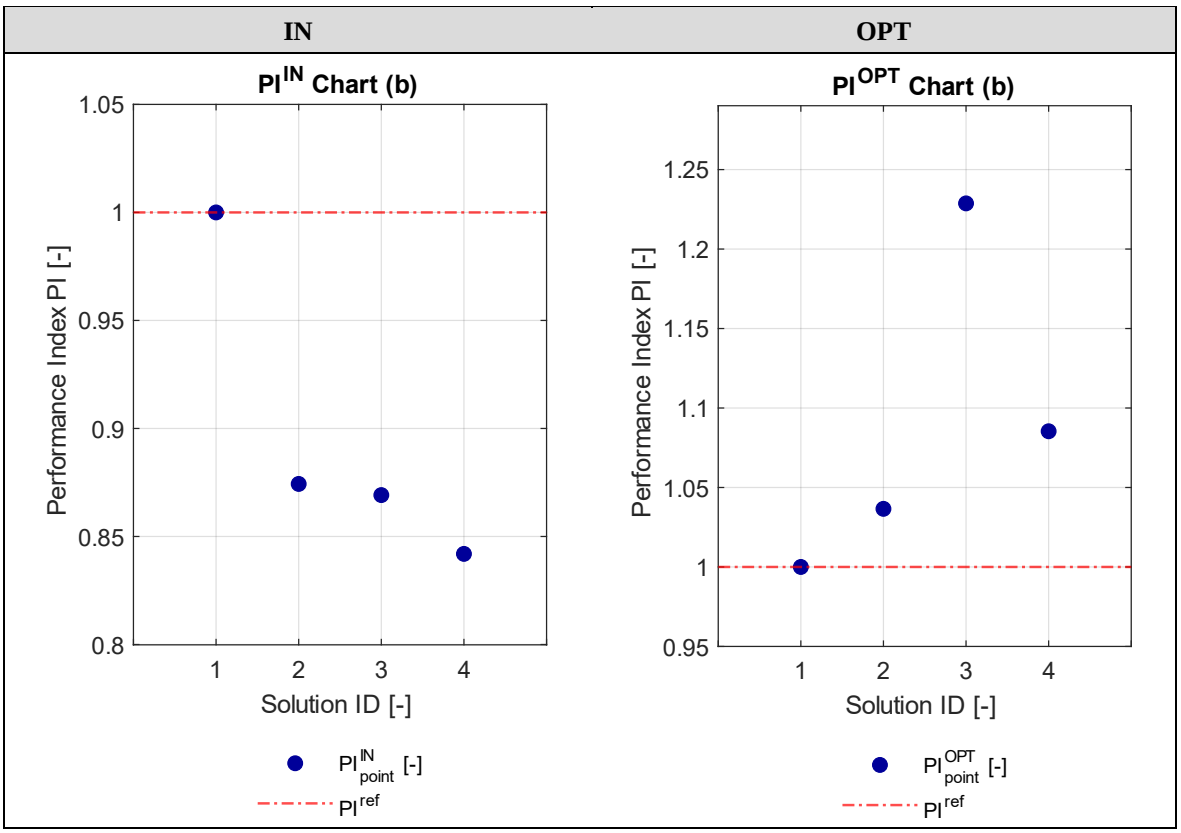

Before the Optimization, all solutions (except the reference scenario – ID = 1) present a PI^{IN} value entirely below the ELV^{ref} automatically imposed by the reference scenario (red dotted line in **Figure 43** (*left*)). However, according to AT (**Table 22**), the analyzed solutions present EL values greater than the worst AT condition (i.e., 25% EL reduction), thus resulting the partially-acceptable design options (solutions with great deterioration). Interestingly, the solution with ID = 4 (the second in the first ranking of **Table 52**) presents a PI^{IN} value much lower than the best acceptable solution in PSL perspective (reference

solution with ID = 1), thus resulting the design option with the worst PI level. As a consequence, where the TRF case study is carried out according to a traditional design perspective, the higher value of PI respect to all other solutions, make that the reference solution with ID = 1 appears to be definitely the most profitable one. Finally, the other solutions result sub-dimensioned when being evaluated through the DeSA, resulting in a lower PI^{IN} value and in a greater value of PSL^{IN}_{rank} (**Table 52**).
After the Optimization, it sees that all solutions (except for the reference solution) present PI^{OPT} values always greater than the PI^{IN} values (**Figure 43** (*right*)), and entirely above the red dotted line ELV^{ref}. According to AT (**Table 22**), the analyzed solutions present EL values greater than the best AT condition (i.e., 0% EL improvement), thus resulting the full-acceptable design options (solutions with improvement). Interestingly, the solution with ID = 3 (the third in the final ranking of **Table 56**) presents a PI value which is entirely above the best acceptable solution in PSL perspective (e.g., solution with ID = 2), resulting the design option with the highest PI level, despite being one of the worst before the Optimization. As a consequence, according to a traditional design perspective, the higher average value of PI respect to all other solutions make that solution with ID = 3 the most profitable one after the optimization. Such a solution becomes over-dimensioned when being evaluated through the DeSA, thus resulting in a lower value of PSL^{OPT}_{rank} (**Table 56**).

Figure 44.a reports the TRF point charts for EI before and after the Optimization phase; whereas **Figure 44.b** shows all LC phases in environmental perspective, considering raw material, manufacturing, use, and EoL.

Figure 44. TRF Case Study – EI(a) and LC(b) phases of all best solutions, before (IN) and after (OPT) the Optimization.

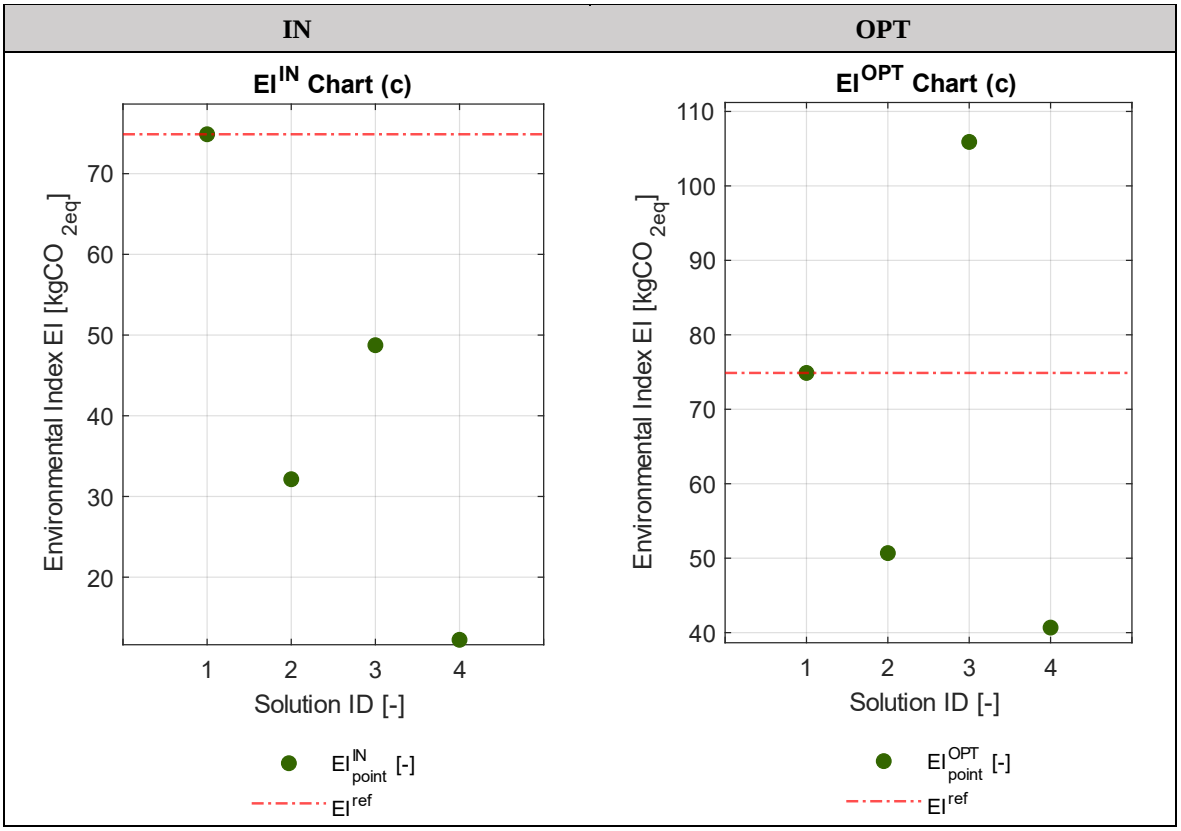

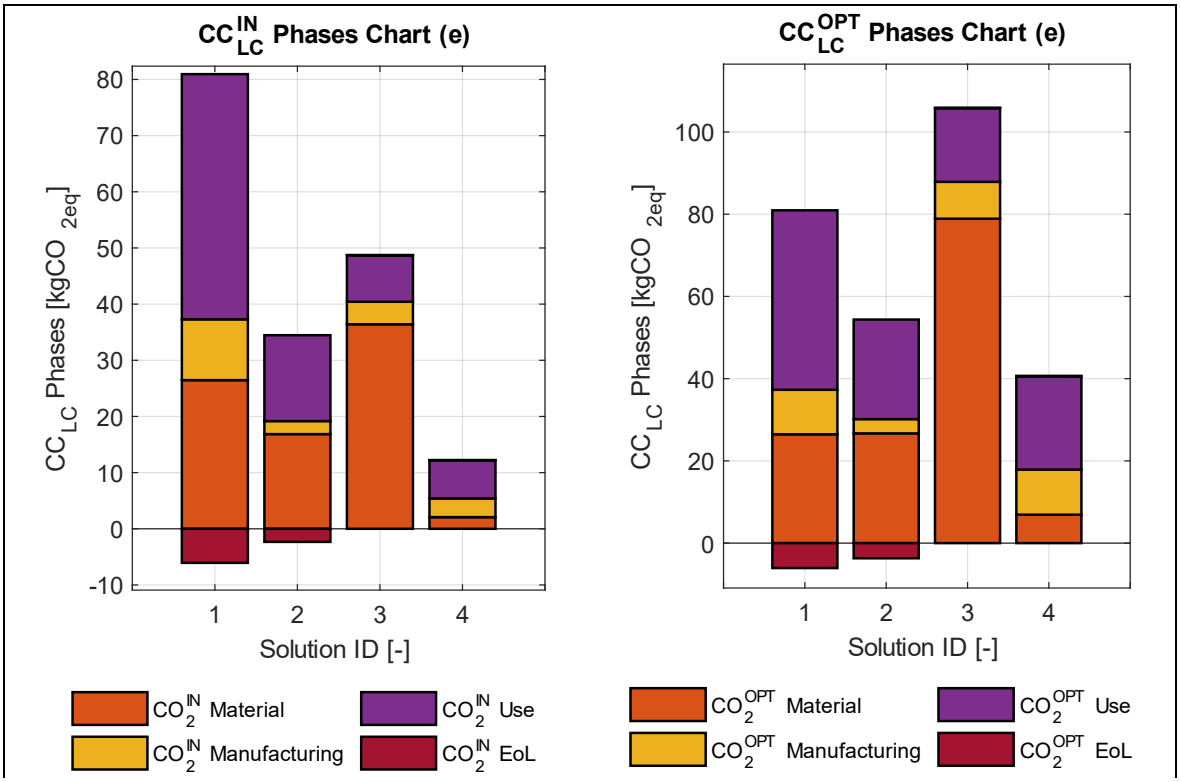

Before the Optimization phase, all solutions (except the reference scenario – ID = 1) present a EI^{IN} value entirely below the CC value of the reference scenario (EI^{ref} - see red dotted line in **Figure 44.a** (*left*)). In this regard, the critical discussion of EI^{IN} values stresses the following key-point: EI^{IN} varies moderately when passing from one solution to another (range: 12 $kgCO_{2eq}$ < EI^{IN} < 48 $kgCO_{2eq}$). The main reasons for this are reported below:

- Considering all solutions (with ID = 2, 3 and 4), the use stage has variable importance over the entire solution LC (between 17% and 56%). Despite this, this phase is minimal compared to the reference solution one (ID = 1, see **Figure 44.b** (*left*)). Furthermore, it is interesting to observe the raw materials phase: on the one hand, the solution with ID = 4 has a minimal CC^{raw} value since the material (NFRP) has a low specific impact, as well as low density value (see **Table B.7** and **Table B.9**). On the other hand, the solutions with ID = 2 and 3 present relatively high values, with a higher relevance (concerning the entire life cycle) than the use phase; this is due to the vast specific impact of the two materials considered (Age-Hardening Wrought Al-Alloys and Carbon Fiber Reinforced Polymer (CFRP), reported in **Table B.9**).

After the Optimization phase, it sees that only two solutions (except the reference scenario – ID = 1) present a EI^{OPT} value entirely below the CC value of the reference scenario (i.e., EI^{ref}), highlighting the partial reduction of environmental impact through optimization of the solutions considered. The optimized solutions with ID = 2 and 4 provide the best environmental performances, as shown in **Figure 44.a** (*right*). In this context, the critical discussion of EI^{OPT} values stresses two main key-points. The first one is that EI^{OPT} varies moderately when passing from one solution to another (range: 40 $kgCO_{2eq}$ < EI^{OPT} < 50 $kgCO_{2eq}$); the second point is that the Optimization generated solutions with an increased environmental impact. The main reasons for this are reported below:

- Considering the solutions with ID = 2 and 4, the use stage has variable importance over the entire solution LC (always between 47% and 56%, because of use stage modelled on a mass basis, as provided by section *2.2 – Environmental Modeling* (**Equations 11-16**)). Despite this, this phase is lower than the reference solution one (ID = 1). Moreover, it is interesting observing the raw materials phase, since it is worsened due to Optimization, but it is still better than the reference scenario material stage. On the one hand, the solution with ID = 4 presents a low CC^{raw} value since the material (NFRP) has a low specific impact and low-density value (**Table B.7** and **Table B.9**). On the other hand, the solution with ID = 2 presents a high value, with a higher relevance (concerning the entire LC) than the use phase; this is due to the vast specific impact of the material considered (Age-Hardening Wrought Al-Alloys (M2) reported in **Table B.9**).
- Considering the solution with ID = 3, the use stage still covers the minority of total CC_{LC} (approximately 17%) since the base material being CFRP (with low density); thus, the phase is lower than the reference solution one (ID = 1, see **Figure 44.b** (*right*)). Moreover, it is interesting observing the raw materials phase: despite the optimization, the solution represents the exception respect to the other ones (see **Figure 44.b** (*right*)), since we have an increase of the environmental impact. The solution has a high impact since it is made by Carbon Fiber Reinforced Polymer (CFRP) (H1), which has a vast specific impact (consequently affecting the materials stage) (see material in **Table B.9**), and a greater mass than in the initial condition (the thickness was increased from 0.75mm to 1.625mm).

Finally, **Figure 45.a** shows the point charts for CI before and after the Optimization; **Figure 45.b** reports instead all LC phases in economic perspective (raw material, manufacturing, use, EoL, respectively). Before the Optimization, only two solutions (except the reference scenario – ID = 1) present a CI^{IN} value that is entirely below the COST value of the reference scenario (i.e., CI^{ref} - see red dotted line in **Figure 45.a** (*left*)). The solutions with ID = 2 and 4 provide the best economic performances, as shown in **Figure 45.a** (*left*). In this context, the critical discussion of CI^{IN} values stresses two main key-points. The first one is that CI^{IN} varies significantly when passing from one solution to another (range: 20 EUR < CI^{IN} < 60 EUR); the second point is that the analysis generated solutions with an increased cost impact. The main reasons for this are reported below:

- Considering the solutions with ID = 2 and 4, the use stage has variable importance over the entire solution LC (always between 4% and 36%, because of use stage modelled on a mass basis, as provided by section *2.3 – Economic Modeling* (**Equations 37-40**)). Despite this, this phase is minimal compared to the reference solution one (ID = 1, see **Figure 45.b** (*left*)). Furthermore, it is interesting to observe the raw materials phase: on the one hand, the solution with ID = 2 has a low $COST^{raw}$ value since the material (Age-Hardening Wrought Al-Alloys) has a low specific cost, as well as low density value (see **Table D.1**). Concerning the EoL phase, since the solution is made by aluminium, the $COST_{EoL}$ is negative and near to zero (see the red bars in **Figure 45.b** (*left*)). On the other hand, the solutions with ID = 4 present relatively high value, with a higher relevance (concerning the entire life cycle) than

the use phase; this is due to the vast specific cost of the material considered (i.e., Natural Fiber Reinforced Polymer (NFRP) (H2), reported in **Table D.1**). Concerning the EoL phase, since the solution is made by composite, the $COST_{EoL}$ is positive (see the red bar in **Figure 45.b** (*left*)).

- Considering the solution with ID = 3, the use stage still covers the minority of total $COST_{LC}$ (approximately 2%) since the base material being CFRP (with low density); thus, the phase is lower than the reference solution one (ID = 1, see **Figure 45.b** (*left*)). Moreover, it is interesting observing the raw materials phase: the solution represents the exception respect to the other ones. The solution has a high material cost since it is made by Carbon Fiber Reinforced Polymer (CFRP) (H1), which has a vast specific cost (consequently affecting the materials stage) (see material in **Table B.11**). Finally, since the base material being composite, it implies that the $COST_{EoL}$ is high respect the other options (the red bars in **Figure 45.b** (*left*)).

Figure 45. TRF Case Study – CI(a) and LC(b) phases of all best solutions, before (IN) and after (OPT) the Optimization.

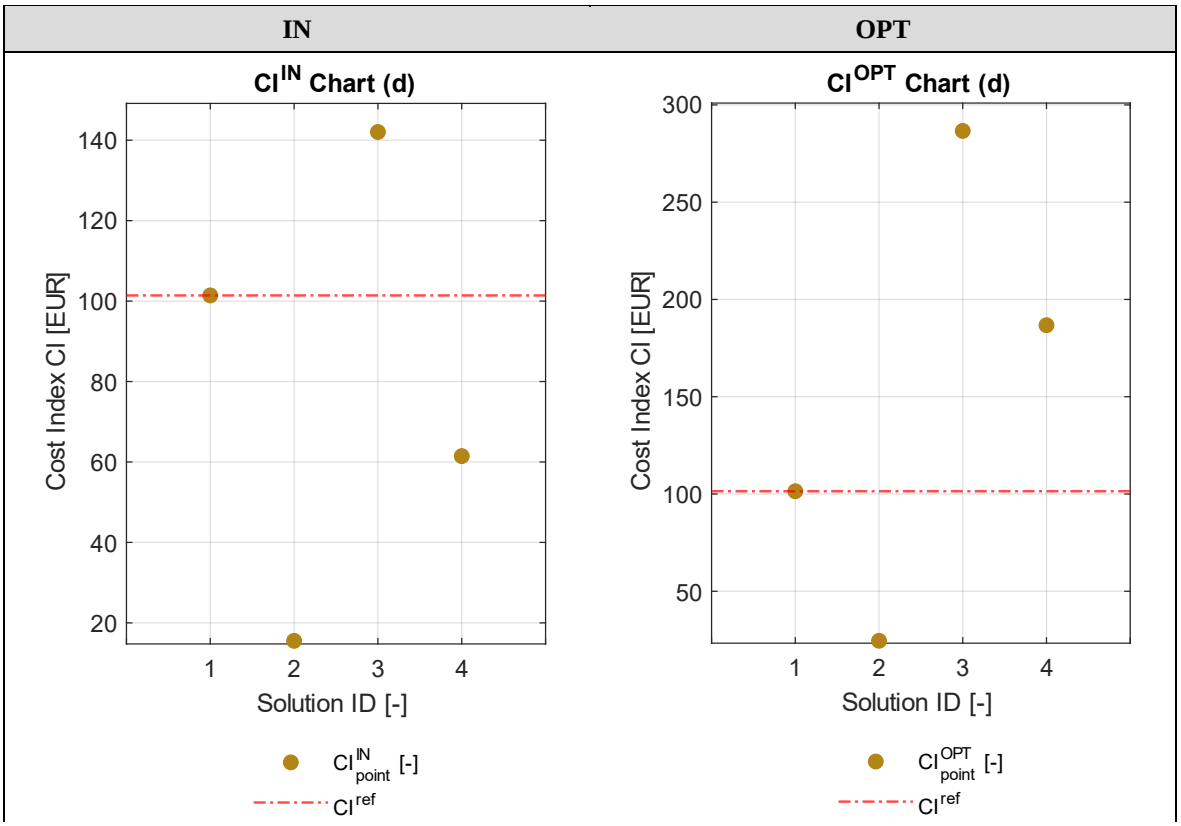

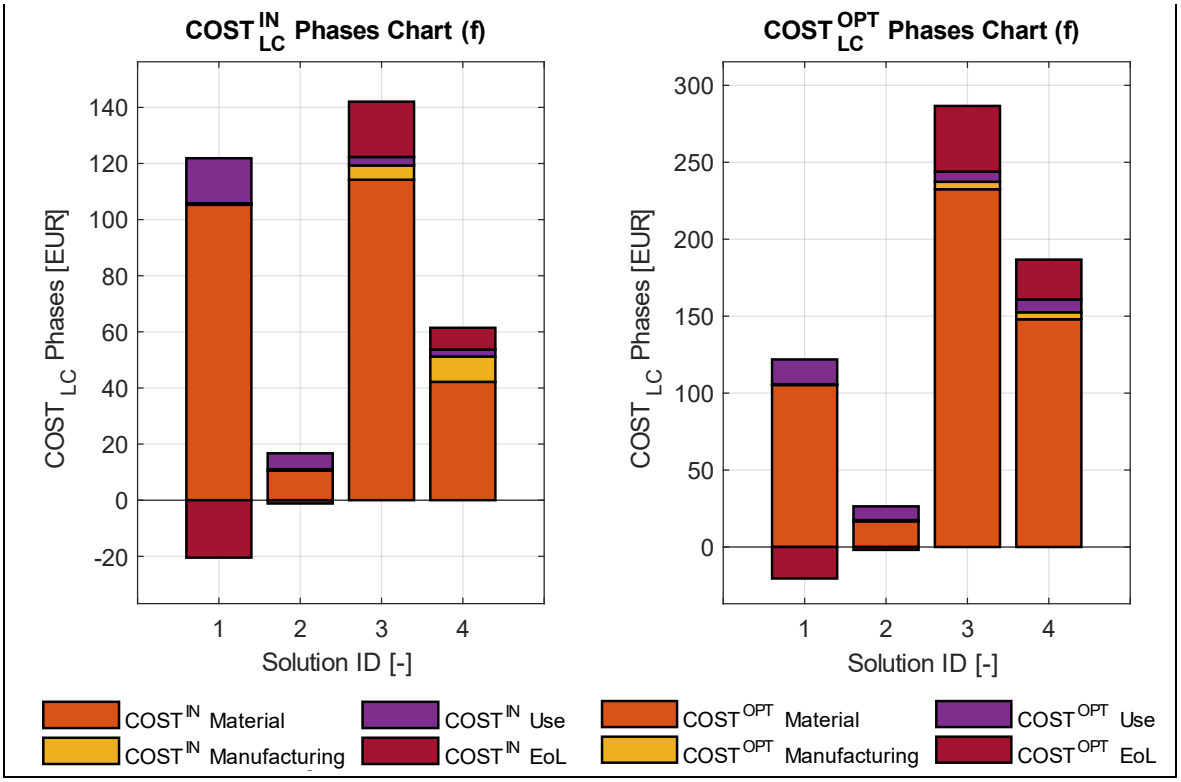

After the Optimization, only one solution (with ID = 3) present a CI^{OPT} value that is entirely below the COST value of the reference scenario (red dotted line CI^{ref}), highlighting the partial reduction of economic cost through optimization of the solutions considered. The optimized solution with ID = 2 provides the best economic performances, as shown in **Figure 45.a** (*right*). In this context, the critical discussion of CI^{OPT} values stresses unique key-point: the Optimization phase generated solutions (except the reference) with an increased economic cost. The main reasons for this are reported below:

- Considering the solutions with ID = 2, the use stage has variable importance over the entire solution LC (approximately 36%, because of use stage modelled on a mass basis). Despite this, this phase is lower than the reference solution one (ID = 1, see **Figure 45.b** (*right*)). Moreover, it is interesting observing the raw materials phase, since it is worsened due to Optimization, but it is still better than the reference scenario material stage. However, the solution has a low $COST^{raw}$ value since the material (Age-Hardening Wrought Al-Alloys) has a low specific cost, as well as low density value (see **Table B.7** and **Table B.11**). Concerning the EoL phase, since the solution is made by aluminium, the $COST_{EoL}$ is negative and near to zero.
- Considering the solutions with ID = 3 and 4, the use stage still covers the minority of total $COST_{LC}$ (between 2% and 4%) since the base material being CFRP and NFRP (with low densities); thus, the phase is lower than the reference solution one (ID = 1, see **Figure 45.b** (*right*)). Concerning the raw materials phase, the solutions present an increase of the economic cost due to the optimization. The solutions have a huge cost since they are made by CFRP (H1) and NFRP (H2), having a vast material specific cost (consequently affecting the materials stage) (see material in **Table B.11**), and a greater mass than in the initial condition (the thickness was increased from 0.75mm to 1.625mm and 2.5mm, respectively).

3.3 3D | EXA-ARB Case Study: Front Lower Control Arm (FLCA)

The suspension system comprises several individual components (i.e., control arms, cross-members, axles, knuckles, brake discs and drums) and is responsible for the following functions: maintain correct vehicle ride height, reduce the effect of shock forces, maintain correct wheel alignment, support vehicle weight, keep the tires in contact with the road, and control the vehicle's direction of travel.

In detail, the lower control arm (FLCA) is a part of the suspension system and takes part to the steering system; its principal roles are to support the entire weight of the front of the vehicle (through the lower ball joint) and control the front wheel movement throughout its travel. Thus, this component determines how well (or poorly) the vehicle performs (ride and handling), allowing the tire to move independently of the vehicle with the least amount of negative feedback to the chassis and steering while keeping the tires planted firmly and squarely on the road. In this context, the lower control arm (FLCA) is chosen as applicative three-dimensional (3D) case study and Functional Unit (FU) for DeSA methodology.

3.3.1 Screening

Starting point of the screening phase is primary shape design constraint choice (see); in this case study, three-dimensional (3D) shape is chosen. **Figure 46** illustrates the initial FEM model of the FLCA.

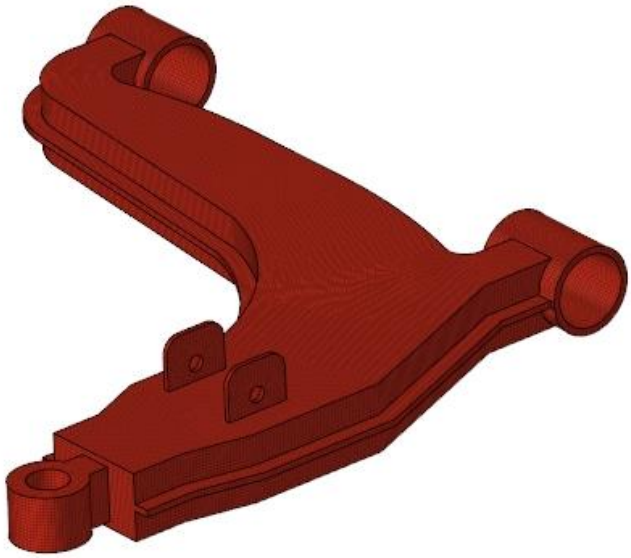

Figure 46. FLCA FEM model.

Then, the production database is created, according to materials and manufacturing processes data availability. Exploratory approach (EXA) is considered: the production database provides physical and mechanical properties through variability ranges (min-max ranges). For the FLCA component, the list of available materials is made of metals and alloys (unique material class in the case study database): each material is defined by ID (MAT_{ID}), mechanical (i.e., density, Young modulus, etc.), environmental (i.e., climate change), and

economic properties (i.e., cost). **Table 57** presents the list of materials chosen, while Appendix D reports all materials properties used for the analysis. The list of allowable processes is made of manufacturing technologies able to generate three-dimensional (3D) shapes: each process is defined by an ID (PR_{ID}), mechanical, environmental, and economic features. Appendix D reports also all processes data used for the FLCA case study.

Table 57. List of available materials and processes in FLCA production database.

Production Database				
Material Section (MAT)				
	Material ID	**Material Class**	**Material Subclass**	**Material Name**
Materials	M1	Metals and Alloys	Ferrous	Cast Iron (Ductile)
	M2	Metals and Alloys	Ferrous	High Carbon Steel
	M3	Metals and Alloys	Ferrous	Low Alloy Steel
	M4	Metals and Alloys	Ferrous	Medium Carbon Steel
	M5	Metals and Alloys	Ferrous	Stainless Steel
	M6	Metals and Alloys	Non-Ferrous	Cast Al-Alloys
	M7	Metals and Alloys	Non-Ferrous	Wrought Magnesium Alloys
	M8	Metals and Alloys	Non-Ferrous	Nickel-based Superalloys
	M9	Metals and Alloys	Non-Ferrous	Titanium Alloys
Manufacturing Technologies Section (MAN)				
	Process ID	**Process Class**	**Process Subclass**	**Process Name**
Processes	CA1	Casting	Die Casting Processes	Gravity Die casting
	CA2	Casting	Investment Casting Processes	Investment Casting
	CA3	Casting	Die Casting Processes	Low Pressure Die Casting
	DE1	Deformation	Bulk Deformation Processes	Forging
	PO1	Powder Methods	Powder Pressing Processes	Pressing and Sintering

The second step of screening is the application of design constraints (directly provided by the designer). The unique physical constraints applied to the case study is the process constraint Batch size (B), with the objective to explore all possible combinations generated by the proposed methodology but economic batch limitation.

The final step of the screening is the determination of all design solutions that satisfy the design requirements (imposed by designer) and that are feasible from a technical point of view. Several solutions are automatically generated thanks to the application of design constraints and design choices in terms of geometry, materials, and processes. As provided by theoretical background reported in previous paragraphs, all combinations that do not meet the above requirements are not inserted in the list of feasible solutions.

3.3.2 Design and Sustainability analysis

The goal and scope of this phase is to analyse and compare the design and sustainability performances of alternative FLCA design solutions - obtained in the screening step - for the front lower control arm component over its whole life cycle.

First step is the design analysis step (**Figure 4**), where FEM simulation modelling of all feasible solutions is performed. Considering the ARB scenario, the load case is assessed on the basis of structural integrity (as ratio between the yield strength of the material and the maximum stress level on the component calculated through the FEM simulations (see **Equation 16**)) provided by the generic design alternative, calculating the performance level PI. The case is obtained from linear static analysis, using a force applied to the ball joint (where the wheel assembly is mounted) of front lower arm (see the detail in **Figure 47**).

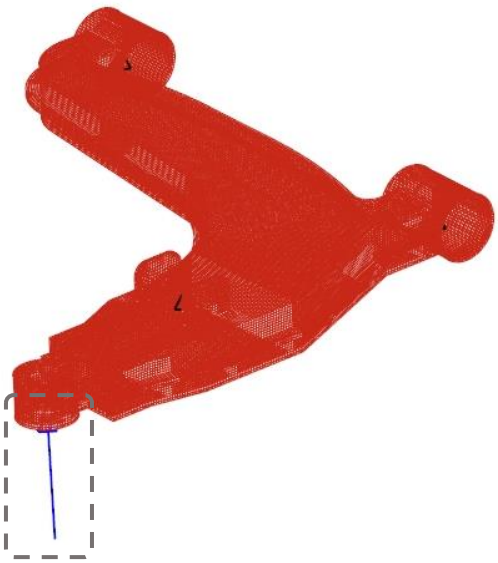

Figure 47. Force (represented as blue arrow) applied to FLCA ball joint for linear static analysis.

Figure 48 shows The BCs of the control arm component: the inner surface nodes of ball joint, the connection with shock absorber and spring, the front and rear bushes are tied respectively to node A, B and C, by means of 1D rigid element (RBE2) to restrict degree of freedom (represented by blue spider webs in figure).

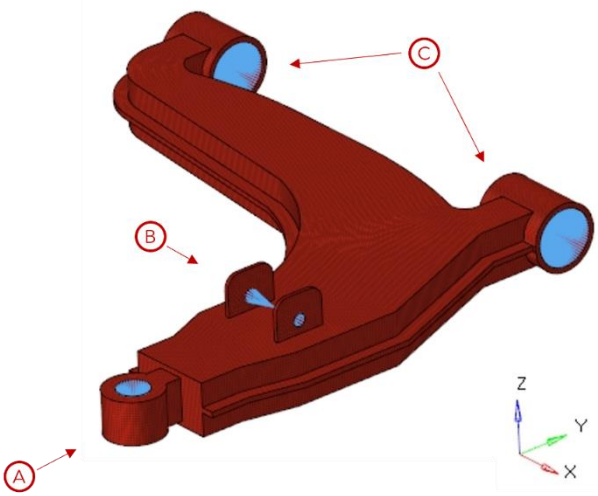

Figure 48. Front lower control arm BCs nodes.

RBE2 consists of one independent node and one or more dependent nodes; nodes A, B and C act as independent node. The load is applied to node A as a force vector (according to the global system reported in **Figure 48**); one component in x-direction (longitudinal), the second component in y-direction (lateral), and the third component in z-direction (vertical). By assumption, the force is calculated considering a static distribution of the vehicle mass (as shown in **Table 58**) on each wheel (F_{wheel}) and multiplying this result by load coefficients consistent with the case study (see **Equations 93-94**):

$$m_{veh} = 1315\ kg \rightarrow\ F_{wheel} = (m_{veh} \cdot g)/4 \approx 3287.5\ N \tag{93}$$

$$\begin{cases} F_x = -2 \cdot F_{wheel} \approx -6575\ N \\ F_y = 1.5 \cdot F_{wheel} \approx 4932\ N \\ F_z = 3.5 \cdot F_{wheel} \approx 11510\ N \end{cases} \tag{94}$$

Table 58. FLCA Case Study - Vehicle features inputs.

Vehicle Features Inputs	
Feature	**Value**
Vehicle Mass	1315 [kg]
Vehicle Lifetime	200000 [km]
Vehicle Class	C
Powertrain	ICEV
Driving Cycle	Worldwide Harmonized Light Vehicles Test Procedure (WLTP)
CO_2 Emissions	108 [g/km]

The z-directional motion of node B (the point where the connection between shock absorber and lower arm is made) is prohibited. Finally, nodes C (centre node of both front and rear bushes) are fixed and no translational motion in x, y and z-directions is allowed, as well as y and z-rotational motion; only x-axis rotation degree of freedom is allowed.

Considering that data characterizing the generic solution S_i are provided in terms of ranges (i.e., EX approach), the LH method is applied to implement such data in the FEM simulations. For this case study a number of simulations (n_{sim}) variable between 2 and 5 is assumed; this variability mainly depends on the data of the solution considered (**Figure 13** and **Equations 1 – 5**). **Table B.13** and **Table B.14** in Appendix D show design data of materials and processes available for FLCA case study (as well as the material, shape, & process compatibility matrices).

The environmental analysis step performs the LCA of all feasible sub-simulations S_{ij} obtained from the design analysis, calculating the environmental level EI. The reference vehicle on which the FU (i.e., FLCA) is assumed to be installed is the VOLKSWAGEN Golf 1.5 TSI combustion engine, with a life-distance of 200,000 km; the component lifetime is assumed equal to the one of the vehicle (no substitution during operation is assumed). As described in a previous section (2.2.2 - Environmental modelling) the system boundaries include the following life cycle phases: materials production, component manufacturing, use stage and EoL treatments. **Table 58** provides car technical features, instead **Table B.15** and **Table B.16** in Appendix D show environmental impacts of materials and processes available for the case study.

The economic analysis step performs the LCC of all feasible sub-simulations S_{ij} obtained from the design analysis and assessed in environmental analysis, calculating the economic level CI. As described in a previous section (*2.2.3 - Economic modelling*), the system boundaries include the following life cycle phases: materials production, component manufacturing, use stage and EoL treatments.

The economic batch size (B) chosen for FU is 7500 pieces, and the fraction of time for which the equipment is productive (i.e., the load factor (L)) is set to 0.5 (or 50%), fixed for all processes available in the production database. In the same way, the capital write-off time is equal for all processes. **Table 59** provides economic features, instead **Table B.17** and **Table B.18** in Appendix D show the economic impacts of materials and processes available for the FLCA case study.

Table 59. FLCA Case Study - Economic features inputs.

Economic Features Inputs	
Feature	**Value**
Batch Size	7500 [pc.]
Load Factor	50 [%]
Capital Write-off Time	5 [yr.]
EoL Grid-Mix	EU-28
Fuel Price	1.8 [EUR/l]

3.3.3 First Classification

Once the Design and Sustainability analysis is performed for the design solutions, the PSL is calculated through PI, EI, and CI indexes. After the first elasticity screening, the first ranking of the acceptable alternatives is occurred.

The PSL calculation step performs the calculation of the PSL by a weighted sum formula to combine the weights of criteria with the performance/sustainability scores for each design alternative (see section 2.3.1). The PSL scale factor (K) assumed for the case study is equal to 10.

The first elasticity screening step identifies all design solutions that are acceptable from an elasticity perspective. Since the FLCA case study is defined considering an EX approach with ARB scenario, such a screening is performed by means of ELV and FL parameters. For this reason, ELV is assumed by designer equal to 1 (that means a structural integrity level (PI) equal to 2), while FL is assumed equal to 0.5, that is, all alternatives that have less than 50% of EL range to the right of ELV vertical line are rejected and they are not considered in the first ranking. The ranking step provides that the PSL values related to the acceptable solutions are compared; such a ranking is performed by means of the average value of the PSL range (PSL_{ss}), according to explorative approach (**Equation 75**).

3.3.4 Optimization

In the optimization phase the acceptable solutions S^{acc}_{i} (and sub-solutions S^{acc}_{ij}, considering the EX approach) obtained from the first elasticity screening are optimized, to improve the PSL of the front lower arm, without compromising the mechanical performance (in this case, structural integrity) of the analyzed design solutions. Since the type of primary shape chosen during the screening phase is three-dimensional (3D), the methodology will work on the (sub-)solutions using the Structural Optimization: starting from given FLCA volume and the boundary condition data (loads, constraints, etc., as shown in **Figure 49**), the numerical framework of structural optimization allows to obtain fully or partially automated design solution, that provide the best performance in relation with a user-defined goal and given design constraints (e.g., structural or manufacturing).

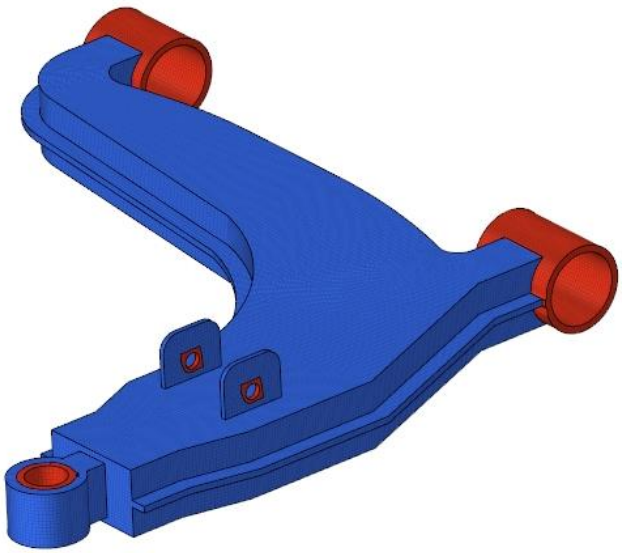

Figure 49. Representation of Design Space (DS – blue elements) and Non-Design Space (NDS – red elements) in FLCA case study.

As described before, in the methodology the Topology Optimization is chosen as structural optimization framework.

In this context, the FLCA geometry (already developed in Design and Sustainability Analysis – 2.2) is meshed, and the designed loads and structural BCs are applied to the meshed model; they remain unaltered when passing from one solution to another. In contrast to FEM analysis, the elements of the FLCA model are designated as falling within one of two categories reported here (see **Figure 49**):

- Design space (DS): elements in which the element density (ρ_{el}) can vary within the topology optimization and may potentially be removed or altered for the final design.
- Non-design space (NDS): elements which remain unchanged during the optimization procedure (typically the locations where BCs, loads, or other constraints are applied).

Since the design approach chosen by the designer is "Exploratory" (EXA), the physical and mechanical properties that characterize materials of all acceptable solutions are already

defined in the design analysis in terms of variability ranges (**Table 28** reports an overview of the required input data for the FEM optimization, considering EXA approach). Therefore, the methodology works as follows:

- In the EX approach the framework explores the generic i-th acceptable solution S^{acc}_i with N_i sub-solutions S^{acc}_{ij} (j =1, …, N_i), each of which has to be modelled through a FEM simulation. The acceptable solution S^{acc}_i (or sub-solutions S^{acc}_{ij}) and number of required FEM simulations N^{acc}_i is already determined during FEM modelling in Design Analysis (2.2.1), thus:

$$S_{ij}^{acc} = S_{ij} = S_{ij}\left(G, BC, MAT_{ij}, N_i^{acc}\right)$$

$$N_i^{acc} = N_i = N_i(MAT_i, n_{min}, n_{max}, \delta)$$

- For each acceptable sub-solution S^{acc}_{ij} identified in the previous simulation modelling step, the optimization simulation is performed through the combined use of MATLAB and Altair HyperWorks simulation software; the solver used in this phase is Optistruct. The optimization problem for each solution is formulated according to the following strategy (already reported in **Table 29**): the main objective of the topology optimization problem is the mass minimization, applying a strength constraint (as lower bound respect to yield strength (σ_y) of specific material).

- After the optimization simulations are performed, the main steps are the outcomes extraction, thus the component shape reconstruction to use in the next and final methodology phase (i.e., Final Classification), where the indexes described in the DeSA (i.e., PI, EL, EI, CI) are calculated. The methodology envisages the following steps, according to the modelling framework reported in **Table 30**, **Table 31**, **Table 32**, and **Table 33** (see **Equations 77-80**):

    - Writing ".dens" and ".out" files for each acceptable sub-solution S^{acc}_{ij} submitted to the optimization phase. The ".dens" file presents the list of elements with the fictitious density value (ρ^{el}) obtained from the topology optimization (see **Table 31**). The ".out" file presents, in the form of a table, the percentage of elements having a specific density range (see **Table 32**).
    - Extracting data from ".dens" and ".out" files just obtained.
    - Writing density matrix (P) and calculating mean density vector ($\bar{\rho}$). The density matrix (P) is calculated from the ".dens" files by extracting the data for each sub-solution (see **Table 31**). The mean density vector ($\bar{\rho}$) is obtained by averaging the density values over the j-th element (see **Equation 77**).
    - Writing density range matrix (T) and calculating mean range vector ($\bar{\tau}$) relative to density ranges. In this case, the density range matrix (T) is obtained from the ".out" files by extracting the data for each sub-solution; then, the average range vector ($\bar{\tau}$) is calculated as the mean of the percentage values over the density ranges (10 in total), according to **Equation 78** (**Table 32**).
    - Setting a density threshold value (THR), chosen by the designer considering the mean range vector ($\bar{\tau}$) calculated and using the following rule:

$$T_{des}^{el}\ such\ that:\ \sum_{r=1}^{r} \overline{\tau_r^{el}} \cong T_{des}^{el} \rightarrow r \rightarrow THR$$

T^{el}_{des} represents the percentage of elements that the designer wants to remain in the optimized shape reconstruction; the methodology extracts the density range (r) for which the cumulative sum of the components of the vector $\bar{\boldsymbol{\tau}}$ is equal to T^{el}_{des} (as shown in **Equation 79**). Finally, THR is obtained considering the density range (r) extracted.

- Output extraction, obtaining the elements that respect THR. The threshold obtained is compared with the values present in the mean density vector ($\bar{\rho}$); if the generic value of the vector is greater than THR, the j-th element respects the constraint imposed by the designer, otherwise the element is discarded and not considered in the shape reconstruction, as shown in **Table 33**.

The elements thus obtained from the previous phase will be used to create a new FEM model following the optimization results. In this phase, the methodology, based on the results obtained from the data extraction phase, automatically reconstructs the component geometry (as shown in **Figure 24**). Then, the designer will use this reconstructed model to redesign **MANUALLY** the geometry (based on this new information and suggestions) and to re-prepare the FEM model. This model will be used in the final stage of the methodology, the final classification.

3.3.5 Final classification

Once the Optimization is performed for the acceptable sub-solutions S_{ij}, the final classification phase is carried out by means of the following steps: Design and Sustainability Re-Analysis and final PSL calculation. After the final elasticity screening, the final ranking of the acceptable and optimized alternatives is occurred.

The final PSL calculation step performs the calculation of the PSL always using a weighted sum formula to combine the weights of criteria with the performance and sustainability scores for each design alternative (as already shown in section 2.3.1). The PSL scale factor (K) assumed is the same used in the previous paragraphs (equal to 10).

The final elasticity screening step identifies all design and optimized solutions that are acceptable from an elasticity perspective. Since the FLCA case study is defined considering an EX approach with ARB scenario, such a screening is performed by means of ELV and FL parameters already defined previously: ELV is assumed equal to 1 (that means a structural integrity level (PI) equal to 2), while FL is assumed equal to 0.5 (i.e., all alternatives that have less than 50% of EL range to the right of ELV vertical line are rejected and they are not considered in the final ranking).

The final ranking step provides that the PSL values related to the acceptable and optimized solutions are compared; such a ranking is performed by means of the average value of the PSL range (PSL_{ss}), according to explorative approach (**Equation 82**).

3.3.6 Results & Discussion

Table 60 reports the 30 solutions generated in the screening stage that satisfy both design requirements (imposed by designer) and are feasible from a technical perspective.

Table 60. FLCA Case Study - List of solutions created in the first screening phase (IN); outcomes obtained through First Elasticity Screening and First Ranking.

FLCA Solutions List – BEFORE OPTIMIZATION						
ID	**Design Solution ID**	**PSL^{IN}_{range}**	**EL^{IN}_{range}**	**PSL^{IN}_{ss}**	**First Elasticity Screening**	**First Ranking**
1	1_Solid_M1_CA2	[71.68,81.99]	[0.35,1.14]	76.83	NO	No Rank
2	2_Solid_M2_CA2	[60.21,73.56]	[0.59,2.70]	66.88	OK, With FL	10
3	3_Solid_M3_CA2	[57.87,70.99]	[0.56,3.74]	64.43	OK, With FL	12
4	4_Solid_M4_CA2	[55.32,73.87]	[0.41,1.85]	64.60	OK, With FL	11
5	5_Solid_M5_CA2	[37,62.66]	[-0.11,2.14]	49.83	OK, With FL	16
6	6_Solid_M6_CA2	[85.83,126.66]	[-0.25,1.36]	106.25	NO	No Rank
7	7_Solid_M7_CA2	[83.41,116.69]	[-0.34,0.43]	100.05	NO	No Rank
8	8_Solid_M8_CA2	[17.09,31.58]	[0.41,5.60]	24.34	OK, With FL	20
9	9_Solid_M1_CA3	[86.84,96.44]	[0.35,1.14]	91.64	NO	No Rank
10	10_Solid_M2_CA3	[76.55,81.14]	[0.59,2.70]	78.85	OK, With FL	8
11	11_Solid_M3_CA3	[72.99,83.7]	[0.56,3.74]	78.34	OK, With FL	9
12	12_Solid_M4_CA3	[76.15,87.57]	[0.41,1.85]	81.86	OK, With FL	5
13	13_Solid_M5_CA3	[44.34,64.72]	[-0.11,2.14]	54.53	OK, With FL	15
14	14_Solid_M6_CA3	[118.29,162.04]	[-0.25,1.36]	140.16	NO	No Rank
15	15_Solid_M7_CA3	[133.41,163.17]	[-0.34,0.43]	148.29	NO	No Rank
16	16_Solid_M8_CA3	[19.17,32.03]	[0.41,5.60]	25.60	OK, With FL	19
17	17_Solid_M2_DE1	[78.83,86.93]	[0.59,2.70]	82.88	OK, With FL	4
18	18_Solid_M3_DE1	[75.8,85.6]	[0.56,3.74]	80.70	OK, With FL	7
19	19_Solid_M4_DE1	[80.92,88.97]	[0.41,1.85]	84.95	OK, With FL	2
20	20_Solid_M5_DE1	[46.16,65.90]	[-0.11,2.14]	56.03	OK, With FL	14
21	21_Solid_M6_DE1	[143.02,170.5]	[-0.25,1.35]	156.76	NO	No Rank
22	22_Solid_M7_DE1	[157.11,173.21]	[-0.34,0.43]	165.16	NO	No Rank
23	23_Solid_M8_DE1	[19.13,32.58]	[0.41,5.60]	25.86	OK, With FL	17
24	24_Solid_M9_DE1	[18.90,21.34]	[2.27,3.69]	20.12	OK	21
25	25_Solid_M2_PO1	[79.00,87.04]	[0.59,2.70]	83.02	OK, With FL	3
26	26_Solid_M3_PO1	[75.73,85.68]	[0.56,3.74]	80.70	OK, With FL	6
27	27_Solid_M4_PO1	[81.38,88.88]	[0.41,1.85]	85.13	OK, With FL	1
28	28_Solid_M5_PO1	[46.43,65.67]	[-0.11,2.14]	56.05	OK, With FL	13
29	29_Solid_M6_PO1	[142.81,172.22]	[-0.25,1.36]	157.51	NO	No Rank
30	30_Solid_M8_PO1	[19.49,32.18]	[0.41,5.60]	25.84	OK, With FL	18

A Design Solution ID is defined for generic design alternative as a combination of shape (primary component shape defined by the designer – 1D, 2D, or 3D), material (MAT_{ID}, see **Table 57**), and process (PR_{ID}, see **Table 57**). Considering that generic i-th solution S_i is defined in terms of material variability range (i.e., EX approach, see Table *8*), it is explored with N_i sub-solutions S_{ij} ($j = 1, \ldots, N_i$), each of which is modelled through a FEM simulation. The number of required FEM simulations N_i is determined using the range sizes of different material properties (**Table B.13** in Appendix D) and number of simulations (n_{sim}) variable between 2 and 5 (assumed by the designer). With these assumptions, the LH method provides 9 simulations, defined on the basis of material types reported in **Table 57**, with a

total of 44 sub-simulations. **Table 61** reports simulations created by LH method and the N_i associated by the generic solution.

Table 61. FLCA Case Study - List of simulations created by LH method.

ID	LH Simulation ID	Number of Sub-simulations
1	M6	5
2	M1	3
3	M2	4
4	M3	4
5	M4	4
6	M8	5
7	M5	5
8	M10	5
9	M7	5
	Total Sub-simulations	44

Looking at the list of solutions, gravity die casting (with Process ID: CA1 – shown in **Table 57**) is not compatible with any of the available material. Therefore, no solution made with the die casting process is generated. 21 out of 30 solutions (70%) comply with the first elasticity screening, subdivided in two main groups:

- full-acceptable solutions, that present EL range always greater than ELV line (see green lines in **Table 60**);
- FL-acceptable solutions, that present EL range less than ELV line (see yellow lines reported in **Table 60**).

All solutions analyzed in the design and sustainability analysis phase are represented through ellipses (or bubbles) in the PSL-EL bubble chart of **Figure 50**.

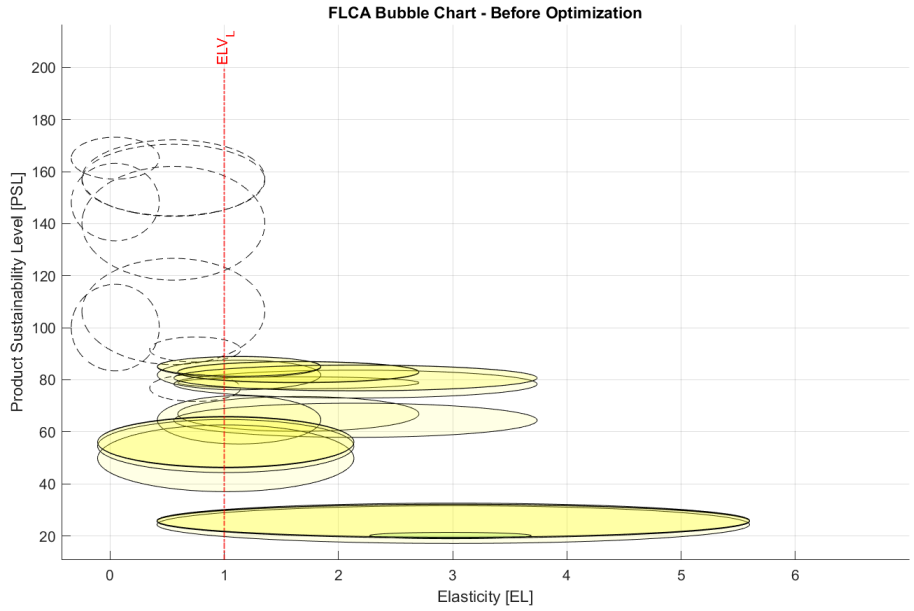

Figure 50. Front lower control arm bubble chart (with FL = 0.5), before the Optimization phase. Dashed bubbles represent discarded solutions.

The full-acceptable solutions S^{acc}_{i} are those identified by bubbles whose area is entirely to the right of the ELV line – green bubbles in **Figure 50**); on the other hand, the FL-acceptable solutions S^{acc}_{i} are those identified by bubbles whose area is to the right of the ELV line by more than 50% (in yellow in **Figure 50**). The other solutions (those that have more than half of the bubble area to the left of the ELV line) are not acceptable and therefore they are rejected. Moreover, **Table 60** reports PSL_{ss} for all acceptable design options, also including the first ranking, from which the best acceptable solution results to be the one identified by ID = 27 (highest value of PSL^{IN}_{ss}).

Next, the acceptable the sub-solutions S^{acc}_{ij} obtained from the first elasticity screening will be optimized to improve the PSL, without compromising the mechanical performance of the analyzed design solutions. The type of primary shape chosen during the screening phase is three-dimensional (3D); thus, the methodology will work on the (sub-)solutions S^{acc}_{ij} using the Structural Optimization (i.e., Topology Optimization). After the optimization simulations are performed, the main steps are the outcomes extraction, thus the component shape reconstruction to use in the Final Classification, where the indexes described in the DeSA (i.e., PI, EL, EI, CI) are calculated and used for PSL calculation. According to the modelling framework reported in **Table 30**, **Table 31**, **Table 32**, and **Table 33** (see **Equations 77-80**), the ".dens" and ".out" files for each acceptable sub-solution S^{acc}_{ij} submitted to the optimization phase are written and extracted. The density matrix (P) and the mean density vector ($\bar{\rho}$) are calculated; the first one from the ".dens" files by extracting the data for each sub-solution, the second one by averaging the density values over the j-th element (as already shown in **Equation 77**). The same operation in performed for the density range matrix (T) and the mean range vector ($\bar{\tau}$) relative to density ranges; the first one is obtained from the ".out" files by extracting the data for each sub-solution, the second one by averaging the percentage values over the j-th element (as already shown in **Equation 78**). **Table 62** reports the mean range vector ($\bar{\tau}$) relative to density ranges of FLCA acceptable sub-solution S^{acc}_{ij}. Therefore, the density threshold value (THR) is chosen by the designer considering the mean range vector ($\bar{\tau}$) shown above and using the following rule:

$$T^{el}_{des}\ such\ that: \sum_{r=1}^{r} \overline{\tau^{el}_{r}} \cong T^{el}_{des} \rightarrow r \rightarrow THR$$

Table 62. FLCA Mean range vector obtained from outcomes extraction phase.

	Mean Range Vector ($\bar{\tau}$)	
Density Range	**Avg Solution Value [%]**	**Cumulate Sum [%]**
0.0 - 0.1	96.69	96.69
0.1 - 0.2	0.52	97.21
0.2 - 0.3	0.32	97.53
0.3 - 0.4	0.22	97.75
0.4 - 0.5	0.18	97.93
0.5 - 0.6	0.13	98.06
0.6 - 0.7	0.12	98.18
0.7 - 0.8	0.11	98.29
0.8 - 0.9	0.11	98.40
0.9 - 1.0	1.6	100
	Total Sum	100

The percentage of elements that the designer wants to remain in the optimized shape reconstruction (T^{el}_{des}) is defined equal to approximately to 97~98%; thus, the methodology extracts the density range (r) for which the cumulative sum of the components of the vector $\bar{\boldsymbol{\tau}}$ is equal to 97~98%, i.e., THR = 0.25.

The THR just defined is compared with the values present in the mean density vector ($\bar{\rho}$); if the generic value of the vector is greater than THR, the j-th element respects the constraint imposed by the designer, otherwise the element is discarded and not considered in the shape reconstruction (as already shown in **Table 33**).

The finite elements obtained will be used to create a new FEM model following the optimization results. In this phase, the methodology, based on the results obtained from the data extraction phase, automatically reconstructs the component geometry (as shown in **Figure 51.a**). Then, the designer will use this reconstructed model to redesign **MANUALLY** the geometry (based on this new information and suggestions) and to re-prepare the FEM model. **Figure 51.b** illustrates the FEM model of the FLCA, reconstructed based on the methodology suggestions; this model is used in the Final Classification.

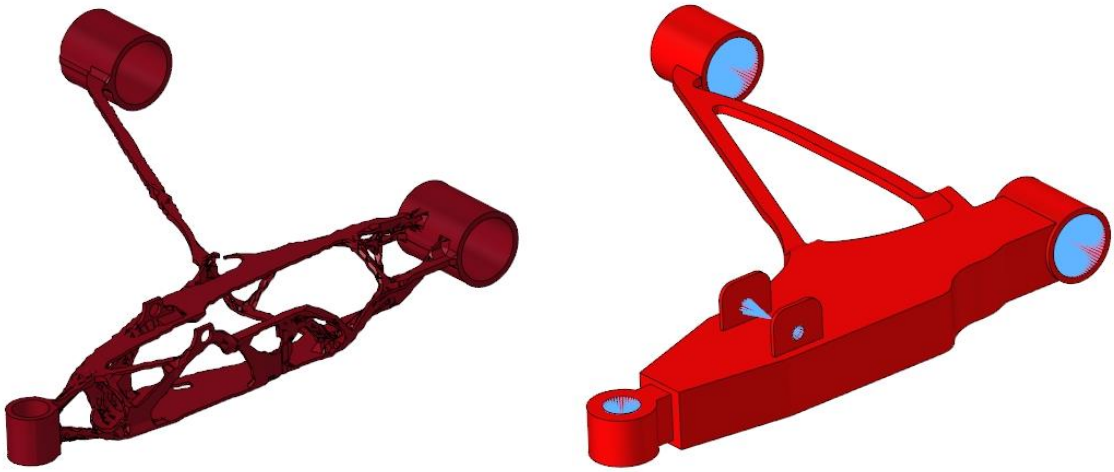

Figure 51. Optimized FLCA FEM model; model automatically created by the methodology (left side); model reconstructed by the designer (right side).

Table 63 and **Table 64** report the 21 solutions analyzed in the Optimization phase and assessed through the final screening stage (then satisfy both design requirements (imposed by the designer) and are feasible from a technical perspective). Considering that generic i-th solution S^{acc}_{i} is defined in terms of material variability range (i.e., EX approach), it is explored with N^{acc}_{i} sub-solutions S^{acc}_{ij} (j =1, …, N_i), each of which is modelled through a FEM simulation. The number of required FEM simulations N^{acc}_{i} is already determined during FEM modelling in Design Analysis (see **Table 61**).

Therefore, 13 out of 21 solutions (≈ 62%) - approximatively 40% respect the total number of design alternatives - comply with the final elasticity screening, always subdivided in two main groups:

- full-acceptable and optimized solutions, that present EL range always greater than ELV line (see green lines in **Table 63** and **Table 64**);

- FL-acceptable and optimized solutions, that present EL range less than ELV line (see yellow lines in **Table 63** and **Table 64**).

Table 63. FLCA Case Study - List of solutions created after the Optimization phase (OPT); outcomes obtained through Final Elasticity Screening and Final Ranking.

FLCA Solutions List – AFTER OPTIMIZATION						
ID	**Design Solution ID**	**PSL^{OPT}_{range}**	**EL^{OPT}_{range}**	**PSL^{OPT}_{ss}**	**Final Elasticity Screening**	**Final Ranking**
2	2_Solid_M2_CA2	[96.76,119.76]	[0.22,1.84]	108.26	OK, With FL	7
3	3_Solid_M3_CA2	[93.26,111.54]	[0.20,2.63]	102.40	OK, With FL	8
4	4_Solid_M4_CA2	[90.41,119.35]	[0.08,1.18]	104.88	NO	No Rank
5	5_Solid_M5_CA2	[58.65,96.75]	[-0.32,1.40]	77.70	NO	No Rank
8	8_Solid_M8_CA2	[27.29,47.85]	[0.08,4.05]	37.57	OK, With FL	12
10	10_Solid_M2_CA3	[130.22,136.09]	[0.22,1.83]	133.15	OK, With FL	5
11	11_Solid_M3_CA3	[124.06,139.61]	[0.20,2.63]	131.83	OK, With FL	6
12	12_Solid_M4_CA3	[125.62,146.40]	[0.08,1.18]	136.01	NO	No Rank
13	13_Solid_M5_CA3	[73.16,102.70]	[-0.32,1.40]	87.93	NO	No Rank
16	16_Solid_M8_CA3	[32.45,49.47]	[0.08,4.05]	40.96	OK, With FL	11
17	17_Solid_M2_DE1	[136.95,147.78]	[0.22,1.84]	142.37	OK, With FL	2
18	18_Solid_M3_DE1	[132.38,145.11]	[0.19,2.63]	138.75	OK, With FL	3
19	19_Solid_M4_DE1	[139.48,150.65]	[0.08,1.18]	145.07	NO	No Rank
20	20_Solid_M5_DE1	[78.75,105.53]	[-0.32,1.40]	92.14	NO	No Rank
23	23_Solid_M8_DE1	[32.47,50.58]	[0.08,4.05]	41.52	OK, With FL	9
24	24_Solid_M9_DE1	[31.34,34.68]	[1.54,2.64]	33.01	OK	13
25	25_Solid_M2_PO1	[137.29,148.00]	[0.22,1.84]	142.65	OK, With FL	1
26	26_Solid_M3_PO1	[132.09,145.40]	[0.19,2.63]	138.74	OK, With FL	4
27	27_Solid_M4_PO1	[140.80,150.51]	[0.08,1.18]	145.65	NO	No Rank
28	28_Solid_M5_PO1	[79.25,105.12]	[-0.32,1.40]	92.18	NO	No Rank
30	30_Solid_M8_PO1	[33.11,49.88]	[0.08,4.05]	41.49	OK, With FL	10

Table 64. FLCA Case Study - List of solutions compared before (IN) and after (OPT) the Optimization phase.

FLCA Solutions List – COMPARISON BEFORE/AFTER OPTIMIZATION					
ID	**Design Solution ID**	**PSL^{IN}_{ss}**	**PSL^{OPT}_{ss}**	**$\%PSL_{ss}$**	**Final Ranking**
1	1_Solid_M1_CA2	76.83	-	-	-
2	2_Solid_M2_CA2	66.88	108.26	61.86%	7
3	3_Solid_M3_CA2	64.43	102.40	58.94%	8
4	4_Solid_M4_CA2	64.60	104.88	62.35%	No Rank
5	5_Solid_M5_CA2	49.83	77.70	55.95%	No Rank
6	6_Solid_M6_CA2	106.25	-	-	-
7	7_Solid_M7_CA2	100.05	-	-	-
8	8_Solid_M8_CA2	24.34	37.57	54.39%	12
9	9_Solid_M1_CA3	91.64	-	-	-
10	10_Solid_M2_CA3	78.85	133.15	68.88%	5
11	11_Solid_M3_CA3	78.34	131.83	68.28%	6
12	12_Solid_M4_CA3	81.86	136.01	66.15%	No Rank
13	13_Solid_M5_CA3	54.53	87.93	61.25%	No Rank
14	14_Solid_M6_CA3	140.16	-	-	-
15	15_Solid_M7_CA3	148.29	-	-	-
16	16_Solid_M8_CA3	25.60	40.96	59.98%	11

FLCA Solutions List – COMPARISON BEFORE/AFTER OPTIMIZATION [CONTINUE]					
ID	**Design Solution ID**	**PSL^{IN}_{ss}**	**PSL^{OPT}_{ss}**	**$\%PSL_{ss}$**	**Final Ranking**
17	17_Solid_M2_DE1	82.88	142.37	71.77%	2
18	18_Solid_M3_DE1	80.70	138.75	71.93%	3
19	19_Solid_M4_DE1	84.95	145.07	70.77%	No Rank
20	20_Solid_M5_DE1	56.03	92.14	64.44%	No Rank
21	21_Solid_M6_DE1	156.76	-	-	-
22	22_Solid_M7_DE1	165.16	-	-	-
23	23_Solid_M8_DE1	25.86	41.52	60.58%	9
24	24_Solid_M9_DE1	20.12	33.01	64.04%	13
25	25_Solid_M2_PO1	83.02	142.65	71.82%	1
26	26_Solid_M3_PO1	80.70	138.74	71.91%	4
27	27_Solid_M4_PO1	85.13	145.65	71.09%	No Rank
28	28_Solid_M5_PO1	56.05	92.18	64.47%	No Rank
29	29_Solid_M6_PO1	157.51	-	-	-
30	30_Solid_M8_PO1	25.84	41.49	60.61%	10

All solutions analyzed in the design and sustainability re-analysis phase are represented again through bubbles in the PSL-EL bubble chart of **Figure 52**.

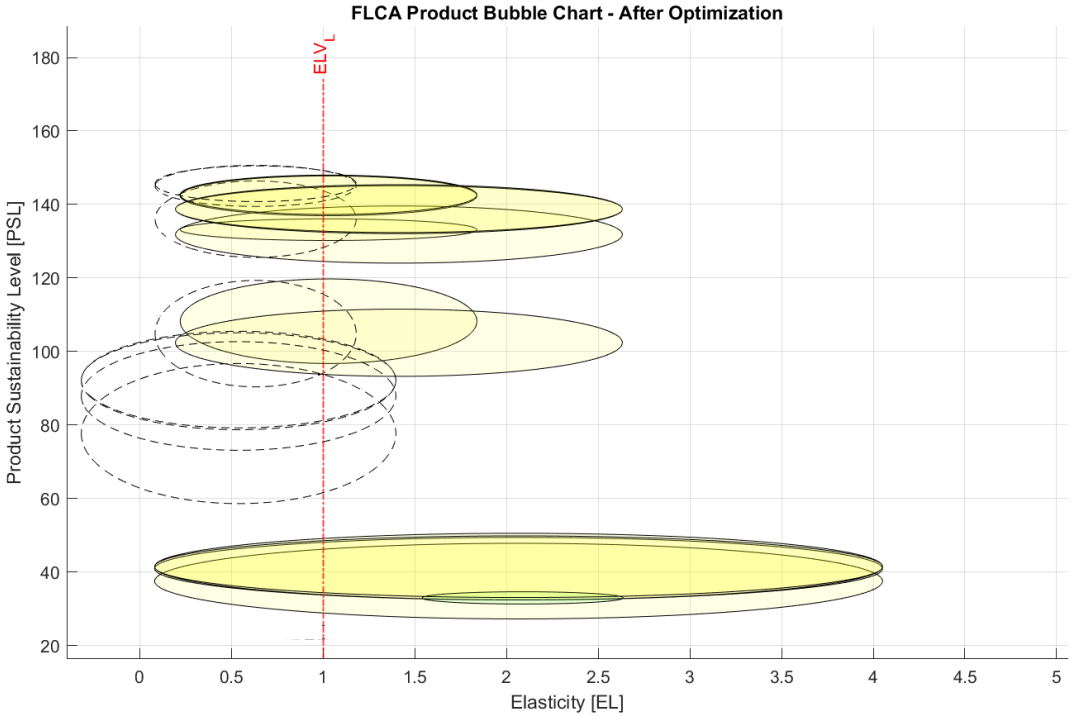

Figure 52. Front lower control arm bubble chart (with FL = 0.5), after the Optimization phase. Dashed bubbles represent discarded solutions.

The full-acceptable and optimized solutions $S^{acc/opt}_{i}$ are those identified by bubbles whose area is entirely to the right of the ELV line - in green in **Figure 52**; on the other hand, the FL-acceptable and optimized solutions $S^{acc/opt}_{i}$ are those identified by yellow bubbles whose area is to the right of the ELV line by more than 50%. The other solutions (those that have more than half of the bubble area to the left of the ELV line) are not acceptable and therefore they are rejected. Moreover, reports PSL_{ss} for all acceptable and optimized design

alternatives, including the final ranking, from which the best acceptable solution results to be the one identified by ID = 25.

The methodology finally calculates the improvement (or worsening) of each acceptable solution S^{acc} obtained during the first classification and further analyzed in Optimization and Final Classification phases (see **Equation 82**). We see that the analyzed solutions' improvement is between 54% and 72%; the elasticity (EL_{range}) presents lower values than the limit value (i.e. ELV = 1) but it is still acceptable considering FL. Therefore, it implies that the optimization has reached the structural limit of the several design alternatives analyzed; further reducing the solutions' mass (in order to increase their PSL) would compromise their mechanical performance.

The solutions analysis is based on the integrated single score index PSL, as well as the specific sustainability indexes (PI, EI, and CI).

Regarding the Sustainability Level, **Figure 53** (*left*) shows the variability range of PSL^{IN} for the first five FLCA solutions considered acceptable during the first ranking.

Figure 53. FLCA Case Study - Product sustainability level of five best solutions, before (IN) and after (OPT) the Optimization phase.

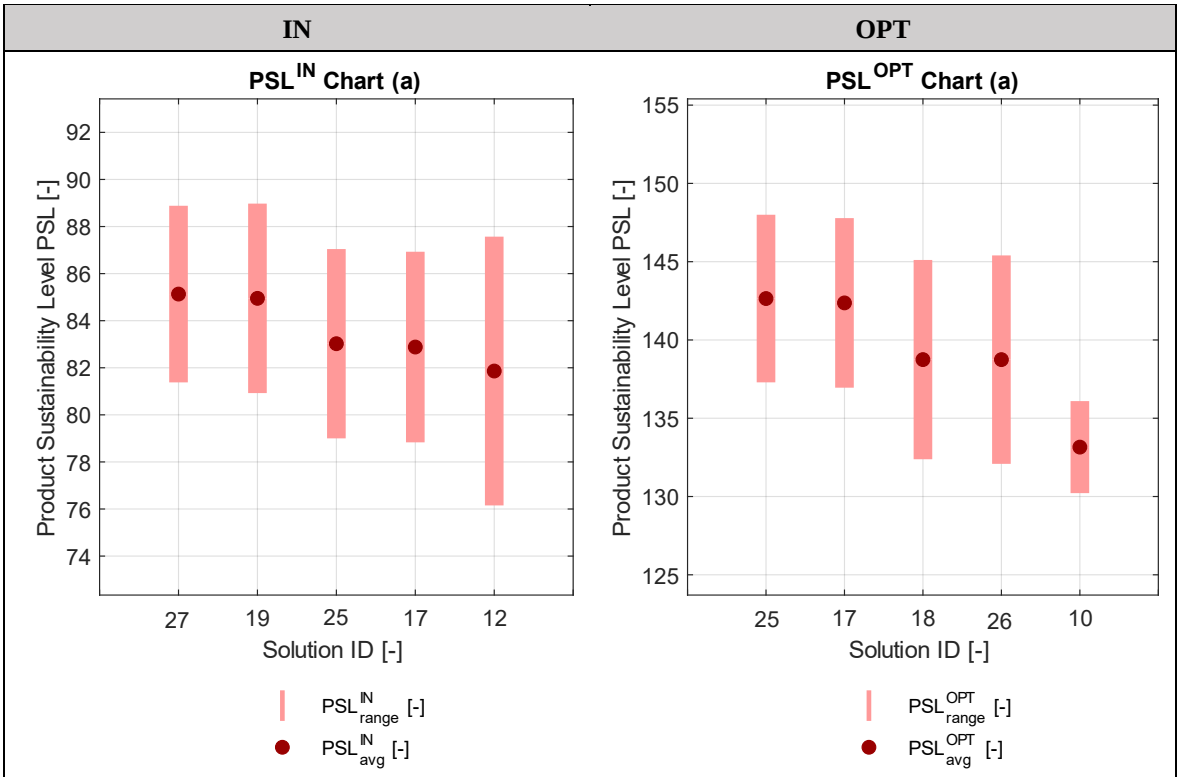

It is interesting to stress that the best design option (solution identified by ID = 27) results slightly preferable compared to the other solutions considered; indeed, PSL^{IN} varies moderately when passing from one solution to another (range: $76 < PSL^{IN} < 89$). Instead, the design alternative with ID = 12, since it is defined by family of materials that presents the high variability in CC and COST inventory data (i.e., Medium Carbon Steel – M4), presents a PSL value lower than the other solutions considered.

Another relevant outcome of the FLCA case study is that all acceptable solutions have low PI ranges; i.e., the elasticity (EL^{IN}_{range}) presents lower values than the limit value (ELV = 1),

but it is still acceptable considering FL. This indicates a possible slight margin for improvement in the lightweight perspective (starting point for the Optimization phase). Indeed, reducing excessively the component mass would certainly provide beneficial effects in terms of the overall sustainability level (an increase of PSL^{IN}_{rank}). However, it would compromise the mechanical performance of design alternatives here analyzed.

Figure 53 (*right*) shows the variability range of PSL^{OPT} for the first five FLCA solutions considered acceptable during the final ranking. In this context, the best design option (ID = 25) results different from the best design alternative obtained in the first ranking phase - before the optimization – the solution with ID = 27. This means that reducing excessively the mass certainly provided beneficial effects in terms of the overall sustainability level (with an increase of PSL^{OPT}) but compromising the mechanical performance of design alternative considered. Therefore, the solution with ID = 27 was discarded during the final elasticity screening, making way for another solution. Moreover, the best new solution results slightly preferable compared to the other solutions considered; indeed, PSL^{OPT} varies moderately when passing from one solution to another (range: $130 < PSL^{OPT} < 147$). Finally, the design alternative with ID = 10 is defined by family of materials that presents the low variability in CC and COST inventory data (i.e., High Carbon Steel – M2); thus, it presents a PSL with a variability lower than the other solutions considered.

Finally, it is interesting to observe that all acceptable solutions have low PI ranges; i.e., the elasticity (EL^{OPT}_{range}) presents lower values than the limit value (ELV = 1), but it is still acceptable considering FL. This implies that the several design alternatives here analyzed have reached the structural limit thanks to the optimization. Further reducing the solutions' mass (in order to increase their PSL) would compromise their mechanical performance. Indeed, only two solutions (ID = 25 and 17) in the first ranking increased their PSL (thus moving up in position), without compromising their performance; the other three, however, were discarded in the final screening phase, making way for three new solutions.

On the contrary, the outcomes of the study change considering design, environmental and economic points of view, separately (PI, EI and CI indexes). In this context, **Figure 54** reports the bar charts for PI before and after the Optimization phase.

Before the Optimization, all five solutions present a range for PI^{IN} which falls on the ELV imposed by the designer (see red dotted line in **Figure 54**), but whose area is above the ELV line by more than 50%; thus, resulting the FL-acceptable of design options. Interestingly, the solutions with ID = 25 and 17 (the third and fourth in the first ranking of **Table 60**) present a range for PI which is greater than the best acceptable solution in PSL perspective (solution with ID = 27 in **Figure 54** (*left*)), resulting the design options with the highest PI levels, even when basing the assessment on the minimum value of the range. As a consequence, where the FLCA case study is carried out according to a traditional design perspective, the higher average value of PI and the high variability of PI make the solutions with ID = 25 and 17 to be definitely the most profitable ones. It is worthy to be noticed that such solutions result over-dimensioned when being evaluated through the DeSA, thus resulting in a lower value of PSL^{IN}_{rank} (**Table 60**).

After the Optimization, all five solutions present PI^{OPT} which falls on the ELV imposed by the designer (see red dotted line), but whose area is above the ELV line by more than 50%; thus, resulting the FL-acceptable of design options. Interestingly, solutions with ID = 18 and 26 (the third and fourth in the final ranking of **Table 64**) present PI greater than the best acceptable solution in PSL perspective (e.g., solution with ID = 25 in **Figure 54** (*right*)), thus resulting the design options with the highest PI levels, even when basing the assessment

Figure 54. FLCA Case Study - PI of five best solutions, before (IN) and after (OPT) the Optimization.

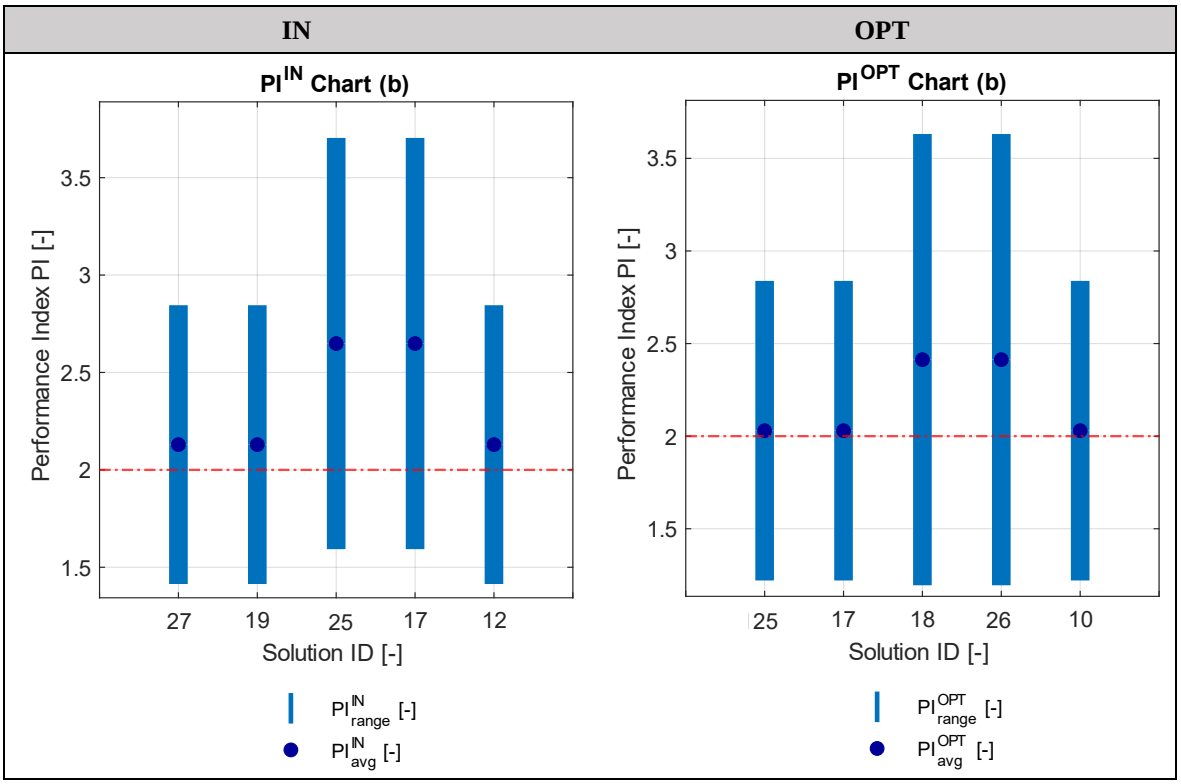

on the minimum value of the range. As a consequence, according to a traditional design perspective, the higher average value of PI and the high variability of PI make solutions with ID = 18 and 26 the most profitable ones after the optimization step. Finally, it is important to highlight that these solutions results still over-dimensioned when being evaluated through the DeSA, thus resulting in a lower value of PSL^{OPT}_{rank}.

Figure 55.a reports the FLCA bar charts for EI before and after the Optimization phase; whereas **Figure 55.b** shows all LC phases in environmental perspective, considering raw material, manufacturing, use, and EoL.

Before the Optimization, solutions with ID = 27, 19, and 12 provide the best environmental performances, as shown in **Figure 55.a** (*left*). In this regard, the critical discussion of EI^{IN} values stresses two main key-points. The first one is that EI^{IN} varies minimally when passing from one solution to another (range: 182 $kgCO_{2eq}$ < EI^{IN} < 185 $kgCO_{2eq}$); the second point is that the variability range that characterizes the four solutions considered is much limited (less than ± 1 for all options). The main reasons for this are reported below:

- Considering all solutions, the use stage covers the vast majority of total CC_{LC} (approximately 80%), and the impact is the almost the same for the alternatives (152 $kgCO_{2eq}$), since the base material being steel (same density ranges, see **Table B.13**) for each of those (use stage modelled on a mass basis, as provided by section *2.2 – Environmental Modeling*). This implies that also CC_{EoL} is more or less the same for all options (see the red bars in **Figure 55.b** (*left*)). Moreover, the variability of EI^{IN} is due to materials and manufacturing phases, but the lower variability in CC

inventory data and the relatively lesser influence on total CC_{LC} (it does not exceed 20% of total for alternatives) make the final EI^{IN} range small.

Figure 55. FLCA Case Study – EI(a) and LC(b) phases of all best solutions, before (IN) and after (OPT) the Optimization.

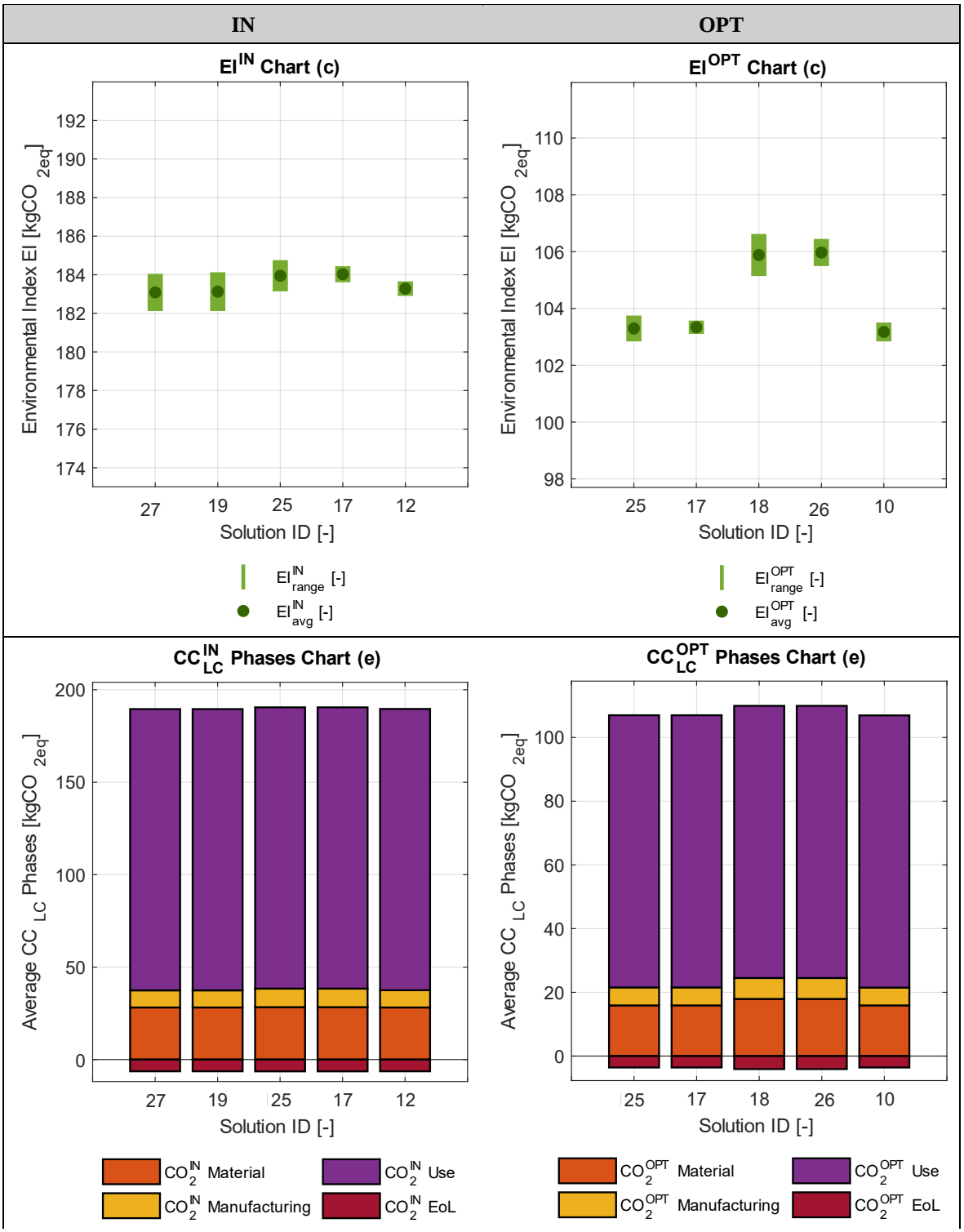

- Considering in detail the solutions with ID = 25 and 17, the use stage always covers the vast majority of total CC_{LC} (approximately 80%), and the impact is the almost

the same for the alternatives (152 $kgCO_{2eq}$), since the base material being steel for each of those. According to the use stage modelled on a mass basis (*2.2 – Environmental Modeling*), the impact in the use stage is due to the density of the material considered. This implies that also CC_{EoL} is more or less the same for all options (see the red bars in **Figure 55.b** (*left*)). Instead, the variability of EI^{IN} is also due to materials and manufacturing phases, but in this case the greater variability in CC inventory data regarding the manufacturing processes (it takes almost the 5% of total for alternatives) make the final EI^{IN} range slightly greater than the other solutions analyzed.

After the Optimization phase, all solutions present an EI^{OPT} ranges smaller than the EI^{IN} ones, highlighting the reduction of environmental impact through optimization of the solutions considered. In this context, the optimized solutions with ID = 25, 17, and 10 provide the best environmental performances, as shown in **Figure 55.a** (*right*). In this regard, the critical discussion of EI^{OPT} values stresses two main key-points. The first one is that EI^{OPT} varies minimally when passing from one solution to another (range: 103 $kgCO_{2eq}$ < EI^{OPT} < 107 $kgCO_{2eq}$); the second point is that the variability range that characterizes the four solutions considered is much limited (less than ± 0.5 for all options). The main reasons for this are reported below:

- Considering all solutions, the use stage covers the vast majority of total CC_{LC} (approximately 80%), and the impact is the almost the same for the alternatives (85 $kgCO_{2eq}$), since the base material being steel (same density ranges, see **Table B.13**) for each of those solutions. This implies that the environmental impact of use stage ($CO^{OPT}{}_{2eq}$ Use) is reduced approximately of 44% respect to impact before the optimization. Moreover, this means that also CC_{EoL} is more or less the same for all options but reduced since the solutions have minor mass (see the red bars in **Figure 55.b** (*right*)). Moreover, the variability of EI^{OPT} is due to materials and manufacturing phases, but the lower variability in CC inventory data and the relatively lesser influence on total CC_{LC} (it does not exceed 20% of total for alternatives) – as well as the mass reduction obtained during the optimization - make the final range for EI^{OPT} small.

- Considering in detail the solutions with ID = 18 and 27, the use stage always covers the vast majority of total CC_{LC} (approximately 80%), and the impact is the almost the same for the alternatives (85 $kgCO_{2eq}$), since the base material being steel for each of those. This implies that the environmental impact of use stage ($CO^{OPT}{}_{2eq}$ Use) is reduced approximately of 44% respect to impact before the optimization. According to the use stage modelled on a mass basis (*2.2.2 – Environmental Modeling*), the impact in the use stage is due to the density of the material considered. The CC_{EoL} is more or less the same for all options but reduced since the solutions have minor mass (see the red bars in **Figure 55.b** (*right*)). Instead, the variability of EI^{OPT} is also due to materials and manufacturing phases, but in this case the greater variability in CC inventory data regarding the manufacturing processes (it takes almost the 5% of total for

alternatives) – even if the mass reduction is obtained during the optimization – make the final EI^{OPT} slightly greater than the other solutions analyzed.

Finally, **Figure 56.a** shows the bar charts for CI before and after the Optimization; **Figure 56.b** reports instead all LC phases in economic perspective (raw material, manufacturing, use, EoL, respectively).

Figure 56. FLCA Case Study – CI(a) and LC(b) phases of all best solutions, before (IN) and after (OPT) the Optimization.

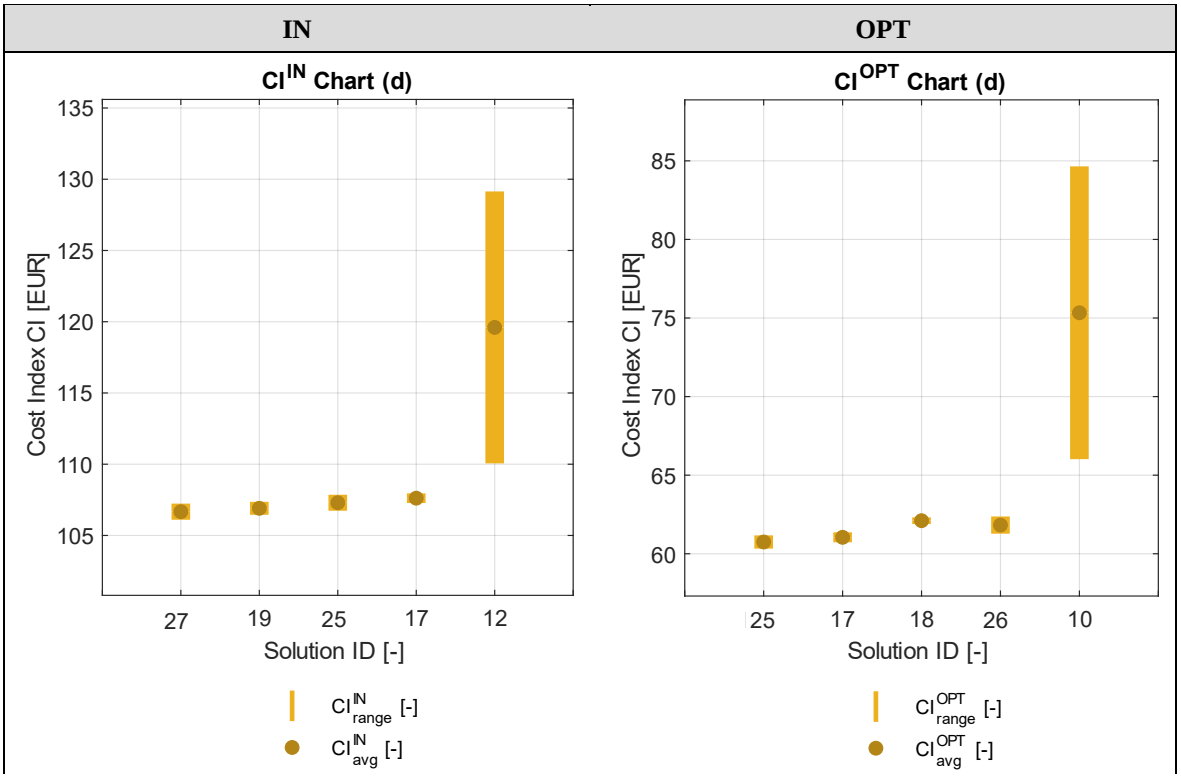

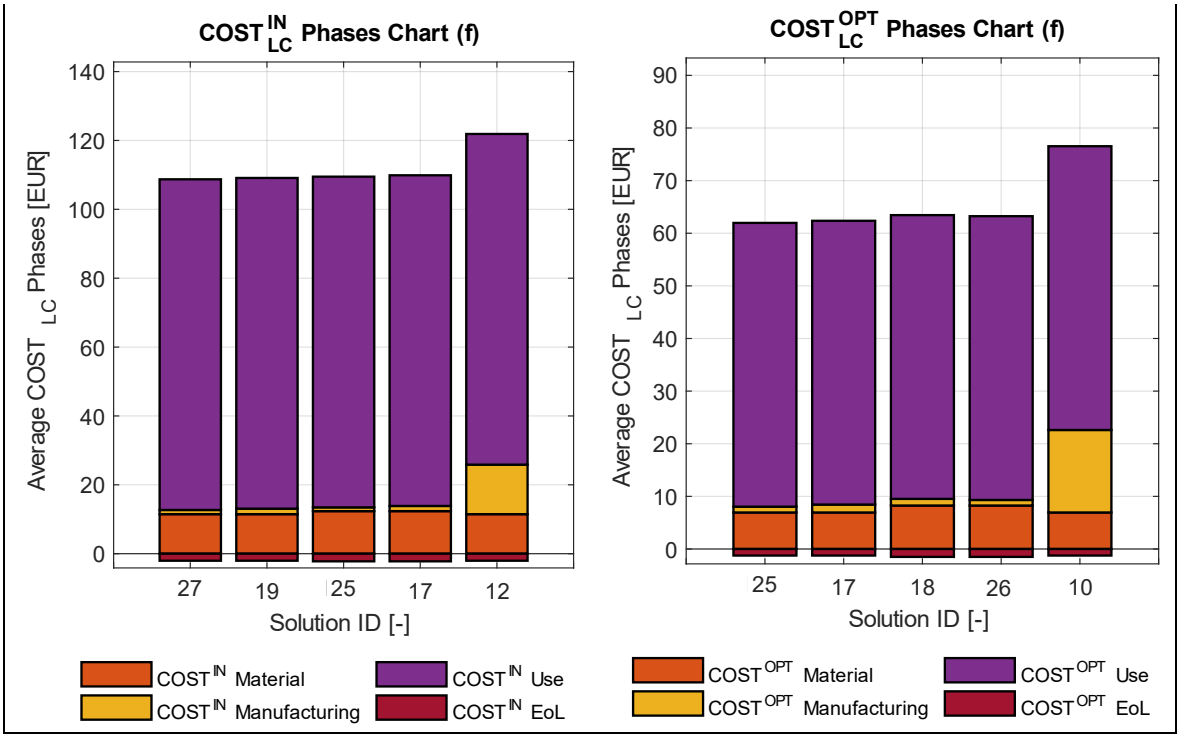

Before the Optimization, all solutions (except the one with ID = 12) provide the best economic performances, as shown in **Figure 56.a** (*left*). In this regard, the critical discussion of CI^{IN} values stresses two main key-points. The first one is that CI^{IN} varies moderately when passing from one solution to another (range: 105 EUR < CI^{IN} < 130 EUR); the second point is that the variability range that characterizes the four solutions considered is high (between ± 0.5 and ± 9). The main reasons for this are reported below:

- Considering all solutions (except ID = 12), the use stage covers the vast majority of total $COST_{LC}$ (approximately 90%), and the impact is the almost the same for the alternatives (96 EUR), since the base material being steel (same density ranges, see **Table B.13**) for each of those (use stage modelled on a mass basis, as provided by section *2.3 – Economic Modeling*). This implies that also $COST_{EoL}$ is more or less the same for all options (see the red bars in **Figure 56.b** (*left*)). Moreover, the CI^{IN} variability is due to materials and manufacturing phases, but the lower variability in COST inventory data and the relatively lesser influence on total $COST_{LC}$ (it does not exceed 10% of total for alternatives), making final CI^{IN} range small.
- Considering in detail the solutions with ID = 26 and 17, the use stage always covers the vast majority of total $COST_{LC}$ (approximately 90%), and the cost is the almost the same for the alternatives (96 EUR), since the base material being steel for each of those. According to the use stage modelled on a mass basis (*2.3 – Economic Modeling*), the cost in the use stage is due to the density of the material considered. This implies that also $COST_{EoL}$ is more or less the same for all options (see the red bars in **Figure 56.b** (*left*)). Instead, the variability of CI^{IN} is also due to materials and manufacturing phases, but in this case the higher variability in COST inventory data regarding the manufacturing processes (it takes almost the 5% of total alternatives), making the final range for CI^{IN} slightly greater than the other solutions analyzed.

The solutions with ID = 12 represents the exception: it has a high impact on the manufacturing phase, since it is processed by means of low pressure die casting (CA3), which has a high specific impact cost (consequently affecting the manufacturing stage) (see process in **Table B.18**).
After the Optimization, all solutions present a range for CI^{OPT} smaller than the CI^{IN} ranges, highlighting the reduction of economic cost through optimization of the solutions considered. In this context, all optimized solutions (except the one with ID = 10) provide the best economic performances, as shown in **Figure 56.a** (*right*). In this regard, the critical discussion of CI^{OPT} values stresses two main key-points. The first one is that CI^{OPT} varies moderately when passing from one solution to another (range: 60 EUR < CI^{OPT} < 85 EUR); the second point is that the variability range that characterizes the four solutions considered is high (between ± 0.3 and ± 69). The main reasons for this are reported below:

- Considering all solutions (except the one with ID = 10), the use stage covers the vast majority of total $COST_{LC}$ (approximately 88%), and the impact is the almost the same for the alternatives (54 EUR), since the base material being steel (same density value, see **Table B.13**) for each of those solutions. This implies that the cost of use stage ($COST^{OPT}$ Use) is reduced approximately of 44% respect to impact before the optimization. Moreover, this means that also $COST_{EoL}$ is more or less the same for all options but reduced since the solutions have minor mass (see the red bars in **Figure 56.b** (*right*)). Moreover, the variability of CI^{OPT} is due to materials and manufacturing phases, but the lower variability in COST inventory data and the relatively lesser influence on total $COST_{LC}$ (it does not exceed 12% of total for alternatives) – as well as the mass reduction obtained during the optimization - make that the final range for CI^{OPT} is small.
- Considering in detail the solutions with ID = 18 and 25, the use stage always covers the vast majority of total $COST_{LC}$ (approximately 88%), and the impact is the almost the same for the alternatives (54 $kgCO_{2eq}$), since the base material being steel for each of those. This implies that the cost of use stage ($COST^{OPT}$ Use) is reduced approximately of 44% respect to impact before the optimization. According to the use stage modelled on a mass basis, the impact in the use stage is due to the density of the material considered. The $COST_{EoL}$ is more or less the same for all options but reduced since the solutions have minor mass (see the red bars in **Figure 56.b** (*right*)). Instead, the variability of CI^{OPT} is also due to materials and manufacturing phases, but in this case the greater variability in COST inventory data regarding the manufacturing processes (it takes almost the 5% of total for alternatives) – even if the mass reduction is obtained during the optimization - make that the final range for CI^{OPT} slightly greater than the other solutions analyzed.

Despite the reduction of the economic cost due to optimisation, the solutions with ID = 10 represents the exception (see **Figure 56.b** (*right*)): a high impact on the manufacturing phase, since it is processed by means of low pressure die casting (CA3), implies a high specific impact cost; thus, affecting the manufacturing stage (see process in **Table B.18**).

3.4 3D | TRA-ARB Case Study: Engine Mounting Bracket (EMB)

In automotive context, one of the main drivers of manufactures is traveling comfort: resonant vibrations come from unbalanced masses within the engine body; this is causing the designers to direct their attention to the utilization of systems such as to improve the vehicle's riding comfort.

In this scenario, the engine mounting bracket (EMB) is most important part of vehicle in reducing vibrations and harshness for the smooth ride of the vehicle. The main function of an EMB is to properly balance the engine and transmission on the vehicle chassis for good balance control when vehicle is in motion (as well as good isolation). In this context, the engine bracket (EB) is chosen as applicative three-dimensional (3D) case study and Functional Unit (FU) for DeSA methodology.

3.4.1 Screening

Starting point of the screening phase is primary shape design constraint choice (see **Table 4**). **Figure 57** illustrates the initial FEM model of the EMB; for this reason, three-dimensional (3D) shape is chosen.

Figure 57. EMB FEM model.

Then, the production database is created, with materials and manufacturing processes available to the designer. In this context, Traditional approach (TRA) is considered: the production database provides physical and mechanical properties through constant values.

For the EMB component, the list of available materials is made of only metals and alloys, defining each material by ID (MAT_{ID}), mechanical (i.e., density, Young modulus, etc.), environmental (i.e., climate change), and economic properties (i.e., cost). In turn, the list of allowable processes is made of manufacturing technologies able to generate three-dimensional (3D) shapes: each process is defined by ID (PR_{ID}), mechanical, environmental, and economic features. **Table 65** presents the list of materials and processes chosen, while Appendix D reports all properties used for the EMB case study.

Table 65. List of available materials and processes in EMB production database.

Production Database				
Material Section (MAT)				
Material ID		**Material Class**	**Material Subclass**	**Material Name**
Materials	M1	Metals and Alloys	Ferrous	High Carbon Steel
	M2	Metals and Alloys	Ferrous	Low Alloy Steel
	M3	Metals and Alloys	Ferrous	Stainless Steel
	M4	Metals and Alloys	Non-Ferrous	Age-Hardening Wrought Al-Alloys
	M5	Metals and Alloys	Non-Ferrous	Titanium Alloys
Manufacturing Technologies Section (MAN)				
Process ID		**Process Class**	**Process Subclass**	**Process Name**
Processes	CA1	Casting	Investment Casting Processes	Investment Casting
	DE1	Deformation	Bulk Deformation Processes	Forging
	PO1	Powder Methods	Powder Pressing Processes	Pressing and Sintering

The second step of screening is the application of design constraints provided by the designer. The unique physical constraints applied is the Batch size (B) constraint, with the objective to explore all possible combinations generated by the proposed methodology with economic batch limitation.

The final step of the screening is the determination of all design solutions that satisfy the design requirements and that are technically feasible. The application of design constraints and design choices in terms of geometry, materials, and processes automatically generates several design solutions. As already said by theoretical background reported in previous paragraphs, all combinations that do not meet the above requirements are discarded and not inserted in the list of feasible solutions.

3.4.2 Design and Sustainability analysis

The goal and scope of this phase is to analyse and compare the design and sustainability performances of alternative EMB design solutions - obtained in the screening step - for the engine mount bracket component over its whole life cycle.

First step is the design analysis step, where FEM simulation modelling of all feasible solutions is performed. As shown in the previous case study, the load case is always assessed on the basis of structural integrity; considering the REF scenario, the ratio is calculated between the stress level on the reference scenario and the maximum stress level on the component calculated through the FEM simulations (**Equation 16**) provided by the generic design alternative, calculating the performance level PI. The case is obtained from linear static analysis, using a combined use of forces and pressures applied to surfaces where the bolts are mounted (see the details in **Figure 58**).

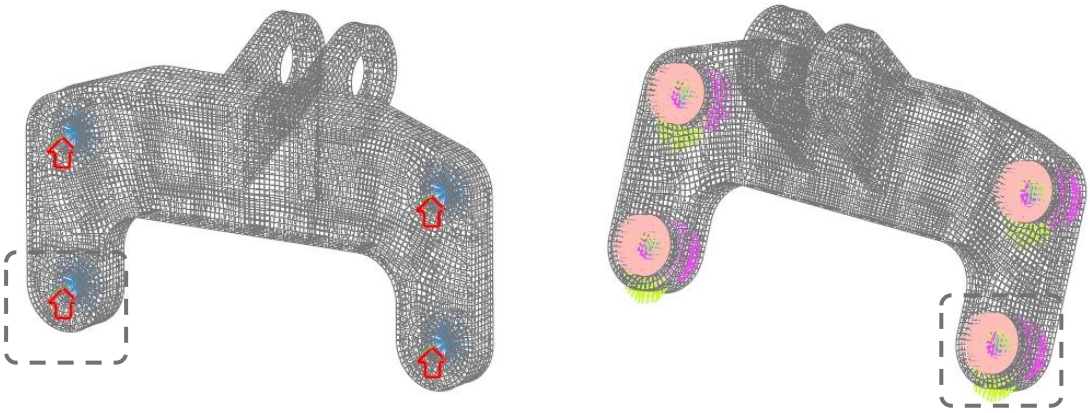

Figure 58. Pretension Forces (represented as red arrows) applied to EMB surfaces for linear static analysis (left image); pressures (represented as colored arrows) applied to EMB surfaces for linear static analysis (right image).

Figure 59 shows the BCs of the engine mount component: the connection with engine and the link between bracket and vehicle chassis are defined by zone A and B, respectively.

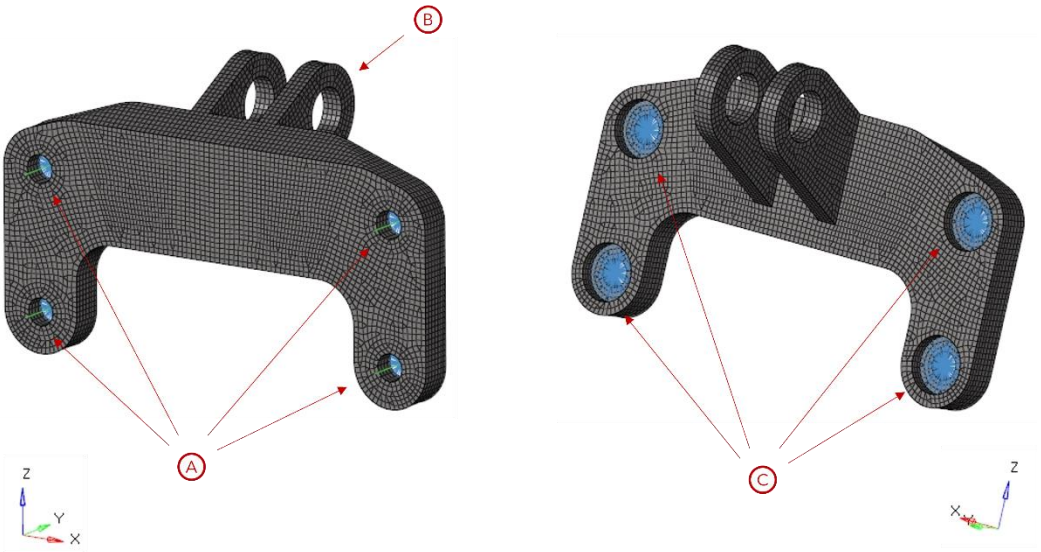

Figure 59. Engine bracket BCs zones.

The connection between engine and bracket is modelled through bolted joints, shown in **Figure 60**: the bolts head are modelled with 1D deformable element (RBE3) in order to restrict degree of freedom without adding further stiffness to the FEM model (see red spider webs). Instead, bolts stem are modelled with 1D solid circular section beam element (see blue lines). The screws characteristics are shown in **Table 66**.

Table 66. Screw's characteristics.

Screw Properties	
Class	8.8
Diameter (D)	10 [mm]
Yield Stress (σ_y)	640 [MPa]

Each screw is pretensioned with a force (i.e., F_{pre}) defined by the following **Equation 96**:

$$F_{pre} = 0.6 \cdot \sigma_y \cdot A = 0.6 \cdot \sigma_y \cdot \frac{\pi \cdot D^2}{4} \approx 30160\ N \tag{96}$$

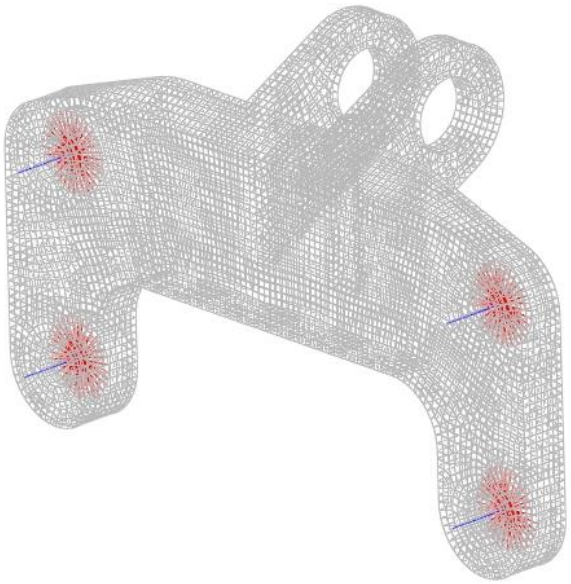

Figure 60. Bolt joints representation.

The load is applied to zone C as a pressure vector (according to the global system in **Figure 59**); one component in x-direction (longitudinal), the second one in y-direction (lateral), and the latter component in z-direction (vertical). By assumption, the pressure load is calculated considering a static distribution of the engine mass on each bracket used for mounting the engine to the cradle (i.e., F_{eng}) and multiplying this result by load coefficients consistent with the case study. Finally, the resultant forces are divided by the load application surface (i.e., the crowns where the bolts heads are placed, S_{cr}, equal to 265 mm^2) (**Equations 97-100**). The engine mass must be consistent with the vehicle used for the case study simulation (in this case, a vehicle with a V4 engine):

$$m_{eng} = 100{\sim}150\ kg \rightarrow\ m_{eng} = 150\ kg \tag{97}$$

$$F_{eng} = \frac{m_{eng}}{4} \cdot g \approx 375\ N \tag{98}$$

$$\begin{cases} F_x = 0.5 \cdot F_{eng}\ \approx 190N \\ F_y = 0.5 \cdot F_{eng} \approx 190N \\ F_z = 1.5 \cdot F_{eng} \approx 570N \end{cases} \tag{99}$$

$$\begin{cases} p_x = \dfrac{F_x}{4 \cdot S_{cr}}\ \approx 0.18\ MPa \\ p_y = \dfrac{F_y}{4 \cdot S_{cr}} \approx 0.18\ MPa \\ p_z = \dfrac{F_z}{4 \cdot S_{cr}} \approx 0.55\ MPa \end{cases} \tag{100}$$

The y-directional motion of zone A (i.e., where the connection between engine bracket and engine is made) is prohibited. Finally, in zone B (i.e., the link between engine cradle and bracket) a cylindrical constraint is applied, locking the displacements respect to the axial and radial axes.

Considering that data characterizing the generic solution S_i are provided in terms of single values (according to the TR approach), the methodology applies such data in the FEM simulations straightforwardly. **Table B.19** and **Table B.20** in Appendix D show design data of materials and processes available for EMB case study (with material, shape, & process compatibility matrices).

The environmental analysis step performs the LCA of all feasible simulations S_i obtained from the design analysis, calculating the environmental level EI. The reference vehicle on which the FU (i.e., EMB) is assumed to be installed is the VOLKSWAGEN Golf 2.0 TSI GTI combustion engine, with a life-distance of 150,000 km; the engine bracket lifetime is assumed equal to the one of the vehicle (no substitution during operation is assumed). As described in a previous section (*2.2.2 - Environmental modelling)* the system boundaries include the following life cycle phases: materials production, component manufacturing, use stage and EoL treatments. **Table 67** provides car technical features, instead **Table B.21** and **Table B.22** in Appendix D show environmental impacts of materials and processes available for the case study.

Table 67. EMB Case Study - List of vehicle features inputs.

Vehicle Features Inputs	
Feature	**Value**
Vehicle Mass	1355 [kg]
Vehicle Lifetime	150000 [km]
Vehicle Class	C
Powertrain	ICEV
Driving Cycle	WLTP
CO_2 Consumption	149 [g/km]

The economic analysis step performs the LCC of all feasible simulations S_i obtained from the design analysis and assessed in environmental analysis, calculating the economic level CI. As described in a previous section (*2.2.3 - Economic modelling*), the system boundaries include all life cycle phases (i.e., materials production, component manufacturing, use stage and EoL treatments). The economic batch size (B) chosen for FU is 5000 pieces, and the fraction of time for which the equipment is productive (i.e., the load factor (L)) is set to 0.5 (or 50%), fixed for all processes available in the production database. In the same way, the capital write-off time is equal for all processes. **Table 68** provides economic features, instead **Table B.23** and **Table B.24** in Appendix D show economic impacts of materials and processes available for the case study.

Table 68. EMB Case Study - Economic features inputs.

Economic Features Inputs	
Feature	**Value**
Batch Size	5000 [pc.]
Load Factor	50 [%]
Capital Write-off Time	5 [yr.]
EoL Grid-Mix	EU-28
Fuel Price	1.8 [EUR/l]

3.4.3 First Classification

Once the Design and Sustainability analysis is performed for the EMB design solutions, the PSL is calculated through PI, EI, and CI indexes. After the first elasticity screening, the first ranking of the acceptable alternatives is occurred.

The PSL calculation step performs the calculation of the PSL by a weighted sum formula to combine the weights of criteria with the performance/sustainability scores for each design alternative (section 2.3.1 – *PSL calculation*). The PSL scale factor (K) assumed for the EMB case study is equal to 10.

The first elasticity screening step identifies all design solutions that are acceptable from an elasticity perspective. Since the EMB case study is defined considering a TR approach with ARB scenario, such a screening is performed by means of ELV and acceptability threshold (AT). For this reason, ELV is assumed by designer equal to 1 (that means a structural integrity level (PI) equal to 2), while AT is calculated according to **Table 21**, where all alternatives that have less than 25% of ELV vertical line are rejected and they are not considered in the first ranking.

The first ranking step provides that the PSL values related to the acceptable solutions are compared; such a ranking is performed directly by means of the value of PSL of each solution, according to traditional approach (see **Equation 74**).

3.4.4 Optimization

In the optimization phase the acceptable solutions S^{acc}_{i} (TR approach) obtained from the first elasticity screening are optimized, to improve the PSL without compromising the mechanical performance (e.g., structural integrity) of the analyzed design solutions. The primary shape typology chosen during the screening phase is three-dimensional (3D); thus, the methodology will work on the solutions using the Structural Optimization. Starting from given EMB volume and the boundary condition data (loads, constraints, etc., as shown in **Figure 59**), the numerical framework of structural optimization allows to obtain fully or partially automated design solution, that provide the best performance in relation with a user-defined goal and given design constraints (e.g., structural or manufacturing). Topology Optimization (TO) is chosen as structural optimization framework in DeSA.

In this context, the EMB geometry (already developed in *Design and Sustainability Analysis – 2.2*) is meshed, and the designed loads and structural BCs are applied to the meshed model (remaining unaltered when passing from one solution to another). In order to perform the FEM optimization, the elements of the EMB model are designated as falling within one of two categories reported here (see **Figure 61**):

- Design space (DS): elements in which the element density (ρ_{el}) can vary within the topology optimization and may potentially be removed or altered for the final design.
- Non-design space (NDS): elements which remain unchanged during the optimization procedure (typically the locations where BCs, loads, or other constraints are applied).

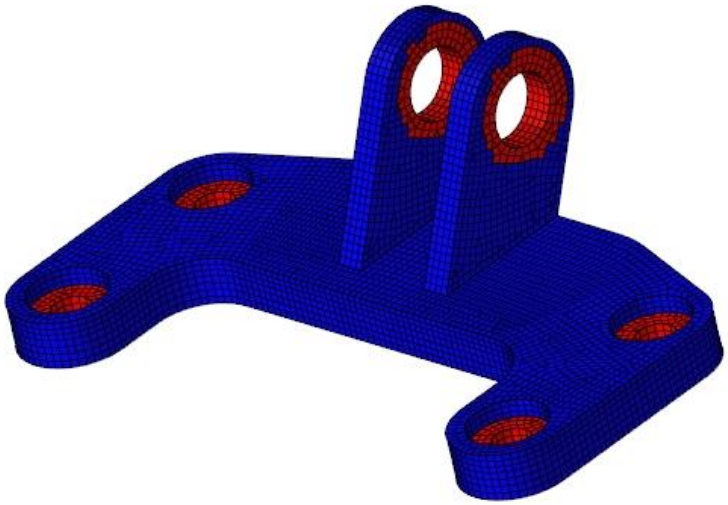

Figure 61. Representation of Design Space (DS – blue elements) and Non-Design Space (NDS – red elements) in EMB case study.

Since the design approach chosen by the designer is Traditional (TRA), the physical and mechanical properties that characterize materials of all acceptable solutions are already defined in the design analysis in terms of specific values (**Table 28** reports an overview of the required input data for the FEM optimization, in TRA approach). Therefore, the methodology works as follows:

- In the TR approach the framework explores straightforwardly the generic i-th acceptable solution S^{acc}_i through a FEM simulation. The acceptable solution S^{acc}_i is already determined during FEM modelling in Design Analysis, thus:

$$S_i^{acc} = S_i = S_i(G, BC, MAT_i)$$

- For each acceptable solution S^{acc}_i so identified in the previous simulation modelling step, the optimization simulation is performed through the combined use of MATLAB and Altair HyperWorks simulation software; the solver used in this phase is Optistruct. The optimization problem for each solution is formulated according to the following strategy, (already reported in **Table 29**): mass minimization as the main objective of the topology optimization, applying a strength constraint to optimization problem (as lower bound respect to yield strength (σ_y) of specific material).

- After the optimization simulations are performed, the main steps are the outcomes extraction and the component shape reconstruction to use in the next and final methodology phase (Final Classification). The methodology envisages the following steps, according to the modelling framework reported in **Table 31** to **Table 33**:

    - Writing .dens and .out files for each acceptable solution S^{acc}_i submitted to the optimization phase. The .dens file presents the list of elements with the fictitious density value (ρ^{el}) obtained from the topology optimization (**Table 31**). The .out file presents, in the form of a table, the percentage of elements having a specific density range (**Table 32**).
    - Extracting data from .dens and .out files just obtained.
    - Writing density matrix (P) and calculating mean density vector ($\bar{\rho}$). The density matrix (P) is calculated from the .dens files by extracting the data for each sub-solution (**Table 31**). The mean density vector ($\bar{\rho}$) is obtained by averaging the density values over the j-th element (see **Equation 77**).
    - Writing density range matrix (T) and calculating mean range vector ($\bar{\tau}$) relative to density ranges. In this case, the density range matrix (T) is obtained from the .out files by extracting the data for each sub-solution; then, the average range vector ($\bar{\tau}$) is calculated as the mean of the percentage values over the density ranges (10), according to the **Equation 78** (**Table 32**).
    - Setting a density threshold value (THR), chosen by the designer considering the mean range vector ($\bar{\tau}$) calculated and using the following rule:

$$T_{des}^{el}\ such\ that: \sum_{r=1}^{r} \overline{\tau_r^{el}} \cong T_{des}^{el} \rightarrow r \rightarrow THR$$

    T^{el}_{des} represents the percentage of elements that the designer wants to remain in the optimized shape reconstruction; the methodology extracts the density range (r) for which the cumulative sum of the components of the vector $\bar{\boldsymbol{\tau}}$ is equal to T^{el}_{des} (as shown in **Equation 79**). Finally, THR is obtained considering the density range (r) extracted.
    - Output extraction, obtaining the elements that respect the designer-defined THR. The threshold is compared with the values present in the mean density vector ($\bar{\rho}$); if the generic value of the vector is greater than THR, the j-th element respects the constraint imposed by the designer, otherwise the element is discarded and not considered in the shape reconstruction.

- The elements thus obtained from the previous phase will be used to create a new FEM model following the optimization results. The methodology, based on the results obtained from the data extraction phase, automatically reconstructs the component geometry (as shown in **Figure 24**). Then, the designer will use this reconstructed model to redesign **MANUALLY** the geometry (based on this new information and suggestions) and to re-prepare the FEM model. This model will be used in the final stage of the methodology, i.e., the final classification.

3.4.5 Final classification & Results

Once the Optimization is performed for the acceptable solutions S_i, the final classification phase is carried out by means of the following steps: Design and Sustainability Re-Analysis and final PSL calculation. After the final elasticity screening, the final ranking of the acceptable and optimized alternatives is occurred.

The final PSL calculation step performs the calculation of the PSL always using a weighted sum formula to combine the weights of criteria with the performance/sustainability scores for each design alternative (as already shown in section 2.3.1). The PSL scale factor (K) assumed for the case study is the same used in the previous paragraphs.

The final elasticity screening step identifies all design and optimized solutions that are acceptable from an elasticity perspective. Since the EMB case study is defined considering a TR approach with ARB scenario, the screening is performed by means of ELV and acceptability threshold (AT) already defined previously: ELV is assumed equal to 1 (that means a structural integrity level (PI) equal to 2), while AT is calculated according to **Table 21**. The alternatives that have less than 25% of ELV vertical line are rejected and they are not considered in the final ranking.

The final ranking step provides that the PSL values related to the acceptable and optimized solutions are compared; such a ranking is performed directly by means of the value of PSL of each solution, according to traditional approach (see **Equation 80**).

3.4.6 Results & Discussion

Table 69 reports the 13 solutions generated in the screening phase, satisfying both design requirements (imposed by designer) and are technically feasible.

Table 69. EMB Case Study - List of solutions created in the first screening phase (IN); outcomes obtained through First Elasticity Screening and First Ranking.

EMB Solutions List – BEFORE OPTIMIZATION						
ID	**Design Solution ID**	**PSL^{IN}**	**EL^{IN}**	**PSL^{IN}_{rank}**	**First Elasticity Screening**	**First Ranking**
1	1_Solid_M1_CA1	18.46	1.67	18.46	OK	4
2	2_Solid_M2_CA1	53.35	0.11	53.35	NO	No Rank
3	3_Solid_M3_CA1	21.71	0.34	21.71	NO	No Rank
4	4_Solid_M4_CA1	41.57	-0.28	41.57	NO	No Rank
5	5_Solid_M1_DE1	177.22	1.67	177.22	OK	2
6	6_Solid_M2_DE1	194.17	0.11	194.17	NO	No Rank
7	7_Solid_M3_DE1	109.85	0.34	109.85	NO	No Rank
8	8_Solid_M4_DE1	294.26	-0.28	294.26	NO	No Rank
9	9_Solid_M5_DE1	41.75	0.95	41.75	OK, With AT	3
10	10_Solid_M1_PO1	187.89	1.67	187.89	OK	1
11	11_Solid_M2_PO1	204.81	0.11	204.81	NO	No Rank
12	12_Solid_M3_PO1	112.84	0.34	112.84	NO	No Rank
13	13_Solid_M4_PO1	299.72	-0.28	299.72	NO	No Rank

As always, a Design Solution ID is defined for generic design alternative as a combination of shape (primary component shape defined by the designer – 1D, 2D, or 3D), material (MAT_{ID}), and process (PR_{ID}) (see **Table 65**).

Considering that generic i-th solution S_i is defined in terms of material single values (i.e., TR approach), it is explored straightforwardly through a FEM simulation. Looking at the list of solutions, 4 out of 13 solutions (≈30% respect the total number of design alternatives) comply with the first elasticity screening, subdivided in two groups:

- Solutions with low deterioration, that present the reduction of EL_i between 5% and 25% respect to ELV line (see yellow lines in **Table 69**);
- Solution with improvement, that present EL_i greater than ELV line (see green lines reported in **Table 69**).

The solutions analyzed in the design and sustainability analysis phase are represented through points in the PSL-EL point chart of **Figure 62**.

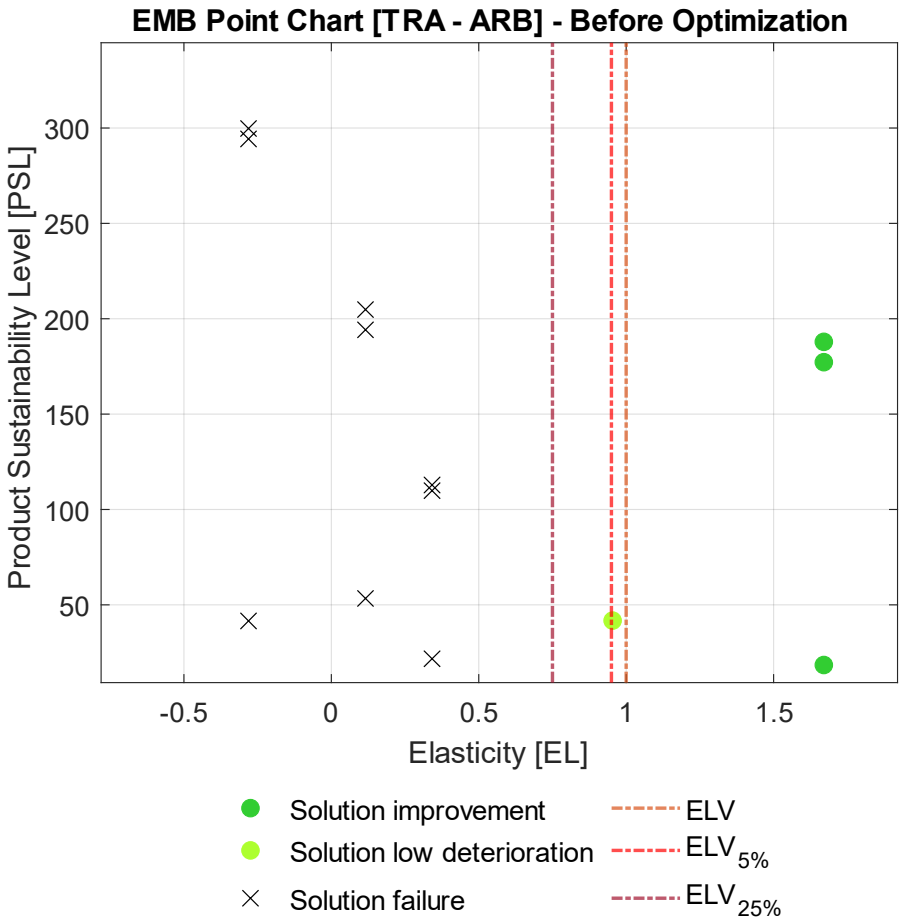

Figure 62. Engine bracket point chart (with AT) before the Optimization phase. Cross points represent discarded solutions.

The full-acceptable solutions S^{acc}_i (or solutions with improvement) are those identified by points whose area is entirely to the right of the ELV line – green points in **Figure 62**). On the other hand, the partially-acceptable solutions S^{acc}_i (or solutions with great deterioration) are those identified by points whose area is between 0% and -5% lines of reduction –

according to **Table 21** - respect to ELV (in light green points in **Figure 62**). In this context, the unique partially-acceptable solution is the solution with ID = 9. The other solutions (those that have the point area to the left of the -25% line of reduction respect to ELV) are not acceptable and therefore they are rejected. In this case, no solution is present in this typology. Moreover, **Table 69** reports PSL_{rank} for all acceptable design options, also including the first ranking; the best acceptable solution results to be the one identified by ID = 10.

Next, the acceptable solutions S^{acc}_i obtained from the first elasticity screening will be optimized to improve the product PSL without compromising the mechanical performance. The type of primary shape chosen during the screening phase is three-dimensional (3D); thus, the methodology will work on the solutions S^{acc}_i using the Structural Optimization.

After the optimization simulations are performed, the main steps are the EMB outcomes extraction, thus the EMB component shape reconstruction to use in the Final Classification, where the indexes described in the DeSA (i.e., PI^{OPT}, EL^{OPT}, EI^{OPT}, CI^{OPT}) are calculated and used for final PSL calculation. According to the modelling framework reported in **Table 30** to **Table 33**, the ".dens" and ".out" files for each acceptable solution S^{acc}_i submitted to the optimization phase are written and extracted. The density matrix (P) and the mean density vector ($\bar{\rho}$) are calculated; the first one from the ".dens" files by extracting the data for each solution, the second one by averaging the density values over the j-th element (**Equation 77**). The same operation in performed for the density range matrix (T) and the mean range vector ($\bar{\tau}$) relative to density ranges; the first one is obtained from the ".out" files by extracting the data for each solution, the second one by averaging the percentage values over the j-th element (**Equation 78**). **Table 70** reports the mean range vector ($\bar{\tau}$) relative to density ranges of EMB acceptable solution S^{acc}_i. Therefore, the density threshold value (THR) is chosen by the designer considering the mean range vector ($\bar{\tau}$) shown above and using the following rule:

$$T_{des}^{el}\ such\ that: \sum_{r=1}^{r} \overline{\tau_r^{el}} \cong T_{des}^{el} \rightarrow r \rightarrow THR$$

Table 70. EMB Mean range vector obtained from outcomes extraction phase.

Mean Range Vector ($\bar{\tau}$)		
Density Range	**Avg Solution Value [%]**	**Cumulate Sum [%]**
0.0 - 0.1	99.34	99.34
0.1 - 0.2	0.44	99.78
0.2 - 0.3	0.14	99.92
0.3 - 0.4	0.045	99.965
0.4 - 0.5	0.018	99.983
0.5 - 0.6	0.017	100
0.6 - 0.7	0	100
0.7 - 0.8	0	100
0.8 - 0.9	0	100
0.9 - 1.0	0	100
	Total Sum	100

The percentage of elements that the designer wants to remain in the optimized shape reconstruction (T^{el}_{des}) is defined equal to approximately to 99%; thus, the methodology

extracts the density range (r) for which the cumulative sum of the components of the vector $\bar{\tau}$ is equal to 99%, i.e., THR = 0.05. The THR value is compared with the values present in the mean density vector ($\bar{\rho}$); if the generic value of the vector is greater than THR, the j-th element respects the constraint imposed by the designer, otherwise the element is discarded and not considered in the shape reconstruction (as already shown in **Table 33**).

The elements thus obtained from the previous phase will be used to create a new FEM model following the optimization results. In this phase, the methodology, based on the results obtained from the data extraction phase, automatically reconstructs the EMB geometry (as shown in **Figure 63.a**). Then, the designer will use this reconstructed model to redesign **MANUALLY** the geometry (based on this new information and suggestions) and to re-prepare the FEM model. **Figure 63.b** illustrates the FEM model of the EMB, reconstructed based on the methodology suggestions and used in the Final Classification.

Figure 63. Optimized EMB FEM model; model automatically created by the methodology (left side); model reconstructed by the designer (right side).

Table 71 and **Table 72** report the 4 solutions analyzed in the Optimization phase and assessed through the final screening stage, satisfying both design requirements and are feasible from a technical perspective.

Considering that generic i-th solution $S^{acc}{}_i$ is defined in terms of material single values (i.e., TR approach), it is explored with N^{acc} solutions $S^{acc}{}_i$ (where i = 1, ..., N_{acc} - the number of acceptable solutions obtained from first elasticity screening), each of which was modelled through a FEM simulation.

Table 71. EMB Case Study - List of solutions created after the Optimization phase (OPT); outcomes obtained through Final Elasticity Screening and Final Ranking.

EMB Solutions List – AFTER OPTIMIZATION						
ID	**Design Solution ID**	**PSL^{OPT}**	**EL^{OPT}**	**$PSL^{OPT}{}_{rank}$**	**Final Elasticity Screening**	**Final Ranking**
1	1_Solid_M1_CA1	16.98	1.44	16.98	OK	4
5	5_Solid_M1_DE1	188.55	1.44	188.55	OK	2
9	9_Solid_M5_DE1	39.66	0.78	39.66	OK, With AT	3
10	10_Solid_M1_PO1	201.44	1.44	201.44	OK	1

Table 72. EMB Case Study - List of solutions compared before (IN) and after (OPT) the Optimization.

EMB Solutions List – COMPARISON BEFORE/AFTER OPTIMIZATION					
ID	**Design Solution ID**	**PSL^{IN}_{rank}**	**PSL^{OPT}_{rank}**	**$\%PSL_{rank}$**	**Final Ranking**
1	1_Solid_M1_CA1	18.46	16.98	-8.02%	4
5	5_Solid_M1_DE1	177.22	188.55	6.39%	2
9	9_Solid_M5_DE1	41.75	39.66	-5.01%	3
10	10_Solid_M1_PO1	187.89	201.44	7.21%	1

Therefore, all solutions - 100% respect the total number of design alternatives - comply with the final elasticity screening, subdivided in two main groups:

- Solutions with great deterioration, that present the reduction of EL_i between 5% and 25% respect to ELV line (see yellow lines in **Table 71** and **Table 72**);
- Solution with improvement, that present EL_i greater than ELV line (see green lines reported in Table 71 and **Table 72**);

All solutions analyzed in the design and sustainability re-analysis phase are represented again through points in the PSL-EL point chart of **Figure 64**.

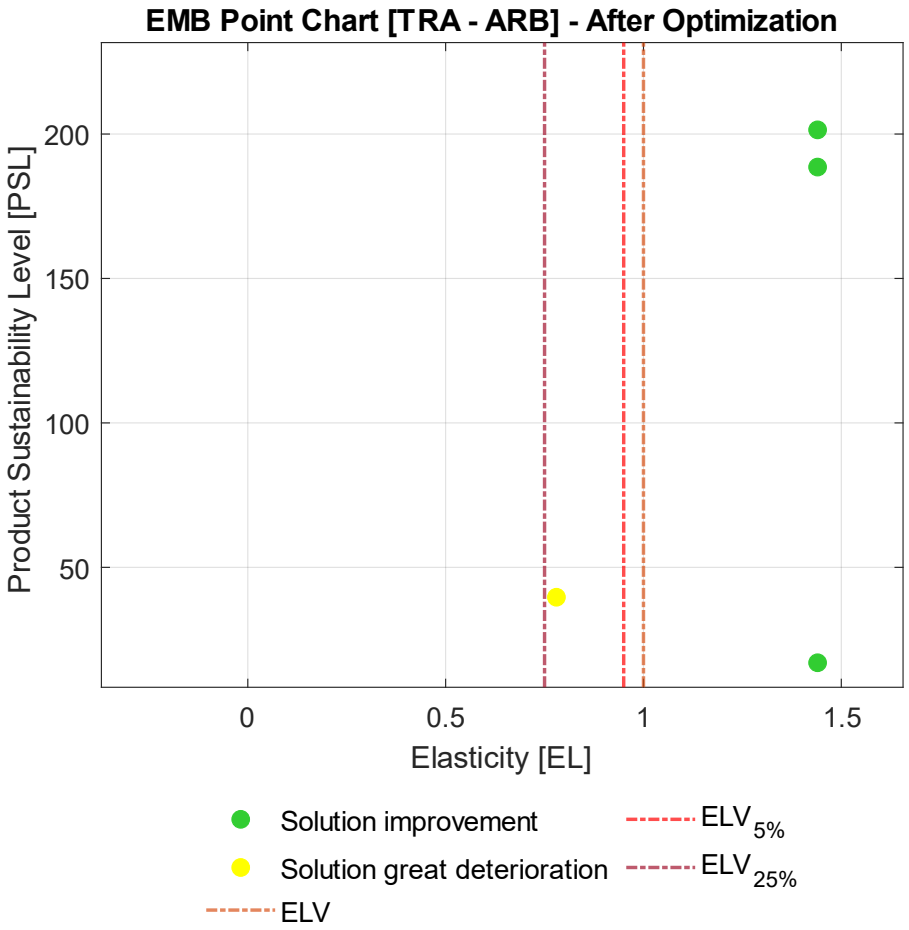

Figure 64. Engine bracket point chart (with AT), after the Optimization phase. Cross points represent discarded solutions.

The full-acceptable and optimized solutions $S^{acc/opt}_i$ (or solutions with improvement) are those identified by points whose area is entirely to the right of the ELV line – green points in **Figure 64**). On the other hand, the partially-acceptable and optimized solutions $S^{acc/opt}_i$ (or solutions with great deterioration) are those identified by points whose area is between -5% and -25% lines of reduction respect to ELV (in yellow). The other solutions (those that have the point area to the left of the -25% line of reduction respect to ELV) are not acceptable and therefore they are rejected. However, despite the optimization no solution is present in this typology.

Moreover, Table 71 reports PSL_{rank} for all acceptable and optimized design alternatives, including the final ranking. For this reason, the best acceptable and optimized solution results to be the one identified by ID = 10 (the same as before optimization).

The methodology finally calculates the improvement (or worsening) of each acceptable solution S^{acc} obtained during the first classification and further analyzed in Optimization and Final Classification phases (see **Table 72**). We see that the analyzed solutions' improvement is between -5% and 7%; moreover, the elasticity (EL) presents values greater than the arbitrary value (i.e. ELV = 1) – except the optimized solution with ID = 9. This implies that several acceptable and optimized design alternatives S^{acc} presented a reduction of PSL, without compromising their mechanical performance.

The solutions analysis is based on the integrated single score index PSL, as well as the specific sustainability indexes (PI, EI, and CI).

Regarding the Sustainability Level, **Figure 65** (*left*) shows the outcomes of PSL^{IN} for all EMB solutions considered acceptable during the first ranking.

Figure 65. EMB Case Study – PSL of all best solutions, before (IN) and after (OPT) the Optimization.

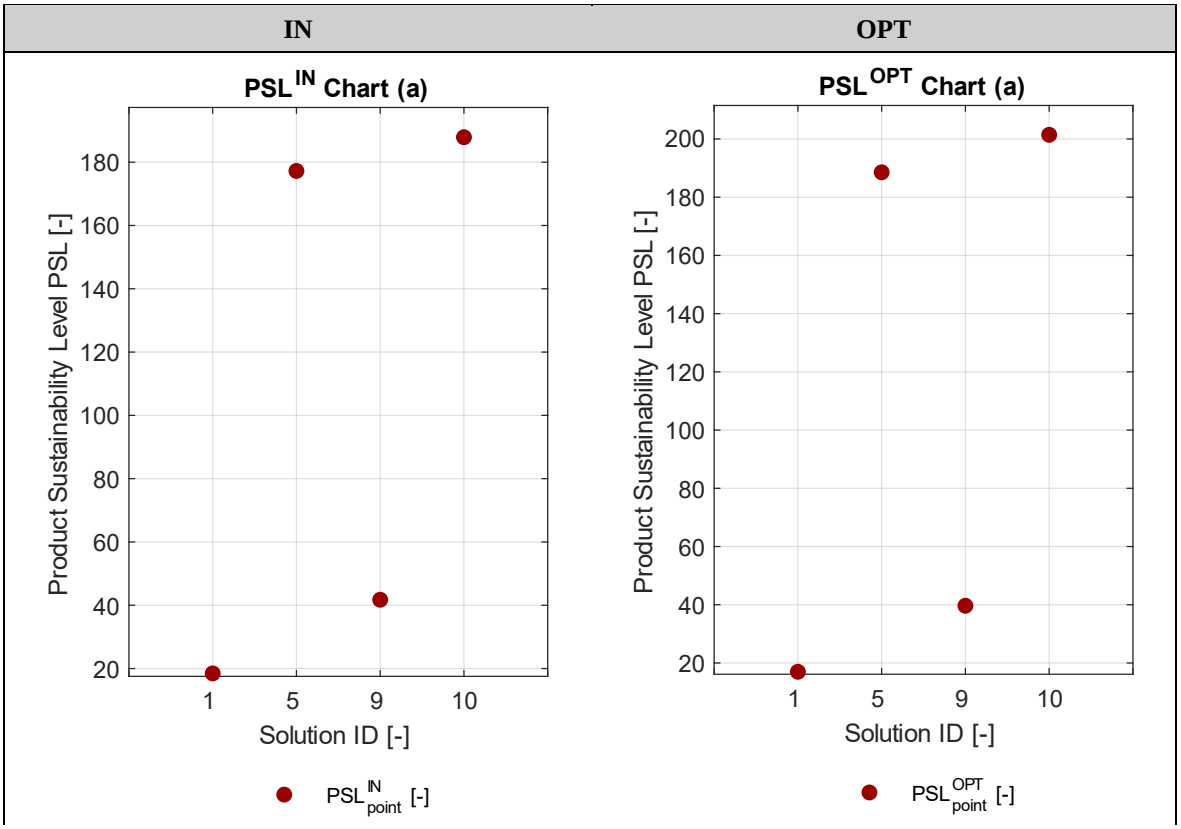

It is interesting to highlight that the best design option (ID = 10) results preferably compared to the other solutions considered (highest respect the other solutions). Moreover, 2 out of 4 solutions present an PSL^{IN} value higher than the value of the other solutions (see green points in **Figure 62** and red points in **Figure 65** (*left*)). Instead, the design alternatives with ID = 1 and 9 present a PSL value lower than the other solutions considered: concerning the first one, it presents the high manufacturing COST (i.e., Investment Casting - CA1) due to lowest lifespan respect to the other processes. The second one is defined by material that presents the highest values in CC and COST material data (i.e., Titanium Alloys – M5).
Another relevant outcome of the EMB case study is that all acceptable solutions (except one) have high PI ranges; i.e., the elasticity (EL^{IN}) presents higher values than the limit value (ELV = 1). This clearly indicates a significant margin for improvement in the lightweight perspective (starting point for the Optimization phase). Indeed, reducing component mass would certainly provide beneficial effects not only on the environment (decrease of CC in all LC stages), but also in terms of the overall sustainability level (an increase of PSL_{rank}). The solution with ID = 9 represents an exception; indeed, reducing excessively the component mass would provide beneficial effects in terms of the overall sustainability level (an increase of PSL^{IN}_{rank}), but compromising the mechanical performance (in this case, structural integrity). However, it is considered an acceptable solution thanks to AT.
Figure 65 (*right*) shows the outcomes of PSL^{OPT} for all EMB solutions considered acceptable during the final ranking. It is interesting to stress that the best design option (ID = 10) results preferably when considering the value of the range (higher respect the other solutions) even after the optimization. Moreover, 2 out of 4 solutions present an optimized PSL^{OPT} value higher than the value of the other solutions (see green points in **Figure 64** and red points in **Figure 65** (*right*)). Again, the design alternatives with ID = 1 and 9 present optimized PSL value lower than the other solutions considered: the first one is due to the high manufacturing COST (i.e., Investment Casting - CA1) linked to the minimal lifespan. The second one is made by a material that presents the highest values in CC and COST material data (i.e., Titanium Alloys – M5).
Another relevant outcome of the EMB case study is that all acceptable and optimized solutions (except one) still have high PI ranges; i.e., the elasticity (EL^{OPT}) presents higher values than the limit value (ELV = 1). This clearly indicates a margin for further improvement in the lightweight perspective, reducing component mass and providing beneficial effects in terms of the overall sustainability level (an increase of PSL_{rank}). The solution with ID = 9 represents the exception; however, even if the mass reduction provided beneficial effects in terms of the overall sustainability level, but partially compromising the mechanical performance, it is still considered an acceptable solution thanks to AT.

On the contrary, the outcomes of the study change considering design, environmental and economic points of view, separately (PI, EI and CI indexes). In this context, **Figure 66** reports the bar charts for PI before and after the Optimization phase.
Before the Optimization, all solutions (except the solution – ID = 9) present a PI^{IN} value which is entirely above the ELV arbitrary imposed by the designer (see red dotted line in **Figure 66** (*left*)). According to AT, the analyzed solutions present EL values greater than the best AT condition (i.e., EL greater than ELV), thus resulting the full-acceptable design options (solutions with improvement). Interestingly, the solution with ID = 1 (the fourth in the first ranking of **Table 69**) presents a PI value equal to the best acceptable solution in PSL perspective (solution with ID = 10 in **Figure 66** (*left*)), thus resulting the design option with an optimal PI level. As a consequence, where the EMB case study is carried out according

to a traditional design perspective, the high value of PI equal to all other solutions, make that the solution with ID = 1 appears to be profitable. It is worthy to be noticed the solutions (except ID = 9) result over-dimensioned when being evaluated through the DeSA, thus resulting in a greater values of PI^{IN} and in a lower value of PSL^{IN}_{rank} (**Table 69**).

Figure 66. EMB Case Study - PI of all solutions, before (IN) and after (OPT) the Optimization.

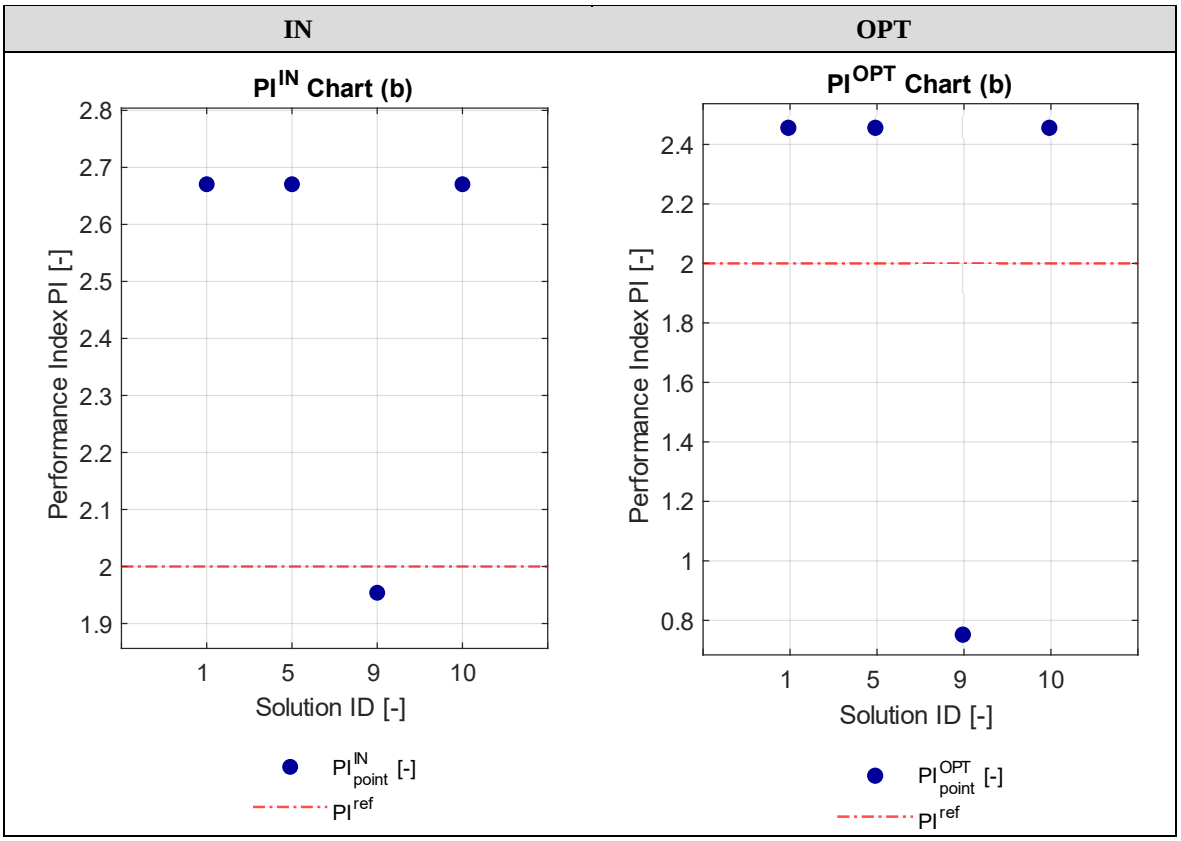

After the Optimization, all solutions (except the solution ID = 9) present a PI^{OPT} value entirely above the ELV arbitrary imposed by the designer (see red dotted line in **Figure 66** (*right*)). According to AT, the optimized solutions present EL^{OPT} values greater than the best AT condition (i.e., EL greater than ELV), thus resulting the full-acceptable design options (solutions with improvement). The solution with ID = 1 (the fourth in the final ranking of **Table 71**) presents a PI value equal to the best acceptable solution in PSL perspective (solution with ID = 10 in **Figure 66** (*right*)), thus resulting the design option with an optimal PI level. As a consequence, the high value of PI equal to all other solutions, make that the solution with ID = 1 appears to be profitable. The solutions (except the solution with ID = 9) result still over-dimensioned even after the optimization phase, thus resulting in a greater values of PI^{OPT} and in a lower value of PSL^{OPT}_{rank}.

Figure 67.a reports the EMB point charts for EI before and after the Optimization phase; whereas **Figure 67.b** shows all LC phases in environmental perspective, considering raw material, manufacturing, use, and EoL.

Figure 67. EMB Case Study – EI(a) and LC(b) of all solutions, before (IN) and after (OPT) the Optimization.

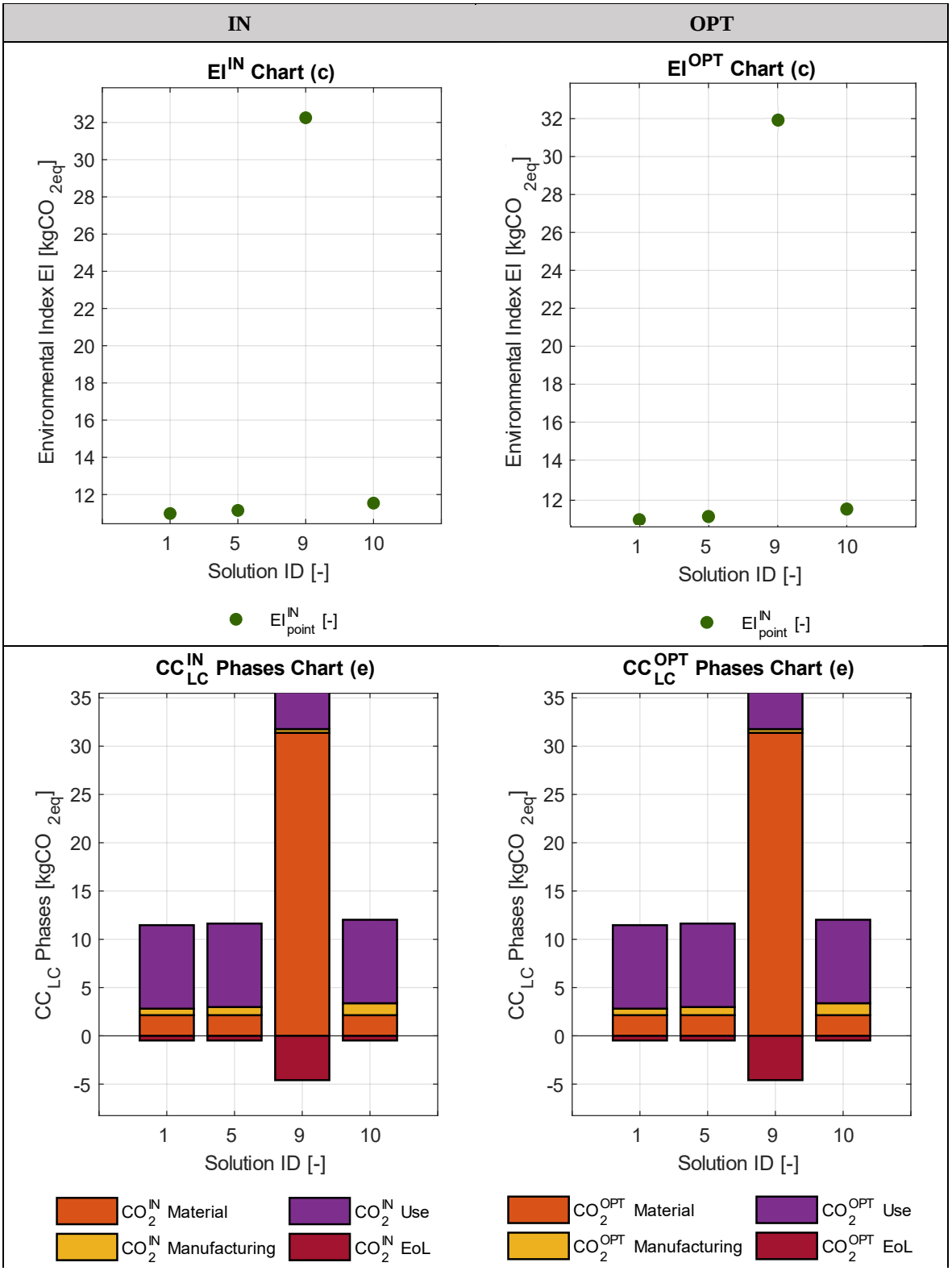

Before the Optimization, all solutions (except the solution ID = 9) provide the best environmental performances, as shown in **Figure 67.a** (*left*). In this regard, the critical discussion of EI^{IN} values stresses two main key-points. The first one is that EI^{IN} varies minimally when passing from one solution to another (range: 10 $kgCO_{2eq}$ < EI^{IN} < 12

$kgCO_{2eq}$); the second point is that the solution with ID = 9 presents EI^{IN} much greater respect to other solution (approximatively, 32 $kgCO_{2eq}$). The main reasons for this are reported here:

- Considering all solutions (except the solution with ID=9), the use stage covers the vast majority of total CC_{LC} (approximately 80%), and the impact is the almost the same for the alternatives (9 $kgCO_{2eq}$), since the base material being steel (same density ranges, see **Table B.19**) for each of those (use stage modelled on a mass basis, as provided by section *2.2.2 – Environmental Modeling*). This implies that also CC_{EoL} is more or less the same for all options (see the red bars in **Figure 67.b** (*left*)). Moreover, the values of EI^{IN} are due to materials and manufacturing phases, but the lower variability in CC inventory data and the relatively lesser influence on total CC_{LC} (it does not exceed 20% of total for alternatives) make EI^{IN} small.
- Considering in detail the solution with ID = 9, the use stage always covers a part of total CC_{LC} (approximately 15%), and the impact is lower than the other alternatives (5 $kgCO_{2eq}$), since the base material being Titanium (M5). According to the use stage modelled on a mass basis, the impact in the use stage is due to the density of the material considered. Instead, the value of EI^{IN} is also due to materials and manufacturing phases, but in this case the vast CC specific impact regarding the raw material (see Titanium Alloys (M5) in **Table B.21**), taking almost the 75% of total and making that the final value for EI^{IN} much greater than the other solutions analyzed (**Figure 67.b** (*left*)). This implies that also CC_{EoL} is greater respect the other options (see the red bars in figure).

After the Optimization, all solutions (except the solution – ID = 9) provide the best environmental performances, as shown in **Figure 67.a** (*right*), highlighting the partial reduction of environmental impact through optimization of the solutions considered. In this regard, the critical discussion of EI^{OPT} values stresses two main key-points. The first one is that EI^{OPT} varies minimally when passing from one solution to another (range: 9 $kgCO_{2eq}$ < EI^{OPT} < 10 $kgCO_{2eq}$); the second point is that the solution with ID = 9 presents EI^{OPT} much greater respect to other solution (approximatively, 30 $kgCO_{2eq}$), but however a decreased environmental impact thanks to the optimization. The main reasons for this are reported here:

- Considering all optimized solutions (except the solution with ID=9), the use stage covers the vast majority of total CC_{LC} (approximately 80%), and the impact is the almost the same for the alternatives (7.7 $kgCO_{2eq}$), since the base material being steel (same density ranges, see **Table B.19**) for each of those (use stage modelled on a mass basis, as provided by section *2.2 – Environmental Modeling*). This implies that the environmental impact of use stage ($CO^{OPT}{}_{2eq}$ Use) is reduced approximately of 11% respect to impact before the optimization. Moreover, CC_{EoL} is more or less the same for all options (see the red bars in **Figure 67.b** (*right*)). Finally, the EI^{OPT} values are due to materials and manufacturing phases, but the lower CC inventory data and the relatively lesser influence on total CC_{LC} (it does not exceed 20% of total for alternatives) make the final range for EI^{OPT} small.
- Considering in detail the solutions with ID = 9, the use stage always covers a part of total CC_{LC} (approximately 15%), and the impact is lower than the other alternatives (4.5 $kgCO_{2eq}$), since the base material being Titanium (M5). According to the use

stage modelled on a mass basis, the impact in the use stage is due to the density of the material considered. This implies that the environmental impact of use stage (CO^{OPT}_{2eq} Use) is reduced approximately of 10% respect to impact before the optimization. Instead, the value of EI^{OPT} is also due to materials and manufacturing phases, but in this case the vast CC specific impact regarding the raw material (see Titanium Alloys (M5) in **Table B.21**), taking almost the 75% of total and making that the final value for EI^{OPT} much greater than the other solutions analyzed – even if the mass reduction is obtained during the optimization - (**Figure 67.b** (*left*)). This implies that also CC_{EoL} is greater respect the other options.

Finally, **Figure 68.a** shows the point charts for CI before and after the Optimization; **Figure 68.b** reports instead all LC phases in economic perspective (raw material, manufacturing, use, EoL, respectively).

Figure 68. EMB Case Study – CI(a) and LC(b) of all solutions, before (IN) and after (OPT) the Optimization.

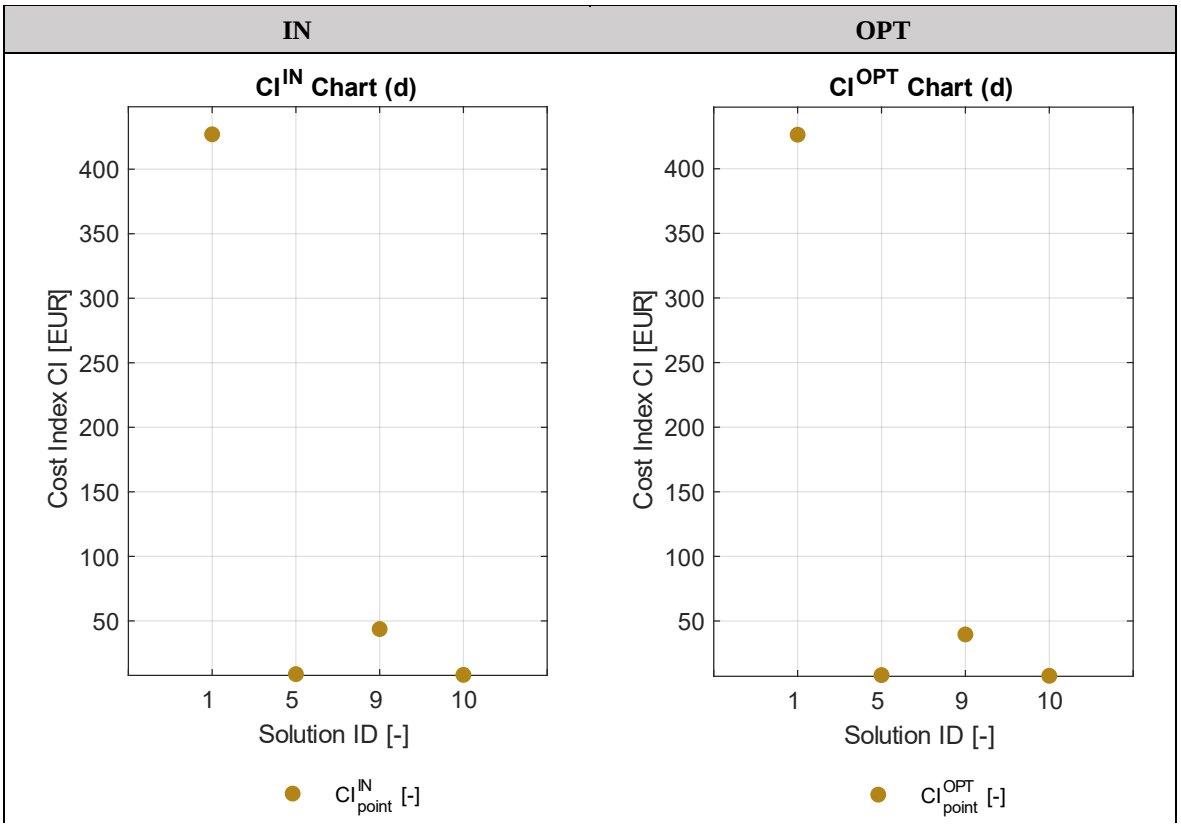

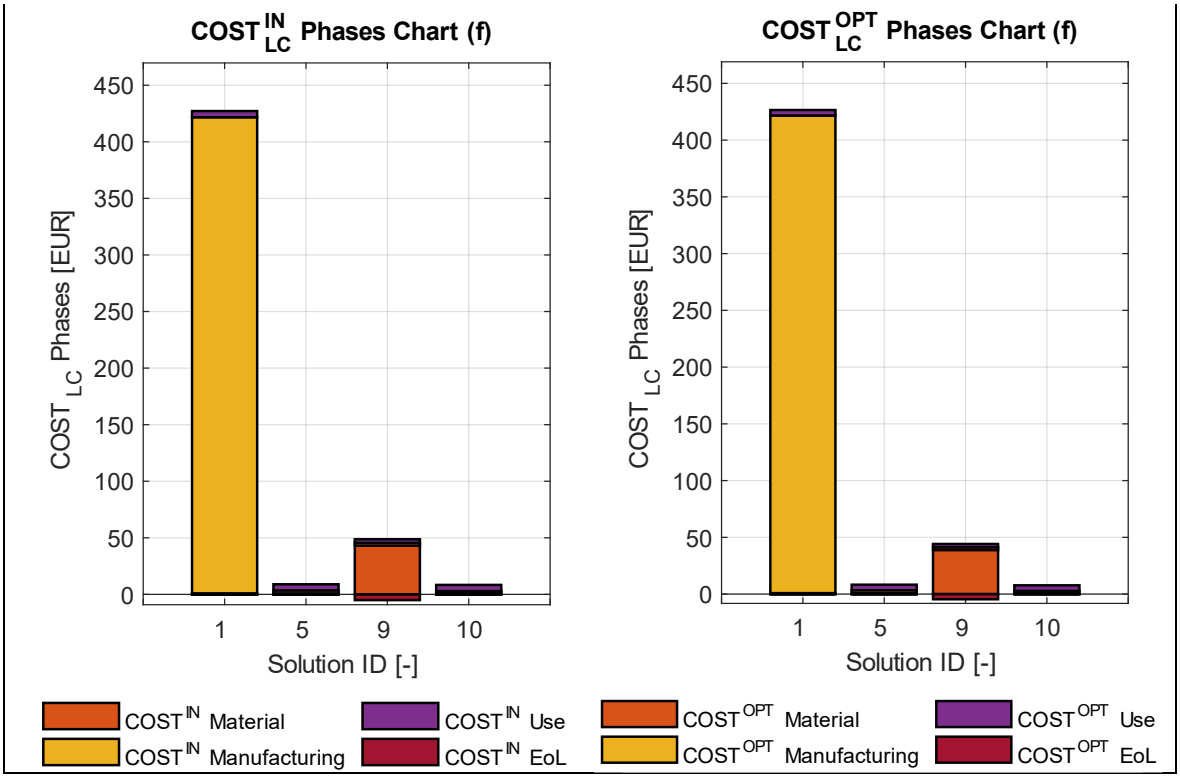

Before the Optimization, all solutions (except the solution – ID = 1) provide the best economic performances, as shown in **Figure 68.a** (*left*). In this regard, the critical discussion of CI^{IN} values stresses two main key-points. The first one is that CI^{IN} varies minimally when passing from one solution to another (range: 10 EUR < CI^{IN} < 45 EUR); the second point is that the solution with ID = 1 presents CI^{IN} much greater respect to other solution (approximatively, 430 EUR). The main reasons for this are reported here:

- Considering the solutions with ID = 5 and 10, the use stage covers the majority of total $COST_{LC}$ (approximately between 62% and 66%), and the cost is the almost the same for the alternatives (5 EUR), since the base material being steel (same density ranges, see **Table B.19**) for each of those (use stage modelled on a mass basis, as provided by section *2.2.3 – Economic Modeling*). This implies that also $COST_{EoL}$ is more or less the same for all options (see the red bars in **Figure 68.b**(*left*)). Moreover, the values of CI^{IN} are due to materials and manufacturing phases, but the lower value in COST inventory data and the relatively lesser influence on total $COST_{LC}$ (not exceed 38% of total for alternatives) make the final range for CI^{IN} small.
- Considering in detail the solutions with ID = 1 and 9, the use stage always covers a minimal part of total $COST_{LC}$ (approximately between 1% and 6%), and the cost is lower than the other alternatives (3-5 EUR). According to the use stage modelled on a mass basis, the impact in the use stage is due to the density of the materials considered. Instead, the value of CI^{IN} is also due to materials and manufacturing phases: for the first solution, the vast COST specific cost regards the manufacturing stage (see Investment Casting (CA1) in **Table B.24**), taking almost the 98% of total and making that the final value for CI^{IN} much greater than the other solutions analyzed (**Figure 68.b** (*left*)). Concerning the second solution, the high COST specific cost regards the raw material stage (see Titanium Alloys (M5) in **Table**

B.23), taking almost the 98% of total and making that the final value for CI^{IN} much greater than the other solutions analyzed.

After the Optimization, all solutions (except the solution – ID = 1) provide the best economic performances, as shown in **Figure 68.a** (*right*); however, highlighting the partial reduction of economic cost through optimisation of the solutions considered. In this regard, the critical discussion of CI^{OPT} values stresses two main key-points. The first one is that CI^{OPT} varies minimally when passing from one solution to another (range: 7 EUR < CI^{OPT} < 39 EUR); the second point is that the solution with ID = 1 presents CI^{OPT} much greater respect to other solution (approximatively, 420 EUR), but however a decreased cost thanks to the optimization. The main reasons for this are reported here:

- Considering the optimized solutions with ID = 5 and 10, the use stage covers the majority of total $COST_{LC}$ (approximately between 60% and 65%), and the cost is the almost the same for the alternatives (4.5 EUR), since the base material being steel (same density ranges, see **Table B.19**) for each of those (use stage modelled on a mass basis, as provided by section *2.3 – Economic Modeling*). This implies that the economic cost of use stage ($COST^{OPT}_{2eq}$ Use) is reduced approximately of 10% respect to impact before the optimization. This implies that also $COST_{EoL}$ is more or less the same for all options (see the red bars in **Figure 68.b** (*right*)). Moreover, the values of CI^{OPT} are due to materials and manufacturing phases, but the lower value in COST inventory data and the relatively lesser influence on total $COST_{LC}$ (it does not exceed 38% of total for alternatives) make that the final range for CI^{OPT} is small – thanks to the optimization (**Figure 68.b** (*right*)).
- Considering in detail the solutions with ID = 1 and 9, the use stage always covers a minimal part of total $COST_{LC}$ (approximately between 1% and 6%), and the cost is lower than the other alternatives (2-4.5 EUR). According to the use stage modelled on a mass basis, the impact in the use stage is due to the density of the materials considered. Instead, the value of CI^{OPT} is also due to materials and manufacturing phases: for the first solution, the vast COST specific cost regards the manufacturing stage (Investment Casting (CA1) in **Table B.24**), taking almost the 98% of total and making that the final value for CI^{OPT} much greater than the other solutions analyzed (**Figure 68.b** (*right*)). Concerning the second solution, the high COST specific cost regards the raw material stage (Titanium Alloys (M5) in **Table B.23**), taking almost the 98% of total and making that the final value for CI^{OPT} much greater than the other solutions analyzed – even if the mass reduction is obtained during the optimization.

4. Conclusions

The present work is aimed to propose an innovative framework assisting designers in the early product development phase of single mono-material automotive components. The methodology considers both design and sustainability pillars (i.e., environment and economy) at the same time and on the same level of importance starting from:

- physical features and load case of the specific automotive component to design
- functional and structural requirements
- available LC inventory data in terms of materials and manufacturing processes to be investigated
- vehicle features of the specific automotive component to design (ICEV and BEV)

From a practical point of view, the framework automatically generates different concept solutions evaluated through design and sustainability indicators, aggregated within a single score index based on MCDA methods; thus, the ranking and the choice of the most promising design option(s) are carried out. The conceived eco-design framework is developed within a computer-modeling tool in an integrated HyperWorks/MATLAB simulation environment.

Below, the study's conclusions are summed up; starting from a "State of Art" and "Materials & Methods" summaries, the framework/tool's utility is described evidencing the enhancements to existing literature and possible future developments.

- **Review of existing State of Art.** For the automotive field, the focus is to define novel design solutions through dedicated eco-design methodologies, which consider mechanical performance and sustainability pillars at the same level of importance, evaluated under the entire LC perspective.
  Thus, LCSA has been considered a suitable approach for assessing product sustainability in the early design phase based on considerations related to the whole LC. Such a methodology compares quantitatively different product concepts, provides insights about rooms for improvement, and transparently describes the potential trade-off.
  The implementation of LCSA brings the adoption of MCDA methods which support product developers and designers to solve decision-making problems when a series of alternatives are evaluated based on multiple criteria and alternatives. Different MCDA methods exist and are used in automotive contexts, such as the Weighted Sum Method, Analytical Hierarchy Process, TOPSIS, VIKOR, ELECTRE, and PROMETHEE.
  For these reasons, the faculty of combining different sustainability criteria and ranking alternatives makes the integration of life cycle thinking methodologies (LCA, LCC, and S-LCA) and MCDA a promising research area.
  A general State of Art (SoA) review is conducted considering the following topic: "Ecodesign methods/tools (EDM/T) in the automotive sector". Literature offers an extensive series of papers dealing with eco-design within the automotive field, which vary significantly in terms of objective, type, complexity, and availability of inventory data. Most of these researches apply sustainability analysis as a supporting tool functional to validate lightweight designs. The aspects of sustainability (economy, environment, and society) and the design dimension are considered, as well as MCDA methods (that can link together all of these dimensions) and lightweight perspective.
  Concerning the design dimension and lightweighting, several studies present a framework for designing automotive components from a weight reduction perspective.

Indeed, the most widely used optimization technique is Topology optimization (TO), which is carried out to reduce the structure's weight without compromising the intended performance. In this context, the reviewed papers perform topological optimization of various lightweight solutions (such as vehicle transmission, steering knuckle, engine parts, and vehicle Body-in-White parts). However, no relevant reference is made to the sustainability aspects, and the concept LW alternatives are obtained according to the classical design approach.

Considering the environmental pillar, from the SoA review, it is evident that most papers deal with LCA analysis from a lightweighting perspective, highlighting that environmental sustainability is a topic discussed in the scientific community and by companies in the automotive industry. In this context, several studies perform detailed assessments of the considered car assets, assuming different impact categories to express the final outcomes and including all LC stages (production, use, and EoL). That said, no reference is made to the performance and design requirements of the considered components since the concept alternatives are analyzed on the assumption that they are rigorously equivalent from a functional perspective.

Regarding the economic perspective, few papers uniquely discuss the economic aspect, dealing with components that generally use the LC cost model focused on manufacturing and developing their studies according to two perspectives: manufacturer and user. In other cases, the user perspective is assumed, and the component acquisition cost represents the whole production stage. In contrast, in other studies, the direct production expenditure is summed up to the use stage and EoL. Also, considering the lightweight perspective, LCC is used to compare traditional materials for a given component with innovative and lightweight ones to evaluate the component manufacturing costs and the expected use stage cost reduction due to mass saving. As said for the environmental pillar, no reference is made to the performance aspects in the considered papers; the concept alternatives analyzed are economically assessed on the assumption that they are rigorously equivalent from a functional perspective.

Several product-oriented S-LCA studies targeted to the automotive sector were found and reviewed, covering applications related to vehicle components/parts, alternative fuels, materials for automotive parts, automotive shredder residue treatment, and manufacturing technology. Yet, the analysis of the sector-specific publications from social sustainability perspective currently does not allow for fully tailoring the conceptual map to the automotive sector due to the limited sample. However, it provides directions about some of the nodes of the conceptual map, in particular regarding system boundaries, indicators, and stakeholders.

Integrating environmental and economic pillars with the standard requirements in product design is gaining vital importance for many companies. Several authors attempt to provide a clear and transparent framework to calculate the LCA and LCC of a given product, process, or system. Very few examples of combined LCC and LCA exist in the literature for the automotive sector; the two methodologies are defined on the same goal and scope settings, but the final results are presented separately (without integration of the several outcomes using MCDA methods).

Many papers presented in SoA refer to applicative eco-design case studies, where the assessment is performed according to the principles of LCSA methodology. Thus, substantial focus in eco-design literature is represented by developing reliable methods and tools ready for application to real case studies, considering all sustainability pillars integrated through MCDA methods. In this context, several articles are concerned with the above aspects: many studies refine holistic assessment methods that integrate overall sustainability pillars (i.e., environmental, economic, and social) in a single-score

indicator through the application of MCDA methods. From the analysis of these papers, it is clear that the overall sustainability analysis is carried out downstream of the design process. Moreover, it is performed only to validate alternative solutions whose conception/development has already been finalized (i.e., they are rigorously equivalent from a functional perspective). With these considerations, few studies strive to integrate the sustainability aspect within the design process through a systematic computer-aided design procedure. They present an approach implemented in a software framework that supports the designers in optimizing component-based automotive solutions from a lightweight eco-design perspective. The advanced methods are based on the integration of CAE, LCM, and LCA tools, which directly connect with the CAD environment. The frameworks assist product developers in conceiving different design alternatives obtained as a combination of material, shape, and manufacturing process through structural optimization tools. That said, the studies above represent exciting attempts to systematically orient design towards sustainability targets. However, such methods are functional only to assist the designer in generating optimized solutions; the conception phase and the data processing do not take place automatically since the advanced tools cannot generate alternative design options on their own.
From the review of existing SoA that deal with the automotive eco-design, the following key considerations emerge, emphasizing the limits and weaknesses of existing literature:

- Several study define several methodologies that deal with the sole design perspective, which is used to optimize solutions without considering the sustainability perspective;
- the vast majority of papers is represented by applicative case studies that deal with the sole sustainability issue (i.e., environment, economy, society), which is used to validate solutions already finalized and defined from a performance point of view;
- a limited number of applicative LCSA case studies consider both design and sustainability pillars, but results are provided separately for the different aspects, without a proper evaluation of the effects that innovative solutions involve on the integrated design/sustainability profile;
- few papers deal with the development of eco-design methods targeted at investigating different design options, but both concept generation and modelling process are not carried out through an automated procedure.

- **Materials & Methods.** Given these gaps in the literature, the proposed methodology develops an innovative eco-design framework for assisting designers in the early development phase of mono-material automotive components. The overall methodology is implemented within an automated simulation tool developed in MATLAB/Hypermesh environment and it is composed by the following four main phases:

  - **Screening**. In this section, the generation of all the alternative design solutions that satisfy design requirements and are feasible from a technological point of view (feasible solutions) is performed.
    The starting point is creating and developing the production database, providing all possible design solutions obtained as a combination of material and manufacturing technology. The database includes all materials and processes that are available to the designer, structured in two major sections: materials (organized into classes belonging to macro-families - metals, polymers, glasses/ceramics, and hybrids materials), and manufacturing technologies

(classified into a hierarchical order and characterized in terms of the following features - applicable materials, applicable primary shapes, and process properties related to the component to be designed).
The next step of the screening phase is the designer's definition of the following design constraints: primary shape constraint (Prismatic-1D, Sheet-2D, Three-dimensional-3D) and process constraints (i.e., the requirements on physical and technological features which characterize the specific case study).
Thanks to design constraints and the designer-provided production database, the screening of possible design solutions is carried out. Primary shape (chosen by the designer - constant input), materials and manufacturing processes (provided by production database – variable inputs), and process constraints (provided by the case study) are combined to perform the screening, thus obtaining all the feasible solutions. Consequently, all the alternatives that do not meet the design requirements or are not technologically feasible are discarded. The final output of the screening is the list of the feasible solutions identified as a permitted "material-shape-process" combination.

- **Design and Sustainability analysis**. In this phase, the description of the design, environmental and economic pillars, and the definition of related mid-point indicators (obtaining the acceptable solutions) is made. It is structured in three main sections which deal with design, environmental, and economic aspects.
In the *design analysis*, the Finite Element Method (FEM) simulation modelling is applied to all feasible solutions provided by the screening. The FEM analysis is aimed at assessing the design performance by means of a tailored indicator which quantifies the specific service provided by the different solutions. For the setting of FEM analysis, the framework requires that the designer characterizes the case study by providing the component Geometry (G) and the component Boundary Conditions (BCs). The model meshing is done on the component geometry, and the designed loads and structural boundary constraints (i.e., BCs) are applied on the meshed model; G and BCs remain unaltered when passing from one solution to another.
For the development of the design analysis phase, two approaches are defined and developed in the methodology, depending on the information available to the designer (see **Table 73**):

Table 73. Two typologies of design approach developed in DeSA methodology.

Design Approach	
Traditional Approach (TRA)	**Exploratory approach (EXA)**
Physical and mechanical properties are expressed by means of single (and constant) values.	Physical and mechanical properties are expressed through variability ranges (min-max ranges).

The TR approach (TRA) is straightforward: specify the properties in FE model and launch the simulation of generic i-th solution S_i (obtained as a feasible combination of material-shape-process in the screening phase). Instead, EX approach (EXA) provides properties in terms of variability ranges; thus, the framework explores the generic i-th solution S_i with N_i sub-solutions S_{ij} (j =1, …, N_i), each of which has to be modelled through a FEM simulation. The

number of required FEM simulations strongly depends on the specific case study; N_i is determined using the range sizes of different material properties (through the LHS method).
Regardless the approach, the design performance is assessed by means of a tailored indicator representative of service levels accomplished by the product, named Performance Index (PI) and defined as the ratio between the reference or arbitrary service levels (user-defined, depending on the case study) and the service levels on the component calculated through the FEM simulations. Two scenarios are defined in the methodology, depending on the information available to the designer (see **Table 74**).
To quantify the distance (or the over-dimensioning) of the generic solution S_i (or sub-solution S_{ij}) with respect to reference or arbitrary value, the methodology defines the Elasticity (EL), which expresses the potential to lighten a solution without compromising the mechanical performance.

Table 74. Two typologies of design scenario developed in DeSA methodology.

Design Scenario	
Arbitrary scenario (ARB)	**Reference scenario (REF)**
The solutions S_i (or sub-solutions S_{ij}) are analyzed defining a designer-defined scenario.	The solutions S_i (or sub-solutions S_{ij}) are analyzed using an existing reference scenario

In the ***Environmental analysis***, the feasible solution S_i (or S_{ij}) provided by the design analysis are evaluated respect to the environmental profile, named Environmental Index (EI), which evaluation is carried out through the LCA methodology by means of the Climate Change (CC). The CC is determined taking into account the overall component LC, defined according to the following main stages: materials (raw materials extraction and production up to the manufacturing of the semi-finished products), manufacturing (manufacturing processes required to convert the semi-finished products into the final component), use (production of energy consumed during operation and exhaust air emissions), EoL (disposal of EoL components and materials, including reuse, recycling, or energy recovery). The CC calculation framework involves an environmental characterization of all solutions (obtained in the design analysis), carried out by means of an environmental database which provides all the input data needed for the sustainability assessment. This database is subdivided in two sections: Use/EoL setting parameters, specific impact values.
In the ***Economic analysis***, the feasible solution S_i (or S_{ij}) provided by the design analysis (and evaluated respect to environmental profile) are analyzed respect to the economic aspect, named Cost Index (CI), which evaluation is carried out through the LCC methodology by means of cost indicator (COST). The COST is developed taking into account the overall component LC, according to the following main stages: materials (materials and feedstocks acquisition cost and production cost up to the manufacturing of the semi-finished products), manufacturing (manufacturing processes cost required to convert the semi-finished products into the final component), use (contribution of propulsion system and the contribution of externalities as pollutant emissions during operation), EoL (disposal of EoL components and materials, including

component reuse and recycling). The COST calculation framework involves an economic characterization of all solutions (obtained in the design analysis stage), performed through an economic database which provides all the input data needed for the assessment. This database is subdivided in three sections: use/EoL setting parameters, manufacturing cost values, specific cost values.
Once the Design and Sustainability analysis is performed for the solutions S_i (or S_{ij}), the first classification phase is carried out by means of the following steps: PSL calculation, elasticity screening and first ranking.
In the *PSL calculation*, the PSL index is calculated based on MCDA methods. The evaluation is performed by means of three main steps (normalization, weighting, and aggregation), which varies according to the scenario and approach chosen by the designer (i.e., ARB and REF, TRA and EXA, respectively). Regardless of the type of design approach, in the arbitrary scenario (ARB) the normalization is performed through the "Max method", which provides that design and sustainability indexes are normalized using the maximum value obtained from each index. Instead, in the reference scenario (REF) the normalization is performed through a method similar to the "Max method", where the design and sustainability indexes are normalized using the values coming from the existing reference solution. As regards the weighting, an equal weight is assigned to all indexes, since it is assumed that all elements have the same level of importance. In the score aggregation step, the normalized data are systematically aggregated into a single score using the weights and the normalized indexes defined above.
In the *First Elasticity screening*, the list of acceptable design solutions (S^{acc}), defined as all solutions that at the same time satisfy elasticity requirements and are feasible from a technological point of view, is identified. The application of this phase varies depending on the information available to the designer, i.e., if the materials (as well as manufacturing process, etc…) considered in the production database are specific (TR approach) or ranges-defined (EX approach), and if the design scenario is designer- or reference-defined (ARB scenario and REF scenario, respectively) (See **Table 75**).

Table 75. Possible combinations of approaches (TRA, EXA) and scenarios (ARB, REF) defined in the DeSA methodology.

Approaches/Scenarios Combinations		
	Arbitrary Scenario (ARB)	Reference Scenario (REF)
Traditional Approach (TRA)	TRA - ARB	TRA - REF
Explorative Approach (EXA)	EXA - ARB	EXA - REF

In the *First ranking* phase, the PSL values of the acceptable solutions are compared, and the ranking is compiled. The solutions that do not pass the elasticity screening step are not taken into account in this phase. Also in this case, this phase varies depending on the information available to the designer, i.e., if the data considered in the production database are specific- (TR approach) or ranges-defined (EX approach).

- **Optimization**. In this phase, the optimization of all the acceptable alternative design solutions that still satisfy design requirements and are feasible from a technological point of view (acceptable and optimized solutions) is conducted. The purpose is to improve the product PSL, without compromising the mechanical performance of the analyzed design solutions. Depending on the primary shape (PS), the methodology will work on the solutions differently; two options are defined in the methodology:

    - Parameter modification (1D/2D shapes): the methodology will accomplish the variation of one or more geometric parameters in order to calculate the sustainability indexes. The outcomes are sent DIRECTLY to the final screening (in Classification phase) since the geometry is already modified to obtain above indexes.
    - Structural optimization (3D shapes): the numerical framework of Topology Optimization allows to obtain fully or partially automated design solution in relation with a user-defined goal and given design constraints. The outcomes are extracted, and the SUGGESTED shape is automatically created from the methodology. Thus, the designer will have to redesign the model based on this new information and suggestions and re-prepare the FEM model (used as input for the Classification phase).

- **Classification**. Finally, once the Optimization is performed, in this phase the calculation of PSL index and final ranking of optimized competing design alternatives are made. Design and Sustainability Re-Analysis, final PSL calculation, final elasticity screening and final ranking are the main steps.
  In *Design and Sustainability Re-Analysis*, the feasible and optimized design solutions obtained in the Optimization phase are evaluated once again by means of the aggregated single-score indicator PSL, performing a holistic assessment where both design performance and sustainable profiles are considered. This section is structured in three main sections identical to the *Design and Sustainability Analysis* phase (which deal with design, environmental, and economic aspects respectively), but applied to feasible and optimized solutions provided by the Optimization. The framework requires that the designer characterizes the case study by providing the component Geometry (G) and the component Boundary Conditions (BCs). In this case G is obtained through the shape reconstruction step (performed in the Optimization phase). Thus, the model meshing is done on the new geometry (G^{opt}), while the designed loads and structural boundary constraints (i.e., BCs) are applied on the meshed model. G^{opt} and BCs remain unaltered when passing from one solution to another.
  In the *Final PSL calculation*, the optimized PSL index is calculated based on MCDA methods. The evaluation is performed always by means of three main steps (normalization, weighting, and aggregation), which varies according to the scenario and approach chosen by the designer (i.e., ARB and REF, TRA and EXA, respectively). In the arbitrary scenario (ARB) the normalization is performed through the "Max method", providing that indexes are normalized using the maximum value came from each index. In the reference scenario (REF) the normalization is performed through a method similar to the "Max method", where the indexes are normalized using the values coming from the existing reference solution. Concerning the weighting, an equal weight is assigned to all indexes; in the score aggregation step, the normalized data are systematically

aggregated into a single score using the weights and the normalized indexes defined above.

In the *Final Elasticity screening*, the list of acceptable and optimized design solutions ($S^{acc(opt)}$), defined as all optimized solutions that at the same time satisfy elasticity requirements and are feasible from a technological point of view, is identified. The application of this phase varies depending on the information available to the designer, i.e., if the data considered in the production database are specific (TR approach) or ranges-defined (EX approach), and if the design scenario is designer- or reference-defined (ARB scenario and REF scenario, respectively) (See **Table 75**).

In the *Final ranking phase*, the PSL values of the acceptable and optimized solutions are compared, and the final ranking is compiled. The solutions that do not pass the final elasticity screening step are not taken into account in this phase. Also in this case, this phase varies depending on the information available to the designer, i.e., if the data considered in the production database are specific- (TR approach) or ranges-defined (EX approach). Moreover, this section calculates the improvement (or worsening) of each acceptable solution obtained during the first classification and further analyzed in Optimization and Final Classification phases, defining the percentage variation between the initial condition of solution (before the optimization) and the optimized one (after optimization).

- **Enhancements with respect to existing literature, utility and possible future developments of the tool/framework.** In the light of:

    - criticisms of current LCSA practices
    - review of DeSA framework and operation

  the enhancements of the research with respect to existing literature are illustrated below. The conceived method is characterized by the following main features:

    - the methodology automatically generates a series of design alternatives starting from physical features, load cases and functional/structural requirements, directly provided by the designer;
    - the alternatives are subject to a simultaneous and integrated design/sustainability assessment by means of dedicated indexes. The final ranking and the choice of the most promising design option(s) are carried out on the basis of an overall single score obtained through MCDA methods;
    - the framework is implemented within an automated simulation tool, specifically developed to be easily adaptable to objectives and constraints of whichever case study, as well as easily usable by professionals of the automotive industry. The added value of the conceived tool is enabling designers to clearly identify potentialities and criticalities of the considered alternatives, thus representing a valuable support for decision-making in the eco-design field.

  That said, the main limitations of the methodology are reported below. The framework is characterized by the following limits:

- a relevant amount of inventory data (production database: environmental and economic data on materials and manufacturing processes) are needed;
- the environmental and economic assessments take into account only primary processes (secondary and joining processes are not included);
- the social assessment is not considered due to the limited information available (as said during the SoA review);
- only one MCDA method (i.e., the "Max" method) is used when integrating the various indices defined in the framework.

The utility of the research is located within the context of Design for Sustainability (DfS), more specifically the branch “Design for Energy Efficiency” (DfEE). The conceived framework investigates three aspects of automotive use stage which are strictly connected to each other, the energy, economy, and environment.

Since a thorough design phase requires that recommendations coming from Design for environment and energy efficiency are corroborated by a series of interconnected aspects such as manufacturability, material usage, durability, reliability and recyclability, the contribution of the framework/tool can be intended as incorporating sustainability issues into design optimization together with the selection process of materials and technologies when developing lightweight design solutions.

The possible end-users of the tool are represented by practitioners in the context of automotive light-weighting (automotive designer, as well as environmental consultants, research centers, universities) and OEM’s that want to assume the sustainability concern as a driver of design process.

Possible future developments of the work can be outlined following three distinct fronts: extension to secondary and joining processes in the environmental and economic assessment, the integration with Social Life Cycle Assessment (S-LCA) analysis, and the implementation of several MCDA methods. The first point would give a comprehensive overview on the environmental and economic potentialities of light-weighting within the automotive context. For the second point, the integration of social instruments (together with environmental and economic pillars) would allow evaluating, in phase of design, aspects not only technical but equally essential; this would lead to a holistic tool able to merge design performance with the overall sustainability profile in the automotive asset. Finally, the third point would give a comprehensive overview of the different outcomes that can be obtained using different MCDA approaches in the automotive context, thus, standardizing as much as possible the results of the users of the methodology proposed in this work.

Acknowledgements

The methodology presented in this thesis was carried out in the Department of Industrial Engineering of the University of Florence.

Foremost, I would like to express my sincere gratitude to all the people working in this Department, starting from my Tutors, Prof. Eng. Massimo Delogu and Prof. Eng. Niccolò Baldanzini, for their availability and professionalism. They always found time to follow this activity despite their busy schedules.

My sincere gratitude goes to Dr. Eng. Francesco Del Pero, who supervised the activity, had a lot of patience (especially in the last weeks of writing the thesis), and allowed me to improve through peer-to-peer comparison. For these reasons, I am genuinely grateful to him. A part of this research was funded by collaboration with the fka group. The author wishes to thank all fka members for their contribution, support, and collaboration.

I am grateful to the members of the internal Ph.D. Board for the interest they had in my work, to the Students that prepared their degree thesis collaborating with me for the things I learned from them, and to my colleagues for the friendship, participation, and familiarity I experienced in these three years.

Thanks to my family and all my friends, near and far, for their support and patience throughout my Ph.D. research.

Finally, I would like to thank my girlfriend Sara: she loves me for who I am, despite my flaws, supports me in my decisions, and stands by me. My sincerest thanks go to her.

Bibliography

1. Alves, C., Ferrão, P.M.C., Silva, A.J., et al., "Ecodesign of automotive components making use of natural jute fiber composites", J Clean Prod 18 (2010): 313–327, doi:10.1016/j.jclepro.2009.10.022

2. Andriankaja, H., Bertoluci, G., Millet, P.D., "An approach to define a robust set of environmental tools for car parts manufacturer", Proceedings of the Ecologic Vehicles. Renewable Energies 26-29 March (2009). Monaco

3. Andriankaja, H., Vallet, F., Le Duigou, J., Eynard, B., "A method to ecodesign structural parts in the transport sector based on product life cycle management", J Clean Prod 94 (2015): 165–176. doi: 10.1016/j.jclepro.2015.02.026

4. Aruldoss, M., Lakshmi, T.M., and Venkatesan, V.P., "A Survey on Multi Criteria Decision Making Methods and Its Applications," Am J Inf Syst 1 (2013): 31-43, https://doi.org/10.12691/ajis-1-1-5.

5. Ashby, M.F., Materials Selection in Mechanical Design, 4th ed. (Boston: Butterworth-Heinemann, 2011)
6. Atilgan, B., Azapagic. A., "An integrated life cycle sustainability assessment of electricity generation in Turkey", Energy Policy 93 (2016): 168–186, doi: 10.1016/j.enpol.2016.02.055

7. Bachmann, TM, "Towards life cycle sustainability assessment: drawing on the NEEDS project's total cost and multi-criteria decision analysis ranking methods", Int J Life Cycle Assess 18 (2012):1698–1709. doi: 10.1007/s11367-012-0535-3

8. Barbieri, S.G., Giacopini, M., Mangeruga, V., Mantovani, S., "A Design Strategy Based on Topology Optimization Techniques for an Additive Manufactured High Performance Engine Piston", Procedia Manufacturing 11 (2017): 641-649, https://doi.org/10.1016/j.promfg.2017.07.162

9. Baroth, A., Karanam, S., McKay, R., "Life Cycle Assessment of Lightweight Noryl * GTX * Resin Fender and Its Comparison with Steel Fender", 2012 SAE World Congress, Detroit, MI, April 24 − 26; 2012

10. Baumann, H., Arvidsson, R., Tong, H., Wang, Y., "Does the Production of an Airbag Injure more People than the Airbag Saves in Traffic?", J Ind Ecol 17 (2013): 517–527, doi:10.1111/jiec.12016

11. Berzi, L., Delogu, M., Giorgetti, A., Pierini, M., 2013. On-field investigation and process modelling of End-of-Life Vehicles treatment in the context of Italian craft-type Authorized Treatment Facilities. Waste Manag. 33(4):892–906.

12. Berzi, L., Delogu, M., Pierini, M., and Romoli, F., "Evaluation of the End-of-Life Performance of a Hybrid Scooter with the Application of Recyclability and Recoverability Assessment Methods," Resour. Conserv. Recycl. 108 (2016): 140-155, https://doi.org/10.1016/j.resconrec.2016.01.013.

13. Blom, M., Solmar, C., "How to socially assess biofuels: a case study of the UNEP/SETAC Code of Practice for social-economical LCA", Master's thesis in cooperation with the division of Quality and Environmental Management at Luleå University of Technology, commissioned by Enact Sustainable Strategies in Stockholm (2009)

14. Bocoum I, Macombe C, Revéret J-P., "Anticipating impacts on health based on changes in income inequality caused by life cycles", Int J Life Cycle Assess 20 (2015): 405–417. doi:10.1007/s11367-014-0835-x

15. Braithwaite, P., "Sustainability Assessment of the Development of the New X-TYPE Jaguar", SAE International, Warrendale, PA (2001)

16. Castro, D.M. and Silv Parreiras, F., "A review on multi-criteria decision-making for energy efficiency in automotive engineering", Applied Computing and Informatics, Vol. 17 No. 1 (2021): 53-78, https://doi.org/10.1016/j.aci.2018.04.004

17. Cavazzuti, M., Costi, D., Baldini, A., Moruzzi, P., "Automotive Chassis Topology Optimization: a Comparison Between Spider and Coupé Designs", Proceedings of the World Congress on Engineering 2011, WCE 2011. 3.

18. Cecchel, S., Chindamo, D., Collotta, M., Cornacchia, G. et al., "Lightweighting in Light Commercial Vehicles: Cradle-to-Grave Life Cycle Assessment of a Safety-Relevant Component," Int J Life Cycle Assess 23 (2018): 2043-2054, https://doi.org/10.1007/s11367-017-1433-5

19. Celen, A., "Comparative Analysis of Normalization Procedures in TOPSIS Method: With an Application to Turkish Deposit Banking Market," Informatica 25, no. 2 (2014): 185-208, https://doi.org/10.15388/Informatica.2014.10

20. Chang, Y-J, Sproesser, G., Neugebauer, S., et al., "Environmental and Social Life Cycle Assessment of Welding Technologies", Procedia CIRP 26 (2015): 293–298, doi:10.1016/j.procir.2014.07.084

21. Cheah, L.W., Heywood, J., 2011. Meeting U.S. passenger vehicle fuel economy standards in 2016 and beyond. Energy Policy 2011-39:454–66.

22. Chiandussi, G., Gaviglio, I., Ibba, A., "Topology optimisation of an automotive component without final volume constraint specification", Advances in Engineering Software 35(10–11) (2004): 609-617, https://doi.org/10.1016/j.advengsoft.2003.07.002

23. Chien, J.M., McKinstry, K.C., Baek, C., Horvath, A., Dornfeld, D., "Multi-objective Analysis on Joining Technologies", Dornfeld, D., Linke, B. (eds) Leveraging Technology for a Sustainable World. Springer, Berlin, Heidelberg (2012), https://doi.org/10.1007/978-3-642-29069-5_49

24. Choudry, S.A., Kaspar, J., Vielhaber, M., Landgrebe, D., "Concurrent Assessment of Material and Joining Technology in Lightweight Engineering", Dao, D., Howlett, R.,

Setchi, R., Vlacic, L. (eds) Sustainable Design and Manufacturing 2018. KES-SDM 2018. Smart Innovation, Systems and Technologies, vol 130. Springer, Cham. https://doi.org/10.1007/978-3-030-04290-5_15

25. Choudry, SA, Kaspar, J., Alber, U., Landgrebe, D., "Integration of an Assessment Methodology for the Selection of Joining Technologies in Lightweight Engineering", Procedia CIRP 70 (2018): 217-222, https://doi.org/10.1016/j.procir.2018.02.034

26. Choudry, SA, Kaspar, J., Greinacher, F., Vielhaber, M., "A Prediction-Model for an Improved Decision-making of Joining Technologies in the Early Stage of Automobile Body Development", Procedia CIRP 80 (2019): 10-14, https://doi.org/10.1016/j.procir.2019.01.084

27. Choudry, SA, Müller, S., Alber, U., Riedel, F., Landgrebe, D., "A Multidimensional Assessment and Selection Methodology: Optimized Decision-making of Joining Technologies in Automobile Body Development", Procedia Manufacturing 21 (2018): 281-288, https://doi.org/10.1016/j.promfg.2018.02.122

28. Choudry, SA, Sandmann, S., Landgrebe, D., "A Methodical Approach for an Economic Assessment of Joining Technologies under Risk – Optimized Decision-making in Automobile Body Development", Procedia CIRP 69 (2018): 31-36, DOI:10.1016/J.PROCIR.2017.11.045

29. Chu, Y., Sun, L., Li, L., "Lightweight scheme selection for automotive safety structures using a quantifiable multi-objective approach", Journal of Cleaner Production 241 (2019): 118316, https://doi.org/10.1016/j.jclepro.2019.118316

30. Ciacci, L., Marselli, L., Passarini, F., Santini, A. et al., "A Comparison among Different Automotive Shredder Residue Treatment Processes," Int J Life Cycle Assess 15 (2010): 896-906, https://doi.org/10.1007/s11367-010-0222-1.

31. Cicconi, P., Germani, M., Landi, D., Mengarelli, M., "Life cycle cost from consumer side: A comparison between traditional and ecological vehicles", Energy Conference (ENERGYCON), 2014 IEEE International. IEEE, pp 1440–1445

32. Costa, D., Quinteiro, P., and Dias, A.C., "A Systematic Review of Life Cycle Sustainability Assessment: Current State, Methodological Challenges, and Implementation Issues," Science of the Total Environment 686 (2019): 774-787, https://doi.org/10.1016/j.scitotenv.2019.05.435

33. Cui, X., Wang, S., Hu, SJ, "A method for optimal design of automotive body assembly using multi-material construction", Materials & Design 29 (2) (2008): 381-387, https://doi.org/10.1016/j.matdes.2007.01.024
34. Cui, X., Zhang, H., Wang, S., Zhang, L., Ko, J., "Design of lightweight multi-material automotive bodies using new material performance indices of thin-walled beams for the material selection with crashworthiness consideration", Materials & Design, 32(2) (2011): 815-821, https://doi.org/10.1016/j.matdes.2010.07.018

35. Danilecki, K., Mrozik, M., Smurawski, P., "Changes in the environmental profile of a popular passenger car over the last 30 years – Results of a simplified LCA study",

Journal of Cleaner Production 141 (2017): 208-218, https://doi.org/10.1016/j.jclepro.2016.09.050

36. Das, S., “The Life-Cycle Impacts of Aluminium Body-in-White Automotive Material,” J Miner Met Mater Soc 52 (2000): 41-44, https://doi.org/10.1007/s11837-000-0173-2.
37. Das S., "Life cycle assessment of carbon fiber-reinforced polymer composites", Int J Life Cycle Assess 16 (2011):268–282, doi: 10.1007/s11367-011-0264-z

38. De Medina, "Eco-design for Materials Selection in Automobile Industry", Center for Mineral Technology (CETEM) (2006)

39. Del Duce, A., Egede, P., Öhlschläger, G., Dettmer, T., Althaus, HJ, Bütler, T., Szczechowicz, E., "eLCAr: Guidelines for the LCA of electric vehicles", 2013, DOI: 10.13140/RG.2.1.2782.8244

40. Del Pero, P., Berzi, L., Antonacci, A., and Delogu, M., “Automotive Lightweight Design: Simulation Modeling of Mass-Related Consumption for Electric Vehicles,” Machines 8, no. 3 (2020): 51, https://doi.org/10.3390/machines8030051

41. Del Pero, F., Delogu, M., Pierini, M., "The effect of lightweighting in automotive LCA perspective: Estimation of mass-induced fuel consumption reduction for gasoline turbocharged vehicles", Journal of Cleaner Production 154 (2017): 566-577, https://doi.org/10.1016/j.jclepro.2017.04.013

42. Delogu, M. , Zanchi, L., Dattilo, C.A., Pierini, M., "Innovative composites and hybrid materials for electric vehicles lightweight design in a sustainability perspective", Materials Today Communications 13 (2017): 192-209, https://doi.org/10.1016/j.mtcomm.2017.09.012

43. Delogu, M., Del Pero, F., Pierini, M., "Lightweight Design Solutions in the Automotive Field: Environmental Modelling Based on Fuel Reduction Value Applied to Diesel Turbocharged Vehicles", Sustainability 8(11) (2016): 1167, https://doi.org/10.3390/su8111167

44. Delogu, M., Del Pero, F., Romoli, F., and Pierini, M., “Life Cycle Assessment of a Plastic Air Intake Manifold,” Int J Life Cycle Assess 20 (2015): 1429-1443, https://doi.org/10.1007/s11367-015-0946-z

45. Delogu, M., Maltese, S., Del Pero, F., Zanchi, L. et al., “Challenges for Modelling and Integrating Environmental Performances in concept Design: The Case of an Automotive Component Lightweighting,” International Journal of Sustainable Engineering 11, no. 2 (2018): 135-148, http://doi.org/10.1080/19397038.2017.1420110

46. Deng, Y., Guo, Y., Wu, P., and Ingarao, G., “Optimal Design of Flax Fiber Reinforced Polymer Composite as a Lightweight Component for Automobiles from a Life Cycle Assessment Perspective,” Journal of Industrial Ecology 23 (2019): 986-997, https://doi.org/10.1111/jiec.12836

47. Dér, A., Gabrisch, C., Kaluza, A., Cerdas, F., Thiede, S., Herrmann, C., “Integrating environmental impact targets in early phases of production planning for lightweight structures”, Procedia CIRP 80 (2019): 168-173, https://doi.org/10.1016/j.procir.2019.01.077

48. Diener, D.L. and Tillman, A.-M., “Scrapping Steel Components for Recycling—Isn’t that Good Enough? Seeking Improvements in Automotive Component End-of- Life,” Resources, Conservation and Recycling 110 (2016): 48-60, https://doi.org/10.1016/j.resconrec.2016.03.001.

49. Dhingra, R., Das S., “Life cycle energy and environmental evaluation of downsized vs. lightweight material automotive engines”, J Clean Prod 85 (2014):347–358, doi:10.1016/j.jclepro.2014.08.107

50. Dubreuil, A., Bushi, L., Das, S., Tharumarajah, A., Gong, X., "A comparative Life Cycle Assessment of Magnesium Front End Autoparts", Society of Automotive Engineers (SAE) (2010), DOI: 10.4271/2010-01-0275

51. Duflou, JR, De Moor, J., Verpoest, I., Dewulf, W., "Environmental impact analysis of composite use in car manufacturing", CIRP Ann - Manuf Technol 58 (2009): 9–12, doi:10.1016/j.cirp.2009.03.077

52. Edwards, R., Hass, H., Larivè, J.F., Lonza, L., Maas, H., Rickeard, D., "Well-To-Wheels analysis of future automotive fuels and powertrains in the European context", European Commission – Joint Research Centre – Scientific and policy reports (2014)

53. Egede, P. Environmental Assessment of Lightweight Electric Vehicles; Springer International Publishing: Cham, Switzerland, 2017

54. Ekener-Petersen, E., Höglund, J., Finnveden, G., "Screening potential social impacts of fossil fuels and biofuels for vehicles", Energy Policy 73 (2014): 416–426, doi:10.1016/j.enpol.2014.05.034

55. Elghali L, Clift R, Sinclair P, et al (2007) Developing a sustainability framework for the assessment of bioenergy systems. Energy Policy 35:6075–6083. doi:10.1016/j.enpol.2007.08.036 ENLIGHT D7.2 (2016) Deliverable D

56. Fassi, H.F., Ourihi, R., and Elahrach, K., “An Integrated Method Involving Design-Manufacturing-Environment Applied in Structural Optimization,” Materials Today: Proceedings 38, no. 1 (2021): 135-138, https://doi.org/10.1016/j.matpr.2020.06.118

57. Fauzi, R.T., Lavoie, P., Sorelli, L., Heidari, M.D. et al., “Exploring the Current Challenges and Opportunities of Life Cycle Sustainability Assessment,” Sustainability 11, no. 3 (2019): 636, https://doi.org/10.3390/su11030636.

58. Ferreira, M.B., Salvador, R., Barros, M.V., Souza, J.T.D. et al., “Eco-Efficiency of the Differential Ratio Change in a Heavy-Duty Vehicle and Implications for the

Automotive Industry," Sustainable Production and Consumption 21 (2020): 145-155, https://doi.org/10.1016/j.spc.2019.12.005.

59. Feschet P, Macombe C, Garrabé M, et al., "Social impact assessment in LCA using the Preston pathway", Int J Life Cycle Assess 18(2012): 490–503. doi: 10.1007/s11367-012-0490-z
60. Finkbeiner, M., Hoffmann, R., "Application of Life Cycle Assessment for the Environmental Certificate of the Mercedes-Benz S-Class (7 pp)", Int J Life Cycle Assess 11 (2006): 240–246. doi: 10.1065/lca2006.05.248

61. Finkbeiner, M., Schau, EM, Lehmann, A., Traverso M., "Towards Life Cycle Sustainability Assessment. Sustainability 2 (2010): 3309–3322. doi: 10.3390/su2103309

62. Finnveden, G. R., Hauschild, M.Z., Ekvall, T., Guinee, J., Heijungs, R., Hellweg, S., Koehler, A., Pennington, D., Suh, D., 2009. Recent developments in life cycle assessment. Journal of Environmental Management 91(1): 1–21.

63. Foolmaun, RK, Ramjeeawon, T., "Comparative life cycle assessment and social life cycle assessment of used polyethylene terephthalate (PET) bottles in Mauritius", Int J Life Cycle Assess 18 (2012): 155–171. doi: 10.1007/s11367-012-0447-2

64. Ford, J. D., Berrang-Ford, L., Paterson, J., 2011. A systematic review of observed climate change adaptation in developed nations. Clim. Change 2011, 106 (2), 327 − 336.

65. Funazaki, A., Taneda, K., Tahara, K., and Inaba, A., "Automobile Life Cycle Assessment Issues at End-of-Life and Recycling," JSAE Rev. 24 (2003): 381-386, https://doi.org/10.1016/S0389-4304(03)00081-X.

66. Gemechu, E.D., Sonnemann, G. & Young, S.B., "Geopolitical-related supply risk assessment as a complement to environmental impact assessment: the case of electric vehicles", Int J Life Cycle Assess 22 (2017): 31–39, https://doi.org/10.1007/s11367-015-0917-4

67. Geyer, "Parametric Assessment of Climate Change Impacts of Automotive Material Substitution", Environmental Science and Technology (2008), https://doi.org/10.1021/es800314w

68. Geyer, "The impact of material choice in vehicle design on life cycle greenhouse gas (GHG) emissions", The Donald Bren School of Environmental Science and Management – University of California at Santa Barbara. LCM 2007, 27-29 August 2007, Zurich.

69. Ghadimi, P., Azadni, A.H., Yusof, N.M., and Mat Saman, M.Z., "A Weighted Fuzzy Approach for Product Sustainability Assessment: A Case Study in Automotive Industry," J Clean Prod 33 (2012): 10-21, https://doi.org/10.1016/j.jclepro.2012.05.010

70. Graedel, T. and Allenby, B., Industrial Ecology and the Automobile (Upper Saddle River, NJ: Prentice Hall, 1998)

71. Guinée JB, Heijungs R, Huppes G, et al., “Life Cycle Assessment: Past, Present, and Future”, Environ Sci Technol 45 (2011): 90–96. doi: 10.1021/es101316v

72. Guinée, J., “Life Cycle Sustainability Assessment: What Is It and What Are Its Challenges?” In: Clift R, Druckman A (eds) Taking Stock of Industrial Ecology. Springer International Publishing, pp 45–68 (2016)
73. Haji Vahabzadeh, A., Asiaei, A., Zailani, S., “Green decision-making model in reverse logistics using FUZZY-VIKOR method”, Resour Conserv Recycl 103 (2015): 125–138. doi:10.1016/j.resconrec.2015.05.023

74. Hakamada, M., Furuta, T., Chino, Y., Chena, Y., Kusuda, H., Mabuchi, M., "Life Cycle Inventory Study on Magnesium Alloy Substitution in Vehicles", Energy 32 (2007): 1352 – 1360

75. Halog A, Manik Y (2011) Advancing Integrated Systems Modelling Framework for Life Cycle Sustainability Assessment. Sustainability 3:469–499. doi: 10.3390/su3020469

76. Hapuwatte, B., Daniel Seevers, K., Badurdeen, F., Jawahir, I.S., "Total Life Cycle Sustainability Analysis of Additively Manufactured Products", Procedia CIRP 48 (2016): 376-381,https://doi.org/10.1016/j.procir.2016.03.016

77. Hawkins, T.R., Gausen, O.M. & Strømman, A.H. Environmental impacts of hybrid and electric vehicles—a review. Int J Life Cycle Assess 17, 997–1014 (2012). https://doi.org/10.1007/s11367-012-0440-10

78. Hawkins, T.R., Singh, B., Majeau-Bettez, G. and Strømman, A.H., "Comparative Environmental Life Cycle Assessment of Conventional and Electric Vehicles", Journal of Industrial Ecology, 17 (2013): 53-64. https://doi.org/10.1111/j.1530-9290.2012.00532.x

79. Helton, J.C. and Davis, F.J., “Latin Hypercube Sampling and the Propagation of Uncertainty in Analyses of Complex Systems,” Reliability Engineering & System Safety 81, no. 1 (2003): 23-69, https://doi.org/10.1016/S0951-8320(03)00058-9.

80. Hiederer, R., European Commission., Joint Research Centre., Institute for Environment and Sustainability., 2011. International reference life cycle data system (ILCD) handbook: general guide for life cycle assessment: provisions and action steps. Publications Office, Luxembourg.

81. Hunkeler, D., Lichtenvort, K., Rebitzer, G., et al., "Environmental life cycle costing", SETAC ; CRC Press, Pensacola, Fla. : Boca Raton (2008)

82. Huppes G, van Rooijen M, Kleijn R, Heijung R, de Koning A, van Oers Lauran (2004) Life Cycle Costing and the Environment. Report No. 200307074 commissioned by the Ministry of VROM-DGM for the RIVM Expertise Centre LCA.

83. Inti, S., Sharma, M., and Tandon, V., “An Approach for Performing Life Cycle Impact Assessment of Pavements for Evaluating Alternative Pavement Designs,” Procedia Engineering 145 (2016): 964-971, https://doi.org/10.1016/j.proeng.2016.04.125.

84. IPCC, 2013. Climate Change 2013: The Physical Science Basis, Working Group I Contribution to the Fifth Assessment Report of the Intergovernmental Panel on Climate Change; Cambridge University Press: Cambridge, U.K., 2013.

85. ISO 14040/14044, 2006. Environmental management – Life Cycle Assessment – Principals and framework/ Requirements and guidelines. Genew, Switzerland.

86. ITF (2015), Executive summary, in ITF Transport Outlook 2015, OECD Publishing, Paris. doi:10.1787/9789282107782-3-en

87. Jankovics, D., Barari, A., "Customization of Automotive Structural Components using Additive Manufacturing and Topology Optimization", IFAC-PapersOnLine 52(10) (2019): 212-217, https://doi.org/10.1016/j.ifacol.2019.10.066
88. Jasinski, D., Meredith, J., Kirwan, K., "A comprehensive review of full cost accounting methods and their applicability to the automotive industry", Journal of Cleaner Production 108, Part A (2015):1123-1139, https://doi.org/10.1016/j.jclepro.2015.06.040

89. Javadi, P., Yeganeh, B., Abbasi, M., and Alipourmohajer, S., “Energy Assessment and Greenhouse Gas Predictions in the Automotive Manufacturing Industry in Iran,” Sustainable Production and Consumption 26 (2021): 316-330, https://doi.org/10.1016/j.spc.2020.10.014.

90. Jeya Girubha, R., Vinodh, S., “Application of fuzzy VIKOR and environmental impact analysis for material selection of an automotive component. Mater Des 37 (2012): 478–486. doi: 10.1016/j.matdes.2012.01.022

91. Joint Research Centre, Institute for Environment and Sustainability, International Reference Life Cycle Data System (ILCD) Handbook : general guide for life cycle assessment : detailed guidance, Publications Office, 2011, https://data.europa.eu/doi/10.2788/38479.

92. Joshi, S.V., Drzal, L.T., Mohanty, A.K., Arora, S., "Are natural fiber composites environmentally superior to glass fiber reinforced composites?", Composites: Part A 35 (2004):371-376

93. Kaluza, A., Kleemann, S., Fröhlich, T., Herrmann, C., Vietor, T., "Concurrent Design & Life Cycle Engineering in Automotive Lightweight Component Development", Procedia CIRP 66 (2017): 16-21, https://doi.org/10.1016/j.procir.2017.03.293

94. Kamalakkannan, S. and Kulatunga, A.K., “Optimization of Eco-Design Decisions Using a Parametric Life Cycle Assessment,” Sustainable Production and Consumption 27(2021): 1297-1316, https://doi.org/10.1016/j.spc.2021.03.006

95. Karlewski, H., "Social Life Cycle Assessment in der Automobilindustrie", Doctoral Thesis, Technische Universität Berlin (2016)

96. Kaspar, J., Choudry, SA, Vielhaber, M., "Concurrent Selection of Material and Joining Technology – Holistically Relevant Aspects and Its Mutual Interrelations in Lightweight Engineering", Procedia CIRP 72 (2018): 780-785, https://doi.org/10.1016/j.procir.2018.03.093

97. Kaspar, J., Revfi, S., Albers, A., Vielhaber, M., "Cross-Component Material and Joining Selection for Functional Lightweight Design based on the Extended Target Weighing Approach - A Detailed Application Example", Procedia CIRP 84 (2019): 694-700, https://doi.org/10.1016/j.procir.2019.04.192

98. Kaspar, J., Vielhaber, M., "Cross-Component Systematic Approach for Lightweight and Material-Oriented Design", DS 85-1: Proceedings of NordDesign 2016, Volume 1, Trondheim, Norway, 10th - 12th August 2016

99. Kelly, JC, Sullivan, JL, Burnham, A., Elgowainy, A., "Impacts of Vehicle Weight Reduction via Material Substitution on Life-Cycle Greenhouse Gas Emissions", Environ Sci Technol 49 (2015):12535–12542, doi: 10.1021/acs.est.5b03192

100. Khoonsari, SHM, "Life Cycle Cost Analysis for Passenger Cars: Steel versus Composites", Troy, Michigan, USA, 2009

101. Kim, H-J, Keoleian, GA, Skerlos, SJ, "Economic Assessment of Greenhouse Gas Emissions Reduction by Vehicle Lightweighting Using Aluminum and High-Strength Steel", J Ind Ecol 15 (2011): 64–80, doi: 10.1111/j.1530-9290.2010.00288.x

102. Kim, H.C. and Wallington, T.J., "Life Cycle Assessment of Vehicle Lightweighting: A Physics-Based Model of Mass-Induced Fuel Consumption," Environ Sci Technol 47 (2013):14358-14366, https://doi.org/10.1021/es402954w.

103. Kloepffer W (2008) Life cycle sustainability assessment of products: (with Comments by Helias A. Udo de Haes, p. 95). Int J Life Cycle Assess 13:89–95. doi:10.1065/lca2008.02.376

104. Koffler C., "Life cycle assessment of automotive lightweighting through polymers under US boundary conditions", Int J Life Cycle Assess 19 (2013): 538–545, doi:10.1007/s11367-013-0652-7

105. Koffler, C., Zahller, M., "Life Cycle Assessment of Polyners in an Automotive Bolster", PE International Technical Reports (2012). Available on the internet at: https://www.pe-international.com/

106. La Rosa, A.D., Recca, G., Summerscales, J., Latteri, A. et al., "Biobased versus Traditional Polymer Composites. A Life Cycle Assessment Perspective," J Clean Prod 74, no. 1 (2014): 135-144, https://doi.org/10.1016/j.jclepro.2014.03.017

107. Leal Filho, W., Tripathi, S.K., Andrade Guerra, J.B.S.O.D., Giné-Garriga, R. et al., “Using the Sustainable Development Goals towards a Better Understanding of Sustainability Challenges,” International Journal of Sustainable Development & World Ecology 26, no.2 (2019): 179-190, https://doi.org/10.1080/13504509.2018.1505674.

108. Lee J-M, Min B-J, Park J-H, Kim D-H, Kim B-M, Ko D-C., "Design of Lightweight CFRP Automotive Part as an Alternative for Steel Part by Thickness and Lay-Up Optimization", Materials 12(14) (2019): 2309, https://doi.org/10.3390/ma12142309

109. Lee K-H, Kang D-H., "Structural optimization of an automotive door using the kriging interpolation method", Proceedings of the Institution of Mechanical Engineers, Part D: Journal of Automobile Engineering 221(12) (2007): 1525-1534, doi:10.1243/09544070JAUTO403

110. Lewis, A. M. , Kelly, J. C., Keoleian, G. A., "Evaluating the life cycle greenhouse gas emissions from a lightweight plug-in hybrid electric vehicle in a regional context," 2012 IEEE International Symposium on Sustainable Systems and Technology (ISSST), 2012, pp. 1-6, doi: 10.1109/ISSST.2012.6403806

111. Li, G., Xu, F., Huang, X., Sun, G., "Topology Optimization of an Automotive Tailor-Welded Blank Door", Journal of Mechanical Design 137 (2015)

112. Li, N., "Automotive Magnesium Applications and Life Cycle Environmental Assessment", Ford Motor Company. Dearborn, Michigan USA. 3rd International Conference on SF6 and the environment, Scottsdale, AZ. December 1-3, 2004

113. Lopes, P.V., Silva, F.J.G., Campilho, R.D.S.G., Baptista, A. et al., “Designing a Novel and Greener Truck Asphalt Container,” Procedia Manufacturing 38 (2019): 324-332, https://doi.org/10.1016/j.promfg.2020.01.042

114. Luz, SM, Caldeira-Pires, A., Ferrão, PMC, "Environmental benefits of substituting talc by sugarcane bagasse fibers as reinforcement in polypropylene composites: Ecodesign and LCA as strategy for automotive components", Resour Conserv Recycl 54 (2010): 1135–1144, doi: 10.1016/j.resconrec.2010.03.009

115. Maclean, H.L. and Lave, L.B., “Life Cycle Assessment of Automobile/Fuel Options,” Environmental Science & Technology 37, no. 23 (2003): 5445-5452, https://doi.org/10.1021/es034574q.

116. Macombe, C., “Searching for social peace: a theory of justice to determine the nature of impacts in social LCA”, Montpellier, France, pp 56–62 (2014)

117. Macombe, C., Leskinen, P., Feschet, P., Antikainen, R., "Social life cycle assessment of biodiesel production at three levels: a literature review and development needs", J Clean Prod 52 (2013): 205–216, doi: 10.1016/j.jclepro.2013.03.026

118. Manik, Y., Leahy, J., Halog, A., "Social life cycle assessment of palm oil biodiesel: a case study in Jambi Province of Indonesia", Int J Life Cycle Assess 18 (2013): 1386–1392, doi:10.1007/s11367-013-0581-5

119. Mantovani, S., Lo Presti, I., Cavazzoni, L., Baldini, A., "Influence of Manufacturing Constraints on the Topology Optimization of an Automotive Dashboard", Procedia Manufacturing 11 (2017): 1700-1708, https://doi.org/10.1016/j.promfg.2017.07.296

120. Martínez-Blanco J, Lehmann A, Muñoz P, et al., "Application challenges for the social Life Cycle Assessment of fertilizers within life cycle sustainability assessment", J Clean Prod 69 (2014): 34–48. doi: 10.1016/j.jclepro.2014.01.044

121. Martinez-Sanchez V, Kromann MA, Astrup TF., "Life cycle costing of waste management systems: Overview, calculation principles and case studies", Waste Manag 36 (2015): 343–355. doi: 10.1016/j.wasman.2014.10.033

122. Mathe S (2014) Integrating participatory approaches into social life cycle assessment: the SLCA participatory approach. Int J Life Cycle Assess 19:1506–1514. doi:10.1007/s11367-014-0758-6

123. Mayyas A.T., Mayyas, A.R., Omar, M., "Sustainable lightweight vehicle design: A case study in eco-material selection for body-in-white", Lightweight Composite Structures in Transport, Woodhead Publishing, (2016):267-302, https://doi.org/10.1016/B978-1-78242-325-6.00011-6

124. Mayyas, A., Qattawi, D., Omar, M., Shan, D., 2012a. Design for sustainability in automotive industry: A comprehensive overview. Renewable and Sustainable Energy Reviews: 16, 1845-1862 (2012).

125. Mayyas, AT, Qattawi, A., Mayyas, AR, Omar, MA, "Life cycle assessment-based selection for a sustainable lightweight body-in-white design", Energy 39 (2012b): 412–425, doi: 10.1016/j.energy.2011.12.033

126. Mayyas, A.T., Qattawi, A., Mayyas, A.R., Omar, M., "Quantifiable measures of sustainability: a case study of materials selection for eco-lightweight auto-bodies", Journal of Cleaner Production, Special Volume: Sustainable consumption and production for Asia: Sustainability through green design and practice 40 (2013): 177–189.

127. McArthur, J.W. and Rasmussen, K., "Change of Pace: Accelerations and Advances during the Millennium Development Goal Era," World Development 105 (2018): 132-143, https://doi.org/10.1016/j.worlddev.2017.12.030.

128. Mcauley, J., 2003. Global sustainability and key needs in future automotive design. Environmental Science & Technology, 2003-37:5414–6.

129. Merulla, A., Gatto, A., Bassoli, E., Ion Munteanu, S., Gheorghiu, B., Alin Pop, M., Bedo, T., Munteanu, D., "Weight reduction by topology optimization of an engine subframe mount, designed for additive manufacturing production", Materials

Today: Proceedings 19(3) (2019): 1014-1018, https://doi.org/10.1016/j.matpr.2019.08.015

130. Moawad, A., Sharer, P., Rousseau, A., 2013. Light-Duty Vehicle Fuel Consumption Displacement Potential up to 2045; ANL/ESD/11-4; Argonne National Laboratory: Lemont, IL, 2013.

131. Mohammed H. Saad, Mohammad A. Nazzal, Basil M. Darras, "A general framework for sustainability assessment of manufacturing processes", Ecological Indicators, 97 (2019): 211-224,https://doi.org/10.1016/j.ecolind.2018.09.062

132. Ness, B., Urbel-Piirsalu, E., Anderberg, S., and Olsson, L., "Categorising Tools for Sustainability Assessment," Ecological Economics 60, no. 3 (2007): 498-508, https://doi.org/10.1016/j.ecolecon.2006.07.023.

133. Neugebauer S, Traverso M, Scheumann R, et al., "Impact Pathways to Address Social Well-Being and Social Justice in SLCA—Fair Wage and Level of Education", Sustainability 6 (2014): 4839–4857. doi: 10.3390/su6084839

134. Norris CB (2013) Data for social LCA. Int J Life Cycle Assess 19:261–265. doi:10.1007/s11367-013-0644-7

135. Ogden, JM, Williams, RH, Larson, ED, "Societal lifecycle costs of cars with alternative fuels/engines", Energy Policy 32 (2004): 7–27 doi: 10.1016/S0301-4215(02)00246-X

136. Onat, NC, Gumus, S., Kucukvar M., Tatari, O., "Application of the TOPSIS and intuitionistic fuzzy set approaches for ranking the life cycle sustainability performance of alternative vehicle technologies", Sustain Prod Consum 6 (2016a):12–25, doi:10.1016/j.spc.2015.12.003

137. Onat, NC, Kucukvar, M., Tatari, O., Zheng, QP, "Combined application of multi-criteria optimization and life-cycle sustainability assessment for optimal distribution of alternative passenger cars in U.S", J Clean Prod 112 (2016b):291–307, doi:10.1016/j.jclepro.2015.09.021

138. Pallaro E, Subramanian N, Abdulrahman MD, Liu C (2015) Sustainable production and consumption in the automotive sector: Integrated review framework and research directions. Sustain Prod Consum 4:47–61. doi: 10.1016/j.spc.2015.07.002

139. Park, HS, Dang, XP, Roderburg, A., Nau B., "Development of plastic front side panels for green cars", CIRP J Manuf Sci Technol 6 (2013): 44–52, doi: 10.1016/j.cirpj.2012.08.002

140. Poulikidou, S., Jerpdal, L., Bjorklund, A., and Åkermo, M., "Environmental Performance of Self-Reinforced Composites in Automotive Applications. Case Study on a Heavy Truck Component," Mater Des 103 (2016): 321-329, https://doi.org/10.1016/j.matdes.2016.04.090.

141. Rahman, M.H.A. & Salleh, Assoc. Prof. Ir. Ts. Dr. Mohd & Abdullah, A. & Yahaya, S. & Razak, Suffian & M. Kamal, M.R. & Marjom, Zolkarnain & Anuar, L. & Saad, N.A.M., "A new design optimization of light weight front lower control arm", Journal of Advanced Manufacturing Technology 12 (2018): 89-102

142. Rajendran, S., Scelsi, L., Hodzic, A., et al., "Environmental impact assessment of composites containing recycled plastics", Resour Conserv Recycl 60 (2012): 131–139, doi:10.1016/j.resconrec.2011.11.006

143. Raugei, M., Morrey, D., Hutchinson, A., Winfield, P., "A coherent life cycle assessment of a range of lightweighting strategies for compact vehicles", J Clean Prod (2015), doi:10.1016/j.jclepro.2015.05.100

144. Rebitzer, G., Ekvall, T., Frischknecht, R., Hunkeler, D., Norris, G., Rydberg, T., 2004. Life cycle assessment Part 1: framework, goal and scope definition, inventory analysis, and applications. Environ Int 2004;30:701–20.

145. Reimer, L., Kaluza, A., Cerdas, F., Meschke, J. et al., "Design of Eco-Efficient Body Parts for Electric Vehicles Considering Life Cycle Environmental Information," Sustainability 12, no. 14 (2020): 5838, https://doi.org/10.3390/su12145838

146. Reppe, P., Keoleian, G., Messick, R., Costic, M., "Life Cycle Assessment of a Transmission Case: Magnesium vs. Aluminum", SAE International Congress and Exposition, Detroit, MI, February 23 − 26; 1998

147. Reuter, B., Schulz, C., Schlagenhalft, G., Lienkamp, M., "Social risk analysis related to the material selection during an early stage of product development", SETAC Europe 20th LCA Case Study Symposium, 25 November Novi Sad, Serbia (2014)

148. Ribeiro, C., Ferreira, J.V., Partidario, P., "Life Cycle Assessment of a Multi-Material Car Component", International Journal of Life Cycle Assessment 12 (5) (2207): 336-345 DOI: 10.1065/lca2006.12.304

149. Rödger, J.-M., Bey, N., Alting, L., and Hauschild, M.Z., "Life Cycle Targets Applied in Highly Automated Car Body Manufacturing—Method and Algorithm," J Clean Prod 194 (2018): 786-799, https://doi.org/10.1016/j.jclepro.2018.04.148.

150. Roes, AL, Marsili, E., Nieuwlaar, E., Patel, MK, "Environmental and Cost Assessment of a Polypropylene Nanocomposite", J Polym Environ 15 (2007): 212–226, doi: 10.1007/s10924-007-0064-5

151. Rossi, M., Germani, M., and Zamagni, A., "Review of Ecodesign Methods and Tools. Barriers and Strategies for an Effective Implementation in Industrial Companies," J Clean Prod 129 (2016): 361-373, https://doi.org/10.1016/j.jclepro.2016.04.051

152. Rousseaux, P., Gremy-Gros, C., Bonnin, M., Henriel-Ricordel, C. et al., "'Eco-Tool-Seeker': A New and Unique Business Guide for Choosing Ecodesign Tools," J Clean Prod 151 (2017): 546-577, https://doi.org/10.1016/j.jclepro.2017.03.089.

153. Russo, D. and Matina, D., “Structural Optimization and LCA for a Computer-Aided Sustainable Design,” in Proceedings of the ASME 2012 International Design Engineering Technical Conferences and Computers and Information in Engineering Conference. Volume 2: 32nd Computers and Information in Engineering Conference, Parts A and B, Chicago, IL, August 12-15, 2012, 329-338, https://doi.org/10.1115/DETC2012-70814

154. Russo, D. and Rizzi, C., “An ECO-DESIGN Approach Based on Structural Optimization in a CAD Framework” Computer-Aided Design & Application 11, no. 5 (2014): 579-588, http://doi.org/10.1080/16864360.2014.902691

155. Sadeghzadeh, K., Salehi, MB., “Mathematical analysis of fuel cell strategic technologies development solutions in the automotive industry by the TOPSIS multi-criteria decision making method”, Int J Hydrog Energy 36 (2011): 13272–13280. doi:10.1016/j.ijhydene.2010.07.064

156. Safaei Mohamadabadi, H., Tichkowsky, G., Kumar, A., “Development of a multi-criteria assessment model for ranking of renewable and non-renewable transportation fuel vehicles”, Energy 34 (2009): 112–125. doi: 10.1016/j.energy.2008.09.004

157. Sakundarini, N. Taha, Z., Abdul-Rashid, SH, Ghazila, RAR, "Optimal multi-material selection for lightweight design of automotive body assembly incorporating recyclability", Materials & Design 50 (2013): 846-857, https://doi.org/10.1016/j.matdes.2013.03.085

158. Sala, S., Ciuffo, B., and Nijkamp, P., “A Systemic Framework for Sustainability Assessment,” Ecological Economics 119 (2015): 314-332, https://doi.org/10.1016/j.ecolecon.2015.09.015.

159. Sala, S., Farioli, F., Zamagni, A., “Life cycle sustainability assessment in the context of sustainability science progress (part 2)”, Int J Life Cycle Assess 18 (2013): 1686–1697. doi:10.1007/s11367-012-0509-5

160. Salvado, Miguel F., Susana G. Azevedo, João C. O. Matias, and Luís M. Ferreira, "Proposal of a Sustainability Index for the Automotive Industry" Sustainability 7, no. 2 (2015): 2113-2144. https://doi.org/10.3390/su7022113

161. Santos, J., Gouveia, R.M., and Silva, F.J.G., “Designing a New Sustainable Approach to the Change for Lightweight Materials in Structural Components Used in Truck Industry,” J Clean Prod 164 (2017): 115-123, https://doi.org/10.1016/j.jclepro.2017.06.174.

162. Saur, K., Schuckert, M., Beddies, H., Eyerer, P., "Foundations for Life Cycle Analysis of Automotive Structures - The Potential of Steel, Aluminum and Composites", Total Life Cycle Conference and Exposition, Vienna, Austria, October 16 − 19; Society of Automotive Engineers: 1995

163. Schau, EM, Traverso, M., Finkbeiner, M., "Life cycle approach to sustainability assessment: a case study of remanufactured alternators", J Remanufacturing 2 (2012): 1–14

164. Schau, EM, Traverso, M., Lehmann, A., Finkbeiner, M., "Life Cycle Costing in Sustainability Assessment—A Case Study of Remanufactured Alternators", Sustainability 3 (2011): 2268–2288, doi: 10.3390/su3112268

165. Schmidt, W.P., Dahlqvist, E., Finkbeiner, M., Krinke, S., Lazzari, S., Oschmann, D., Pichon, S., Thiel, C., "Life cycle assessment of lightweight and end-of-life scenarios for generic compact class vehicles", Int J Life Cycle Assess 9 (2004): 405-416

166. Schmidt, W-P, Taylor A., "Sustainable management of vehicle design", Int J Veh Des 46 (2008): 143–155. doi: 10.1504/IJVD.2008.017179

167. Schöggl, JP, Baumgartner, RJ, Hofer, D., "Improving sustainability performance in early phases of product design: A checklist for sustainable product development tested in the automotive industry", Journal of Cleaner Production, 140(3) (2017): 1602-1617, https://doi.org/10.1016/j.jclepro.2016.09.195

168. Schuh, G., Korthals, K., Backs, M., "Environmental Impact of Body Lightweight Design in the Operating Phase of Electric Vehicles", In: Nee AYC, Song B, Ong S-K (eds) Reengineering Manufacturing for Sustainability. Springer Singapore, (2013): 105–110

169. Simoes, C.L., Figueiredo de Sa, R., Ribeiro, C.J., Bernardo, P. et al., "Environmental and Economic Performance of a Car Component: Assessing New Materials, Processes and Designs," J Clean Prod 118, no. 1 (2016): 105-117, https://doi.org/10.1016/j.jclepro.2015.12.101.

170. Singh, KR, "An Approach for Operationalization of Social Life Cycle Assessment in Steel Industry" (2014)

171. Solomon, S., D. Qin, M. Manning, Z. Chen, M. Marquis, K.B. Averyt, M. Tignor and H.L. Miller (eds.), "Climate Change 2007: The Physical Science Basis. Contribution of Working Group I to the Fourth Assessment Report of the Intergovernmental Panel on Climate Change". Cambridge University Press, Cambridge, United Kingdom and New York, NY, USA, 2007a

172. Solomon, S., D. Qin, M. Manning, Z. Chen, M. Marquis, K.B. Averyt, M. Tignor, and H.L. Miller (eds.), "Climate change 2007: the synthesis report. Contribution of Working Group I to the Fourth Assessment Report of the Intergovernmental Panel on Climate Change". Cambridge, United Kingdom and New York: Cambridge University Press. 996 p., 2007b

173. Soo, VK, Compston, P., Subic, A., Doolan, M., "The Impact of Different Joining Decisions for Lightweight Materials on Life Cycle Assessment", AutoCRC 3rd Technical Conference (2014)

174. Spreafico, C., “Can TRIZ (Theory of Inventive Problem Solving) Strategies Improve Material Substitution in Eco-Design?” Sustainable Production and Consumption 30 (2022): 889-915, https://doi.org/10.1016/j.spc.2022.01.010

175. Srivastava, S., Pande, S., Kapadiya, B., Salunkhe, S., "Topology optimization of steering knuckle structure", International Journal for Simulation and Multidisciplinary Design Optimization 11 (2020): 1-8, 10.1051/smdo/2019018

176. Stoycheva, S., Marchese, D., Paul, C., Padoan, S., Juhmani, A., Linkov, I., "Multi-criteria decision analysis framework for sustainable manufacturing in automotive industry", Journal of Cleaner Production 187 (2018): 257-272, https://doi.org/10.1016/j.jclepro.2018.03.133

177. Subic, A., Schiavone, F., Leary, M., Manning, J., "Comparative Life Cycle Assessment (LCA) of passenger seats and their impact on different vehicle models", Int J Veh Des 53 (2010): 89–109, doi: 10.1504/IJVD.2010.032985

178. Sun, X., Liu, J., Lu, B., Zhang, P. et al., “Life Cycle Assessment-Based Selection of a Sustainable Lightweight Automotive Engine Hood Design,” Int J Life Cycle Assess 22 (2017): 1373-1383, https://doi.org/10.1007/s11367-016-1254-y

179. Sun, X., Meng, F., Liu, J., and McKechnie, J., “Life Cycle Energy Use and Greenhouse Gas Emission of Lightweight Vehicle—A Body-in-White Design,” J Clean Prod 220 (2019): 1-8, https://doi.org/10.1016/j.jclepro.2019.01.225

180. Swarr, TE, Hunkeler, D, Klöpffer, W, et al., “Environmental life-cycle costing: a code of practice”, Int J Life Cycle Assess 16 (2011): 389–391. doi: 10.1007/s11367-011-0287-5

181. Tharumarajah, A., Koltun, P., "Improving environmental performance of magnesium instrument panels" Resour Conserv Recycl 54 (2010): 1189–1195, doi:10.1016/j.resconrec.2010.03.014

182. Tharumarajah, A., Koltun, P., "Is there an environmental advantage of using magnesium components for light-weighting cars?", J Clean Prod 15 (2007): 1007–1013, doi:10.1016/j.jclepro.2006.05.022

183. Traverso M, Asdrubali F, Francia A, Finkbeiner M. “Towards life cycle sustainability assessment: an implementation to photovoltaic modules”, Int J Life Cycle Assess 17 (2012): 1068–1079. doi: 10.1007/s11367-012-0433-8

184. UNEP/SETAC, “Towards a Life Cycle Sustainability Assessment: Making Informed Choices on Products UNEP/SETAC Life Cycle Initiative,” UNEP-SETAC Life-Cycle Initiative, Paris, France, 2011.

185. UNEP/SETAC C, “Guidelines for Social Life Cycle Assessment of Products”, UNEPSETAC Life-Cycle Initiative, Paris, France, 2009

186. Ungureanu, CA, Das, S., Jawahir, IS, "Life-cycle cost analysis: aluminum versus steel in passenger cars", 2007

187. U.S. EPA, 2012. National Highway Traffic Safety Administration, 2012. 2017 and Later Model Year Light-Duty Vehicle Greenhouse Gas Emissions and Corporate Average Fuel Economy Standards; U.S. EPA; U.S. NHTSA: Washington, DC, 2012.

188. U.S. EPA, 2013. Light-Duty Automotive Technology, Carbon Dioxide Emissions, and Fuel Economy Trends: 1975 Through 2012; EPA-420-R-13 − 001; 2013.

189. U.S. EPA, 2014. Light Duty Automotive Technology, Carbon Dioxide Emissions, and Fuel Economy Trends: 1975 − 2014, PA-420-R-14-023; U.S. EPA: Washington, DC, 2014

190. Vafaei, N., Ribeiro, R.A., Camarinha-Matos, L.M., "Normalization Techniques for Multi-Criteria Decision Making: Analytical Hierarchy Process Case Study," in Camarinha-Matos, L.M., Falcão, A.J., Vafaei, N., Najdi, S. (Eds), Technological Innovation for Cyber-Physical Systems, DoCEIS 2016, IFIP AICT, vol. 470 (Cham: Springer, 2016), 261-269, https://doi.org/10.1007/978-3-319-31165-4_26.

191. Vermeulen, I., Block, C., Van Caneghem, J., et al., "Sustainability assessment of industrial waste treatment processes: The case of automotive shredder residue", Resour Conserv Recycl 69 (2012): 17–28, doi: 10.1016/j.resconrec.2012.08.010

192. Viana, F.A., "Things You Wanted to Know about the Latin Hypercube Design and Were Afraid to Ask," in Proceedings of the 10th World Congress on Structural and Multidisciplinary Optimization, Albany, NY, 2013.

193. Vinodh, S., Jayakrishna, K., "Environmental impact minimization in an automotive component using alternative materials and manufacturing processes", Mater Des 32 (2011): 5082–5090, doi: 10.1016/j.matdes.2011.06.025

194. Visentin, C., Da Silva Trentin, A.W., Braun, A.B., and Thomé, A., "Life Cycle Sustainability Assessment: A Systematic Literature Review through the Application Perspective, Indicators, and Methodologies," J Clean Prod 270 (2020): 122509, https://doi.org/10.1016/j.jclepro.2020.122509.

195. Wang, J.J., Jing, Y.Y., Zhang, C.F., and Zhao, J.H., "Review on Multi-Criteria Decision Analysis Aid in Sustainable Energy Decision-Making," Renew Sustain Energy Rev 13 (2009): 2263-2278, https://doi.org/10.1016/j.rser.2009.06.021

196. Ward's auto (2017) World Vehicle Population Rose 4.6% in 2016. https://wardsintelligence.informa.com/WI058630/World-Vehicle-Population-Rose-46-in-2016. Accessed 17 Oct 2017

197. Weiss, M.A., Heywood, J.B., Drake, E.M., Schafer, A., AuYeung, F.F., "On the road in 2020. A life-cycle analysis of new automobile technologies", Energy laboratory report. Energy Laboratory – Massachusetts Institute of Technology – Cambridge, Massachusetts (2000)

198. Witik, RA, Payet, J., Michaud, V., et al., "Assessing the life cycle costs and environmental performance of lightweight materials in automobile applications", Compos Part Appl Sci Manuf 42 (2011): 1694–1709, doi: 10.1016/j.compositesa.2011.07.024

199. Wong, YS, Lu, W-F, Wang, Z., "Life Cycle Cost Analysis of Different Vehicle Technologies in Singapore", World Electr. Veh. J. 4(4) (2010): 912-920, https://doi.org/10.3390/wevj4040912

200. WorldAutoSteel, 2012. Life Cycle Assessment: Good for the Planet, Good for the Auto Industry. WorldAutoSteel, Rue Colonel Bourg 120 B-1140 Brussels, Belgium. On the Internet at www.worlautosteel.org (accessed: November 2014).

201. Wu R, Yang D, Chen J (2014) Social Life Cycle Assessment Revisited. Sustainability 6:4200–4226. doi: 10.3390/su6074200

202. Yoo, S., Doh, J., Lim, J., Kang, O., Lee J., Kang, K., "Topologically optimized shape of CFRP front lower control arm", International Journal of Automotive Technology 18(4) (2017): 625−630, DOI 10.1007/s12239−017−0062−0

203. Zah, R., Hischier, R., Leao, A.L., Braun, I., "Curauà fibers in the automobile industry – A sustainability assessment", J Cleaner Production; 15 (2006): 1032-40

204. Zamagni, A., Amerighi, O., Buttol, P., “Strengths or bias in social LCA?” Int J Life Cycle Assess 16 (2011): 596–598. doi: 10.1007/s11367-011-0309-3

205. Zamagni, A., Pesonen, H-L, Swarr, T., “From LCA to Life Cycle Sustainability Assessment: concept, practice and future directions”, Int J Life Cycle Assess 18 (2013): 1637–1641. doi: 10.1007/s11367-013-0648-3

206. Zanchi, L., "Life Cycle Sustainability Assessment: application to the automotive sector and challenges for the lightweighting", (2016)

Appendix A – DeSA Graphic User Interface (GUI)

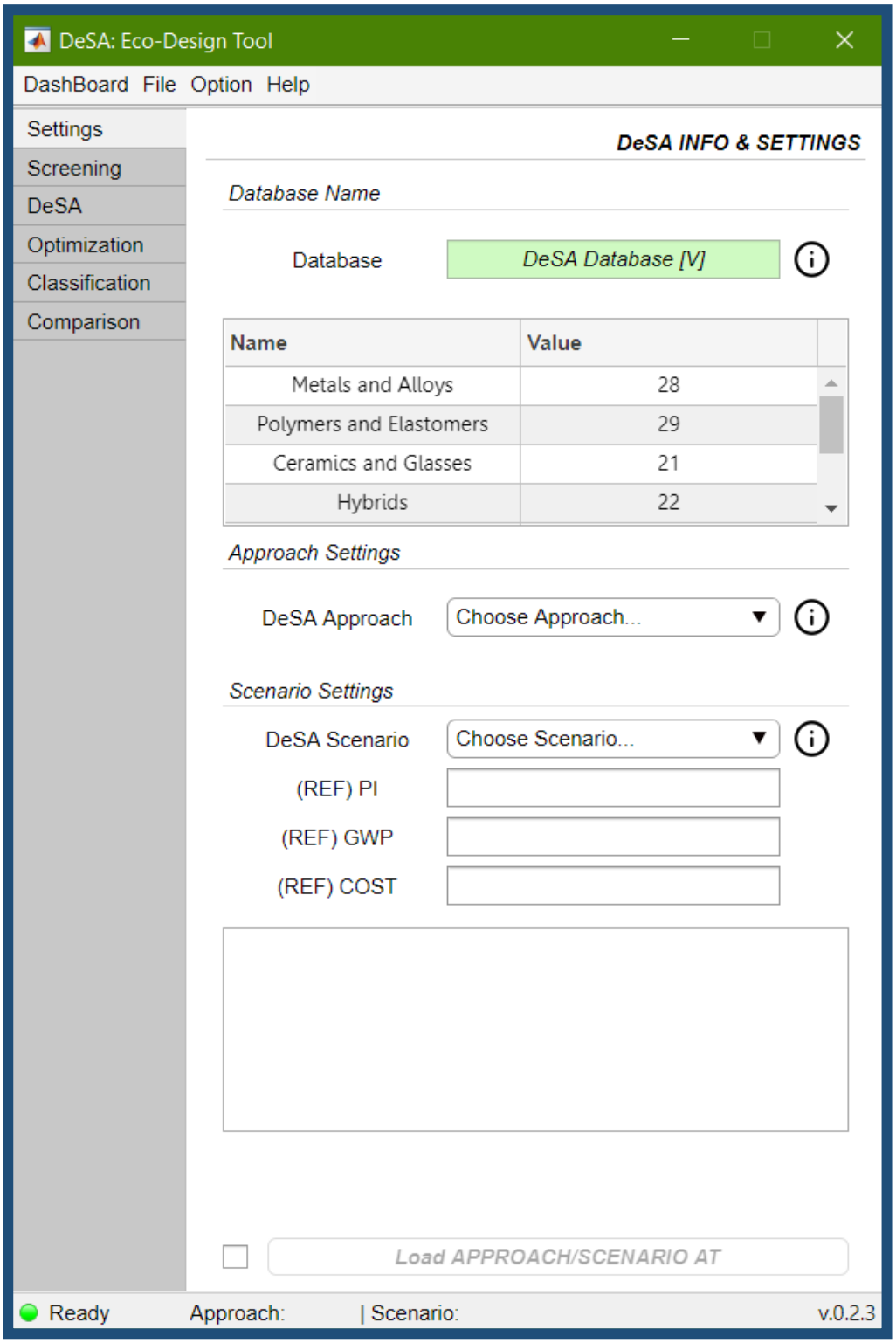

Figure A.1. GUI of Approaches/Scenarios settings in DeSA methodology.

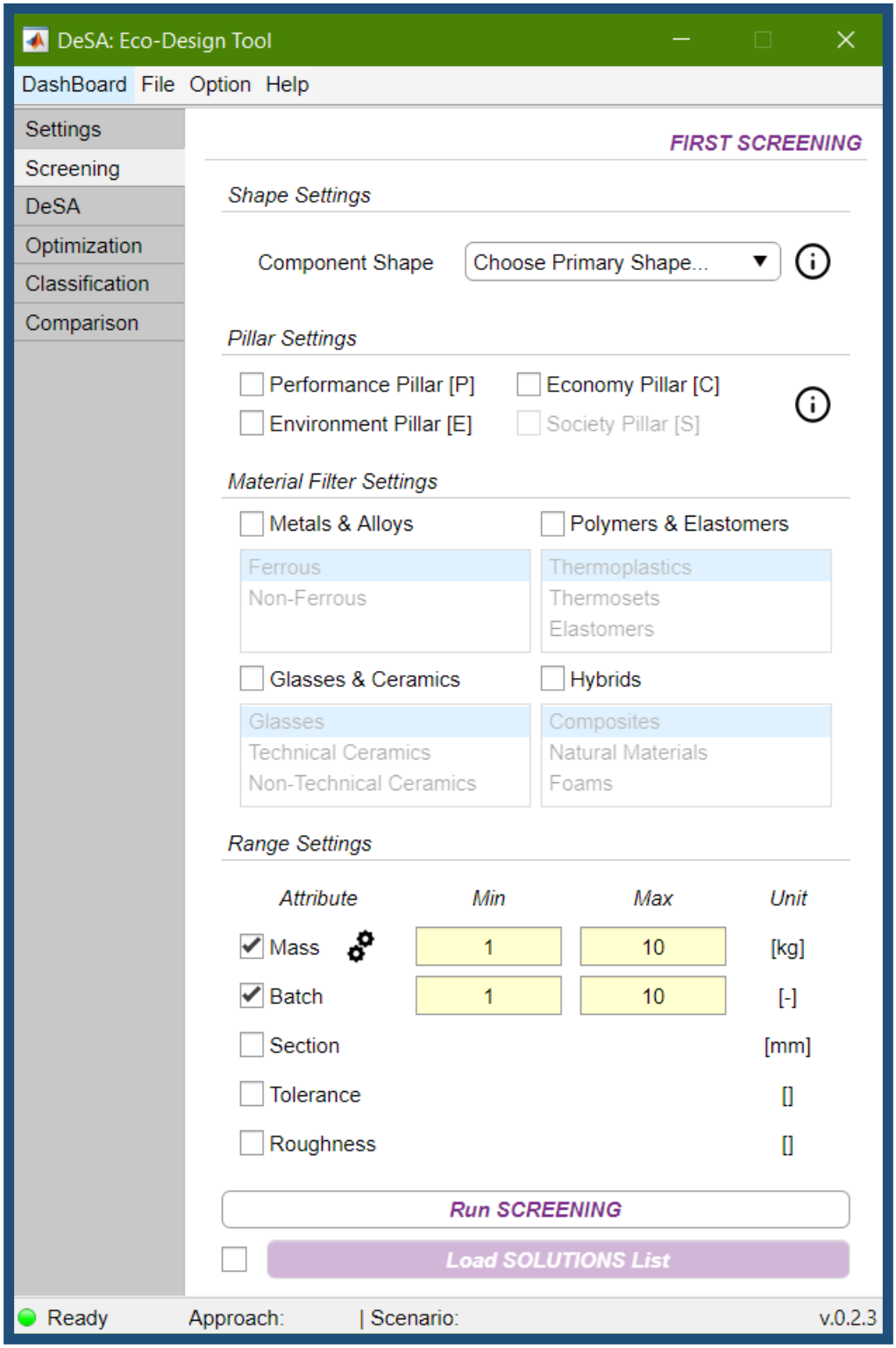

Figure A.2. GUI of First Screening phase of DeSA methodology.

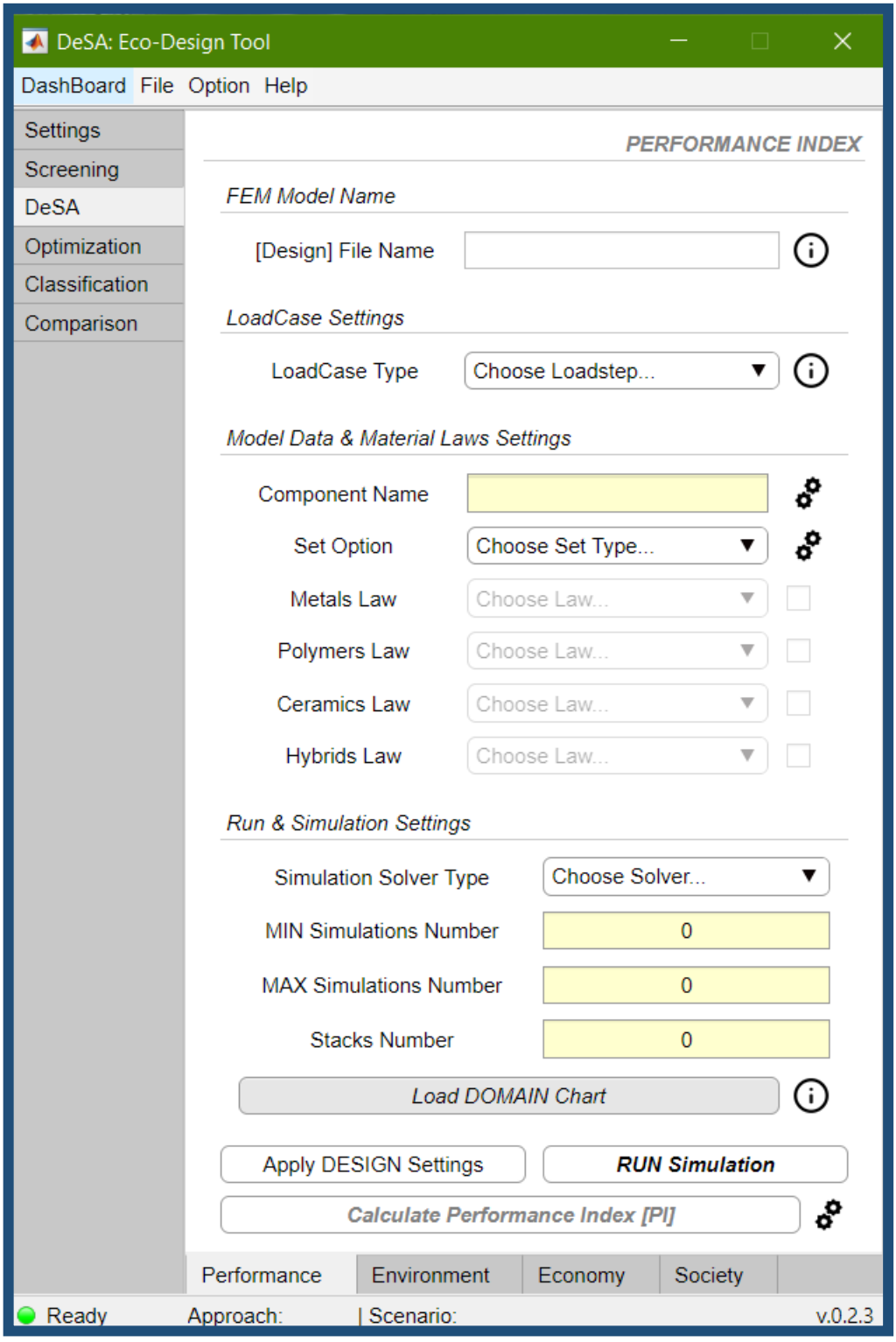

Figure A.3. GUI of Design phase in Design and Sustainability phase of DeSA methodology.

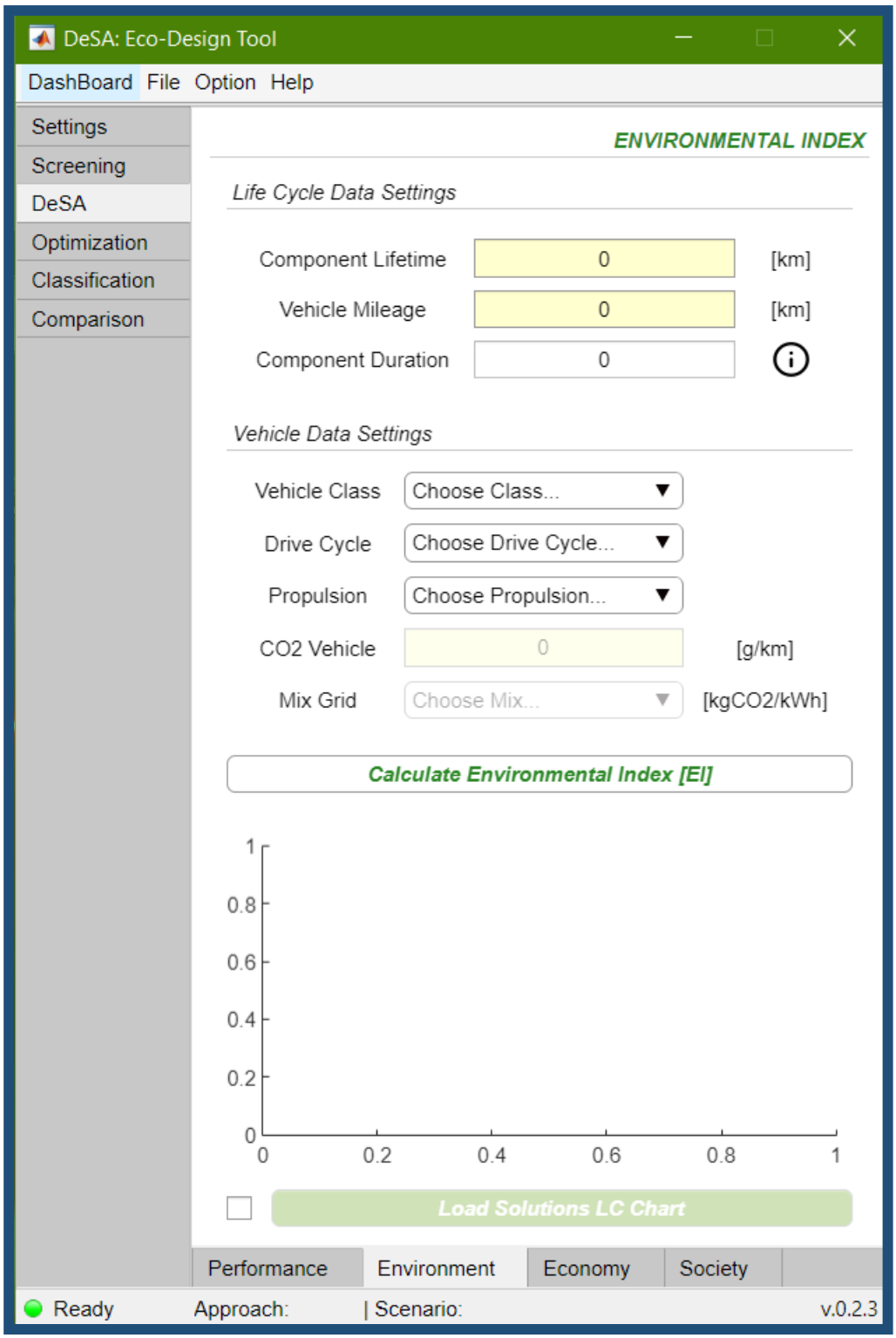

Figure A.4. GUI of Environmental phase in Design and Sustainability phase of DeSA methodology.

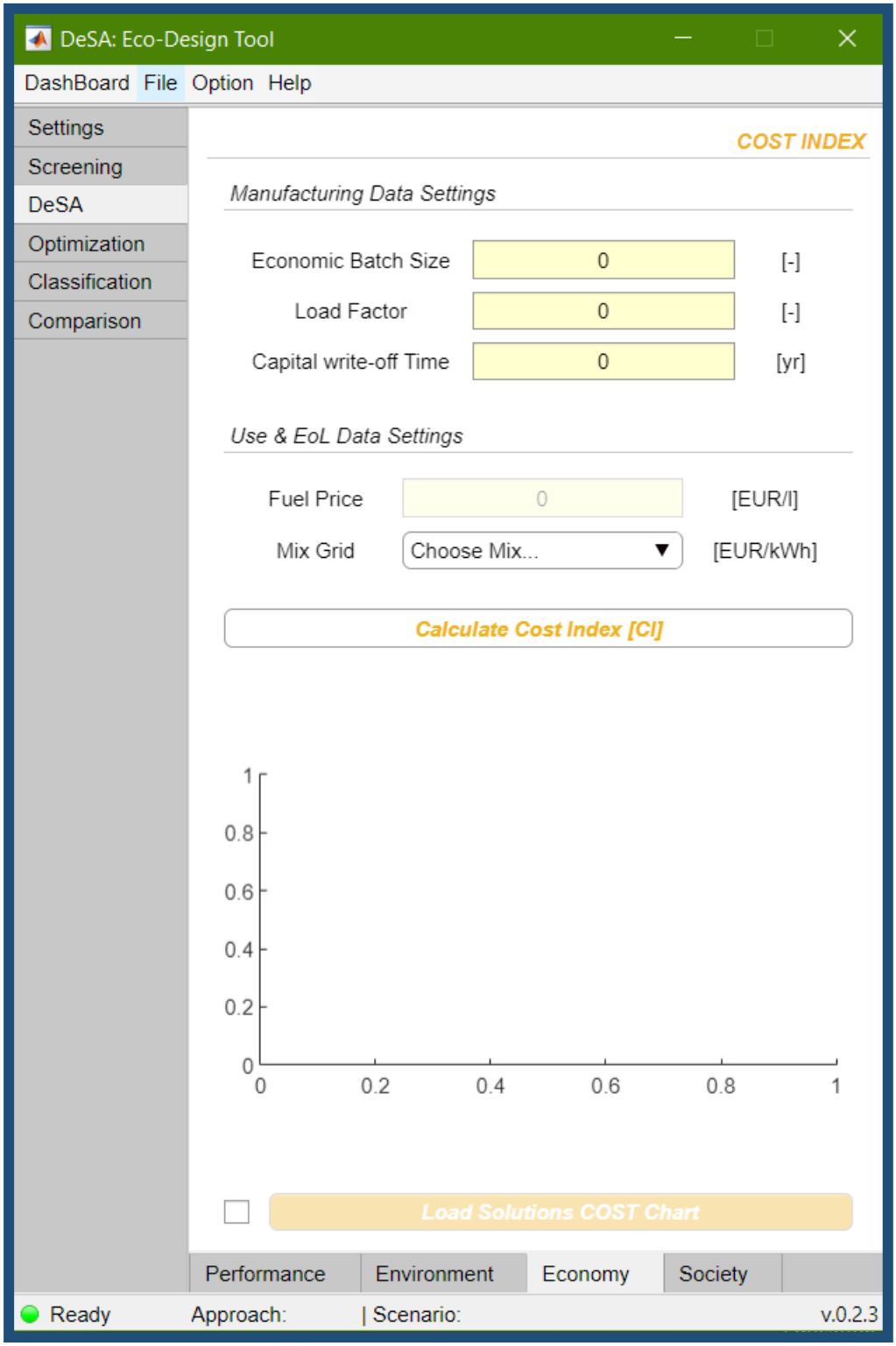

Figure A.5. GUI of Economic phase in Design and Sustainability phase of DeSA methodology.

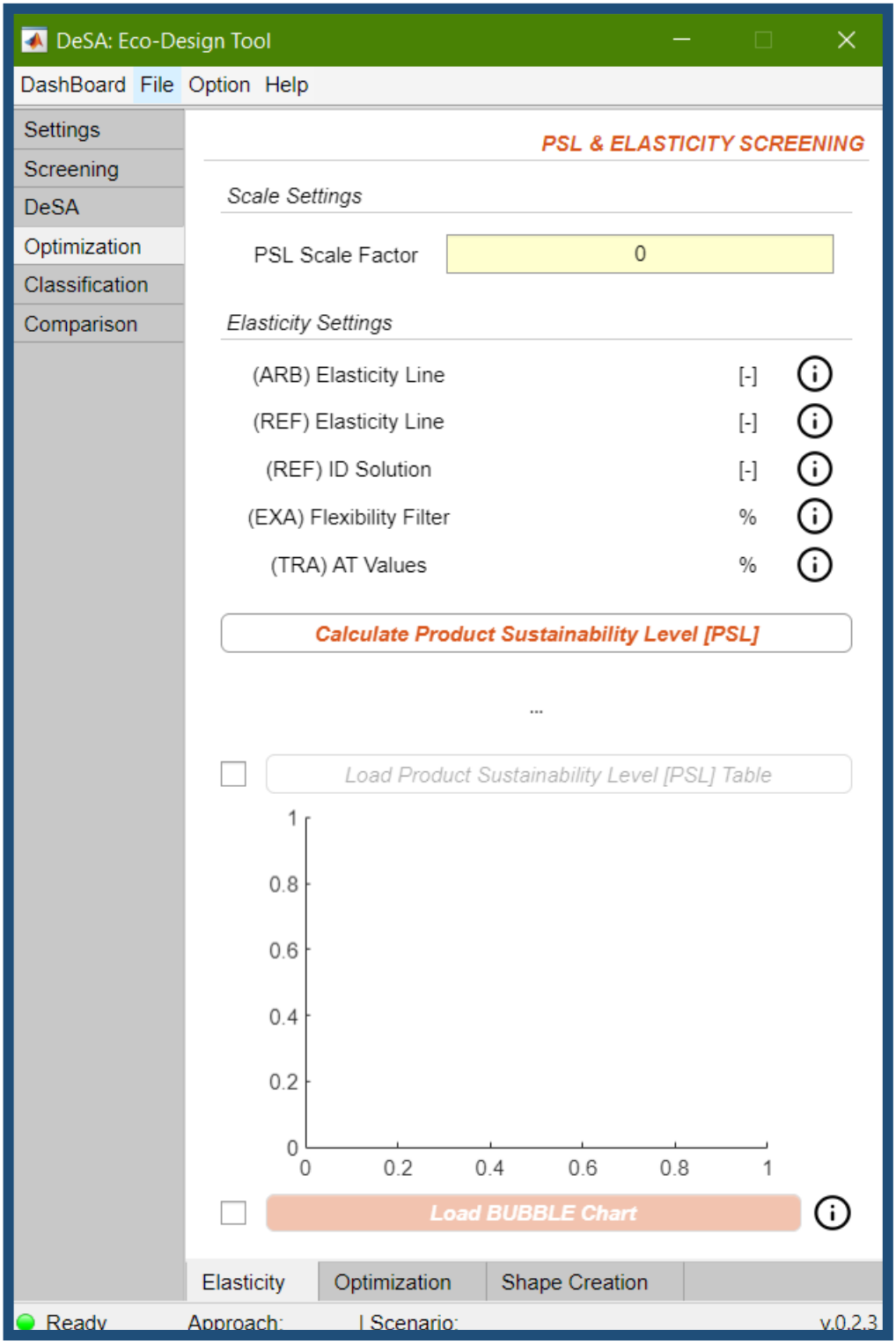

Figure A.6. GUI of First Elasticity Screening in DeSA methodology.

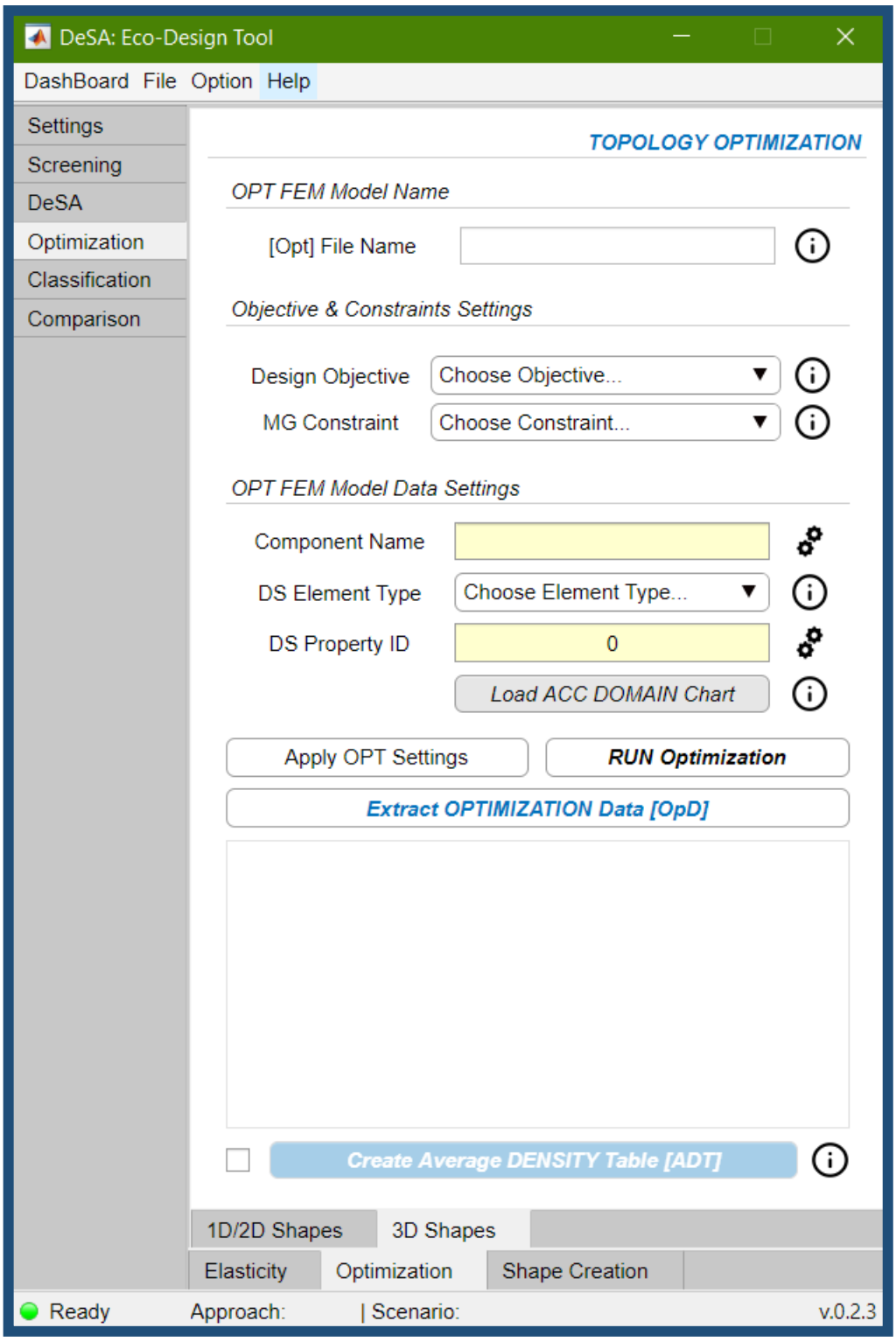

Figure A.7. GUI of Optimization phase (for 3D shapes) in DeSA methodology.

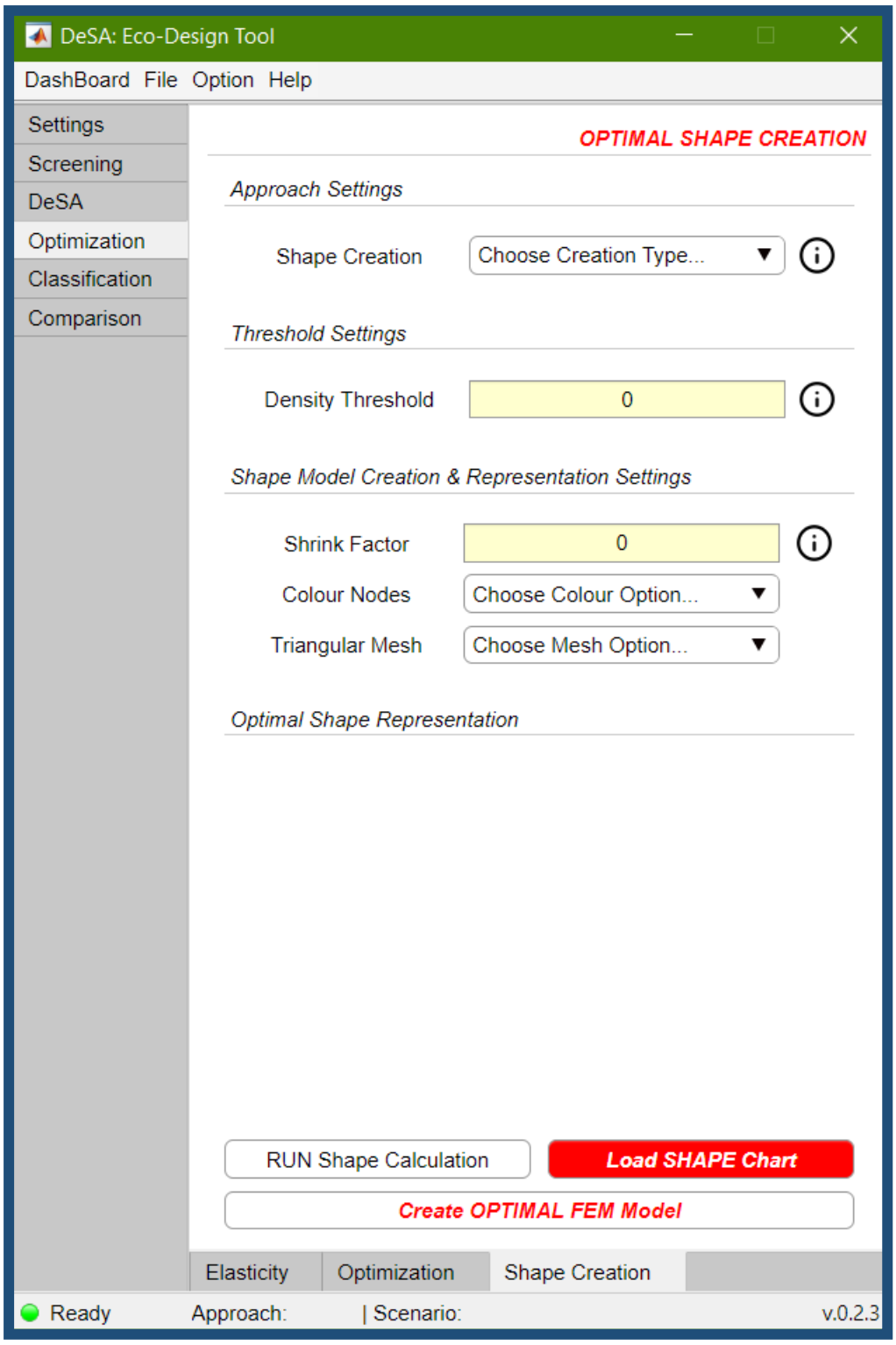

Figure A.8. GUI of Shape Reconstruction phase (for 3D shapes) in DeSA methodology.

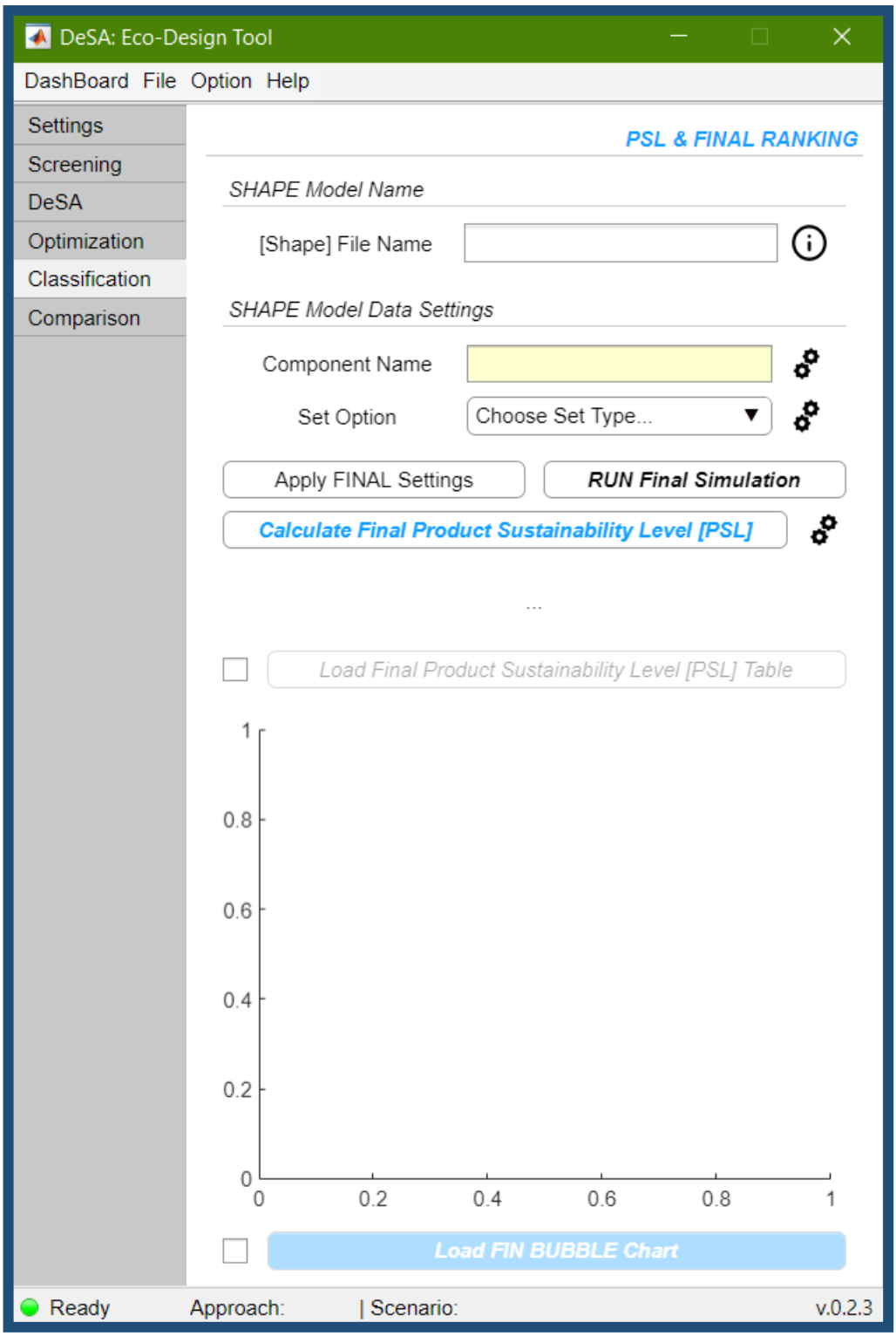

Figure A.9. GUI of Design and Sustainability Re-analysis phase in DeSA methodology.

Appendix B – Case Studies Data

Table B.1. TB Case Study - Design materials data in production database.

TB - Production Database							
Material Section (MAT)							
ID	**Material Class**	**Material Subclass**	**Material name**	**Density [kg/m^3]**	**Young's Modulus [MPa]**	**Poisson Ratio [-]**	**Yield Strength [MPa]**
M1	Metals and Alloys	Ferrous	Cast Iron (Ductile)	7050-7250	165000-180000	0.26-0.28	250-680
M2	Metals and Alloys	Ferrous	High Carbon Steel	7800-7900	200000-215000	0.285-0.295	400-1160
M3	Metals and Alloys	Ferrous	Stainless Steel	7600-8100	189000-210000	0.265-0.275	170-1000
M4	Metals and Alloys	Non-Ferrous	Age-Hardening Wrought Al-Alloys	2500-2900	68000-80000	0.32-0.36	95-610
M5	Metals and Alloys	Non-Ferrous	Titanium Alloys	4400-4800	110000-120000	0.35-0.37	750-1200
H1	Hybrids	Composites	CFRP	1500-1600	69000-150000	0.305-0.307	550-1050
H2	Hybrids	Composites	GFRP	1750-1970	15000-28000	0.314-0.315	110-192

Table B.2. TB Case Study - Design processes data and Compatibility Matrices in production database.

TB - Production Database					
Process Section (MAN)					
ID	**Process Class**	**Process Subclass**	**Process name**	**Mass range [kg]**	**Economic Batch size [-]**
CA1	Casting	Die Casting Processes	High Pressure Die casting	0.01-50	10000- 1000000
CA2	Casting	Investment Casting Processes	Investment Casting	0.001-100	1- 10000
DE1	Deformation	Bulk Deformation Processes	Extrusion	1-1000	0- 100000000
CO1	Composite Forming	Advanced Composite Forming Processes	Resin Transfer Molding (RTM)	0.8-50	1000- 1000000
CO2	Composite Forming	Conventional Composite Forming Processes	Lay-Up Methods	1-6000	1-500

TB - Production Database [CONTINUE]						
Process Section (MAN)						
ID	**Process Class**	**Process Subclass**	**Process name**	**Section thickness [mm]**	**Tolerance [mm]**	**Roughness [µm]**
CA1	Casting	Die Casting Processes	High Pressure Die casting	0.5-12	0.15-0.5	0.8-1.6
CA2	Casting	Investment Casting Processes	Investment Casting	1-75	0.05-0.25	0.5-3.2
DE1	Deformation	Bulk Deformation Processes	Extrusion	1-900	0.5-1	0.8-3.2
CO1	Composite Forming	Advanced Composite Forming Processes	Resin Transfer Molding (RTM)	2-6	0.25-1	0.25-1.6
CO2	Composite Forming	Conventional Composite Forming Processes	Lay-Up Methods	2-10	0.8-2	0.5-3.2

TB - Compatibility Process/Shape						
ID	**1D - Circular**	**1D - Noncircular**	**2D - Flat**	**2D - Dished**	**3D - Solid**	**3D-Hollow**
CA1	1	1	0	0	1	0
CA2	1	1	0	0	1	1
DE1	1	1	0	0	0	0
CO1	1	1	1	1	1	1
CO2	1	1	1	1	1	1

TB - Compatibility Process/Material							
ID	**M1**	**M2**	**M3**	**M4**	**M5**	**H1**	**H2**
CA1	0	0	0	1	0	0	0
CA2	1	1	1	1	0	0	0
DE1	0	0	0	1	0	0	0
CO1	0	0	0	0	0	1	1
CO2	0	0	0	0	0	1	1

Table B.3. TB Case Study - Environmental materials data in production database.

TB - Production Database						
Material Section (MAT)						
ID	**Material Class**	**Material Subclass**	**Material name**	**cc Primary [kgCO_{2eq}/kg]**	**cc EoL - Energy recovery [kgCO_{2eq}/kg]**	**Substitution Factor [-]**
M1	Metals and Alloys	Ferrous	Cast Iron (Ductile)	1.7-1.8	0-0	0.25-0.25
M2	Metals and Alloys	Ferrous	High Carbon Steel	1.71-1.89	0-0	0.25-0.25
M3	Metals and Alloys	Ferrous	Stainless Steel	4.73-5.23	0-0	0.25-0.25
M4	Metals and Alloys	Non-Ferrous	Age-Hardening Wrought Al-Alloys	12.2-13.4	0-0	0.15-0.15
M5	Metals and Alloys	Non-Ferrous	Titanium Alloys	44.1-48.7	0-0	0.15-0.15
H1	Hybrids	Composites	CFRP	32.9-36.4	0-0	0-0
H2	Hybrids	Composites	GFRP	9.5-10.5	0-0	0-0

Table B.4. TB Case Study - Environmental Compatibility Matrices in production database.

TB - Compatibility Process/Material							
ID	**M1**	**M2**	**M3**	**M4**	**M5**	**H1**	**H2**
	[kgCO_{2eq}/kg]	**[kgCO_{2eq}/kg]**	**[kgCO_{2eq}/kg]**	**[kgCO_{2eq}/kg]**	**[kgCO_{2eq}/kg]**	**[kgCO_{2eq}/kg]**	**[kgCO_{2eq}/kg]**
CA1	0-0	0-0	0-0	0.386-1.06	0-0	0	0
CA2	0.386-1.06	0.386-1.06	0.386-1.06	0.386-1.06	0-0	0	0
DE1	0-0	0-0	0-0	0.386-1.06	0-0	0	0
CO1	0-0	0-0	0-0	0-0	0-0	1.67-1.84	1.67-1.84
CO2	0-0	0-0	0-0	0-0	0-0	1.67-1.84	1.67-1.84

Table B.5. TB Case Study - Economic materials data in production database.

TB - Production Database						
Material Section (MAT)						
ID	**Material Class**	**Material Subclass**	**Material name**	**cost Primary [EUR/kg]**	**Material Scrap fraction [-]**	**LHV [MJ]**
M1	Metals and Alloys	Ferrous	Cast Iron (Ductile)	0.517-0.569	0.3-0.3	0-0
M2	Metals and Alloys	Ferrous	High Carbon Steel	0.605-0.665	0.3-0.3	0-0
M3	Metals and Alloys	Ferrous	Stainless Steel	6.6-7.26	0.3-0.3	0-0
M4	Metals and Alloys	Non-Ferrous	Age-Hardening Wrought Al-Alloys	1.87-2.05	0.3-0.3	0-0
M5	Metals and Alloys	Non-Ferrous	Titanium Alloys	45.6-50.2	0.3-0.3	0-0
H1	Hybrids	Composites	CFRP	31.9-35.2	0.3-0.3	31.3-31.3
H2	Hybrids	Composites	GFRP	15.4-17	0.3-0.3	12-12

Table B.6. TB Case Study - Economic processes data in production database.

TB - Production Database					
Process Section (MAN)					
ID	**Process Class**	**Process Subclass**	**Process name**	**Tool Cost [EUR]**	**Tool Lifespan [pc.]**
CA1	Casting	Die Casting Processes	High Pressure Die casting	5880-89400	20000-1000000
CA2	Casting	Investment Casting Processes	Investment Casting	65.3-653	1-5
DE1	Deformation	Bulk Deformation Processes	Extrusion	653-3260	100-10000
CO1	Composite Forming	Advanced Composite Forming Processes	Resin Transfer Molding (RTM)	653-2610	500-5000
CO2	Composite Forming	Conventional Composite Forming Processes	Lay-Up Methods	65.3-1310	200-1000

TB - Production Database [CONTINUE]						
Process Section (MAN)						
ID	**Process Class**	**Process Subclass**	**Process name**	**Production Rate [pc./hr]**	**Capital Cost [EUR]**	**Overhead Rate [EUR/hr]**
CA1	Casting	Die Casting Processes	High Pressure Die casting	2-200	131000-653000	60-60
CA2	Casting	Investment Casting Processes	Investment Casting	1-200	261-1310	60-60
DE1	Deformation	Bulk Deformation Processes	Extrusion	1-10	131000-1310000	60-60
CO1	Composite Forming	Advanced Composite Forming Processes	Resin Transfer Molding (RTM)	5-20	6530-39200	60-60
CO2	Composite Forming	Conventional Composite Forming Processes	Lay-Up Methods	0.1-0.5	65.3-653	60-60

Table B.7. TRF Case Study - Design materials data in production database.

TRF - Production Database							
Material Section (MAT)							
ID	**Material Class**	**Material Subclass**	**Material name**	**Density [kg/m^3]**	**Young's Modulus [MPa]**	**Poisson Ratio [-]**	**Yield Strength [MPa]**
M1	Metals and Alloys	Ferrous	Stainless Steel	7850	210000	0.3	500
M2	Metals and Alloys	Non-Ferrous	Age-Hardening Wrought Al-Alloys	2750	70000	0.3	300
H1	Hybrids	Composites	Carbon Fiber Reinforced Polymer (CFRP)	1485	80000	0.305	700
H2	Hybrids	Composites	Natural Fiber Reinforced Polymer (NFRP)	1220	25000	0.315	150

Table B.8. TRF Case Study - Design processes data and Compatibility Matrices in production database.

TRF - Production Database					
Process Section (MAN)					
ID	**Process Class**	**Process Subclass**	**Process name**	**Mass range [kg]**	**Economic Batch size [-]**
DE1	Deformation	Sheet Deformation Processes	Sheet Stamping Drawing and Blanking	0.001-5	1000-1000000000
CO1	Composite Forming	Advanced Composite Forming Processes	Resin Transfer Molding (RTM)	0.8-50	1000-1000000
MO1	Thermoplastic Molding	Thermoforming	Molding	0.001-25	10000-1000000

TRF - Production Database [CONTINUE]						
Process Section (MAN)						
ID	**Process Class**	**Process Subclass**	**Process name**	**Section thickness [mm]**	**Tolerance [mm]**	**Roughness [µm]**
DE1	Deformation	Sheet Deformation Processes	Sheet Stamping Drawing and Blanking	0.2-5	0.1-0.8	0.5-12.5
CO1	Composite Forming	Advanced Composite Forming Processes	Resin Transfer Molding (RTM)	2-6	0.25-1	0.25-1.6
MO1	Thermoplastic Molding	Thermoforming	Molding	0.4-6.3	0.07-1	0.2-1.6

TRF - Compatibility Process/Shape						
ID	**1D - Circular**	**1D - Noncircular**	**2D - Flat**	**2D - Dished**	**3D - Solid**	**3D-Hollow**
DE1	0	0	1	1	0	0
CO1	1	1	1	1	1	1
MO1	1	1	1	1	1	1

TRF - Compatibility Process/Material				
ID	**M1**	**M2**	**H1**	**H2**
DE1	1	1	0	0
CO1	0	0	1	0
MO1	0	0	0	1

Table B.9. TRF Case Study - Environmental materials data in production database.

TRF - Production Database						
Material Section (MAT)						
ID	**Material Class**	**Material Subclass**	**Material name**	**cc Primary [$kgCO_{2eq}/kg$]**	**cc EoL - Energy recovery [$kgCO_{2eq}/kg$]**	**Substitution Factor [-]**
M1	Metals and Alloys	Ferrous	Stainless Steel	2.2	0	0.25
M2	Metals and Alloys	Non-Ferrous	Age-Hardening Wrought Al-Alloys	4	0	0.15
H1	Hybrids	Composites	Carbon Fiber Reinforced Polymer (CFRP)	16	1.26	0
H2	Hybrids	Composites	Natural Fiber Reinforced Polymer (NFRP)	1.1	1.26	0

Table B.10. TRF Case Study - Environmental Compatibility Matrices in production database.

TRF - Compatibility Process/Material				
ID	**M1**	**M2**	**H1**	**H2**
	[$kgCO_{2eq}/kg$]	**[$kgCO_{2eq}/kg$]**	**[$kgCO_{2eq}/kg$]**	**[$kgCO_{2eq}/kg$]**
DE1	0.5	0.5	0	0
CO1	0	0	1.7	0
MO1	0	0	0	1.7

Table B.11. TRF Case Study - Economic materials data in production database.

TRF - Production Database						
Material Section (MAT)						
ID	**Material Class**	**Material Subclass**	**Material name**	**cost Primary [EUR/kg]**	**Material Scrap fraction [-]**	**LHV [MJ]**
M1	Metals and Alloys	Ferrous	Stainless Steel	7	0.2	0
M2	Metals and Alloys	Non-Ferrous	Age-Hardening Wrought Al-Alloys	2	0.2	0
H1	Hybrids	Composites	Carbon Fiber Reinforced Polymer (CFRP)	32	0.3	31.3
H2	Hybrids	Composites	Natural Fiber Reinforced Polymer (NFRP)	16	0.3	15

Table B.12. TRF Case Study - Economic processes data in production database.

TRF - Production Database					
Process Section (MAN)					
ID	**Process Class**	**Process Subclass**	**Process name**	**Tool Cost [EUR]**	**Tool Lifespan [pc.]**
DE1	Deformation	Sheet Deformation Processes	Sheet Stamping Drawing and Blanking	13000	200000
CO1	Composite Forming	Advanced Composite Forming Processes	Resin Transfer Molding (RTM)	700	5000
MO1	Thermoplastic Molding	Thermoforming	Molding	2600	200000

TRF - Production Database [CONTINUE]						
Process Section (MAN)						
ID	**Process Class**	**Process Subclass**	**Process name**	**Production Rate [pc./hr]**	**Capital Cost [EUR]**	**Overhead Rate [EUR/hr]**
DE1	Deformation	Sheet Deformation Processes	Sheet Stamping Drawing and Blanking	500	10000	60
CO1	Composite Forming	Advanced Composite Forming Processes	Resin Transfer Molding (RTM)	10	10000	60
MO1	Thermoplastic Molding	Thermoforming	Molding	100	30000	60

Table B.13. FLCA Case Study - Design materials data in production database.

FLCA - Production Database							
Material Section (MAT)							
ID	**Material Class**	**Material Subclass**	**Material name**	**Density [kg/m^3]**	**Young's Modulus [MPa]**	**Poisson Ratio [-]**	**Yield Strength [MPa]**
M1	Metals and Alloys	Ferrous	Cast Iron (Ductile)	7050-7250	165000-180000	0.26-0.28	250-680
M2	Metals and Alloys	Ferrous	High Carbon Steel	7800-7900	200000-215000	0.285-0.295	400-1160
M3	Metals and Alloys	Ferrous	Low Alloy Steel	7800-7900	205000-217000	0.285-0.295	400-1500
M4	Metals and Alloys	Ferrous	Medium Carbon Steel	7800-7900	200000-216000	0.285-0.295	305-900
M5	Metals and Alloys	Ferrous	Stainless Steel	7600-8100	189000-210000	0.265-0.275	170-1000
M6	Metals and Alloys	Non-Ferrous	Cast Al-Alloys	2500-2900	68000-80000	0.32-0.36	95-610
M7	Metals and Alloys	Non-Ferrous	Wrought Magnesium Alloys	1500-1950	42000-47000	0.29-0.31	115-410
M8	Metals and Alloys	Non-Ferrous	Nickel-based Superalloys	7750-8650	150000-245000	0.26-0.325	300-1900
M9	Metals and Alloys	Non-Ferrous	Titanium Alloys	4400-4800	110000-120000	0.35-0.37	750-1200

Table B.14. FLCA Case Study - Design processes data and Compatibility Matrices in production database.

FLCA - Production Database					
Process Section (MAN)					
ID	**Process Class**	**Process Subclass**	**Process name**	**Mass range [kg]**	**Economic Batch size [-]**
CA1	Casting	Die Casting Processes	Gravity Die casting	0.5-50	1000-100000
CA2	Casting	Investment Casting Processes	Investment Casting	0.001-100	1-10000
CA3	Casting	Die Casting Processes	Low Pressure Die Casting	0.01-10000	1-100000
DE1	Deformation	Bulk Deformation Processes	Forging	0.01-5000	1000-100000
PO1	Powder Methods	Powder Pressing Processes	Pressing and Sintering	0.01-5	5000-5000000

FLCA - Production Database [CONTINUE]						
Process Section (MAN)						
ID	**Process Class**	**Process Subclass**	**Process name**	**Section thickness [mm]**	**Tolerance [mm]**	**Roughness [µm]**
CA1	Casting	Die Casting Processes	Gravity Die casting	5-45	0.25-2	3.4-6.3
CA2	Casting	Investment Casting Processes	Investment Casting	1-75	0.05-0.25	0.5-3.2
CA3	Casting	Die Casting Processes	Low Pressure Die Casting	3-1000	0.8-3	20-200
DE1	Deformation	Bulk Deformation Processes	Forging	3-250	0.2-1	3.2-12.5
PO1	Powder Methods	Powder Pressing Processes	Pressing and Sintering	1.5-8	0.025-1	1-10

FLCA - Compatibility Process/Shape						
ID	**1D - Circular**	**1D - Noncircular**	**2D - Flat**	**2D - Dished**	**3D - Solid**	**3D-Hollow**
CA1	1	1	0	0	1	0
CA2	1	1	0	0	1	1
CA3	1	1	0	0	1	1
DE1	0	1	0	0	1	0
PO1	1	1	0	0	1	1

FLCA - Compatibility Process/Material										
ID	**M1**	**M2**	**M3**	**M4**	**M5**	**M6**	**M7**	**M8**	**M9**	**M10**
CA1	0	0	0	0	0	0	0	0	0	0
CA2	1	1	1	1	1	1	1	1	0	0
CA3	1	1	1	1	1	1	1	1	0	0
DE1	0	1	1	1	1	1	1	1	1	1
PO1	0	1	1	1	1	1	0	1	0	1

Table B.15. FLCA Case Study - Environmental materials data in production database.

FLCA - Production Database						
Material Section (MAT)						
ID	**Material Class**	**Material Subclass**	**Material name**	**cc Primary [$kgCO_{2eq}/kg$]**	**cc EoL - Energy recovery [$kgCO_{2eq}/kg$]**	**Substitution Factor [-]**
M1	Metals and Alloys	Ferrous	Cast Iron (Ductile)	1.7-1.8	0-0	0.25-0.25
M2	Metals and Alloys	Ferrous	High Carbon Steel	1.71-1.89	0-0	0.25-0.25
M3	Metals and Alloys	Ferrous	Low Alloy Steel	1.93-2.13	0-0	0.25-0.25
M4	Metals and Alloys	Ferrous	Medium Carbon Steel	1.72-1.9	0-0	0.25-0.25
M5	Metals and Alloys	Ferrous	Stainless Steel	4.73-5.23	0-0	0.25-0.25
M6	Metals and Alloys	Non-Ferrous	Cast Al-Alloys	12.20-13.4	0-0	0.15-0.15
M7	Metals and Alloys	Non-Ferrous	Wrought Magnesium Alloys	33.6-37.1	0-0	0.15-0.15
M8	Metals and Alloys	Non-Ferrous	Nickel-based Superalloys	13-14.4	0-0	0.15-0.15
M9	Metals and Alloys	Non-Ferrous	Titanium Alloys	44.1-48.7	0-0	0.15-0.15

Table B.16. TRF Case Study - Environmental Compatibility Matrices in production database.

FLCA - Compatibility Process/Material										
ID	**M1**	**M2**	**M3**	**M4**	**M5**	**M6**	**M7**	**M8**	**M9**	**M10**
	[kgCO_{2eq}/kg]	**[kgCO_{2eq}/kg]**	**[kgCO_{2eq}/kg]**	**[kgCO_{2eq}/kg]**	**[kgCO_{2eq}/kg]**	**[kgCO_{2eq}/kg]**	**[kgCO_{2eq}/kg]**	**[kgCO_{2eq}/kg]**	**[kgCO_{2eq}/kg]**	**[kgCO_{2eq}/kg]**
CA1	0-0	0-0	0-0	0-0	0-0	0-0	0-0	0-0	0-0	0-0
CA2	0.751-0.83	0.807-0.892	0.819-0.906	0.819-0.906	0.809-0.894	0.819-0.906	0.819-0.906	0.748-0.826	0-0	0-0
CA3	0.751-0.83	0.807-0.892	0.819-0.906	0.819-0.906	0.809-0.894	0.819-0.906	0.819-0.906	0.748-0.826	0-0	0-0
DE1	0-0	0.247-0.273	0.238-0.263	0.233-0.258	0.562-0.621	5.24-5.79	0.449-0.497	0.311-0.344	1.05-1.16	0.391-0.432
PO1	0-0	2.7-3.27	2.83-3.43	2.87-3.42	2.89-3.31	20.2-24.4	0-0	2.52-3.05	0-0	4.45-4.91

Table B.17. FLCA Case Study - Economic materials data in production database.

FLCA - Production Database						
Material Section (MAT)						
ID	**Material Class**	**Material Subclass**	**Material name**	**cost Primary [EUR/kg]**	**Material Scrap fraction [-]**	**LHV [MJ]**
M1	Metals and Alloys	Ferrous	Cast Iron (Ductile)	0.517-0.569	0.2-0.2	0-0
M2	Metals and Alloys	Ferrous	High Carbon Steel	0.605-0.665	0.2-0.2	0-0
M3	Metals and Alloys	Ferrous	Low Alloy Steel	0.712-0.783	0.2-0.2	0-0
M4	Metals and Alloys	Ferrous	Medium Carbon Steel	0.563-0.619	0.2-0.2	0-0
M5	Metals and Alloys	Ferrous	Stainless Steel	6.6-7.26	0.2-0.2	0-0
M6	Metals and Alloys	Non-Ferrous	Cast Al-Alloys	1.87-2.05	0.2-0.2	0-0
M7	Metals and Alloys	Non-Ferrous	Wrought Magnesium Alloys	3.74-4.12	0.2-0.2	0-0
M8	Metals and Alloys	Non-Ferrous	Nickel-based Superalloys	24.4-26.8	0.2-0.2	0-0
M9	Metals and Alloys	Non-Ferrous	Titanium Alloys	45.6-50.2	0.2-0.2	0-0

Table B.18. FLCA Case Study - Economic processes data in production database.

FLCA - Production Database					
Process Section (MAN)					
ID	**Process Class**	**Process Subclass**	**Process name**	**Tool Cost [EUR]**	**Tool Lifespan [pc.]**
CA1	Casting	Die Casting Processes	Gravity Die casting	3920-17500	10000-100000
CA2	Casting	Investment Casting Processes	Investment Casting	65.3-653	1-5
CA3	Casting	Die Casting Processes	Low Pressure Die Casting	131-1310	100-1000
DE1	Deformation	Bulk Deformation Processes	Forging	3920-11800	100-1000000
PO1	Powder Methods	Powder Pressing Processes	Pressing and Sintering	3260-10400	10000-50000

FLCA - Production Database [CONTINUE]						
Process Section (MAN)						
ID	**Process Class**	**Process Subclass**	**Process name**	**Production Rate [pc./hr]**	**Capital Cost [EUR]**	**Overhead Rate [EUR/hr]**
CA1	Casting	Die Casting Processes	Gravity Die casting	5-50	13100-52200	60-60
CA2	Casting	Investment Casting Processes	Investment Casting	1-200	261-1310	60-60
CA3	Casting	Die Casting Processes	Low Pressure Die Casting	1-20	1310-6530	60-60
DE1	Deformation	Bulk Deformation Processes	Forging	100-500	261000-653000	60-60
PO1	Powder Methods	Powder Pressing Processes	Pressing and Sintering	120-1200	45700-261000	60-60

Table B.19. EMB Case Study - Design materials data in production database.

EMB - Production Database							
Material Section (MAT)							
ID	**Material Class**	**Material Subclass**	**Material name**	**Density [kg/m^3]**	**Young's Modulus [MPa]**	**Poisson Ratio [-]**	**Yield Strength [MPa]**
M1	Metals and Alloys	Ferrous	High Carbon Steel	7850	212300	0.29	1030
M2	Metals and Alloys	Ferrous	Low Alloy Steel	7850	207700	0.29	430
M3	Metals and Alloys	Ferrous	Stainless Steel	7900	203300	0.27	515
M4	Metals and Alloys	Non-Ferrous	Age-Hardening Wrought Al-Alloys	2845	75500	0.34	275
M5	Metals and Alloys	Non-Ferrous	Titanium Alloys	4800	117740	0.37	750

Table B.20. EMB Case Study - Design processes data and Compatibility Matrices in production database.

EMB - Production Database					
Process Section (MAN)					
ID	**Process Class**	**Process Subclass**	**Process name**	**Mass range [kg]**	**Economic Batch size [-]**
CA1	Casting	Investment Casting Processes	Investment Casting	0.001-100	1-10000
DE1	Deformation	Bulk Deformation Processes	Forging	0.01-5000	1-100000000
PO1	Powder Methods	Powder Pressing Processes	Pressing and Sintering	0.01-5	500-5000000

EMB - Production Database [CONTINUE]						
Process Section (MAN)						
ID	**Process Class**	**Process Subclass**	**Process name**	**Section thickness [mm]**	**Tolerance [mm]**	**Roughness [µm]**
CA1	Casting	Investment Casting Processes	Investment Casting	1-75	0.05-0.25	0.5-3.2
DE1	Deformation	Bulk Deformation Processes	Forging	1-900	0.2-1	3.2-12.5
PO1	Powder Methods	Powder Pressing Processes	Pressing and Sintering	1.5-8	0.025-1	1-10

EMB - Compatibility Process/Shape						
ID	**1D - Circular**	**1D - Noncircular**	**2D - Flat**	**2D - Dished**	**3D - Solid**	**3D-Hollow**
CA1	1	1	0	0	1	1
DE1	0	1	0	0	1	0
PO1	1	1	0	0	1	1

EMB - Compatibility Process/Material					
ID	**M1**	**M2**	**M3**	**M4**	**M5**
CA1	1	1	1	1	0
DE1	1	1	1	1	1
PO1	1	1	1	1	0

Table B.21. EMB Case Study - Environmental materials data in production database.

EMB - Production Database						
Material Section (MAT)						
ID	**Material Class**	**Material Subclass**	**Material name**	**cc Primary [$kgCO_{2eq}/kg$]**	**cc EoL - Energy recovery [$kgCO_{2eq}/kg$]**	**Substitution Factor [-]**
M1	Metals and Alloys	Ferrous	High Carbon Steel	1.71-1.89	0	0.25
M2	Metals and Alloys	Ferrous	Low Alloy Steel	1.93-2.13	0	0.25
M3	Metals and Alloys	Ferrous	Stainless Steel	4.73-5.23	0	0.25
M4	Metals and Alloys	Non-Ferrous	Age-Hardening Wrought Al-Alloys	12.2-13.4	0	0.15
M5	Metals and Alloys	Non-Ferrous	Titanium Alloys	44.1-48.7	0	0.15

Table B.22. EMB Case Study - Environmental Compatibility Matrices in production database.

EMB - Compatibility Process/Material					
ID	**M1**	**M2**	**M3**	**M4**	**M5**
	[$kgCO_{2eq}/kg$]	**[$kgCO_{2eq}/kg$]**	**[$kgCO_{2eq}/kg$]**	**[$kgCO_{2eq}/kg$]**	**[$kgCO_{2eq}/kg$]**
CA1	0.5	0.5	0.5	0.5	0
DE1	0.5	0.5	0.5	0.5	0.5
PO1	0.5	0.5	0.5	0.5	0

Table B.23. EMB Case Study - Economic materials data in production database.

EMB - Production Database						
Material Section (MAT)						
ID	**Material Class**	**Material Subclass**	**Material name**	**cost Primary [EUR/kg]**	**Material Scrap fraction [-]**	**LHV [MJ]**
M1	Metals and Alloys	Ferrous	High Carbon Steel	0.65	0.2	0
M2	Metals and Alloys	Ferrous	Low Alloy Steel	0.75	0.2	0
M3	Metals and Alloys	Ferrous	Stainless Steel	7	0.2	0
M4	Metals and Alloys	Non-Ferrous	Age-Hardening Wrought Al-Alloys	2	0.2	0
M5	Metals and Alloys	Non-Ferrous	Titanium Alloys	50	0.2	0

Table B.24. EMB Case Study - Economic processes data in production database.

EMB - Production Database					
Process Section (MAN)					
ID	**Process Class**	**Process Subclass**	**Process name**	**Tool Cost [EUR]**	**Tool Lifespan [pc.]**
CA1	Casting	Investment Casting Processes	Investment Casting	250	5
DE1	Deformation	Bulk Deformation Processes	Forging	5000	50000
PO1	Powder Methods	Powder Pressing Processes	Pressing and Sintering	5000	20000

EMB - Production Database [CONTINUE]						
Process Section (MAN)						
ID	**Process Class**	**Process Subclass**	**Process name**	**Production Rate [pc./hr]**	**Capital Cost [EUR]**	**Overhead Rate [EUR/hr]**
CA1	Casting	Investment Casting Processes	Investment Casting	100	1000	60
DE1	Deformation	Bulk Deformation Processes	Forging	10	200000	60
PO1	Powder Methods	Powder Pressing Processes	Pressing and Sintering	500	200000	60